Hashemite Kingdom of Jordan

Jordan Journal of Biological Sciences

An International Peer-Reviewed Scientific Journal

Financed by the Scientific Research and Innovation Support Fund

This title is indexed in Scopus

http://jjbs.hu.edu.jo/

المجلة الأردنية للعلوم الحياتية
Jordan Journal of Biological Sciences (JJBS)
http://jjbs.hu.edu.jo

Jordan Journal of Biological Sciences (JJBS) (ISSN: 1995–6673 (Print); 2307-7166 (Online)):

An International Peer- Reviewed Open Access Research Journal financed by the Scientific Research and Innovation Support Fund, Ministry of Higher Education and Scientific Research, Jordan and published quarterly by the Deanship of Scientific Research, Hashemite University, Jordan.

Submission Address

Professor Abu-Elteen, Khaled H
Hashemite University
P.O. Box 330127, Zarqa, 13115, Jordan
Phone: +962-5-3903333 ext. 4357
E-Mail: jjbs@hu.edu.jo

المجلة الاردنية للعلوم الحياتية
Jordan Journal of Biological Sciences (JJBS)
http://jjbs.hu.edu.jo

International Advisory Board (Arranged alphabetically)

Instructions to Authors

Scopes

Study areas include cell biology, genomics, microbiology, immunology, molecular biology, biochemistry, embryology, immunogenetics, cell and tissue culture, molecular ecology, genetic engineering and biological engineering, bioremediation and biodegradation, bioinformatics, biotechnology regulations, gene therapy, organismal biology, microbial and environmental biotechnology, marine sciences. The JJBS welcomes the submission of manuscript that meets the general criteria of significance and academic excellence. All articles published in JJBS are peer-reviewed. Papers will be published approximately one to two months after acceptance.

Type of Papers

The journal publishes high-quality original scientific papers, short communications, correspondence and case studies. Review articles are usually by invitation only. However, Review articles of current interest and high standard will be considered.

Submission of Manuscript

Manuscript, or the essence of their content, must be previously unpublished and should not be under simultaneous consideration by another journal. The authors should also declare if any similar work has been submitted to or published by another journal. They should also declare that it has not been submitted/ published elsewhere in the same form, in English or in any other language, without the written consent of the Publisher. The authors should also declare that the paper is the original work of the author(s) and not copied (in whole or in part) from any other work. All papers will be automatically checked for duplicate publication and plagiarism. If detected, appropriate action will be taken in accordance with International Ethical Guideline. By virtue of the submitted manuscript, the corresponding author acknowledges that all the co-authors have seen and approved the final version of the manuscript. The corresponding author should provide all co-authors with information regarding the manuscript, and obtain their approval before submitting any revisions. Electronic submission of manuscripts is strongly recommended, provided that the text, tables and figures are included in a single Microsoft Word file. Submit manuscript as e-mail attachment to the Editorial Office at: JJBS@hu.edu.jo. After submission, a manuscript number will be communicated to the corresponding author within 48 hours.

Peer-review Process

It is requested to submit, with the manuscript, the names, addresses and e-mail addresses of at least 4 potential reviewers. It is the sole right of the editor to decide whether or not the suggested reviewers to be used. The reviewers' comments will be sent to authors within 6-8 weeks after submission.
Manuscripts and figures for review will not be returned to authors whether the editorial decision is to accept, revise, or reject. All Case Reports and Short Communication must include at least one table and/ or one figure.

Preparation of Manuscript

The manuscript should be written in English with simple lay out. The text should be prepared in single column format. Bold face, italics, subscripts, superscripts etc. can be used. Pages should be numbered consecutively, beginning with the title page and continuing through the last page of typewritten material.

The text can be divided into numbered sections with brief headings. Starting from introduction with section 1. Subsections should be numbered (for example 2.1 (then 2.1.1, 2.1.2, 2.2, etc.), up to three levels. Manuscripts in general should be organized in the following manner:

Title Page

The title page should contain a brief title, correct first name, middle initial and family name of each author and name and address of the department(s) and institution(s) from where the research was carried out for each author. The title should be without any abbreviations and it should enlighten the contents of the paper. All affiliations should be provided with a lower-case superscript number just after the author's name and in front of the appropriate address.
The name of the corresponding author should be indicated along with telephone and fax numbers (with country and area code) along with full postal address and e-mail address.

Abstract

The abstract should be concise and informative. It should not exceed **350 words** in length for full manuscript and Review article and **150 words** in case of Case Report and/ or Short Communication. It should briefly describe the purpose of the work, techniques and methods used, major findings with important data and conclusions. No references should be cited in this part. Generally non-standard abbreviations should not be used, if necessary they should be clearly defined in the abstract, at first use.

Keywords

Immediately after the abstract, **about 4-8 keywords** should be given. Use of abbreviations should be avoided, only standard abbreviations, well known in the established area may be used, if appropriate. These keywords will be used for indexing.

Abbreviations

Non-standard abbreviations should be listed and full form of each abbreviation should be given in parentheses at first use in the text.

Introduction

Provide a factual background, clearly defined problem, proposed solution, a brief literature survey and the scope and justification of the work done.

Materials and Methods

Give adequate information to allow the experiment to be reproduced. Already published methods should be mentioned with references. Significant modifications of published methods and new methods should be described in detail. Capitalize trade names and include the manufacturer's name and address. Subheading should be used.

Results

Results should be clearly described in a concise manner. Results for different parameters should be described under subheadings or in separate paragraph. Results should be explained, but largely without referring to the literature. Table or figure numbers should be mentioned in parentheses for better understanding.

Discussion

The discussion should not repeat the results, but provide detailed interpretation of data. This should interpret the significance of the findings of the work. Citations should be given in support of the findings. The results and discussion part can also be described as separate, if appropriate. The Results and Discussion sections can include subheadings, and when appropriate, both sections can be combined

Conclusions

This should briefly state the major findings of the study.

Acknowledgment

A brief acknowledgment section may be given after the conclusion section just before the references. The acknowledgment of people who provided assistance in manuscript preparation, funding for research, etc. should be listed in this section.

Tables and Figures

Tables and figures should be presented as per their appearance in the text. It is suggested that the discussion about the tables and figures should appear in the text before the appearance of the respective tables and figures. No tables or figures should be given without discussion or reference inside the text.

Tables should be explanatory enough to be understandable without any text reference. Double spacing should be maintained throughout the table, including table headings and footnotes. Table headings should be placed above the table. Footnotes should be placed below the table with superscript lowercase letters. Each table should be on a separate page, numbered consecutively in Arabic numerals.

Each figure should have a caption. The caption should be concise and typed separately, not on the figure area. Figures should be self-explanatory. Information presented in the figure should not be repeated in the table. All symbols and abbreviations used in the illustrations should be defined clearly. Figure legends should be given below the figures.

References

References should be listed alphabetically at the end of the manuscript. Every reference referred in the text must be also present in the reference list and vice versa. In the text, a reference identified by means of an author's name should be followed by the year of publication in parentheses (e.g.(Brown,2009)). For two authors, both authors' names followed by the year of publication (e.g.(Nelson and Brown, 2007)). When there are more than two authors, only the first author's name followed by "*et al*." and the year of publication (e.g. (Abu-Elteen *et al*., 2010)). When two or more works of an author has been published during the same year, the reference should be identified by the letters "a", "b", "c", etc., placed after the year of publication. This should be followed both in the text and reference list. e.g., Hilly, (2002a, 2002b); Hilly, and Nelson, (2004). Articles in preparation or submitted for publication, unpublished observations, personal communications, etc. should not be included in the reference list but should only be mentioned in the article text (e.g., Shtyawy,A., University of Jordan, personal communication). Journal titles should be abbreviated according to the system adopted in Biological Abstract and Index Medicus, if not included in Biological Abstract or Index Medicus journal title should be given in full. The author is responsible for the sccuracy and completeness of the references and for their correct textual citation. Failure to do so may result in the paper being withdraw from the evaluation process. Example of correct reference form is given as follows:-

Reference to a journal publication:

Bloch BK. 2002. Econazole nitrate in the treatment of *Candida vaginitis*. *S Afr Med J.* , **58**:314-323.

Ogunseitan OA and Ndoye IL. 2006. Protein method for investigating mercuric reductase gene expression in aquatic environments. *Appl Environ Microbiol*., **64**: 695-702.

Hilly MO, Adams MN and Nelson SC. 2009. Potential fly-ash utilization in agriculture. *Progress in Natural Sci.*, **19**: 1173-1186.

Reference to a book:

Brown WY and White SR.1985. **The Elements of Style**, third ed. MacMillan, New York.

Reference to a chapter in an edited book:

Mettam GR and Adams LB. 2010. How to prepare an electronic version of your article. In: Jones BS and Smith RZ (Eds.), **Introduction to the Electronic Age**. Kluwer Academic Publishers, Netherlands, pp. 281–304.

Conferences and Meetings:

Embabi NS. 1990. Environmental aspects of distribution of mangrove in the United Arab Emirates. Proceedings of the First ASWAS Conference. University of the United Arab Emirates. Al-Ain, United Arab Emirates.

Theses and Dissertations:

El-Labadi SN. 2002. Intestinal digenetic trematodes of some marine fishes from the Gulf of Aqaba. MSc dissertation, The Hashemite University, Zarqa, Jordan.

Nomenclature and Units

Internationally accepted rules and the international system of units (SI) should be used. If other units are mentioned, please give their equivalent in SI.

For biological nomenclature, the conventions of the *International Code of Botanical Nomenclature, the International Code of Nomenclature of Bacteria,* and the *International Code of Zoological Nomenclature* should be followed.
Scientific names of all biological creatures (crops, plants, insects, birds, mammals, etc.) should be mentioned in parentheses at first use of their English term.

Chemical nomenclature, as laid down in the *International Union of Pure and Applied Chemistry* and the official recommendations of the *IUPAC-IUB Combined Commission on Biochemical Nomenclature* should be followed. All biocides and other organic compounds must be identified by their Geneva names when first used in the text. Active ingredients of all formulations should be likewise identified.

Math formulae

All equations referred to in the text should be numbered serially at the right-hand side in parentheses. Meaning of all symbols should be given immediately after the equation at first use. Instead of root signs fractional powers should be used. Subscripts and superscripts should be presented clearly. Variables should be presented in italics. Greek letters and non-Roman symbols should be described in the margin at their first use.

To avoid any misunderstanding zero (0) and the letter O, and one (1) and the letter l should be clearly differentiated. For simple fractions use of the solidus (/) instead of a horizontal line is recommended. Levels of statistical significance such as: $^{*}P < 0.05$, $^{**}P < 0.01$ and $^{***}P < 0.001$ do not require any further explanation.

Copyright

Submission of a manuscript clearly indicates that: the study has not been published before or is not under consideration for publication elsewhere (except as an abstract or as part of a published lecture or academic thesis); its publication is permitted by all authors and after accepted for publication it will not be submitted for publication anywhere else, in English or in any other language, without the written approval of the copyright-holder. The journal may consider manuscripts that are translations of articles originally published in another language. In this case, the consent of the journal in which the article was originally published must be obtained and the fact that the article has already been published must be made clear on submission and stated in the abstract. It is compulsory for the authors to ensure that no material submitted as part of a manuscript infringes existing copyrights, or the rights of a third party.

Ethical Consent

All manuscripts reporting the results of experimental investigation involving human subjects should include a statement confirming that each subject or subject's guardian obtains an informed consent, after the approval of the experimental protocol by a local human ethics committee or IRB. When reporting experiments on animals, authors should indicate whether the institutional and national guide for the care and use of laboratory animals was followed.

Plagiarism

The JJBS hold no responsibility for plagiarism. If a published paper is found later to be extensively plagiarized and is found to be a duplicate or redundant publication, a note of retraction will be published, and copies of the correspondence will be sent to the authors' head of institute.

Galley Proofs

The Editorial Office will send proofs of the manuscript to the corresponding author as an e-mail attachment for final proof reading and it will be the responsibility of the corresponding author to return the galley proof materials appropriately corrected within the stipulated time. Authors will be asked to check any typographical or minor clerical errors in the manuscript at this stage. No other major alteration in the manuscript is allowed. After publication authors can freely access the full text of the article as well as can download and print the PDF file.

Publication Charges

There are no page charges for publication in Jordan Journal of Biological Sciences, except for color illustrations,

Reprints

Ten (10) reprints are provided to corresponding author free of charge within two weeks after the printed journal date. For orders of more reprints, a reprint order form and prices will be sent with article proofs, which should be returned directly to the Editor for processing.

Disclaimer

Articles, communication, or editorials published by JJBS represent the sole opinions of the authors. The publisher shoulders no responsibility or liability what so ever for the use or misuse of the information published by JJBS.

Indexing

JJBS is indexed and abstracted by:

DOAJ (Directory of Open Access Journals)	CABI
Google Scholar	EBSCO
Journal Seek	CAS (Chemical Abstract Service)
HINARI	ETH- Citations
Index Copernicus	Open J-Gat
NDL Japanese Periodicals Index	SCImago
SCIRUS	Clarivate Analytics (Zoological Abstract)
OAJSE	Scopus
ISC (Islamic World Science Citation Center)	AGORA (United Nation's FAO database)
Directory of Research Journal Indexing (DRJI)	SHERPA/RoMEO (UK)
Ulrich's	

المجلة الأردنية للعلوم الحياتية
Jordan Journal of Biological Sciences (JJBS)
ISSN 1995- 6673 (Print), 2307- 7166 (Online)
http://jjbs.hu.edu.jo

The Hashemite University

Deanship of Scientific Research

TRANSFER OF COPYRIGHT AGREEMENT

Journal publishers and authors share a common interest in the protection of copyright: authors principally because they want their creative works to be protected from plagiarism and other unlawful uses, publishers because they need to protect their work and investment in the production, marketing and distribution of the published version of the article. In order to do so effectively, publishers request a formal written transfer of copyright from the author(s) for each article published. Publishers and authors are also concerned that the integrity of the official record of publication of an article (once refereed and published) be maintained, and in order to protect that reference value and validation process, we ask that authors recognize that distribution (including through the Internet/WWW or other on-line means) of the authoritative version of the article as published is best administered by the Publisher.

To avoid any delay in the publication of your article, please read the terms of this agreement, sign in the space provided and return the complete form to us at the address below as quickly as possible.

Article entitled:----------

Corresponding author: ----------

To be published in the journal: Jordan Journal of Biological Sciences (JJBS)

I hereby assign to the Hashemite University the copyright in the manuscript identified above and any supplemental tables, illustrations or other information submitted therewith (the "article") in all forms and media (whether now known or hereafter developed), throughout the world, in all languages, for the full term of copyright and all extensions and renewals thereof, effective when and if the article is accepted for publication. This transfer includes the right to adapt the presentation of the article for use in conjunction with computer systems and programs, including reproduction or publication in machine-readable form and incorporation in electronic retrieval systems.
Authors retain or are hereby granted (without the need to obtain further permission) rights to use the article for traditional scholarship communications, for teaching, and for distribution within their institution.

☐ **I am the sole author of the manuscript**

☐ **I am signing on behalf of all co-authors of the manuscript**

☐ **The article is a 'work made for hire' and I am signing as an authorized representative of the employing company/institution**

Please mark one or more of the above boxes (as appropriate) and then sign and date the document in black ink.

Signed:_____ **Name printed:** _____
Title and Company (if employer representative) : _____
Date: _____

Data Protection: By submitting this form you are consenting that the personal information provided herein may be used by the Hashemite University and its affiliated institutions worldwide to contact you concerning the publishing of your article.

Please return the completed and signed original of this form by mail or fax, or a scanned copy of the signed original by e-mail, retaining a copy for your files, to:

Hashemite University
Jordan Journal of Biological Sciences
Zarqa 13115 Jordan
Fax: +962 5 3903338
Email: jjbs@hu.edu.jo

EDITORIAL PREFACE

Jordan Journal of Biological Sciences (JJBS) is a r efereed, quarterly international journal financed by the Scientific Research and Innovation Support Fund, Ministry of Higher Education and Scientific Research in cooperation with the Hashemite University, Jordan. JJBS celebrated its 11th commencement this past January, 2019. JJBS was founded in 2008 to create a peer-reviewed journal that publishes high-quality research articles, reviews and short communications on novel and innovative aspects of a wide variety of biological sciences such as cell biology, developmental biology, structural biology, microbiology, entomology, molecular biology, biochemistry, medical biotechnology, biodiversity, ecology, marine biology, plant and animal biology, plant and animal physiology, genomics and bioinformatics.

We have watched the growth and success of JJBS over the years. JJBS has published 11 volumes, 45 issues and 479 articles. JJBS has been indexed by SCOPUS, CABI's Full-Text Repository, EBSCO, Clarivate Analytics- Zoological Record and recently has been included in the UGC India approved journals. JJBS Cite Score has improved from 0.18 in 2015 to 0.60 in 2018.

A group of highly valuable scholars have agreed to serve on the editorial board and this places JJBS in a position of most authoritative on bi ological sciences. I am honored to have six eminent associate editors from various countries. I am also delighted with our group of international advisory board members coming from 15 countries worldwide for their continuous support of JJBS. With our editorial board's cumulative experience in various fields of biological sciences, this journal brings a substantial representation of biological sciences in different disciplines. Without the service and dedication of our editorial; associate editorial and international advisory board members, JJBS would have never existed.

In the coming year, we hope that JJBS will be indexed in Clarivate Analytics and MEDLINE (the U.S. National Library of Medicine database) and others. As you read throughout this volume of JJBS, I would like to remind you that the success of our journal depends on the number of quality articles submitted for review. Accordingly, I would like to request your participation and colleagues by submitting quality manuscripts for review. One of the great benefits we can provide to our prospective authors, regardless of acceptance of their manuscripts or not, is the feedback of our review process. JJBS provides authors with high quality, helpful reviews to improve their manuscripts.

Finally, JJBS would not have succeeded without the collaboration of authors and referees. Their work is greatly appreciated. Furthermore, my thanks are also extended to The Hashemite University and the Scientific Research and Innovation Support Fund, Ministry of Higher Education and Scientific Research for their continuous financial and administrative support to JJBS.

Professor Khaled H. Abu-Elteen
March, 2019

JJBS

Volume 12, Number 5, December .2019
ISSN 1995-6673

Jordan Journal of Biological Sciences

CONTENTS

Original Articles

Short Communication

JJBS
Jordan Journal of Biological Sciences

Volume 12, Number 5,December 2019
ISSN 1995-6673
Pages 525 - 534

Plant Growth-Promoting Rhizobacteria: An Emerging Method for the Enhancement of Wheat Tolerance against Salinity Stress- (Review)

Randa N. Albdaiwi[1], Hala Khyami-Horani[1*] and Jamal Y. Ayad[2]

[1]*Department of Biological Sciences, Faculty of Science,* [2]*Department of Horticulture and Crop Science, Faculty of Agriculture, The University of Jordan, Amman 11942, Jordan*

Received December 24, 2018; Revised February 12, 2019; Accepted February 16, 2019

Abstract

Salinity is a major threat to crop productivity and agriculture development worldwide. Intensive research has been conducted to overcome such problem focusing primarily on efficient resource management and crop improvement. However, such approaches take a long time and are considerably expensive. Therefore, there is an urgent need to develop new economical methods that are effective in ameliorating the adverse effects of high salinity levels in the soil. The isolation and use of halotolerant Plant Growth-Promoting Rhizobacteria (PGPR), from natural saline habitats, are needed to reduce the adverse effects of salinity on crop species. The ability of PGPR to provide plants with necessary nutrients is considered a promising substitute to chemical fertilizers and organic alternatives to promote growth and improve the yield of crops. PGPR have been reported to enhance germination, and to delay leaf senescence at various salinity levels. Several bacterial activities and mechanisms have been identified including the increase in nutrient availability through biological nitrogen fixation, inorganic phosphate solubilization, and siderophore production, which result in the improvement of nutrient availability and plant hormonal activities. The present review gives an update of scientific progress regarding PGPR utilization for improving staple food crops such as wheat.

Keywords: Halotolerant Plant Growth Promoting, 1-aminocydopropane-1-carboxylic acid (ACC) deaminase, Durum Wheat, Endophyte, Salinity.

1. Introduction

Crop productivity is severely affected by several biotic and abiotic stresses including drought, salinity, extreme temperatures, and pathogens, which can limit growth and development of any given crop. Salinity is an adverse condition affecting crop productivity in arid and semi-arid areas around the world where it caused an annual loss of 1-2% of arable land (Shrivastava and Kumar, 2015). Salinity alters cellular metabolism causing many physiological, morphological, biochemical, and molecular changes in plants. It also affects all aspects of plant growth and development from seed germination up to reproductive growth (Gupta and Huang, 2014). Salinity impact on plant growth and development is mainly attributed to changes in the osmotic status of plants, which has an immediate impact on water availability, accumulation of toxic ions such as Na^+ and Cl^- in the cells, and nutrient imbalances (Munns and Tester, 2008).

Wheat (*Triticum spp*.) is considered one of the most important crops in the world; it is a staple food for over 35 % of the world's population where it provides more calories and proteins than any other cultivated crop (FAOSTAT, 2017). Durum wheat (*T. turgidum subsp. durum*) forms about 10 % of all wheat cultivated areas in the world. Indeed, it is a major cereal crop in the Mediterranean region (Kabbaj *et al.*, 2017). Several studies indicate that the wild progenitor of modern durum wheat is widely distributed in the Jordan Valley region on the eastern side of the Dead Sea with archeological evidences of durum wheat utilization near the Dead Sea region as far back as 9500 years ago (Weide, 2015). High genetic diversity in Jordanian germplasm is considered a valuable resource to improve durum wheat tolerance against different abiotic stresses including drought, heat, and salinity (Abdel-Ghani, 2009; Abu-Romman, 2016; Jaradat, 1992).

High-salt stress has more pronounced effects on durum-wheat growth and development compared with other cereals. This is mainly attributed to its inability to exclude Na^+ from its tissues (Roy *et al.*, 2014). Several approaches have been used to reduce salinity effects on durum wheat, including proper soil practices, irrigation managements, traditional breeding and genetic engineering (Katerji *et al.*, 2009).

The rhizosphere environment harbors many microorganisms that can play a major role in enhancing

* Corresponding author e-mail: horani-h@ju.edu.jo; horani.hala@gmail.com.

plant productivity under saline conditions (Etesami and Beattie, 2018). In such environments, Plant Growth-Promoting Rhizobacteria (PGPR) are considered beneficial microorganisms that possess many growth-promoting traits, which are crucial to improving plant growth and the yield of crops, either directly or indirectly. They can also help in alleviating the adverse effects of many stresses, including salinity. The direct plant-growth promotion occurs when PGPR facilitate the plant nutrients' uptake from the surrounding environments by phosphorus solubilization, nitrogen fixation, and/or by producing siderophore to sequester iron (Etesami and Beattie, 2018). Furthermore, PGPR can modulate plant growth by promoting the production and regulation of phytohormones, such as Indole Acetic Acid (IAA) (Arshadullah *et al.*, 2017), or by lowering plant ethylene production by the activity of the 1-Aminocyclopropane-1-carboxylate (ACC) deaminase enzyme (Glick, 2014). On the other hand, indirect plant-growth promotion by PGPR occurs when they limit or prevent plant damage caused by various pathogenic agents such as bacteria, fungi, and nematodes (Compant *et al.*, 2005). This review focuses on the soil salinity problem as a challenge to improve crops, primarily wheat productivity. It discusses the utilization of PGPR as a strategy to mitigate soil salinity-stress and identifies the mechanisms to cope with such stresses.

2. Soil Salinity: A Global Problem

Soil salinity is a major problem affecting crop productivity in arid and semi-arid areas around the globe with salinity-affected soils covering more than 7 % of total arable lands of the world (Rasool *et al.*, 2013). Climate change and human activities result in increased salt accumulation in the soil; high rates of evapotranspiration, improper drainage and limited leaching of mineral salts from the soil surface result in increased salinity levels in arid and semi-arid regions (Mohan *et al.*, 2017). According to the United States Department of Agriculture (USDA), a given soil with an Electrical Conductivity (EC) of 4 dS m^{-1} is considered as saline soil. The inhibitory effect of excess salt in the soil can impact many plant cellular, physiological, biochemical and molecular processes that will hinder plant growth and eventually reduce crop production (Sairam and Tyagi, 2004).

3. Effect of Soil Salinity on Crop Plants

Plant growth and development are affected by salinity stress at different growth stages including germination, vegetative growth and reproductive development (Shrivastava and Kumar, 2015). Such adverse effects are mainly attributed to changes in cellular water and ionic status in growing plants (Munns and Tester, 2008). Plants are generally divided into four groups according to their salinity tolerance as follows: sensitive, moderately-sensitive, moderately- tolerant and tolerant. Many of the cereal crops are considered sensitive to high salt stress; bread wheat plants can withstand a salinity level up to 6 dSm^{-1}, while maize plants are considered less tolerant and are negatively affected at levels higher than 2 dSm^{-1}. Under salinity stress, the yield of many cereals, such as wheat, rice, and barley, is reduced significantly (Arshadullah *et al.*, 2017).

Salinity can have enormous negative effects on the morphological and physiological properties in wheat. It affects wheat-seed germination, seedling growth, water-uptake, photosynthesis, nutrient uptake, enzymatic activities and yield. Several studies revealed diverse effects of salt stress on different wheat species and cultivars, by which some were found tolerant, while others were susceptible (Hasanuzzaman *et al.*, 2017). Bread wheat (*T. aestivum*) showed moderate salinity-tolerance responses, while durum wheat (*T. turgidum subsp. durum*) was found more sensitive due to its inability to exclude Na^+ from its tissue (Roy *et al.,* 2014). High salinity levels were found to reduce the growth and development of eight Jordanian durum wheat genotypes when compared with non-saline treatments (Abdel-Ghani, 2009); three lines showed low values of susceptibility indices for germination, seminal root length and grain yield.

4. Amelioration of Soil Salinity

Several strategies can be adopted to manage the deleterious effects of soil salinity on p lants such as leaching the excess of soluble salts from the soil, conventional plant breeding and genetic improvement aiming for tolerant varieties; however, all of these strategies have their own limitations. Plant breeding is a relatively slow process depending often on laborious programs, whereas genetically-modified crops are promising, but the limited success to find major genetic determinants of salt tolerance in plants and its acceptance by the general public are quite challenging (Key *et al.*, 2008).

Other tools used for salinity amelioration include the application of biochar, which is a ch arcoal-derived material that can adsorb Na^+ (Akhtar *et al.*, 2015), seed priming with plant growth-promoting substances, such as salicylic acid (Azooz, 2009), and the application of polyamines (Roychoudhury *et al.*, 2011).

Plant salt-tolerance can be improved by the application of eco-friendly strategies and through the use of beneficial microorganisms. The free-living or root-colonizing beneficial bacteria known as PGPR, which reside in the rhizosphere region, have many beneficial effects on plants (Arshadullah *et al.*, 2017). They comprise 2-5 % of the total rhizospheric bacteria surrounding a given plant-root system (Katiyar *et al.*, 2016). PGPR may possess multiple plant growth-promoting traits, which increase plant growth and the yield of crops, and can help in alleviating the effects of abiotic and biotic stresses through direct or indirect mechanisms (Numana *et al.*, 2018).

5. Plant Growth-Promoting Rhizobacteria

PGPR are composed of different groups of soil-living bacteria, which enhance plant growth through different mechanisms; they may be free-living or may colonize plant roots (Numana *et al.*, 2018). The rhizosphere is a region that extends only a few mm from the root system and is directly affected by the plant-root activity. In this region, the bacterial communities are the most dominant living organisms typically ranging from 10^6 to 10^9 CFU g^{-1} of a r hizospheric soil. Bacterial concentrations in the rhizosphere is generally higher than in bulk soils as a result of chemical signals and exudates produced by the roots,

which support bacterial growth and their metabolism (Ahemad and Kibret, 2014). In general, PGPR are classified into two main groups according to their degree of pr oximity to the roots of their host plant: (1) Rhizospheric bacteria that live outside plant roots and include free-living rhizobacteria, which exist in the soil near the root system (rhizosphere), or bacteria colonizing the root surface (rhizoplane), and (2) Endophytic bacteria or endophytes that live inside plant-root tissues and include bacteria which inhabit intercellular spaces, specialized root structures (nodules), or in the vascular system (Menendez and Garcia-Fraile, 2017).

Most of rhizospheric bacteria belong to several phyla including: Cyanobacteria, Actinobacteria, Bacteroidetes, Firmicutes, and Proteobacteria; in addition to several bacterial genera including: *Agrobacterium*, *Arthrobacter*, *Azotobacter*, *Azospirillum*, *Bacillus*, *Burkholderia*, *Caulobacter, Chromobacterium*, *Erwinia*, *Flavobacterium*, *Micrococcus*, *Pseudomonas*, and *Serratia* (Bhattacharyya and Jha, 2012). On the other hand, dominant endophytic bacterial phyla include: Proteobacteria, Actinobacteria and to a lesser extent Bacteroidetes and Firmicutes. The most common genera of bacterial endophytes include: *Pseudomonas, Bacillus, Burkholderia, Stenotrophomonas (Xanthomonas), Micrococcus, Pantoea* and *Mycobacterium*; endophytic bacteria enter into a p lant tissue through primary and/or lateral root cracks, wounds, lenticels, and germinating radicles (Chaturvedi *et al*., 2016). Upon their entrance into a plant tissue, the endophytes may become localized at the place of entry or spread systematically throughout the plant (Glick, 2014).

Compared to the rhizospheric bacteria, endophytes have many advantages to plants as they are able to colonize the internal tissues conferring growth-promoting abilities; this is mainly attributed to the internal protective environment inside the plant compared to its surfaces (Santos *et al*., 2018). Furthermore, endophytic bacteria can utilize carbon sources and other metabolites provided by the plants compared with rhizospheric bacteria that don't have access to such resources. The localization of endophytes in special plant tissues like nodes and xylem vessels allow them to grow in low O_2 environment, which is necessary for their nitrogenase enzyme activity (Yousaf *et al*., 2017). Furthermore, the ability of endophytic bacteria to fix nitrogen by nitrogenase or to produce growth regulators inside plant tissue helps plants to survive against multiple stresses when compared with rhizospheric bacteria (Santoyo *et al*., 2016).

6. Growth-Promoting Mechanisms of PGPR under Stress Conditions

In general, PGPR are composed of a mixed group of unrelated taxa that promote plant growth under stress conditions through different mechanisms (Lugtenberg and Kamilova, 2009). Specific beneficial compounds, synthesized by PGPR, have a direct growth-promoting activity, which enhances the uptake of nutrients and minerals from the surrounding environment (Gouda *et al*., 2018); growth-promotion mechanisms involve nitrogen fixation, inorganic phosphorus mobilization, and sequestering micronutrients by siderophores' production, and modulation of the levels of phytohormones. PGPR can improve plant growth by altering plant-hormone levels; by increasing the production of auxins, cytokinins and gibberellins, or decreasing ethylene production through the activity of ACC deaminase (Glick, 2014). Such alterations in phytohormones lead to increased root length, and/or the number of root hairs that enhance the nutrient uptake by plants. Furthermore, indirect growth-promoting activities of PGPR involve control against plant pathogens by the production of inhibitory substances (Egamberdieva and Lugtenberg, 2014).

6.1. PGPR Enhance Plant Nutrients Uptake

The ability of plants to adapt to soil salinity is highly affected by their mineral nutritional status. Under saline conditions, cellular nutritional imbalance results from the effect of salinity on nutrient availability and their uptake, transport, and distribution within the plant. It may also cause physiological disorders associated with major nutrients resulting in the development of deficiency symptoms (Grattan and Grieve, 1998). Such nutritional imbalance eventually hinders plant growth and development and subsequently their yield. Soil salinity results in osmotic- pressure changes and ionic strength in stressed plants that dramatically affect the cellular processes. Stressed plants were found to require higher amounts of nutrients to reduce the adverse effects of salinity stress (Khoshgoftarmanesh *et al*., 2010). PGPR have been proven to be effective in circulating nutrients in the rhizosphere, and thereby increase their availability for plants, and subsequently reduce the need for chemical fertilizers. Under saline conditions, PGPR can increase nutrients' uptake and plant growth by different mechanisms such as atmospheric nitrogen fixation, solubilization of phosphorus, and sequestering iron by the production of siderophores (Ahemad and Kibret, 2014).

6.1.1. Biological Nitrogen Fixation

Nitrogen is an essential nutrient for plant growth and productivity. It is needed for the cellular synthesis of proteins, enzymes, chlorophyll, DNA and RNA. Although atmospheric nitrogen accounts for about 78 % of N_2, plants are unable to use it in this form. Nitrogen-fixing bacteria convert N_2 into ammonia, thus making it available for plants. Globally, the Biological Nitrogen Fixation (BNF) process accounts for approximately two-thirds of fixed nitrogen, and it is considered the most important feature in PGPR (Raymond *et al*., 2004). In this perspective, N_2-fixing PGPR can form a symbiotic relationship with plants; members of the family rhizobiaceae form symbiosis with leguminous plants (e.g. *Rhizobia*) and non-leguminous trees (e.g. *Frankia*). The non-symbiotic nitrogen-fixing PGPR group includes endophytes or free-living bacteria such as cyanobacteria (e.g. *Azospirillum spp., Azotobacter spp., Gluconacetobacter diazotrophicus* and *Azocarus*) (Riggs *et al*., 2001). In non-leguminous plants, diazotrophs can fix N_2 through the formation of a non-obligate interaction with the host plants (Glick *et al*., 1999). Strains of diazotrophic bacteria, such as *Azotobacter, Azospirillum, Bacillus* and *Paenibacillus,* have gained economic importance due to their nitrogen-fixation ability as they possess the *nif* gene cluster (Goswami *et al*., 2016). The ability of *Providencia spp.* AW4 and *Brevundimonas diminuta* AW7 strains to fix atmospheric nitrogen has been

associated with higher yields and plant height in wheat plants (Rana *et al*., 2011).

6.1.2. Phosphate Solubilization

Phosphorus (P) is a macronutrient, which is abundant in soils in both organic and inorganic forms, and is considered the second most important growth-limiting nutrient after nitrogen. However, the majority of inorganic P present in the soil is found in insoluble forms, which are not available for plants (Zaidi *et al*., 2009). Plants can absorb P in two soluble forms: the monobasic (H_2PO^{-4}) and the dibasic (HPO_2^- ions). High-salt stress results in phosphate- deficiency symptoms due to its effect on P uptake and accumulation in plant tissues. To overcome such P limitation in soils, farmers use phosphate fertilizers that are considerably expensive and environmentally undesirable. An alternative solution to overcome low P levels in soils is the use of PGPR that possess a phosphate-solubilizing activity, known as Phosphate Solubilizing Bacteria (PSB); PSB can help in providing available forms to the plants, and act as a good substitute to chemical fertilizers (Richardson *et al*., 2009). The solubilization of inorganic P results from the action of low molecular-weight organic acids synthesized by various by PSB; these organic acids decrease the pH in the soil surrounding roots, and catalyze the conversion of inorganic phosphate forms to free phosphate ready-to-use by plants (Zaidi *et al*., 2009). Many *Pseudomonas, Bacillus, Rhizobium, Burkholderia, Agrobacterium, Achromobacter Micrococcus, Aerobacter, Flavobacterium* and *Erwinia spp*. are PSB that can solubilize inorganic phosphate compounds such as tricalcium phosphate, dicalcium phosphate, hydroxyl apatite and rock phosphate (Rodríguez *et al*., 2006). Several strains of PGPR have been found to be very efficient in phosphorus-solubilization under high-saline conditions (Upadhyay *et al*., 2012).

6.1.3. Production of Siderophores

Iron is considered an essential micronutrient for plant growth and development. It is a constituent of many cellular enzymes involved in many biochemical reactions such as photosynthesis and respiration (Abbas *et al*., 2015). It is one of the most abundant minerals on earth; however, it is inaccessible for direct assimilation by plants. Under aerobic conditions, the reduced ferrous (Fe^{2+}) form is considered unstable, and is oxidized to ferric (Fe^{3+}) form, which is unstable and form insoluble ferric hydroxide that is unavailable to living organisms. Therefore, the amount of soluble Fe in the soil can hardly maintain microbial and plant growth. In saline soils, Fe availability is much lower than in non-saline conditions, which suppresses plant growth and development (Abbas *et al*., 2015). To overcome such limitation in Fe supply, PGPR secrete siderophores, small iron-binding proteins, which can bind Fe^{+3} with a very high affinity to allow its acquisition by microbial cells (Saha *et al*., 2016). The ability of PGPR to produce siderophores is considered crucial in determining the ability of PGPR to enhance plant growth and development under stress conditions (Saraf *et al*., 2014). Siderophores produced by PGPR enhance the iron uptake by plants, but the cellular mechanisms involved in providing plants with Fe are not fully understood yet (Menendez and Garcia-Fraile, 2017). Furthermore, siderophore- production by PGPR helps in the Fe uptake even in the presence of heavy metals such as nickel and cadmium (Dimkpa *et al*., 2008). It also reduces the impact of other harmful microorganisms and soil-borne pathogens such as bacteria, fungi, and nematodes (Haas and Défago, 2005).

There are many studies on the ability of PGPR producing siderophores to promote the growth of many plants, siderophores production by endophytic *Streptomyces* strains promoted the growth of *Azadirachta indica* plant (Verma *et al*., 2011). *Phyllobacterium endophyticum* PEPV15, a siderophore-producing strain, promoted the growth and quality of strawberry plants (Flores-Felix *et al*., 2015). The production of siderophores by the *Chryseobacterium sp*. strain C138 enabled the growth of tomato plants under an iron-limited supply (Radzki *et al*., 2013). Furthermore, halotolerant PGPR and siderophores produced from different bacterial species enhanced salinity tolerance in different plant species (Menendez and Garcia-Fraile, 2017).

6.2. Phytohormones and PGPR

Phytohormones are small organic molecules that play a major role in plant growth development and enable plants to tolerate different stress conditions (Shaterian *et al.* 2005). PGPR are known to produce or alter the concentrations of different plant-growth hormones such as auxin, gibberellin, cytokinins and ethylene in host plants (Kumar and Sharma, 2017). Under salinity, PGPR can alter the phytohormone status, hence modulating plant growth and development by regulating various cellular and molecular responses. They were found to alter the levels of IAA (Vessey, 2003), gibberellic acid, cytokinins and ethylene (Kaushal and Wani, 2016). The effect of IAA-producing PGPR on plants was reflected in enhanced growth and development under stress conditions (Vessey, 2003). They increased root length, root surface area and the number of root hairs that enhanced the nutrients' uptake and improved plant tolerance against different stresses (Ramos-Solano *et al*., 2008). On the other hand, PGPR modulated the levels of ethylene, an important phytohormone that accumulates under salinity and may have negative effects on plant growth and development (Goswami *et al*., 2016). Several PGPR strains have been found to ameliorate salt-stress conditions by reducing ethylene levels in stressed plant through the production of ACC deaminase, which cleaves ACC, the immediate precursor for ethylene production in plants and alleviates its inhibitory effects on plants (Glick, 2014).

6.2.1. IAA-producing PGPR

Under normal conditions, IAA is involved in root initiation, cell division, and cell enlargement. Its production is inhibited under saline conditions. The decrease in IAA levels in the roots of stressed plants results in impaired germination, plant growth and development (Pérez-Alfocea *et al*., 2010). The production of IAA is considered an important growth-prompting trait in PGPR that is commonly found in more than 80 % of the bacteria existing in the rhizosphere (Spaepen *et al*., 2007). Many PGPR expressed the ability to affect the endogenous levels of IAA and had remarkable effects on plant growth under saline conditions (Jha and Saraf, 2015). IAA produced by PGPR affects the root system by increasing

its growth, the number of lateral roots, and surface area, which subsequently leads to an increase in nutrient absorption and an improvement of plant growth and development (Ramos-Solano *et al.*, 2008).

To produce IAA, most of PGPR utilize L-tryptophan that is secreted by the roots as a precursor (Jha and Saraf, 2015). Auxin-production by PGPR is considered an important factor responsible for establishing the plant-microbe symbiotic relationship, enhancing plant growth and development and helping in alleviating adverse effects of salinity stress on plant growth (Ahmed and Hasnain, 2014). Halotolerant PGPR, capable of IAA production, enhance plant growth under salinity conditions through maintaining the auxin supply in the rhizosphere to help plant root and shoot growth under stress conditions (Albacete *et al.*, 2008). Halotolerant *Azospirillum brasilense* strain NH, associated with wheat plants, was able to produce auxin under high-salt stress of 200 mM NaCl (Nabti *et al.*, 2007). Similarly, halotolerant strains of PGPR including *Serratia plymuthica* RR2-5-10, *S. rhizophila* e-p10, *Pseudomonas fluorescens* SPB2145 and *P. chlororaphis* TSAU13 produced auxin under saline conditions, and enhanced plant tolerance to such adverse conditions (Egamberdieva, 2012). The effect of several auxin-producing PGPR strains (*Pseudomonas*; *P. aureantiaca* TSAU22, *P. extremorientalis* TSAU6 and *P. extremorientalis* TSAU20) on wheat at 100 m M NaCl level was reflected in significantly improved root and shoot (Egamberdieva and Kucharova, 2009). One *Streptomyces* isolate was able to produce IAA in the presence of salt stress and improved significantly wheat growth and development (Sadeghi *et al.*, 2012). Ramadoss *et al.* (2013) found that the inoculation of wheat with IAA-producing halotolerant PGPR ameliorated salt stress in wheat seedlings and increased the root length. Similarly, wheat plants inoculated with *Halobacillus sp.* SL3 and *Bacillus halodenitrificans* PU62 had a significant increase (90 %) in root elongation and in dry weight (17.4 % increase) at 320 mM NaCl stress compared with non-inoculated plants. In order to have a significant impact on plant growth under salinity, it is important to select PGPR with a capability to produce high levels of phytohormones under stress (Paul and Lade, 2014).

6.2.2. ACC deaminase-producing PGPR

Few PGPR were able to cleave ACC into ammonia and ketobutyrate and reduce the level of the ethylene precursor in plants under stress conditions (Glick *et al.*, 2007). Plants under stress conditions, such as salinity, drought, temperature extremes, flooding, pathogen infections, and nutritional stress, synthesize significant amounts of ethylene that have deleterious effects on plants (Bhattacharyya and Jha, 2012). As a consequence of prolonged stress, ethylene negatively affects plant growth and other cellular processes, leading to defoliation, chlorosis, reduced crop performance and senescence in plants that lead to the death of plant tissue (Bhattacharyya and Jha, 2012). ACC deaminase-producing PGPR were able to counteract the effects of the ACC hormone, and subsequently improve plant growth and development under stress conditions (Glick *et al.*, 2007). They also showed positive effects on root elongation, shoot growth, and increased the N, P, and K uptakes in various crops including wheat, tomato, rice among others under salt-stress conditions (Nadeem *et al.*, 2007; Glick, 2014; Cardinale *et al.*, 2015). Siddikee *et al.* (2010) reported that halotolerant-bacteria strains, belonging to different genera (*Bacillus, Brevibacterium, Planococcus, Zhihengliuella, Halomonas, Exiguobacterium, Oceanimonas, Corynebacterium, Arthrobacter* and *Micrococcus)* improved salinity tolerance in plants via ACC deaminase activity. PGPR with ACC deaminase- activity can hydrolyze ACC, the ethylene precursor in plants, to ammonia and α-ketobutyrate, thereby lowering the level of ethylene, improving tolerance against different stresses and subsequently promoting growth (Glick *et al.*, 2007).

6.3. PGPR and Plant Pathogens

In nature, plants are attacked by different types of pathogens including viruses, bacteria, fungi and nematodes, in addition to insects, which cause significant reduction in the yield of any given crop (Haggag *et al.*, 2015). Pathogens contribute to about a 15 % worldwide loss of global food production (Strange and Scott, 2005). Several PGPR were found to decrease or prevent the deleterious effects of pathogens on plants through the production of antibiotics and antifungal metabolites. They can also induce systemic resistance, competition with harmful microbes on invasion sites, and the sequestering of iron from the rhizosphere region (Glick *et al.*, 1999). The utilization of PGPR as a biocontrol agent seems to be a good strategy to reduce the negative impact of such pathogen on plant production (Rebib *et al.*, 2012).

7. Screening of Halotolerant PGPR from Saline Environments

The ability of PGPR, isolated from harsh environments to withstand different stresses, might indicate their abilities to improve stress tolerance in inoculated plants. Only PGPR isolated from stressful environments have the ability to withstand stress conditions, and may promote plant growth and development as they are well-adapted to such conditions (Shrivastava and Kumar, 2015). For salinity stress, most of microbial taxa that show improved tolerance for increased-salinity environments can be divided into two groups (Zahran, 1997): Halophiles which need salt for growth and are sub-classified into slight, moderate, and extreme halophiles; and the halotolerant group that includes microbes with no specific requirement for salt but may grow under normal conditions and saline conditions (up to 33% NaCl). The halotolerant group is sub-classified into slightly halotolerant, moderately halotolerant and extremely halotolerant.

The ability of halotolerant PGPR to promote growth in plants reflects their ability to deploy different cellular mechanisms and alter morphology as well as physiology to colonize roots and improve the plant tolerance to high-salt concentration (Miransari, 2017). The major salinity-tolerance mechanisms of halotolerant PGPR include: a reduced-salt uptake due to the structural properties of their membranes or cell wall, maintenance of intracellular ion hemostasis by the action ions antiporters and transporters, biosynthesis of compatible solutes such as sucrose and glycine betaine, biosynthesis of enzymes that are resilient to high levels of salt, and the production of exopolysaccharides that can form hydrating biofilms. The isolation of indigenous halotolerant PGPR from stressful

environments and the assessment of their stress tolerance mechanisms and growth-promoting traits are important to enable their use as bio-fertilizers for stressed crops (Etesami and Maheshwari, 2018).

Several genera of halotolerant PGPR with plant promoting-growth activities have been isolated from a wide range of habitats including saline soils (Shi *et al*., 2012; Ruppel *et al*., 2013). Zhu *et al.* (2011) isolated *Kushneria sp.* YCWA18, a halotolerant PGPR that can grow on media containing 20 % NaCl and was found to possess high phosphorus-solubilizing ability; Tiwari *et al.* (2011) isolated several halotolerant PGPR that were able to tolerate up to 25 % of NaCl and included different genera: *Bacillus pumilus*, *Pseudomonas mendocina*, *Arthrobacter sp.*, *Halomonas sp.*, and *Nitrinicola lacisaponensis*. These strains were found to possess different plant growth-promoting traits including P solubilization and IAA production, siderophores and ACC deaminase activities. Other examples of halotolerant PGPR isolated from the rhizosphere of different crops growing under saline conditions including *Bacillus megaterium* from maize (Marulanda *et al*., 2010); *Pseudomonas pseudoalcaligenes, P. syringae*, *P. fluorescens*, *Enterobacter aerogenes* and *Bacillus pumilus* from rice (Jha *et al*., 2011); *Azospirillum brasilense* from barley (Omar *et al*., 2009); *Pseudomonas syringae*, *P. fluorescens,* and *Enterobacter aerogenes* from maize (Nadeem *et al*., 2007). In wheat, it was reported that halotolerant PGPR isolated directly from the plants grown in a saline soil were able to increase plant growth (Egamberdieva *et al*., 2008).

8. Mitigation of Salt Stress in Wheat by PGPR

Wheat (*Triticum spp.*) is considered as one of the most important crops in the world. It is a staple food for over 35 % of the world's population where it provides more calories and proteins than any other crop. The wheat plant is a monocotyledonous plant that belongs to the Poaceae family within the Triticeae tribe that includes many domesticated cereals. The average global production of wheat was estimated at 729 million metric tons; of which, only twenty-eight million metric tons were produced from west Asia (FAOSTAT, 2015).

Wheat species show different responses to salinity stress. Bread wheat (*T. aestivum*) has moderate-tolerance responses, while durum wheat (*T. turgidum subsp. durum*) is considered salt- sensitive. This is attributed mainly to its inability to exclude Na^+ from its tissue (Roy *et al.,* 2014). The utilization of PGPR to improve plant growth and tolerance against multiple stresses is an effective and eco-friendly approach (Shrivastava and Kumar, 2015). The mitigation of the effects of salts on wheat by halotolerant PGPR at early stages can improve the chance of establishing a successful crop and improve the yield (Etesami and Beattie, 2018). Several studies (Etesami and Beattie, 2018; Etesami and Maheshwari, 2018; Shrivastava and Kumar, 2015) have been conducted in order to understand the role of halotolerant PGPR in alleviating the devastating effects of salinity and the mechanisms involved in the alleviation and promotion of growth in different plant species including wheat. Such studies have focused on the isolation of halotolerant PGPR directly from saline soils, the rhizosphere of different plants species (Siddikee *et al*., 2011; Ruppel *et al*., 2013) and from endophytic bacteria in the roots of different plant species (Bacilio *et al*., 2004). However, there have been few reports on the effects of halotolerant PGPR on durum-wheat growth under saline conditions, while most reports are related to bread wheat.

Several PGPR strains, which belong to different genera, were isolated from saline habitats and possessed growth-promoting traits which improved wheat tolerance against saline conditions (Table 1). For instance, the inoculation of wheat with four selected PGPR strains (*Pseudomonas fluorescens* 153 and 169 as well as *P. putida* 4 and 108) alleviated the negative effect of salinity on plants (Abbaspoor *et al*., 2009). Upadhyay *et al.* (2011) reported that the inoculation of wheat plants with *Bacillus subtilis* and *Arthobacter* sp. (two halotolerant PGPR) improved the growth under different salinity levels. Several PGPR strains from the genus *Pseudomonas,* that had the ACC-deaminase enzyme, improved wheat plant growth substantially under saline conditions (Egamberdieva and Kucharovaes, 2009). *Klebsiella* strains, with IAA-producing capabilities, increased root length and shoot height of inoculated wheat seedlings significantly compared with non-inoculated control (Sachdev *et al*., 2009). Ramadoss *et al.* (2013) isolated eighty-four halotolerant bacterial strains from saline habitats, from which 25 % enhanced wheat germination and seedling growth at 20 % NaCl level. Five extremely halotolerant isolates of *Bacillus* and *Hallobacillus* possessed several growth-promoting activities such as IAA production, siderophore production, ACC deaminase activity and P solubilization. Chakraborty *et al.* (2011) isolated several highly-halotolerant PGPR from which *Bacillus cereus* showed increased height, number, and length of leaves of different plants. Abbas *et al.* (2015) reported positive effects of IAA-producing PGPR on wheat under saline conditions. Wheat seeds inoculated with the siderophore-producing *P. putida* and *P. aeruginosa* had higher germination percentages, and increased shoot height, shoot and root length, chlorophyll content, spikelets weight, grain yield, and iron content (Sarode *et al*., 2013). Egamberdieva (2009) found that both IAA and ACC deaminase-producing PGPR improved wheat growth under salinity stress. The nitrogen-fixing *Pantoea agglomerans* Lma2 strain, isolated from wheat rhizosphere, was able to produce IAA, siderophores, solubilize P and was found to enhance growth in the presence of salt (Silini-Cherif *et al*., 2012). Orhan (2016) isolated eighteen indigenous halotolerant bacteria from saline soils of the East Anatolian region in Turkey; eight isolates promoted wheat growth in a hydroponic culture under high salt-stress conditions (200 mM NaCl). Pande *et al.* (2016) found that wheat plants' germination and growth under saline conditions improved when they were inoculated separately with six strains of ACC deaminase-producing PGPR.

There have been a few studies for evaluation the effects of salt-tolerant PGPR on seeds and seedling growth under salinity stress on durum wheat. The inoculation of durum wheat cultivar (*Triticum durum* var. *waha*) with *A. brasilense* NH strain, isolated from a saline soil in northern Algeria, improved the growth under salt-stress conditions (Nabti *et al.,* 2007) even under high salt stress (160 and 200 mM NaCl). *A. brasilense* NH enhanced the restoration

of complete vegetative growth and grain production compared with control plants. Similarly, the *Azotobacter chroococcum* AZ6 strain, isolated from rhizospheric soils surrounding durum-wheat plants cultivated in an arid location in Algeria, was inoculated in wheat seedling under salt stress, and the negative effects on plant growth parameters such as root length, plant height, fresh shoot and root weight and dry shoot and root weight were reduced (Silini *et al.*, 2016).

Table 1. The ability of some PGPR strains to promote growth in wheat plants

PGPR strains	PGP traits	Results of inoculation with PGPR	References
Providencia spp. AW4, *Brevundimonas diminuta* AW7	Nitrogen fixation	Increased yield and plant height	Rana *et al.* (2011)
Azotobacter chroococcum AZ6	Nitrogen fixation	Improved the growth under salt-stress conditions	Silini *et al.* (2016)
Pantoea agglomerans Lma2	Nitrogen fixation, siderophores, phosphate solubilization	Enhanced growth in the presence of salt	Silini-Cherif *et al.* (2012)
Azospirillum brasilense NH	Auxin production	Improved the growth under salt-stress conditions	Nabti *et al.* (2007)
Pseudomonas aureantiaca TSAU22, *P. extremorientalis* TSAU6 and *P. extremorientalis* TSAU20	Auxin production	Improved root and shoot growth	Egamberdieva and Kucharova, 2009
Bacillus pumilus	Auxin production, increase of phenolic and flavonoid quercetin	Increased shoot and root length and biomass	Tiwari *et al.* (2011)
Halobacillus sp. SL3 and *Bacillus halodenitrificans* PU62	Auxin production	Increased root elongation and dry weight	Ramadoss *et al.* (2013)
Klebsiella strains	Auxin production	Increased root and shoot length	Sachdev *et al.* (2009)
Pseudomonas putida and *P. aeruginosa*	Siderophore production	Increased germination percentages, shoot and root length, chlorophyll content, spikelets weight, grain yield, and iron content.	Sarode *et al.* (2013)
Bacillus subtilis and *Arthobacter sp*.	Change the activity of antioxidant enzymes	Improved growth under different salinity levels	Upadhyay *et al.* (2011)
Pseudomonas fluorescens 153, 169, *Pseudomonas putida* 108, 4	Undefined traits	Increased shoot growth and grain yield	Abbaspoor *et al.* (2009)

9. Formulation and Commercialization of PGPR

The utilization of PGPR as an agricultural practice is expected to have huge impacts on crop productivity in the near future (Glick, 2014). Recently, PGPR have been utilized commercially in various formulated products as biofertilizers and biocontrol agents (Jha and Saraf, 2015; Goswami *et al.*, 2016). Several bacterial biofertilizers are available in different forms in the market. For instance, it is possible to produce dry powders of Gram-positive spore-forming bacteria, which are known to be resistant to desiccation and heat stress (Kamilova *et al.*, 2015). Nowadays, several companies have become successful in commercializing spore-forming bacterial strains as PGPR-based biofertilizers such as *Bacillus licheniformis* SB3086 that can act as a phosphate-solubilizer strain and an effective biocontrol agent against the Dollar spot disease (Goswami *et al.*, 2016). The same strain is currently distributed as a commercial biocontrol product, known as "EcoGuard". A bioformulation of *Pseudomonas aureofaciens*, which is commercialized by "Ecosoil" (www.ecosoil.com), is currently used as a natural biocontrol agent against different fungal diseases caused by *Pythium aphanidermatum* and *Microdochium patch* (pink snow mold). The "AgBio" product is a commercial formulation of *Streptomyces griseoviridis* strain K61, which is known to inhibit fungal and bacterial diseases that cause seed, root, and stem rotting, and the wilting of different crops.

Further development in biofertilizer formulations with an improved shelf life and more efficient strains is required. Several challenges faced the developers due to the multiplicity of biotic and abiotic stresses that plants encounter during their life cycle. The variability of climatic conditions and the severity of stresses and genetic variation (crop species and cultivars) cause variabilities in the responses of these microorganisms and also disparities in the potentiality of PGPR-based biofertilizers (Kamilova *et al.*, 2015).

10. Conclusion

The rhizosphere is a dynamic environment that enables the existence of symbiotic relationship between plants and other living organism including PGPR. Such beneficial microorganisms exert numerous benefits on plant growth and development which include improved tolerance against different abiotic stresses including salinity and induced resistance against different pathogens. The present review discussed the potential use of PGPR as biostimulants to ameliorate the inhibitory effects of high salinity-stress on plant growth and development with special emphasis on wheat plants. Plant growth-promoting traits, such as nitrogen fixation, phosphate immobilization, siderophore production, are unique properties of many halotolerant PGPR that can improve nutrients' availability of stressed plants in saline soils. Furthermore, the ability of halotolerant PGPR to synthesize several phytohormones that can be utilized by plants to mitigate salinity stress conditions, and the ability of PGPR to induce resistance mechanisms were also discussed. Commercialized products that relay on PGPR are considered eco-friendly alternatives to the use of chemical fertilizers and

pesticides. New formulations and commercial products that use PGPR are expected to have a positive impact on crop productivity and yield of many crops, in addition to securing food supplies to growing populations around the globe.

References

Abbas G, Saqib M, Akhtar J and Haq MAU. 2015. Interactive effects of salinity and iron deficiency on different rice genotypes. *J Plant Nutr Soil Sci*, **178(2)**: 306-311.

Abbaspoor A, Zabihi HR, Movafegh S and Asl MHA. 2009. The efficiency of plant growth promoting rhizobacteria (PGPR) on yield and yield components of two varieties of wheat in salinity condition. *Am.*-Eurasian *J. Sustain Agri*, **3(4)** 824-829.

Abdel-Ghani AH. 2009. Response of wheat varieties from semi-arid regions of Jordan to salt stress. *J Agron Crop Sci,* **195(1)**: 55-65.

Abu-Romman S. 2016. Genotypic response to heat stress in durum wheat and the expression of small *HSP* genes. *Rend Lincei-Sci Fis*, **27(2)**: 261-267.

Ahemad M and Kibret M. 2014. Mechanisms and applications of plant growth promoting rhizobacteria: current perspective. *J King Saud Uni Sci*, **26(1)**: 1-20.

Ahmed A and Hasnain S. 2014. Auxins as one of the factors of plant growth improvement by plant growth promoting rhizobacteria. *Pol J Microbiol*, **63(3)**: 261-266.

Akhtar SS, Andersen MN and Liu F. 2015. Biochar mitigates salinity stress in potato. *J Agron Crop Sci,* **201(5)**: 368-378.

Albacete A, Ghanem ME, Martínez-Andújar C, Acosta M, Sánchez-Bravo J, Martínez V and Pérez-Alfocea F. 2008. Hormonal changes in relation to biomass partitioning and shoot growth impairment in salinized tomato (*Solanum lycopersicum* L.) plants. *J Exp Bot*, **59(15)**: 4119-4131.

Arshadullah M, Hyder SI, Mahmood IA, Sultan T and Naveed S. 2017. Mitigation of salt stress in wheat plant (*Triticum aestivum*) by plant growth promoting rhizobacteria for ACC deaminase. *Int J Adv Pharm Biol Sci*, **4(6)**: 41-46.

Azooz MM. 2009. Salt stress mitigation by seed priming with salicylic acid in two faba bean genotypes differing in salt tolerance. *Int J Agric Biol*, ***11*(4)**: 343-350.

Bacilio M, Rodriguez H, Moreno M, Hernandez JP and Bashan Y. 2004. Mitigation of salt stress in wheat seedlings by a gfp-tagged *Azospirillum lipoferum. Biol Fertil Soils*, **40(3)**: 188-193.

Bhattacharyya PN and Jha DK. 2012. Plant growth-promoting rhizobacteria (PGPR): emergence in agriculture. *World J Microbiol Biotechnol*, **28(4)**: 1327-1350.

Cardinale M, Ratering S, Suarez C, Montoya AMZ, Geissler-Plaum R and Schnell S. 2015. Paradox of plant growth promotion potential of rhizobacteria and their actual promotion effect on growth of barley (*Hordeum vulgare* L.) under salt stress. *Microbiol Res*, **181**: 22-32.

Chakraborty U, Roy S, Chakraborty AP, Dey P and Chakraborty B. 2011. Plant growth promotion and amelioration of salinity stress in crop plants by a salt-tolerant bacterium. *Recent Res Sci Technol*, **3(11)**: 61-70.

Chaturvedi H, Singh V and Gupta G. 2016. Potential of bacterial endophytes as plant growth promoting factors. *J Plant Pathol Microbiol*, **7(376)**: 1-6.

Compant S, Duffy B, Nowak J, Clément C and Barka EA. 2005. Use of plant growth-promoting bacteria for biocontrol of plant diseases: principles, mechanisms of action, and future prospects. *Appl Environ Microbiol*, **71(9)**: 4951-4959.

Dimkpa C, Svatoš A, Merten D, Büchel G and Kothe E. 2008. Hydroxamate siderophores produced by *Streptomyces acidiscabies* E13 bind nickel and promote growth in cowpea (*Vigna unguiculata* L.) under nickel stress. *Can J Microbiol*, **54(3)**: 163-172.

Egamberdieva D and Lugtenberg B. 2014. Use of plant growth-promoting rhizobacteria to alleviate salinity stress in plants. PGPR to alleviate salinity stress on plant growth**.** In: Miransari M (Ed.), **Use of Microbes for the Alleviation of Soil Stresses**, Springer, New York, pp. 73–96.

Egamberdieva D, Kamilova F, Validov S, Gafurova L, Kucharova Z and Lugtenberg B. 2008. High incidence of plant growth-stimulating bacteria associated with the rhizosphere of wheat grown on salinated soil in Uzbekistan. *Environ Microbiol*, **10(1)**:1-9.

Egamberdieva D. 2009. Alleviation of salt stress by plant growth regulators and IAA producing bacteria in wheat. *Acta Physiol Plant*, **31(4)**: 861-864.

Egamberdieva, D and Kucharova Z. 2009. Selection for root colonising bacteria stimulating wheat growth in saline soils. *Biol Fertil Soils,* **45:** 563-571.

Egamberdieva D. 2012. *Pseudomonas chlororaphis*: a salt tolerant bacterial inoculant for plant growth stimulation under saline soil conditions. *Acta Physiol Plant*, **34**: 751–756.

Etesami H and Maheshwari DK. 2018. Use of plant growth promoting rhizobacteria (PGPRs) with multiple plant growth promoting traits in stress agriculture: Action mechanisms and future prospects. *Ecotoxicol Environ Saf*, **156**: 225-246.

Etesami H. Beattie GA. 2018. Mining halophytes for plant growth-promoting halotolerant bacteria to enhance the salinity tolerance of non-halophytic crops. *Front Microbiol*, **9(148)**: 1-20

FAOSTAT. 2015. Food and agriculture organization of the United Nations, Rome (www.fao.org).

FAOSTAT. 2017. Food and agriculture organization of the United Nations, Rome (www.fao.org).

Flores-Felix JD, Silva LR and Rivera LP. 2015. Plants probiotics as a tool to produce highly functional fruits: the case of Phyllobacterium and vitamin C in strawberries. *PLoS One*, **10(4)**: e0122281.

Glick BR, Cheng Z, Czarny J and Duan J. 2007. Promotion of plant growth by ACC deaminase-producing soil bacteria. *Eur J Plant Pathol*, **119:** 329-339

Glick BR, Patten CL, Holguin G and Penrose DM. 1999. **Biochemical and Genetic Mechanisms Used by Plant Growth Promoting Bacteria**. Imperial College Press, London, UK.

Glick BR. 2014. Bacteria with ACC deaminase can promote plant growth and help to feed the world. *Microbiol Res*, **169(1)**: 30-39.

Goswami D, Thakker JN and Dhandhukia PC. 2016. Portraying mechanics of plant growth promoting rhizobacteria (PGPR): **A review**. *Cogent Food Agric*, **2(1):** 1-19.

Gouda S, Kerry RG, Das G, Paramithiotis S, Shin HS and Patra JK. 2018. Revitalization of plant growth promoting rhizobacteria for sustainable development in agriculture. *Microbiol Res*, **206**: 131-140.

Grattan SR and Grieve CM. 1998. Salinity–mineral nutrient relations in horticultural crops. *Sci Hortic*, **78(1-4)**: 127-157.

Gupta B and Huang B. 2014. Mechanism of salinity tolerance in plants: physiological, biochemical, and molecular characterization. *Int J Genomics*, 2014: 1-18.

Haas D and Défago G. 2005. Biological control of soil-borne pathogens by fluorescent pseudomonads. *Nat Rev Microbiol,* **3(4)**: 307.

Haggag WM, Abouziena HF, Abd-El-Kreem F and El Habbasha S. 2015. Agriculture biotechnology for management of multiple biotic and abiotic environmental stress in crops. *J Chem Pharm Res*, **7(10)**: 882-889.

Hasanuzzaman M, Nahar K, Rahman A, Anee TI, Alam MU, Bhuiyan TF, Oku H and Fujita M. 2017. Approaches to enhance salt stress tolerance in wheat. In: Wanyera R and Owuoche J (Eds.). **Wheat Improvement, Management and Utilization**. InTech.

Jaradat AA. 1992. Breeding potential of durum wheat landraces from Jordan: Differential responses to drought. *Hereditas*, **116(3)**: (305-309).

Jha CK and Saraf M.2015. Plant growth promoting rhizobacteria (PGPR): A review. *J Agril Res Dev*, **5(2)**: 108-119.

Jha Y, Subramanian RB and Patel S. 2011. Combination of endophytic and rhizospheric plant growth promoting rhizobacteria in *Oryza sativa* shows higher accumulation of osmoprotectant against saline stress. *Acta Physiol Plant*, **33(3)**: 797-802.

Kabbaj H, Sall AT, Al-Abdallat A, Geleta M, Amri A, Filali-Maltouf A, Belkadi B, Ortiz R and Bassi FM. 2017. Genetic diversity within a global panel of durum wheat (*Triticum durum*) landraces and modern germplasm reveals the history of alleles exchange. *Front Plant Sci*, **8**: 1277.

Kamilova F, Okon Y, de Weert S and Hora K. 2015. Commercialization of microbes: Manufacturing, inoculation, best practice for objective field testing, and registration. In: Lugtenberg B. (Ed.), **Principles of plant-microbe interactions**. Springer, pp. 319–327.

Katerji N, Mastrorilli M, Van Hoorn JW, Lahmer FZ, Hamdy A and Oweis T. 2 009. Durum wheat and barley productivity in saline–drought environments. *Eur J Agron*, **31(1):** 1-9.

Katiyar D, Hemantaranjan A and Singh B. 2016. Plant growth promoting rhizobacteria-an efficient tool for agriculture promotion. *Adv Plants Agri Res*, **4(6)**: 00163.

Kaushal M and Wani SP. 2016. Plant-growth-promoting rhizobacteria: drought stress alleviators to ameliorate crop production in drylands. *Annu Microbiol*, **66(1)**: 35-42.

Key S, Ma JK and Drake PM. 2008. Genetically modified plants and human health. *J Royal Soc Med*, **101(6)**: 290-298.

Khoshgoftarmanesh AH, Schulin R, Chaney RL, , Daneshbakhsh B and Afyuni M. 2010. Micronutrient-efficient genotypes for crop yield and nutritional quality in sustainable agriculture. A review. *Agron Sustain Dev,* **30**: 83-107.

Kumar V and Sharma N. 2017. Plant Growth Promoting Rhizobacteria as Growth Promoters for Wheat: **A review**. *Agri Res Tech*, **12(4)**: 555857.

Lugtenberg B and Kamilova F. 2009. Plant-growth-promoting rhizobacteria. *Annu Rev Microbiol*, **63**: 541-556.

Marulanda A, Azcón R, Chaumont F, Ruiz-Lozano JM and Aroca R. 2010. Regulation of plasma membrane aquaporins by inoculation with a *Bacillus megaterium* strain in maize (*Zea mays* L.) plants under unstressed and salt-stressed conditions. *Planta*, **232(2)**: 533-543.

Menendez E and Garcia-Fraile P. 2017. Plant probiotic bacteria: solutions to feed the world. *AIMS Microbiol*, **3(3)**: 502-524.

Miransari M. 2017. The interactions of soil microbes affecting stress alleviation in agroecosystems. In: Kumar V, Kumar M, Sharma S and Prasad R (Eds.), **Probiotics in Agroecosystem**. Springer, Singapore, pp. 31-50.

Mohan V, Devi K, Anushya A, Revathy G, Kuzhalvaimozhi G and Vijayalakshmi K. 2017. Screening of salt tolerant and growth promotion efficacy of phosphate solubilizing bacteria. *J Acad Ind Res*, **5**: 168-172.

Munns R and Tester M. 2008. Mechanisms of salinity tolerance. *Annu Rev Plant Biol*, **59:** 651-681.

Nabti E, Sahnoune M, Adjrad S, Van Dommelen A, Ghoul M, Schmid M and Hartmann A. 2007. A halophilic and osmotolerant *Azospirillum brasilense* strain from Algerian soil restores wheat growth under saline conditions. *Eng Life Sci*, **7(4)**: 354-360.

Nadeem SM, Zahir ZA, Naveed M and Arshad M. 2007. Preliminary investigations on inducing salt tolerance in maize through inoculation with rhizobacteria containing ACC-deaminase activity. *Can J Microbiol*, **53:** 1141-1149.

Numana M, Bashir S, Khan Y, Mumtaz R, Shinwari ZK, Khan AL, and Ahmed AH. 2018. Plant growth promoting bacteria as an alternative strategy for salt tolerance in plants: A review. *Microbiol Res*, **209**: 21-32.

Omar A, Osman H, Kasim A and El-Daim IA. 2009. Improvement of salt tolerance mechanisms of barley cultivated under salt stress using *Azospirillum brasilense*. In: Ashraf M, Ozturk M and Athar H (Eds.), **Salinity and water stress**. Springer, Dordrecht, pp. 133-147

Orhan F. 2016. Alleviation of salt stress by halotolerant and halophilic plant growth-promoting bacteria in wheat (*Triticum aestivum*). *Braz J Microbiol* **47(3)**: 621-627.

Pande AM, Kulkarni NS and Bodhankar MG. 2016. Effect of PGPR with ACC-deaminase activity on growth performance of wheat cultivated under stress conditions. *Inter J App Res*, **2(1):** 723-726.

Paul D and Lade H. 2014. Plant-growth-promoting rhizobacteria to improve crop growth in saline soils: **A review**. *Agron Sustain Dev*, **34(4):** 737-752.

Pérez-Alfocea F, Albacete A, Ghanem ME and Dodd IC. 2010. Hormonal regulation of source–sink relations to maintain crop productivity under salinity: a case study of root-to-shoot signalling in tomato. *Funct Plant Biol*, **37(7)**: 592-603.

Radzki W, Mañero FG, Algar E, García JL, García-Villaraco A and Solano BR. 2013. Bacterial siderophores efficiently provide iron to iron-starved tomato plants in hydroponics culture. *Antonie Van Leeuwenhoek*, **104(3)**: 321-330.

Ramadoss D, Lakkineni VK, Bose P, Ali S and Annapurna K. 2013. Mitigation of salt stress in wheat seedlings by halotolerant bacteria isolated from saline habitats. *Springer Plus*, **2(1)**: 6.

Ramos-Solano B, BarriusoMaicas J, Pereyra De La Iglesia MT, Domenech J and Gutiérrez Mañero FJ. 2008. Systemic disease protection elicited by plant growth promoting rhizobacteria strains: relationship between metabolic responses, systemic disease protection, and biotic elicitors. *Phytopathology*, **98(4)**: 451-457.

Rana A, Saharan B, Joshi M, Prasanna R, Kumar K and Nain L. 2011. Identification of multi-trait PGPR isolates and evaluating their potential as inoculants for wheat. *Ann Microbiol*, **61(4):** 893-900.

Rasool S, Hameed A, Azooz M, Siddiqi T and Ahmad P. 2013. Salt Stress: Causes, Types and Responses of Plants. In: Ahmad P, Azooz M and Prasad MNV (Eds.), **Ecophysiology and Responses of Plants under Salt Stress**. Springer, pp. 1–24.

Raymond J, Siefert JL, Staples CR and Blankenship RE. 2004. The natural history of nitrogen fixation. *Mol Biol Evol*, **21**: 541–554.

Rebib H, Hedi A, Rousset M, Boudabous A, Limam F and Sadfi-Zouaoui N. 2012. Biological control of *Fusarium* foot rot of wheat using fengycin-producing *Bacillus subtilis* isolated from salty soil. *Afr J Biotechnol*, **11(34)**: 8464-8475.

Richardson AE, Hocking PJ, Simpson RJ and George TS. 2009. Plant mechanisms to optimise access to soil phosphorus. *Crop Pasture Sci*, **60**:124–143.

Riggs PJ, Chelius MK, Iniguez AL, Kaeppler SM and Triplett EW. 2001. Enhanced maize productivity by inoculation with diazotrophic bacteria. *Funct Plant Biol*, **28(9)**: 829-836.

Rodríguez H, Fraga R, Gonzalez T and Bashan Y. 2006. Genetics of phosphate solubilization and its potential applications for improving plant growth-promoting bacteria. *Plant Soil*, **287(1-2)**: 15-21.

Roychoudhury A, Basu S, and Sengupta D N. 2011. Amelioration of salinity stress by exogenously applied spermidine or spermine in three varieties of indica rice differing in their level of salt tolerance. *Plant Physiol*, **168(4):** 317-328.

Roy SJ, Negrão S and Tester M. 2014. Salt resistant crop plants. *Curr Opin Biotechnol*, **26**: 115-124.

Ruppel S, Franken P and Witzel K. 2013. Properties of the halophyte microbiome and their implications for plant salt tolerance. *Funct Plant Biol*, **40(9)**: 940-951.

Sachdev DP, Chaudhari HG, Kasture VM, Dhavale DD and Chopade BA. 2009. Isolation and characterization of indole acetic acid (IAA) producing *Klebsiella pneumoniae* strains from rhizosphere of wheat (*Triticum aestivum*) and their effect on plant growth. *Indian J Exp Biol*, **47(12)**: 993.

Sadeghi A, Karimi E, Dahazi PA, Javid MG, Dalvand Y and Askari H. 2012. Plant growth promoting activity of an auxin and siderophore producing isolate of Streptomyces under saline soil condition. *World J Microbiol Biotechnol*, **28**:1503–1509.

Saha M, Sarkar S, Sarkar B, Sharma BK, Bhattacharjee S and Tribedi P. 2016. Microbial siderophores and their potential applications: a review. *Environ Sci Pollut Res*, **23(5)**: 3984-3999.

Sairam RK and Tyagi A. 2004. Physiology and molecular biology of salinity stress tolerance in plants. *Curr Sci*, **86:** 407–421.

Santos MLD, Berlitz DL, Wiest SLF, Schünemann R, Knaak N and Fiuza LM. 2018. Benefits Associated with the Interaction of Endophytic Bacteria and Plants. *Braz Arch Biol Technol*, **61**: 1-11.

Santoyo G, Moreno-Hagelsieb G, Del Carmen Orozco-Mosqueda M and Glick BR. 2016. Plant growth-promoting bacterial endophytes. *Microbiol Res*, **183**: 92-99.

Saraf M, Pandya U and Thakkar A. 2014. Role of allelochemicals in plant growth promoting rhizobacteria for biocontrol of phytopathogens. *Microbiol Res*, **169(1)**: 18-29.

Sarode P, Rane M, Kadam M and Chincholkar S. 2013. Role of Microbial Siderophores in Improving Crop Productivity in Wheat. In: In: Maheshwari D, Saraf M and Aeron A (Eds), **Bacteria in Agrobiology: Crop Productivity**. Springer, Berlin, Heidelberg, pp. 287–308.

Shaterian J, Waterer D, De Jong H and Tanino KK. 2005. Differential stress responses to NaCl salt application in early-and late-maturing diploid potato (*Solanum* sp.) clones. *Environ Exper Bot*, **54(3)**: 202-212.

Shi W, Takano T and Liu S. 2012. *Anditalea andensis* gen. nov., sp. nov., an alkaliphilic, halotolerant bacterium isolated from extreme alkali–saline soil. *Antonie van Leeuwenhoek*, **102**(4): 703-710.

Shrivastava P and Kumar R. 2015. Soil salinity: a s erious environmental issue and plant growth promoting bacteria as one of the tools for its alleviation. *Saudi J Biol Sci*, **22(2):** 123-131.

Siddikee MA, Chauhan PS, Anandham R, Han GH and Sa T. 2010. Isolation, characterization, and use for plant growth promotion under salt stress, of ACC deaminase-producing halotolerant bacteria derived from coastal soil. *World J Microbiol Biotechnol*, **20(11)**: 1577-1584.

Silini A, Cherif-Silini H and Yahiaoui B. 2016. Growing varieties durum wheat (*Triticum durum*) in response to the effect of osmolytes and inoculation by *Azotobacter chroococcum* under salt stress. *Afr J Microbiol Res*, **10(12)**: 387-399.

Silini-Cherif H, Silini A, Ghoul M and Yadav S. 2012. Isolation and characterization of plant growth promoting traits of a rhizobacteria: *Pantoea agglomerans* lma2. *Pak J Biol Sci*, **15(6)**: 267.

Spaepen S, Vanderleyden J and Remans R. 2007. Indole-3-acetic acid in microbial and microorganism-plant signaling. *FEMS Microbiol Rev*., **31(4)**: 425-448.

Strange RN and Scott PR. 2005. Plant disease: a threat to global food security. *Annu Rev Phytopathol*., **43**: 83-116.

Tiwari S, Singh P, Tiwari R, Meena KK, Yandigeri M, Singh DP and Arora DK. 2011. Salt-tolerant rhizobacteria-mediated induced tolerance in wheat (*Triticum aestivum*) and chemical diversity in rhizosphere enhance plant growth. *Biol. Fert Soil,* **47(8)**: 907.

Upadhyay SK, Maurya SK and Singh DP. 2012. Salinity tolerance in free living plant growth promoting rhizobacteria. *Int J Sci Res*, **3(2)**: 73-78.

Upadhyay SK, Singh JS, Saxena AK and Singh DP. 2011. Impact of PGPR inoculation on growth and antioxidant status of wheat under saline conditions. *Plant Biol*, **14(4)**: 605-611.

Vessey JK. 2003. Plant growth promoting rhizobacteria as biofertilizers. *Plant soil*, **255(2):** 571-586.

Verma VC, Singh SK and Prakash S. 2011. Bio-control and plant growth promotion potential of siderophore producing endophytic Streptomyces from *Azadirachta indica* A. Juss. *J Basic Microbial,* **51(5):** 550-556.

Weide A. 2015. On the identification of domesticated emmer wheat, *Triticum turgidum* subsp. *dicoccum* (Poaceae), in the Aceramic Neolithic of the Fertile Crescent. *Arch Inf*, **38(1)**: 381-424.

Yousaf M, Rehman Y and Hasnain S. 2017. High-yielding wheat varieties harbour superior plant growth promoting-bacterial endophytes. *Appl Food Biotech*, **4(3)**: 143-154.

Zahran HH. 1997. Diversity, adaptation and activity of the bacterial flora in saline environments. *Biol Fertil Soils*, **25(3)**: 211-223.

Zaidi A, Khan MS, Ahemad M and Oves M. 2009. Plant growth promotion by phosphate solubilizing bacteria. *Acta Microbiol Immunol Hung*, **56**: 263–284.

Zhu F, Qu L, Hong X and Sun X. 2011. I solation and characterization of a phosphate-solubilizing halophilic bacterium *Kushneria* sp. YCWA18 from Daqiao Saltern on the coast of Yellow Sea of China. *Evid Based Complementary Altern Med*, **2011**; 1-6.

JJBS

Volume 12, Number 5,December 2019
ISSN 1995-6673
Pages 535 - 541

Jordan Journal of Biological Sciences

Evaluation of *Pseudomonas fluorescens* Extracts as Biocontrol Agents Against some Foodborne Microorganisms

Diaa A. Marrez*, Gomaa N. Abdel-Rahman and Salah H. Salem

Food Toxicology and Contaminants Department, National Research Centre, Dokki, Cairo, P.O. Box: 12622, Egypt

Received December 18, 2018; Revised February 10, 2019; Accepted February 16, 2019

Abstract

Foodborne pathogens are among the serious problems in food industries. To control food spoilage microorganisms, five strains of *Pseudomonas fluorescens* were used as biocontrol agents against foodborne pathogenic bacteria and mycotoxigenic fungi. The antimicrobial activity of the *P. fluorescens* cell-free supernatants and their fractions were evaluated against six strains of foodborne pathogenic bacteria and five strains of toxigenic fungi. The bioactive fractions were identified using Gas Chromatography-Mass Spectroscopy (GC-MS). All cell- free supernatants of the *P. fluorescens* strains showed antibacterial activity against all tested bacteria with an inhibition zone ranging between 7.8 and 15.2 mm. While, only *P. fluorescens* FP10 exhibited antifungal activity against all tested fungi with a maximum inhibition zone of 19.3 mm, against *Aspergillus steynii*. The chloroform fractions of *P. fluorescens* FP6, FP7 and FP10 showed high activity against the tested pathogenic bacteria and toxigenic fungi. The GC-MS analysis of chloroform fractions of these strains showed the presence of two pyrrol compounds in all fractions as major compounds, Pyrrolo[1,2-a] pyrazine-1,4-dione, hexahydro-3-(2-methylpropyl)- and Pyrrolo[1,2-a] pyrazine-1,4-dione, hexahydro-3-(propylmethyl). The present study maintains that *P. fluorescens* cell-free supernatants and chloroform fractions would be ideal for application in food industry as biocontrol agents against foodborne pathogens.

Keywords: *Pseudomonas fluorescens*, Foodborne pathogens, Biocontrol, Mycotoxigenic fungi.

1. Introduction

Foodborne pathogens are among the major threats to food safety. Most foodborne illnesses occur by infections with pathogenic microbes that have contaminated the food chain at one or more points from farm to fork (Feltes *et al*., 2017). In addition, foodborne illnesses can be also caused by microbial toxins that contaminate food (Addis and Sisay, 2015). Mycotoxins are produced by certain fungal species as secondary metabolites that grow on several foods, including cereals, nuts and dried fruits. A variety of fungal species mostly from the genera *Aspergillus*, *Penicillium*, *Fusarium* and *Alternaria* are known to produce mycotoxins. Most important mycotoxins are aflatoxins, ochratoxin, fumonisins, deoxynivalenol, trichothecenes, zearalenone, and patulin (Karlovsky *et al*., 2016). Some strains of foodborne pathogenic bacteria including *Bacillus cereus*, *Staphylococcus aureus* and *Clostridium botulinum* produce toxins in food causing different symptoms ranging from vomiting in the case of the *S. aureus* toxin to high-risk neurological symptoms in the case of the botulinum toxin (Schirone *et al*., 2017).

Cooking and chilling are the major control measures to eliminate the foodborne microbes. Most foodborne diseases can be controlled by avoiding cross-contamination. This can be achieved by applying Good Manufacturing Practices (GMP) and Good Hygienic Practices (GHP) such as storing raw and cooked food separately and washing hands before and after touching raw food materials. Such food hygiene practices must be adhered to during production, storage, transportation and preparation of food, to minimize the growth and spread of pathogens (Malhotra *et al*., 2015). There are various methods that can be used to preserve food, including conventional methods such as drying, heating, freezing, fermentation, salting and modern preservation technology including biopreservative and active antimicrobial packaging systems (Sung *et al*., 2013; Darwesh *et al*., 2018).

Food biopreservation refers to the use of microorganisms or their metabolites to inhibit or destroy the undesirable microorganisms in foods to improve the microbiological safety and extend the shelf life of foods. Several studies have reported that use of microorganisms, such as bacteria, yeast, fungi, actinomycetes and algae and their antimicrobial metabolites as biopreservative substances (Marrez and Sultan, 2016; Sultan *et al*., 2016; Marrez *et al*., 2017). Some bacterial strains are able to produce antagonistic substances used as antimicrobial and biocontrol agents against microorganisms in food. In this respect, *Pseudomonas* spp. is one of the most considerable species used in the biocontrol of foodborne pathogenic bacteria and mycotoxigenic fungi (Sabry *et al*., 2016). *P. fluorescens* shows antagonistic effects against some toxigenic fungi such as *A. flavus, A. niger, P. italicum*, *P. simplicissmum* and *Fusarium* sp. (Srivastava and Shalini, 2008; Mushtaq *et al*., 2010). Moreover, it produces antibacterial agents against foodborne pathogenic bacteria *Staphylococcus aureus*, *Klebsiella pneumoniae* and *Proteus mirabilis* (Kadhim, 2015). The main objective of

* Corresponding author e-mail: diaamm80@hotmail.com.

this study is to evaluate the antagonistic potential of some *P. fluorescens* strains against foodborne pathogenic microorganisms. Furthermore, it aims at identifying the bioactive compounds of the most active fractions against foodborne pathogens using GC-MS.

2. Materials and Methods

2.1. Origin of the Bacterial Isolates

Five *Pseudomonas fluorescens* strains (FP3, FP4, FP6, FP7 and FP10) were obtained from Hydrobiology Department, Veterinary Division, National Research Centre, Egypt. These strains were maintained on tryptic soya agar (TSA) with 10 % glycerol and stored at -80°C.

2.2. Preparation of Bacterial Culture Filtrate

From the glycerol stock, fresh cultures were prepared on plates of TSA. A single colony of each bacterial strain was inoculated and grown in a tryptic soya broth (TSB) with constant shaking at 150 rpm for forty-eight hours at 35±2°C. The culture was centrifuged at 6,000 rpm for ten minutes to separate the bacterial cells. The supernatant was centrifuged again at 10,000 rpm for ten minutes at 4°C and passed through a bacteriological filter (0.45 µm). The cell-free supernatant was used to assess its antimicrobial activity against foodborne pathogenic bacteria and mycotoxigenic fungi (Nandakumar *et al*., 2002).

2.3. Extraction of Secondary Metabolites

The cell-free supernatants of *P. fluorescens* strains were extracted three times with equal volumes of ethyl acetate, diethyl ether, butanol, chloroform and hexane at room temperature. Each organic phase was combined and evaporated to dryness at 40°C using a rotary evaporator. The obtained crude extracts were evaluated for their antimicrobial activity.

2.4. Antimicrobial Assay

2.4.1. Test Microorganisms

The antimicrobial activity of the cell-free supernatants of the *P. fluorescens* strains and their fractions were assayed against six species of pathogenic bacteria, two Gram-positive bacteria (*Bacillus cereus* EMCC 1080 and *Staphylococcus aureus* ATCC 13565) and four Gram-negative bacteria (*Salmonella typhi* ATCC 25566, *Escherichia coli* 0157 H7 ATCC 51659, *Pseudomonas aeruginosa* NRRL B-272 and *Klebsiella pneumoniae* LMD 7726). Five fungal species were used for antifungal assay, *Aspergillus flavus* NRRL 3357, *A. parasiticus* SSWT 2999, *A. westerdijikia* CCT 6795, *A. steynii* IBT LKN 23096, and *A. carbonarius* ITAL 204.

2.4.2. Well Diffusion Method

The antimicrobial activity of the cell-free supernatants of *P. fluorescens* strains against the tested bacteria and fungi was evaluated using the well diffusion technique described by Kheiralla *et al*. (2016). A suspension was prepared from each culture of the bacterial and fungal strains and adjusted by turbidimetry to a 0.5 McFarland standard. Using cotton swabs, nutrient agar plates were uniformly inoculated with TSB of bacterial cultures and potato dextrose agar (PDA) medium were inoculated with 50 µL of each fungal culture and uniformly spread using a sterile L-glass rod. A sterilized glass Pasteur pipette was used to make wells of 5 mm in diameter on the agar. Fifty µL of each strain cell-free supernatant were placed individually into each well. Fifty µL of tetracycline (500 µg mL^{-1}) were used as the antibacterial positive control and 50 µL of nystatin (1000 U mL^{-1}) were used as antifungal positive control. The dishes were immediately incubated at 37°C/24 h for bacteria and at 25°C/48 h for fungi. After incubation, the zones of inhibition were measured. The results' average was calculated from at least three replicates for each assay (Emam *et al*., 2018).

2.4.3. Disc Diffusion Method

From the twenty-four-hour incubated nutrient agar slant of each bacterial species, a loop full of the microorganism was inoculated in a tube containing 5 mL of tryptic soy broth. The broth culture was incubated at 35°C for two-six hours until it achieved the turbidity of 0.5 McFarland standard. The activity of the fractions of the *P. fluorescens* strains were examined against all the tested bacterial species using the disc diffusion method of Kirby-Bauer technique (Bauer *et al*., 1966). Using cotton swabs, nutrient agar plates were uniformly inoculated with the tryptic soy broth of the bacterial cultures. A concentration of 10 mg mL^{-1} for each fraction was prepared by dissolving 10 mg in 1 mL of dimethyl sulfoxide (DMSO). Sterilized discs (6 mm) from Whatman No. 1 filter paper were loaded by each fraction and dried completely under sterile conditions. The discs were placed on the seeded plates by using a sterile forceps. The DMSO and tetracycline (500 µg mL^{-1}) represented the negative control and positive control, respectively. Inoculated plates were incubated at 37°C for twenty-four hours, and then the inhibition zones were measured and expressed as the diameter of the inhibition zone including the diameter of the paper disc.

The fungal strains were plated onto Potato Dextrose Agar (PDA) and incubated for five days at 25°C. The spore suspension (2×10^8 CFU mL^{-1}) of each fungus was prepared in a 0.01 % tween 80 solution compared with the 0.5 McFarland standard. Petri dishes containing a PDA medium were inoculated with 50 µL of each fungal culture and uniformly spread using sterile L-glass rod. Sterilized discs (6 mm) were loaded by each fraction (10 mg mL^{-1}) and dried completely under sterile conditions, then were placed on the seeded plates by using a sterile forceps. The DMSO and commercial fungicide nystatin (1000 U mL^{-1}) were considered as a negative and positive control, respectively. The inoculated plates were incubated at 25°C for 48 hours, and then the antifungal activity was assessed by measuring the zone of inhibition (Medeiros *et al*., 2011). The results average was calculated from at least three replicates for each assay.

2.5. GC-MS Analysis

The GC/MS analysis was performed using a Thermo Scientific, Trace GC Ultra / ISQ Single Quadrupole MS, TG-5MS fused silica capillary column (30m, 0.251mm, 0.1 mm film thickness). For the GC/MS detection, an electron ionization system with ionization energy of 70 eV was used; Helium gas was used as the carrier gas at a constant flow rate of 1ml min^{-1}. The injector and MS transfer line temperature was set at 280°C.

The oven temperature was programmed at an initial temperature of 50°C (hold 2 min) to150°C at an increasing

rate of 7°C min^{-1}. then to 270°C at an increasing rate of 5°C min^{-1} (hold 2min) then to 310°C as a final temperature at an increasing rate of 3.5°C min^{-1} (hold 10 min). The quantification of all of the identified components was investigated using a r elative peak area percentage. A tentative identification of the compounds was performed based on the comparison of their relative retention time and mass spectra with those of the NIST, WILLY library data of the GC/MS system.

2.6. Statistical Analysis

Results were subjected to one-way analysis of variance (ANOVA) of the general liner model (GLM) using SAS (1999) statistical package. The results were the average of three replicates ($p \leq 0.05$).

3. Results and Discussion

3.1. Antimicrobial Activity of P. fluorescens Cell-Free Supernatant

Five strains of *Pseudomonas fluorescens* (FP3, FP4, FP6, FP7 and FP10) were screened for the antimicrobial activity of their cell-free supernatants against six species of foodborne pathogenic bacteria and five species of mycotoxigenic fungi as shown in Table 1. The cell-free supernatants of all five strains showed antibacterial activity against both gram positive and gram negative bacteria. The zone of inhibition ranged from 7.8 to 15.2 mm. the highest antibacterial activity was recorded by the supernatant of FP6 followed by FP3 against *S. aureus* with inhibition zones 15.2 and 15.0 mm, respectively.

The results in Table 2 reveal that the cell-free supernatant of *P. fluorescens* FP10 produced antifungal substances which inhibited the growth of all tested fungi, followed by FP6 and FP7 which inhibited the growth of all tested fungi except *A. flavus* and *A. parasiticus*, respectively. The highest antifungal activity was recorded by FP7 against *A. westrdijikia* with an inhibition zone of 22.0 mm.

The inhibitory activity of *Pseudomonas* spp. against foodborne pathogenic bacteria and fungi has been previously demonstrated. Freedman *et al*. (1989) reported that *P. aeruginosa, P. putida, P. tapaci* and *P. fiuorescens* showed antibacterial activity against *S. typhimurium* and *S. aureus*. Charyulu *et al*. (2009) found that *P. fluorescens* had antibacterial activity against *Salmonella typhi, Streptococcus mutans, Bacillus subtilis,* and *Shigella sonnei*. Also, Rekha *et al*. (2010) screened the antibacterial activity of *P. fluorescens* against ten pathogenic bacteria and the results indicated that *P. fluorescens* had a s ignificant value against *Salmonella typhi, S. sonnei*, *Streptococcus mutans* and *Bacillus subtilis,* but no activity was observed against *Staphylococcus aureus, Aeromonas hydrophila, V. cholerae, Escherichia coli, K. pneumoniae* and *Serratia marcescens.* Sharma and Kaur (2010) indicated that all of the cultures of the cell-free supernatants from *Pseudomonas* isolates inhibited the growth of *B. subtilis, B. cereus* and *Xanthomonas* sp. as well as human pathogens such as *Salmonella typhi, Shigella* sp. *Klebsiella* sp., *E. coli,* and *Staphylococcus* sp.

Table 1. Antibacterial activity of the cell-free supernatants of *P. fluorescens* strains against some foodborne pathogenic bacteria.

Bacteria	Inhibition zone (mm) (Mean ± S.E)					
	Positive control	FP3	FP4	FP6	FP7	FP10
B. cereus	27.0±1.32^{a}	13.5±1.80^{d}	11.2±1.04^{e}	13.8±1.25^{c}	14.5±0.50^{b}	14.0±2.29^{bc}
S. aureus	26.3±1.04^{a}	15.0±1.80^{bc}	10.5±1.00^{e}	15.2±0.76^{b}	11.5±2.29^{d}	14.8±0.76^{c}
E. coli	26.2±1.04^{a}	14.3±2.93^{b}	12.5±2.29^{d}	11.5±2.29^{e}	13.3±0.76^{c}	12.8±1.25^{c}
S. typhi	24.8±1.61^{a}	10.8±1.60^{e}	12.7±1.89^{c}	11.3±2.08^{d}	13.3±1.04^{b}	12.8±1.25^{bc}
P. aeruginosa	22.5±0.50^{a}	8.0±0.50^{cd}	7.8±0.76^{d}	8.2±0.28^{c}	9.2±0.28^{b}	9.5±1.32^{b}
K. pneumoniae	25.3±1.25^{a}	11.7±2.02^{c}	11.2±1.25^{d}	11.3±2.25^{d}	12.8±1.04^{b}	13.0±2.18^{b}

Means followed by different subscripts within row are significantly different at the 5% level, (n= 3), S.E: standard error, Positive control: tetracycline.

Table 2. Antifungal activity of the cell-free supernatants of *P. fluorescens* strains against some mycotoxigenic fungi.

Fungi	Inhibition zone (mm) (Mean ± S.E)					
	Positive control	FP3	FP4	FP6	FP7	FP10
A. flavus	28.3±0.76^{a}	0	0	0	16.7±0.76^{b}	13.8±2.25^{c}
A. carbonarius	27.2±1.25^{a}	18.3±3.55^{c}	0	14.2±1.04^{e}	21.2±0.76^{b}	15.8±1.60^{d}
A. steynii	29.5±1.32^{a}	10.8±0.76^{d}	0	18.5±0.50^{c}	18.7±3.68b^{c}	19.3±2.92^{b}
A. parasiticus	25.8±1.90^{a}	14.8±2.02^{c}	17.5±1.27^{b}	9.33±0.58^{d}	0	17.8±1.25^{b}
A. westrdijikia	29.2±1.26^{a}	21.2±1.25^{b}	16.0±0.50^{e}	18.2±1.75^{d}	22.0±0.50^{b}	19.2±1.04^{c}

Means followed by different subscripts within row are significantly different at the 5% level, (n= 3), S.E: standard error, Positive control: nystatin.

Moreover, *Pseudomonas* spp. inhibited the growth of *F. oxysporum* as reported by van Peer *et al*. (1990). While, Laine *et al.* (1996) showed that *P. fiuorescens* and *P. chlororaphis* had inhibition effects against *S. typhi*, *S. aureus*, *Fusarium oxysporum*, *F. culmorum* and *A. niger*. Also, *P. fluorescens* had antifungal activity against *P. ultimum* more than *M. phaseolina* and *P. oryzae* (Fuente *et al*., 2004). *P. fluorescens* recorded antifungal activity

against *Fusarium oxysporum* and *F. udum* (Srivastuva and Shalini, 2008). Also, the *Pseudomonas* isolates had antifungal activity against plant pathogens, *i.e. Aspergillus* sp., *Penicillium* sp., *Fusarium* sp., *Rhizoctonia* sp., *Alternaria* sp. and *Trichoderma* sp (Sharma and Kaur 2010). Mushtaq *et al*. (2010) as well as Rajeswari and Kannabiran (2011) reported that the culture filtrate of *P. fiuorescens* had antifungal activity against *Fusarium oxysporum*, *Penicillium italicum* and *Aspergillus niger*.

3.2. Antimicrobial Activity of P. fluorescens Strains Solvent Fractions

The cell-free supernatants of the *P. fluorescens* strains (FP4, FP6, FP7 and FP10) were selected according to their antimicrobial activity and fractionated using different solvents, ethyl acetate, diethyl ether, butanol, chloroform and hexane. The antibacterial activity of different fractions extracted from selected *P. fluorescens* strains are illustrated in Table 3. The chloroform fraction of *P. fluorescens* FP3 had the highest antibacterial activity against *B. cereus*, *E. coli*, *S. typhi* and *K. pneumoniae*, while the butanol fraction showed the highest activity against *S. aureus* and *P. aeruginosa*. On other hand, the chloroform fraction of *P. fluorescens* FP6 and FP7 had antibacterial activity higher than other fractions against all tested bacteria with the exception of *P. aeruginosa*. The highest activity against *P. aeruginosa* was recorded by the hexane fraction of *P. fluorescens* FP6 and the ethyl acetate fraction of *P. fluorescens* FP7 with inhibition zones of 9.3 and 12.7 mm, respectively. Also, the chloroform fraction of *P. fluorescens* FP10 had the highest activity against *B. cereus*, *S. aureus*, *E. coli* and *S. typhi*, while butanol and diethyl ether fractions showed the highest activity against *P. aeruginosa* and *K. pneumoniae*, respectively.

Table 3. Antibacterial activity of the cell-free supernatant fractions of *P. fluorescens* strains

Bacterial extracts	Inhibition zone (mm) (Mean ± S.E)					
	B. cereus	*St. aureus*	*E. coli*	*S. typhi*	*P. aeruginosa*	*K. pneumoniae*
Negative control	0	0	0	0	0	0
Positive control	26.8±0.4^{a}	25.5±1.2^{b}	22.8±1.0^{b}	25.2±0.2^{a}	13.2±0.9^{a}	26.0±1.3^{a}
P. fluorescens FP3						
Ethyl acetate	9.3±1.1^{d}	8.2±0.6^{g}	11.2±0.7^{e}	7.2±0.2^{k}	9.3±0.7^{c}	8.5±1.0^{gh}
Diethyl ether	0	9.3±0.7^{fg}	0	0	0	0
Butanol	9.8±0.6^{d}	13.2±0.2^{e}	8.5±0.3^{g}	7.8±0.2^{k}	11.5±0.6^{ab}	8.3±0.9^{h}
Chloroform	13.3±0.7^{c}	12.0±0.3^{ef}	12.7±1.3^{de}	12.2±0.4^{fg}	8.5±0.8^{e}	10.5±0.9^{fg}
Hexane	0	9.7±0.9^{fg}	8.7±0.7^{g}	10.0±0.3^{hi}	11.8±1.0^{ab}	7.7±0.4^{h}
P. fluorescens FP6						
Ethyl acetate	8.0±0.6^{d}	0	21.5±1.5^{b}	7.8±0.2^{k}	0	8.0±0.6^{h}
Diethyl ether	11.3±0.7^{cd}	13.7±1.6^{de}	8.8±1.0^{fg}	18.3±0.4^{c}	9.0±0.3^{c}	16.2±0.7^{bc}
Butanol	10.8±0.7^{cd}	8.0±0.6^{g}	7.7±0.2^{g}	7.8±0.6^{k}	8.0±0.3^{c}	0
Chloroform	25.8±0.6^{a}	28.7±2.2^{a}	26.8±0.4^{a}	23.3±0.4^{b}	7.8±0.8^{c}	25.0±0.5^{a}
Hexane	8.5±0.3^{d}	9.5±0.3^{fg}	8.2±0.6^{g}	9.3±0.7^{ij}	9.3±0.6^{c}	8.5±0.8^{gh}
P. fluorescens FP7						
Ethyl acetate	19.5±4.3^{b}	13.0±0.8^{e}	11.8±1.5^{b}	13.5±1.2^{e}	12.7±0.2^{ab}	12.7±0.9^{de}
Diethyl ether	11.2±1.0^{cd}	8.0±0.6^{g}	8.5±1.0^{g}	13.3±0.4^{ef}	0	10.5±0.6^{fg}
Butanol	10.8±0.6^{cd}	8.8±0.4^{g}	11.0±0.8^{ef}	10.2±0.4^{hi}	8.0±0.3^{c}	12.7±1.1^{de}
Chloroform	23.5±0.8^{a}	19.8±1.2^{c}	15.5±0.6^{c}	16.3±0.4^{d}	7.8±0.8^{c}	17.5±0.5^{b}
Hexane	11.3±0.4^{cd}	11.7±0.4^{ef}	11.0±0.5^{ef}	11.0±0.3^{gh}	8.5±0.6^{c}	11.3±0.4^{ef}
P. fluorescens FP10						
Ethyl acetate	11.2±2.2^{cd}	11.7±1.3^{ef}	0	10.0±0.3^{hi}	8.2±0.2^{c}	11.5±0.8^{ef}
Diethyl ether	8.2±0.4^{d}	13.2±0.9^{e}	11.2±0.7^{e}	8.2±0.4^{jk}	8.3±0.4^{c}	14.3±0.7^{cd}
Butanol	10.8±0.9^{cd}	11.7±0.6^{ef}	11.0±0.3^{ef}	11.0±0.3^{gh}	12.0±0.9^{ab}	11.0±0.6^{fg}
Chloroform	14.0±0.3^{c}	16.3±1.9^{d}	13.8±0.7^{cd}	13.0±0.6^{ef}	11.2±0.6^{b}	11.7±0.2^{ef}
Hexane	0	0	7.2±0.2^{g}	8.2±0.2^{jk}	0	7.5±0.5^{h}
LSD	3.3	2.7	2.2	1.3	1.7	2.1

Means followed by different subscripts within column are significantly different at the 5 % level (n= 3), S.E: standard error, Negative control: DMSO, Positive control: tetracycline.

The antifungal activity of the cell-free supernatant fractions of *P. fluorescens* strains are illustrated in Table 4. The chloroform fractions of *P. fluorescens* FP6, FP7 and FP10 showed the highest antifungal activity against all tested mycotoxigenic fungi, while the chloroform fraction of *P. fluorescens* FP3 had the highest activity against *A. flavus*, *A. carbonarus* and *A. parasiticus* since ethyl acetate and butanol fractions showed highest inhibition zones against *A. niger* and *A. westerdijikia*, respectively. The highest antifungal activity was observed by the chloroform fraction of *P. fluorescens* FP6 against *A. niger* with a 24.0 mm inhibition zone.

Generally, *P. fluorescens* FP6, FP7 and FP10 chloroform fractions showed highest antimicrobial activity against the tested foodborne pathogenic bacteria and mycotoxigenic fungi. So, the bioactive compounds

in these fractions should be identified using Gas Chromatography Mass Spectroscopy (GC/MS).

Fassouane *et al*. (1995) found that the extraction of *P. fluorescens* FSJ-3 cell free supernatant with n-butanol exhibited excellent antimicrobial activity against several species of bacteria, yeast and fungi, including *P. aeruginosa*, *Staphylococcus aureus*, *Candida albicans*, *Aspergillus niger* and *A. fumigatus*. The crude extracts of *P. fluorescens* isolates inhibited the growth of *Dreschelaria oryzae*, *R. solani, Magnaporthe grisea* and *Sarocladium oryzae* completely (Reddy *et al*., 2007). In a previous study, the antifungal activity of ethyl acetate and methanol extracts of *P. fluorescens* Pf3 showed that they completely inhibited the mycelial growth of *Botrytis fabae* compared with the hexane extract. Meanwhile, the antifungal activity of the hexane extract of *P. fluorescens* Pf8 showed complete inhibition of the *B. fabae* growth compared with the ethyl acetate and the methanol extracts (Alemu and Alemu, 2013).

Table 4. Antifungal activity of cell-free supernatant fractions of *P. fluorescens* strains**.**

Bacterial extracts	Inhibition zone (mm) (Mean ± S.E)				
	A. flavus	*A. carbonarus*	*A. niger*	*A. parasiticus*	*A. westerdijikia*
Negative control	0	0	0	0	0
Positive control	15.8±0.4^{a}	22.7±0.7^{a}	15.3±0.4^{c}	15.5±0.3^{c}	12.3±0.6^{d}
P. fluorescens FP3					
Ethyl acetate	8.5±0.8^{de}	7.8±0.6^{ef}	9.8±0.6^{d}	0	0
Diethyl ether	0	7.3±0.2^{f}	0	0	0
Butanol	9.0±0.6^{de}	8.5±0.3^{ef}	8.8±0.2^{de}	9.0±0.8^{d}	9.2±0.4^{ef}
Chloroform	9.2±0.2^{d}	9.5±1.3^{de}	0	9.3±1.1^{d}	9.0±0.6^{ef}
Hexane	0	8.3±0.7^{ef}	0	8.2±0.4^{d}	8.8±0.2^{f}
P. fluorescens FP6					
Ethyl acetate	9.2±1.3^{d}	9.0±0.3^{ef}	8.0±0.6^{e}	8.8±1.0^{d}	0
Diethyl ether	9.0±1.3^{de}	8.8±0.4^{ef}	9.3±0.2^{de}	9.7±1.0^{d}	7.8±0.4^{f}
Butanol	9.0±0.8^{de}	0	0	9.5±1.3^{d}	0
Chloroform	20.0±0.3^{a}	22.2±1.1^{a}	24.0±1.3^{a}	20.7±1.5^{a}	22.0±1.0^{a}
Hexane	7.3±0.3^{e}	9.0±1.2^{ef}	9.7±0.4^{d}	0	11.2±0.6^{de}
P. fluorescens FP7					
Ethyl acetate	11.±0.4^{c}	11.7±0.4^{c}	8.0±0.6^{e}	8.5±1.0^{d}	8.7±0.6^{f}
Diethyl ether	7.8±0.6^{de}	0	0	8.3±0.7^{d}	0
Butanol	0	11.2±0.6^{cd}	9.2±1.0^{de}	7.8±0.6^{d}	8.0±0.6^{f}
Chloroform	18.8±1.2^{a}	23.8±1.2^{a}	19.3±1.0^{b}	18.2±1.9^{b}	19.5±2.4^{b}
Hexane	8.3±0.3^{de}	9.5±0.3^{de}	0	8.2±0.4^{d}	9.3±0.6^{ef}
P. fluorescens FP10					
Ethyl acetate	11.3±0.9^{c}	0	8.5±0.3^{de}	0	0
Diethyl ether	7.5±0.3^{de}	9.0±0.3^{ef}	8.7±0.4^{de}	8.0±0.6^{d}	0
Butanol	0	9.5±1.6^{de}	8.5±0.3^{de}	8.7±0.9^{d}	0
Chloroform	11.7±0.2^{c}	14.7±0.7^{b}	9.3±0.6^{de}	9.5±0.3^{d}	15.0±2.0^{c}
Hexane	0	0	0	0	0
LSD	1.7	2.0	1.5	2.3	2.2

Means followed by different subscripts within column are significantly different at the 5 % level (n= 3), S.E: standard error, Negative control: DMSO, Positive control: nystatin.

3.3. Identification of the Compounds Using GC/MS

The results pertaining to the GC/MS analysis of *P. fluorescens* FP6, FP7 and FP10 chloroform fractions are illustrated in Figure 1 a nd Table 5. They reveal the presence of eight metabolites in the chloroform fraction of *P. fluorescens* FP6 with a retention time ranging from 11.32 to 35.46 minutes. The maximum peak area was identified as Pyrrolo[1,2-a]pyrazine-1,4-dione, hexahydro-3-(propylmethyl)- with an area percentage of 41.30 %, followed by Pyrrolo[1,2-a]pyrazine-1,4-dione, hexahydro-3-(2-methylpropyl)- ($C_{14}H_{16}N_2O_2$) as 21.60 % and (2S,6R)-2,6-Dibutyl-4-methylpiperdine ($C_{14}H_{29}N$) as 12.90 %. Meanwhile, the minimum peak was identified as Methaqualone ($C_{16}H_{14}N_2O$) and the peak area percentage was 0.98 %.

On the other hand, five compounds were identified from the chloroform fractions of *P. fluorescens* FP7, as 4-Bromo-5-methyl-1-(phenylmethyl) imidazole ($C_{11}H_{11}BrN_2$), 3-Ethoxy-4-methoxyphenol ($C_9H_{12}O_3$), Pyrrolo[1,2-a]pyrazine-1,4-dione,hexahydro-3-(2-methylpropyl)-, Pyrrolo[1,2-a]pyrazine-1,4-dione, hexahydro-3-(propyl

methyl)- and Cyclotrisiloxane, hexamethyl- ($C_6H_{18}O_3Si_3$) with peak area percentages of 0.76, 5.68, 25.35, 51.60 and 16.61%, respectively. Regarding to the chloroform fraction of *P. fluorescens* FP10, four compounds were found as 3-Ethoxy-4-methoxyphenol, Pyrrolo[1,2-a]pyrazine-1,4-dione, hexahydro-3-(2-methylpropyl)-, Pyrrolo[1,2-a] pyrazine-1,4-dione,hexahydro-3-(propylmethyl)-and Cyclo trisiloxane, hexamethyl- with peak area percentages of 4.14, 26.32, 47.40 and 22.14 %, respectively. Two Pyrrolo compounds were found in all of the fractions as the main compounds, Pyrrolo[1,2-a] pyrazine-1,4-dione, hexahydro-3-(propylmethyl)- and Pyrrolo[1,2-a]pyrazine-1,4-dione, hexahydro-3-(2-methylpropyl)-. Also, Cyclotrisiloxane, hexamethyl- and 3-Ethoxy-4-methoxyphenol were found in all *P. fluorescens* chloroform fractions.

The antibacterial metabolite of *P. fluorescens* strains showed activity against both Gram-negative and Gram-positive bacteria. Also, they have broad-spectrum antifungal activty against phytopathogenic and toxigenic fungi. Narasaiah (2016) reported that *Streptomyces albus* CN-4 secondary metabolites which contain Pyrrolo[1,2-a]pyrazine-1,4-dione, hexahydro-3-(2-methylpropyl)- had antibacterial activity against *Bacillus megaterium, B. subtilis*, *E. coli, Pseudomonas aeruginosa, Staphylococcus aureus* and *Xanthomonas campestris*. Also, they had antifungal activity against *Aspergillus niger, Candida albicans* and *Fusarium solani*. The pure Pyrrolo[1,2-a] pyrazine-1,4-dione, hexahydro-3-(2-methyl propyl)- had antibacterial activity against pathogenic bacteria that cause serious fish and human diseases (Pandey *et al*., 2010). Dash *et al*. (2009) found that Pyrrolo [1,2-a] pyrazine-1,4-dione,hexahydro-3-(2-methylpropyl)- isolated from a sponge-associated marine bacteria prevented biofilm formation by *Loktanella honkongensis* and *Vibrio halioticoli*. Also, Pyrrolo [1,2-a] pyrazine-1,4-dione,hexahydro-3-(2-methylpropyl)- isolated from marine sponge *Spongia officinalis* exhibited potent antibacterial and antifungal activity (Sathiyanarayanan *et al*., 2014). Melo *et al*. (2014) indicated that the chloroform extract of Antarctic endophytic fungus exhibited strong antibacterial activity, mainly against *P. aeruginosa*, *Enterococcus faecalis* and *E. coli*. They added that, Pyrrolo[1,2-a] pyrazine-1,4-dione, hexahydro-3-(2-methylpropyl)- and Pyrrolo[1,2-a]pyrazine-1,4-dione,hexahydro-3-(phenyl-methyl)- from the fungus extract had potential antimicrobial compounds. Also, pyrrolo [1,2-a] pyrazine-1,4-dione, hexahydro-3-(2-methyl propyl)- purified from *Streptomyces* sp. had antibacterial activity against *E. coli*, , *Proteus vulgaris*, *P. aeruginosa*, *S. paratyphi*, *Enterobacter* spp. and *S. aureus*, *B. cereus* (Manimaran *et al*., 2017).

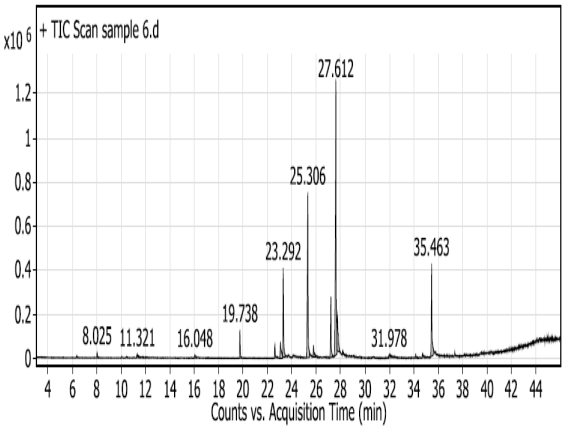

Figure 1. GC-MS chromatogram of *P. fluorescens* FP6 chloroform fractions.

Table 5. GC-MS analysis of chloroform fractions *of P. fluorescens strains* (FP6, FP7 and FP10).

No	RT	Chemical	Structure	Chloroform fractions (Peak area %)		
				Pf 6	Pf 7	Pf 10
1	11.32	4-Bromo-5-methyl-1-(phenylmethyl)imidazole	$C_{11}H_{11}BrN_2$	1.18	0.76	--
2	16.05	Methaqualone	$C_{16}H_{14}N_2O$	0.98	--	--
3	19.70	beta-Lonipinene	$C_{15}H_{24}$	6.13	--	--
4	23.01	3-Ethoxy-4-methoxyphenol	$C_9H_{12}O_3$	3.11	5.68	4.14
5	23.30	(2S,6R)-2,6-Dibutyl-4-methylpiperdine	$C_{14}H_{29}N_4$	12.90	--	--
6	25.30	Pyrrolo[1,2-a]pyrazine-1,4-dione, hexahydro-3-(2-methylpropyl)-	$C_{11}H_{18}N_2O_2$	21.60	25.35	26.32
7	27.61	Pyrrolo[1,2-a]pyrazine-1,4-dione, hexahydro-3-(propylmethyl)-	$C_{14}H_{16}N_2O_2$	41.30	51.60	47.40
8	35.46	Cyclotrisiloxane, hexamethyl-	$C_6H_{18}O_3Si_3$	12.80	16.61	22.14

4. Conclusion

The present *in-vitro* study reveals that all of the studied cell-free supernatants of the *P. fluorescens* strains (FP3, FP4, FP6, FP7 and FP10) were more effective as antibacterial against all the tested pathogenic bacteria. Meanwhile, only the *P. fluorescens* FP10 strain was more effective as antifungal against all studied mycotoxigenic fungi. The main compound identified in chloroform fractions were Pyrrolo[1,2-a]pyrazine-1,4-dione, hexahydro-3-(propylmethyl)- and Pyrrolo[1,2-a]pyrazine-1,4-dione, hexahydro-3-(2-methylpropyl)- that have been proved to possess a biological activity against pathogenic bacteria and toxigenic fungi. Finally, data in the current study reveal that cell-free supernatants and chloroform fractions of *P. fluorescens* strains displayed potential antimicrobial activity against foodborne microorganisms that could be applied as food biopreservative agents.

Conflict of Interest

The authors have no conflicts of interest to declare.

References

Addis M and Sisay D. 2015. A review on major foodborne bacterial illnesses. *J Trop Dis*., **3(4):**176.

Alemu F and Alemu T. 2013. Antifungal activity of secondary metabolites of *Pseudomonas fluorescens* isolates as a b iocontrol

agent of chocolate spot disease (*Botrytis fabae*) of faba bean in Ethiopia. *Afr J Microbiol Res*., **7(47)**:5364-5373.

Bauer A, Kirby W, Sherris J and Turck M. 1966. Antibiotic susceptibility testing by a standardized single disk method. *Amer J Clin Pathol*., **45**:493-496.

Charyulu E, Sekaran G, Rajakumar G and Gnanamani A. 2009. Antimicrobial activity of secondary metabolite from marine isolate, *Pseudomonas* sp. against Gram positive and negative bacteria including MRSA. *Indian J Exper Biol*., **47**:964-968.

Darwesh OM, Sultan YY, Seif MM and Marrez DA. 2018. Bio-evaluation of crustacean and fungal nano-chitosan for applying as food ingredient. *Toxicol Rep.*, **5**:348–356.

Dash S, Jin C, Lee O, Xu Y and Qian P. 2009. Antibacterial and antilarval-settlement potential and metabolite profiles of novel sponge-associated marine bacteria. *J Indust Microbiol Biotechnol*., **36**:1047–1059.

Emam HE, Darwesh OM and Abdelhameed RM. 2018. In-Growth Metal Organic Framework/Synthetic Hybrids as Antimicrobial Fabrics and Its Toxicity. *Coll Surf B:Biointerf.* **165**: 219–228.

Fassouane A, Rebuffat S, Nguyen V and Bodo B. 1995. Isolation and characterization of an antifungal agent active against human pathogenic fungi, produced by *Pseudomonas fluorescens* FSJ-3. *Actes Inst Agron Vet.* (*Maroc*), **15 (4)**:5-10.

Feltes M, Arisseto-Bragotto A and Block J. 2017. Food quality, food-borne diseases, and food safety in the Brazilian food industry. *Food Quality and Safety*, **1**:13-27.

Freedman D, Kondo J and Willrett D. 1989. Antagonism of foodborne bacteria by *Pseudomonas* spp.: a possible role for iron. *J Food Prot.*,**52**:484-489.

Fuente L, Thomashow L, Weller D, Bajsa N, Quagliotto L, Chernin L and Arias A. 2004. *Pseudomonas fluorescens* UP61 isolated from birdsfoot trefoil rhizosphere produces multiple antibiotics and exerts a broad spectrum of biocontrol activity. *Eur J Plant Pathol*., **110**:671–681.

Kadhim S. 2015. Efficacy of the bioactive substance of *Pseudomonas fluorescens* against bacteria from skin infections. *Intern J Pharm Sci Rev and Res*., **34(2)**:193-196.

Karlovsky P, Suman M, Berthiller F, De Meester J, Eisenbrand G, Perrin I, Oswald I, Speijers G, Chiodini A, Recker T and Dussort P. 2016. Impact of food processing and detoxification treatments on mycotoxin contamination. *Mycotoxin Res*., **32**:179-205.

Kheiralla ZH, Hewedy MA, Mohammed HR. and Darwesh OM. 2016. Isolation of Pigment Producing Actinomycetes from Rhizosphere Soil and Application It in Textiles Dyeing. *Res J Pharm Biol Chem Sci.*, **7(5)**: 2128- 2136.

Laine M, Karwoski M, Raaska L and Mattila-Sandholm T. 1996. Antimicrobial activity of *Pseudomonas* spp. against food poisoning bacteria and moulds. *Lett Appl Microbiol*., 22:214-218.

Malhotra B, Keshwani A and Kharkwal H. 2015. Antimicrobial food packaging: potential and pitfalls. *Front Microbiol*., **6**:611.

Manimaran M, Gopal J. and Kannabiran K. 2017. Antibacterial Activity of *Streptomyces* sp. VITMK1 Isolated from Mangrove Soil of Pichavaram, Tamil Nadu, India. *Proc. Natl. Acad. Sci., India, Sect. B Biol. Sci*., **87(2)**:499-506.

Marrez D and Sultan Y. 2016. Antifungal activity of the cyanobacterium *Microcystis aeruginosa* against mycotoxigenic fungi. *J Appl Pharm. Sci*., **6(11)**:191-198.

Marrez D, Sultan Y and Embaby M. 2017. Biological activity of the cyanobacterium *Oscillatoria brevis* extracts as a source of nutraceutical and bio-preservative agents. *Intern J Pharmacol*., **13(8)**:1010-1019.

Medeiros M, de Oliveira D, Rodrigues D and de Freitas D. 2011. Prevalence and antimicrobial resistance of *Salmonella* in chicken carcasses at retail in 15 Brazilian cities. *Rev. Panam. Salud Publica*, **30**:555-560.

Melo I, Santos S, Rosa L, Parma M, Silva L, Queiroz S. and Pellizari V. 2 014. Isolation and biological activities of an endophytic Mortierella alpina strain from the Antarctic moss *Schistidium antarctici*. *Extremophiles*, **18**:15–23.

Mushtaq S, Ali A, Khokhar I and Mukhtar I. 2010. Antagonisitic potential of soil bacteria against foodborne fungi. *World Appl Sci J*., **11**:966-969.

Nandakumar R, Babu S, Radjacommare R, Raguchander T and Samiyappan R. 2002. *Pseudomonas fluorescens* mediated antifungal activity against *Rhizoctonia solani* causing sheath blight in rice. *Phytopathol. Mediterr*., **41**:109-119.

Narasaiah B. 2016. Structural elucidation and antimicrobial activity of secondary metabolites from *Streptomyces albus* CN-4. *Intern J Res Eng Appl Sci*., **6(5)**:77-89.

Pandey A, Naik M and Dubey S. 2010. Organic metabolites produced by *Vibrio parahaemolyticus* strain An3 isolated from goan mullet inhibit bacterial fish pathogens. *Afr J Biotechnol*., **9**:7134-7140.

Rajeswari P and Kannabiran B. 2011. *In vitro* effects of antagonistic microorganisms on *Fusarium oxysporum* [Schlecht. Emend. Synd & Hans] Infecting *Arachis hypogaea* L. *J Phytol*., **3**:83-85.

Reddy K, Choudary K and Reddy M. 2007. Antifungal metabolites of *Pseudomonas fluorescens* isolated from rhizosphere of rice crop. *J Mycol Plant Pathol*., **37(2)**:280-284.

Rekha V, John A and Shankar T. 2010. Antibacterial activity of *Pseudomonas fluorescens* isolated from Rhizosphere soil. *Intern J Biol Technol*., **1(3)**:10-14.

Sabry M, Mabrouk M, Marrez, D, Barakat O and Sedik M. 2016. Antagonistic pigment producing bacterium isolated from rhizosphere soil of medicinal plants. *J Drug Res. Egypt*, **36(1)**: 87-96.

SAS 1999. **Statistical Analysis System**, SAS / STAT User's Guide. Release 6.03 Edn. SAS Institute, Cary, NC, 1028 PP.

Sathiyanarayanan G, Gandhimathi R, Sabarathnam B, Kiran G and Selvin J. 2014. Optimization and production of pyrrolidone antimicrobial agent from marine sponge-associated *Streptomyces* sp. MAPS15. *Bioprocess Biosyst. Eng*., **37**:561-573.

Schirone M, Visciano P, Tofalo R and Suzzi G. 2017. Editorial: Biological Hazards in Food. *Front. Microbiol*., **7**: 2154.

Sharma S and Kaur M. 2010. Antimicrobial activities of rhizobacterial strains of *Pseudomonas* and *Bacillus strains* isolated from rhizosphere soil of carnation (*Dianthus caryophyllus* cv. Sunrise). *Indian J Microbiol*., **50**:229-232.

Srivastava R and Shalini S. 2008. Antifungal activity of *Pseudomonas fluorescens* against different plant pathogenic fungi. *J Env Agric Food Chem*., **7**: 2789-2796.

Sultan Y, Ali M, Darwesh O, Embaby M and Marrez D. 2016. Influence of nitrogen source in culture media on antimicrobial activity of *Microcoleus lacustris* and *Oscillatoria rubescens*. *Res. J. Pharm Biol Chem Sci*., **7(2)**:1444-1452.

Sung S, Sin L, Tee T, Bee S, Rahmat A, Rahman W, Tan A and Vikhraman M. 2013. Antimicrobial agents for food packaging applications. *Trends Food Sci Technol*., **33**:110-123.

van Peer R, van Kuik A, Rattink H and Schippers B. 1990. Control of *Fusarium* wilt in carnation grown on rockwool by *Pseudomonas* sp. strain WCS417 and by Fe-EDDHA. *Neth. J. P1. Path*., **96**:119-132.

JJBS

Volume 12, Number 5,December 2019
ISSN 1995-6673
Pages 543 - 551

Jordan Journal of Biological Sciences

A Study of the Use of Deep Artificial Neural Network in the Optimization of the Production of Antifungal Exochitinase Compared with the Response Surface Methodology

Shaymaa A Ismail[1], Ahmed Serwa[2], Amira Abood[1], Bahgat Fayed[1], Siham A Ismail[1] and Amal M Hashem[1*]

[1]*Department of Chemistry of Natural and Microbial Products, Division of Pharmaceutical and Drug Industries, National Research Centre;*
[2]*Faculty of Engineering in El-Mataria, Helwan University, Cairo, Egypt.*

Received January 9, 2019; Revised February 13, 2019; Accepted February 21, 2019

Abstract

This study aimed the using of deep artificial neural network in the optimization of exochitinase production as an alternative method to response surface methodology. The isolated fungus *Alternaria* sp. strain Sha that was identified by its morphological features then by the 18S rDNA technique, was used for the production of the enzyme by solid state fermentation. A Plackett–Burman design was constructed to screen the effect of seven independent variables on the enzyme production. The overall enzyme production increased from 3.4 to 28.931U/g dry substrate by approximately 8.5 folds with the coefficient of determination (R^2) value being 0.996 using deep artificial neural network in comparison with the R^2 value 0.76 using response surface methodology. It was clear that the deep artificial neural network was more accurate than the response surface methodology in predicting the enzyme activity. Finally, the produced exochitinase showed antifungal activity against the resistant controllable soil-borne fungus *Rhizoctonia solani.*

Keywords: Exochitinase; *Alternaria* sp., Solid state fermentation, Deep artificial neural network, Response surface methodology, Antifungal.

1. Introduction

Chitin is a linear polymer of N-acetylglucosamine, with β-1,4-glycosidic bonds (Blaak *et al*., 1993). It is the second most abundant biopolymer after cellulose in nature that exists as part of fungi, yeasts, nematodes, shrimps, and other invertebrates (Young *et al*., 2005).

Chitinases are chitinolytic enzymes that are capable of degrading the chitin chain by different mechanisms. The degradation can be done by endochitinases randomly within the chain or by exochitinase that degrades the chain from the terminal end leading to the production of diacetylchitobiose or N-acetylglucosamine units (Sahai and Manocha, 1993). Chitinases gained importance due to its agricultural, industrial, and medical applications (Hamid *et al*., 2013).

The microorganisms are considered the main source for exochitinase production. The upsurge in the exochitinase applications urged the efforts to maximize the microbial production of the enzyme to satisfy the industrial needs (Chavan and Deshpande, 2013).

The fermentation conditions have a crucial impact on microorganisms' growth and their metabolic products as well as the production cost (Shivalee *et al*., 2018). The optimization of the fermentation conditions was initially performed using the classical one-variable-at-a-time approach because of its simplicity and ease. However, this method has several limitations as it is time-consuming and involves a great deal of experiments that may increase the production cost, in addition to the loss of the interactive effects between various parameters. Consequently, statistical models have been employed in fermentation technology to overcome these limitations (Desai *et al*., 2008).

Response surface methodology (RSM) is a statistical technique that was originally described by Box and Wilson, (1951) and has been successfully applied in microbiological and biotechnological fields (Astray *et al*., 2016). As a matter of fact, it is the most popular technique used in optimizing the production of microbial enzymes, and has been used occasionally for maximizing the yield of microbial exochitinase (Kumar *et al*., 2012 and Awad *et al*., 2017).

Over the last two decades, artificial neural networks (ANNs) were utilized in different science aspects for modeling and optimization processes. ANN has several advantages as it can use data with noise and can modulate incomplete and highly non-linear behaviors (Astray *et al*., 2016, de Araujo Padilha *et al*., 2017 and Cui *et al*., 2018). In addition to the various advantages of the ANN, the introduction of deep learning has led to more accurate results (Serwa, 2017). ANN has been previously used in the optimization of the production of some microbial

* Corresponding author e-mail: amal_mhashem@yahoo.com.

enzymes such as L- asparaginase (Gurunathan and Sahadevan, 2011), α-galactosidase (Edupuganti *et al*., 2014), α-amylase (Mishra *et al*., 2016) and protease (Ramkumar *et al*., 2018).

In the current study a comparitive study between RSM and deep artificial neural network (DANN) was performed to predict the optimum conditions for exochitinase production by solid state fermentation (SSF). Additionally, the antifungal activity of the produced exochitinase against phytopathogenic fungi was examined.

2. Materials and Methods

2.1. Materials

Wheat bran and sugarcane bagasse were purchased from the local market. Chitin, 4-NitrophenylN-acetyl-β-D-glucosaminide, 4-Nitrophenol and Yeast extract were purchased from Sigma-Aldrich, Saint Louis, USA. Potato dextrose agar (PDA) medium was purchased from Merck, Darmstadt, Germany. All other chemicals were of analytical or HPLC grade.

2.2. Microorganism and Identification

The fungus used in the current study was previously isolated from waste of marine organisms (shrimp and fish) collected from the local seafood market. Its morphological features were studied by field emission high resolution scanning electron microscope (quanta 250). Molecular identification of the strain was carried out in Sigma Scientific Services Co. by the 18S rDNA technique.

2.3. Exochitinase Production

2.3.1. Inoculum Preparation

An inoculum suspension was obtained by scrapping the fungal potato dextrose agar (PDA) slants with 10mL sterile distilled water containing 0.1 % (w/v) tween 80 (Sridevi and Reddy, 2016).

2.3.2. Fermentation Process

The fermentation process was performed in 250mL Erlenmeyer flask containing 5g of wheat bran and 50mg of colloidal chitin moistened with 10mL of a basal salt solution composed of (g %) yeast extract, 1.85; K_2HPO_4, 0.15; $MgSO_4$, 0.01; KCl, 0.2 and $FeSO_4.7H_2O$, 0.01, inoculated with 2mL of inoculum suspension and incubated at 30°C for seven days. The concentration of the salts was constructed on the base of previous studies on the production of chitin and chitosan hydrolyzing enzymes (Hosny *et al*., 2010 and Hashem *et al*., 2018).

At the end of fermentation, 50mL of distilled water was added and mixed in a rotary shaker at 150rpm for one hour. The mixture was centrifuged at 4°C for twenty minutes at 5000 rpm, and the clear supernatant was used as the crude enzyme solution (Sridevi and Reddy, 2016).

2.4. Enzyme Assay

The exochitinase activity was determined using 0.1 % of the synthetic substrate 4-NitrophenylN-acetyl-β-D-glucosaminide in 0.2M acetate buffer pH 5 (Rustiguel *et al*., 2012). The reaction was performed by mixing 50µL of the clear extract with 50µL of the substrate solution and the reaction mixture was incubated at 30°C for fifteen minutes. At the end of the assay time, 1mL of 1M NaOH was added to stop the reaction and the yellow color developed was quantified at 410nm. One unit of exochitinase was defined as the amount of enzyme that released 1µmol of p-Nitro-phenol (equivalent to 1µmolof N-acetylglucosamine) per minute under the assay conditions.

2.5. Optimization of the Enzyme Production

Initially, the effects of varying the fermentation period in addition to the effects of adding various salt solutions (tap water, SR salt solution [consisting of (g %) $MgSO_4$, 0.012; KH_2PO_4, 0.015; $NH_4H_2PO_4$, 0.05; peptone, 0.02 and yeast extract, 0.45], Khanna salt solution [consisting of (mg %) NH_4NO_3, 100; KH_2PO_4, 65; $MgSO_4.7H_2O$, 18.1; KCl, 4.9; $MnSO_4.H_2O$, 0.69; $ZnSO_4.H_2O$, 0.35; $FeCl_3.6H_2O$, 0.33; $CuSO_4.5H_2O$, 0.31 and yeast extract, 100]) were examined in a medium containing 5g wheat bran and 50mg colloidal chitin (Rustiguel *et al*., 2012).

The Plackett–Burman experiment (Plackett and Burman, 1946) was performed in order to identify the variables that influence the exochitinase production. Seven independent variables (temperature, incubation period, volume of moistening agent, age of fungus, concentration of chitin, addition of shrimp shells and sugarcane bagasse) were examined in eight trials by which each variable was tested at two levels (a high +ve and a low –ve levels). Plackett–Burman experimental design based on the first order linear model:

$$Y=B_o+\sum B_iX_i \quad \text{Eq. (1)}$$

Where Y is the response (exochitinase production), B_o is the model intercept, and B_i is the variable estimation. The main effect of each variable was determined by the following equation:

$$E_{(Xi)}=2(\Sigma M_i^+-M_i^-)/N \quad \text{Eq. (2)}$$

Where $E_{(Xi)}$ is the effect of the tested variable. M_i^+ and M_i^- represent exochitinase production from the trials performed at high and low concentrations of the independent variable (Xi), respectively, and N is the number of trials.

2.5.1. Modeling Procedure for Response Surface Methodology

RSM using Box-Behnken design (Box and Behnken, 1960) was performed to optimize exochitinase production. The three most significant independent variables extracted from Plackett–Burman design were examined at three different levels, low (-), high (+) and control (0). For predicting the optimal point, a second order polynomial function in the form of the three factors was fitted to correlate the relationship between the independent variables and the response as follows:

$$Y=ß_0+ß_1X_1+ß_2X_2+ß_3X_3+ß_{11}X_1^2+ß_{22}X_2^2+ß_{33}X_3^2+ß_{12}X_1X_2+ß_{13}X_1X_3+ß_{23}X_2X_3 \quad \text{Eq. (3)}$$

Where Y is the predicted response (exochitinase production), and X_1, X_2 and X_3 are the most significant independent variables; $ß_0$ is the intercept regression coefficient, $ß_1$, $ß_2$, $ß_3$ are linear coefficients, $ß_{11}$, $ß_{22}$, $ß_{33}$ are quadratic coefficients, and $ß_{12}$, $ß_{13}$, $ß_{23}$ are cross product coefficients.

All experiments were performed in triplicates and the average of the results was reported. The results were statistically analyzed using the analysis of variance (ANOVA) techniques, in which p value of ≤ 0.05 was regarded as significant. The statistical software SPSS (version 16.0) was used for the regression analysis of the experimental data obtained.

2.5.2. Modeling Procedure for Artificial Neural Network

The data sets presented to the ANN model were performed in the same order as in the Box-Behnken design. Multi-layer perceptron (MLP) is the most used architecture in ANN models, which was composed of three different kinds of layers: the input, the output and the hidden layers. In the case of DANN (Figure 1), the number of hidden layers is larger than the traditional ANN(Serwa, 2017).

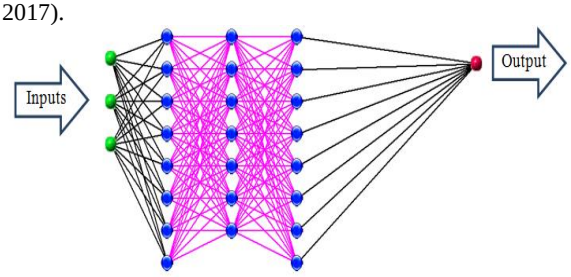

Figure 1. MLP architecture with deep learning.

The back propagation neural networks (BPNN) algorithm is used to adjust the weights of the network. The target output is known from training data which is the exochitinase activity (experimental work results).

The used software that applied the ANN model by DANN has been reported by Serwa, (2017). The relationship between the experimental and the predicted results was expressed by the root mean square error (RMSE). The accuracy of the predicted model was expressed as the overall average accuracy %.

$$RMSE=\sqrt{\frac{\sum_{i=1}^{N}(Xpred-X)^2}{N}} \quad \text{Eq. (4)}$$

Accuracy % = 100-[Absolute error/X*100] Eq. (5)

Overall average accuracy % = ∑ Accuracy %/N Eq. (6)

in which X is the experimental results.

2.6. Some Properties of the Crude Exochitinase

2.6.1. Effect of pH

The effect of different pH's on the activity and stability of the enzyme were examined in the pH range of 4 to 7 and 4 to 5, respectively using 0.2M acetate buffer.

2.6.2. Effect of temperature

The optimum temperatures for the enzyme activity in-addition to its thermostability, were investigated in the range from 30°C to 60°C, and from 35°C to 60°C, respectively.

2.6.3. Effect of Substrate Concentrations

The effect of different substrate concentrations (0.05 to 3mg/ml), was studied at the optimal pH and temperature of the tested enzyme.

2.7. Antifungal Activity of the Produced Exochitinase

The well diffusion method according to Neto *et al*., (2016) was used to examine the antifungal activity of the produced exochitinase against the phytopathogenic fungi *Rhizoctonia solani* and *Dothideomycetes* sp. The experiment was performed in a petri dish containing 20mL of potato dextrose agar inoculated with 0.2ml of the fungal strains spore suspension. Wells of 7mm in diameter were made in the agar plate with a sterile glass Pasteur pipette and 0.1mL of the produced enzyme (45U/mL) was added into the wells. The plates were then incubated at 30ºC for forty-eight hours.

3. Results

3.1. Identification of the Fungal Exochitinase Producer Strain

The fungal isolate used in this study was previously isolated from the waste of marine organisms and screened for its chitinolytic activity (unpublished data). Morphological features of the isolate in terms of sporangia were examined under scanning electron microscope (Figure 2). The molecular identification of the isolate was performed using the 18S rDNA technique and the evolutionary history was inferred using the Maximum Likelihood method. The tree with the highest log likelihood (-1003.8762) is shown in Figure 3. The phylogentic analysis of the isolated fungus revealed that the strain was 100 % identical to other *Alternaria* sp. The data of the 18S rDNA partial sequence was submitted to NCBI under the name *Alternaria* sp. strain Sha and received the accession number of MK139827.

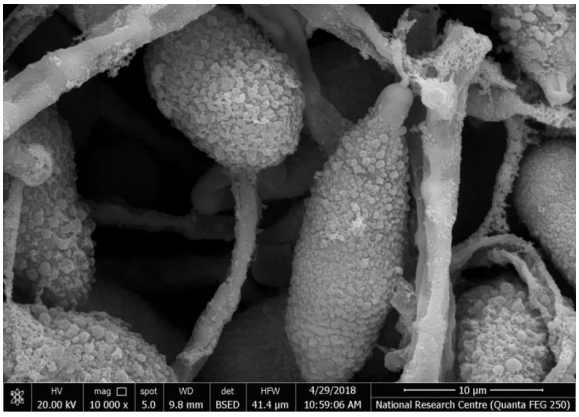

Figure 2. Scanning Electron Micrograph of the fungal isolate.

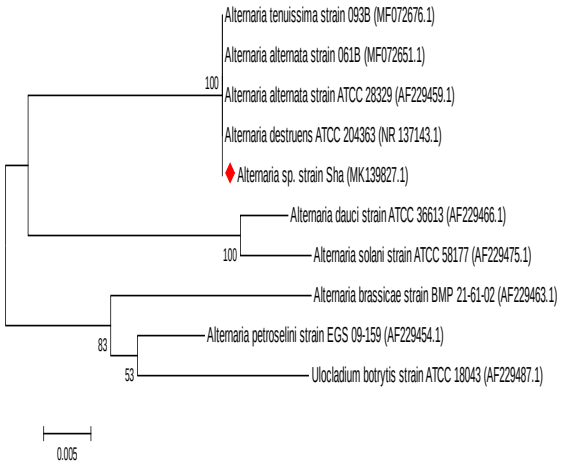

Figure 3. The Phylogenetic tree by the Maximum Likelihood method.

3.2. Optimization of the Enzyme Production by SSF

The production of exochitinase using 5g of wheat bran and 50mg of colloidal chitin as a substrate at different incubation periods indicated that the used strain produced 3.4U/g dry substrate (g ds) after seven days and increased to reach 10.1U/g ds after fourteen days of incubation.

However, a further increase in incubation period leads to a decrease in the enzyme production (Figure 4).

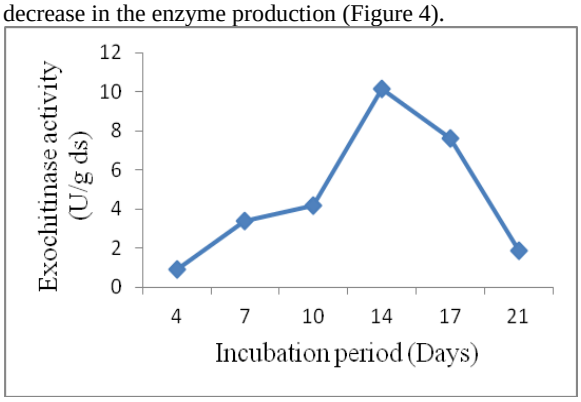

Figure 4. Production of exochitinase at different incubation periods.

The effect of various salt solutions on moistening the solid substrate (5g wheat bran and 50mg chitin) indicated that a 29.1 % increase in the activity was achieved using the SR salt solution compared with the basal salt solution (Table 1).

Table 1. The effect of different salt solutions on the enzyme production

Salt solution	Exochitinase activity (U/g ds)
Basal salt solution	10.147
Khanna salt solution	10.777
SR salt solution	13.102
Tap water	8.924

3.2.1. Selection of the Variables that Influence the Enzyme Production by Plackett–Burman Design

The Plackett–Burman design was applied to identify the variables that influence exochitinase production by SSF in which seven independent variables were studied in eight trials (Table 2). A wide variation in the exochitinase productivity ranging from 2.901 to 16.521U/g ds was observed. A maximum exochitinase activity of 16.521U/g ds was achieved in the third trial in which the optimized medium contained (g/flask) wheat bran; 5g, sugarcane bagasse; 1g and chitin; 75mg moistened by 5mL SR salt solution, then inoculated by 2mL of spore suspension of a five-day-old fungus, and incubated for sixteen days at 27°C.

The multiple regression analysis of the data (Table 3) clarified that all of the examined variables significantly influence the exochitinase production. The first order equation describing the relation between the seven variables and the enzyme activity, obtained after applying the regression analysis of the experimental results, was as follows:

$$Y=29.952 -1.031X_1+0.291X_2-0.273X_3+ 0.288X_4+ 0.043X_5+ 0.978X_6+ 6.441X_7 \quad \text{Eq. (7)}$$

Y is the exochitinase activity. X_1, X_2, X_3, X_4, X_5, X_6, and X_7 are temperature, fermentation period, age of the fungus, volume of the moistening agent, addition of chitin, addition of shrimp shells, and addition of sugarcane bagasse respectively.

The R^2 value for the applied model was 0.9919 and the analysis of variance (ANOVA) indicated that the model terms used were significant since the F value was 278.42 with Prob>F value of 1.69E-15 (less than 0.05).

The main effect of each variable was calculated and represented graphically in figure 5; it was evident that the temperature and the volume of the salt solution have negative values while the other variables have positive values. So the variables which represented positive effects on the enzyme production were set at high levels (+ve), while the variables that exerted negative effects were maintained at low levels (-ve) in the further experimental optimization.

Table 2. Plackett – Burman design and the observed results.

Trials	Temperature (°C)	Incubation period (day)	Volume of moistening agent (mL)	Age of the fungus (days)	Chitin (mg/flask)	Shrimp (g/flask)	Sugarcane bagasse (g/flask)	Exochitinase activity (U/g ds)
1	(27) -	(12) -	(5) -	(9) +	(75) +	(1) +	(0) -	11.043
2	(33) +	(12) -	(5) -	(5) -	(25) -	(1) +	(1) +	8.004
3	(27) -	(16) +	(5) -	(5) -	(75) +	(0) -	(1) +	16.521
4	(33) +	(16) +	(5) -	(9) +	(25) -	(0) -	(0) -	2.901
5	(27) -	(12) -	(15) +	(9) +	(25) -	(0) -	(1) +	11.630
6	(33) +	(12) -	(15) +	(5) -	(75) +	(0) -	(0) -	0
7	(27) -	(16) +	(15) +	(5) -	(25) -	(1) +	(0) -	6.181
8	(33) +	(16) +	(15) +	(9) +	(75) +	(1) +	(1) +	9.736

Table 3. Statistical analysis of Plackett- Burman design showing coefficient values, t-and *P*- values for each variable on exochitinase production.

Variables	Exochitinase analysis			
	Coefficient	*t*-statistics	*P*-value	Confidence level (%)
Intercept	29.952			
Temperature (°C)	-1.031	-27.9452	5.23E-15	100
Incubation time (day)	0.291	5.266116	7.68E-05	99.99
Volume of moistening agent (ml)	-0.273	-12.3397	1.37E-09	100
Age of the fungus (days)	0.288	5.203531	8.7E-05	99.99
Chitin (mg/flask)	0.043	9.697626	4.2E-08	100
Shrimp shell (g/flask)	0.978	4.419094	0.00043	99.96
Sugarcane bagasse (g/flask)	6.441	29.10956	2.75E-15	100

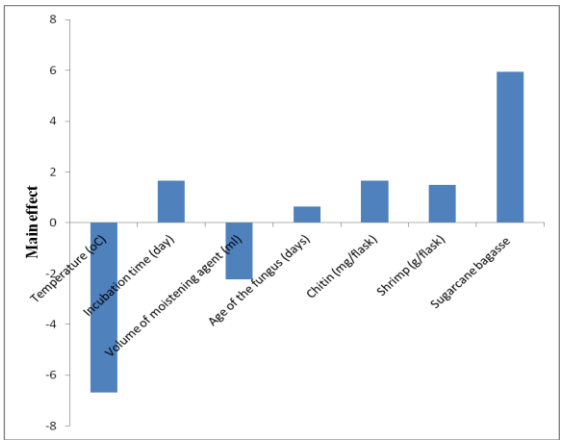

Figure 5. Main effects of the selected independent variables on exochitinase production according to the results of the Plackett – Burman experiment.

3.2.2. Response Surface Methodology Model

RSM using Box-Behnken design was applied in order to reach the optimum concentration of the variables (temperature, addition of sugarcane bagasse, and the volume of moistening agent) that exert the highest main effect on exochitinase production. The results (Table 4) showed an increase in exochitinase production to reach 28.931U/g ds using a medium composed of (g/flask) wheat bran, 5; sugarcane bagasse, 1.5 and colloidal chitin, 0.075, moistened with 5mL of SR salt solution, and incubated at 25°C for sixteen days.

The ANOVA (Table 5) revealed the significance of the model since the model terms had values of Prob> F equal to 7.01 E-07, but the R^2 value of that model was 0.76.

The second order polynomial equation of Box-Behnken model obtained after applying the regression analysis of the experimental results was as follows:

$$Y= 371.167-24.289X_1+1.507X_2-8.967X_3+0.433X_1^2+26.77X_2^2-0.612X_3^2-2.323X_1X_2+0.555X_1X_3+1.062X_2X_3 \quad \text{Eq. (8)}$$

Where Y was the response (exochitinase production) and X_1, X_2, and X_3 were the coded values of the tested variables (temperature, addition of sugarcane bagasse and the volume of moistening agent) respectively.

In order to investigate the interaction between the experimental variables, the three dimensional response surface plots were constructed by representing the regression equation. Figure 6 a-c represents the response surface plots of temperature and the addition of sugarcane bagasse, temperature, and the volume of moistening agent, the addition of sugarcane bagasse, and the volume of moistening agent respectively while keeping the other variables at the zero level.

The competence of the constructed model was confirmed by performing an experiment under the optimized conditions. The exochitinase production was 26.259U/g ds which is in accordance with the predicted value 26.486U/g ds, confirming the validation of the model.

Table 4. Examined concentration of the key variables and results of Box-Behnken Design experiments with the predicted values by RSM and ANN**.**

Trials	Independent variable			Observed exochitinase (U/g ds)	Predictedexochitinase by RSM(U/g ds)	Predictedexochitinase by ANN(U/g ds)
	X1Temperature (oC)	X2 Sugarcane bagasse (g/flask)	X3 Volume of moistening agent(mL)			
1	25(-)	0.5(-)	5(0)	23.790	25.055	23.225
2	29(+)	0.5(-)	5(0)	25.952	28.050	26.522
3	25(-)	1.5(+)	5(0)	28.931	26.486	29.430
4	29(+)	1.5(+)	5(0)	21.465	20.187	20.883
5	25(-)	1(0)	3(-)	15.737	17.999	13.465
6	29(+)	1(0)	3(-)	8.503	11.491	7.692
7	25(-)	1(0)	7(+)	17.725	15.675	17.844
8	29(+)	1(0)	7(+)	20.333	18.045	21.229
9	27(0)	0.5(-)	3(-)	24.915	19.838	25.306
10	27 (0)	1.5(+)	3(-)	20.444	16.179	17.385
11	27(0)	0.5(-)	7(+)	21.510	23.224	20.821
12	27(0)	1.5(+)	7(+)	21.589	23.813	17.891
13	27(0)	1(0)	5(0)	18.071	16.521	15.966

Table 5. Analysis of Box-Behnken Design for exochitinase production.

Term	Regression coefficient	Standard error	t- test	P-value
Intercept	371.167	216.115	1.717	0.097
X_1	-24.289	15.530	-1.564	0.129
X_2	1.507	25.512	0.059	0.953
X_3	-8.967	6.574	-1.364	0.183
X_1^2	0.433	0.286	1.511	0.142
X_2^2	26.770	4.582	5.842	2.457 E-06
X_3^2	-0.612	0.286	-2.138	0.041
X_1X_2	-2.323	0.866	-2.683	0.012
X_1X_3	0.555	0.216	2.563	0.016
X_2X_3	1.062	0.866	1.227	0.230

F value = 10.197; P>F= 7.01 E-07; R^2=0.760; R =0.872; Adjusted R^2=0.685

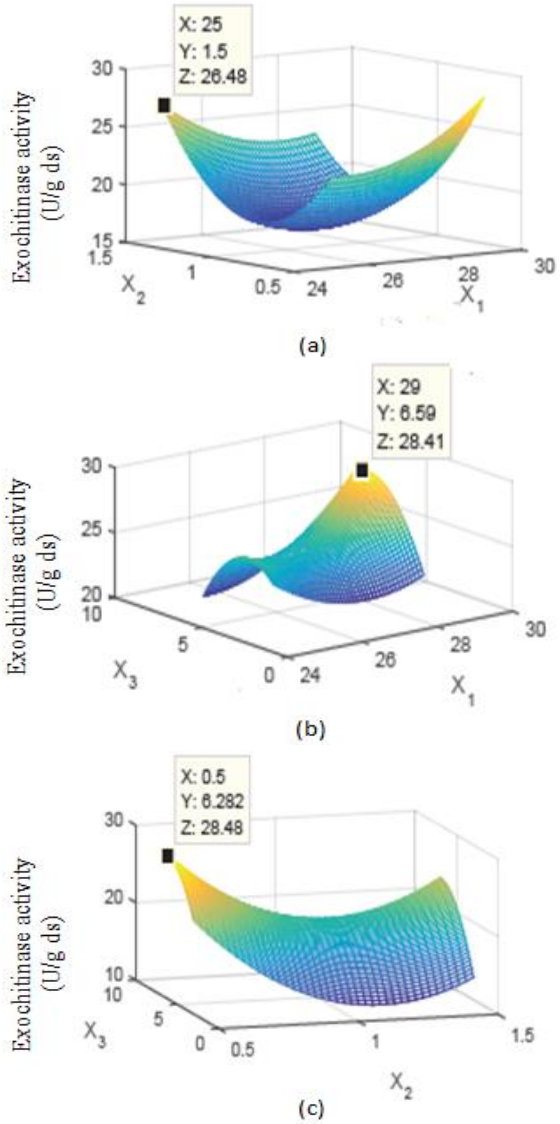

Figure 6. Response surface plot of exochitinase production

(a) Showing the interactive effects of $X_1$and X_2at X_3 = 0.

(b) Showing the Interactive effects of X_1 and X_3 at X_2= 0.

(c) Showing the Interactive effects of X_2 and X_3 at X_1= 0.

in which X_1 is the temperatures (25- 29°C), X_2 is the additions of sugarcane bagasse (0.5-1.5g/flask), and X_3 is the volumes of moistening agent (3-7mL).

3.2.3. Artificial Neural Network Model

The applied neural network was selected based on the fit for validation phase. The predicted results for exochitinase production using DANN are shown in table (4). The analysis of the data indicates that the predicted model was well-fitted since the R^2 value was 0.996. Also, the analysis of the data indicates that there was a small error between experimental and predicted values since the root mean square error was 0.67, and the overall average accuracy % was 96.3 %.

Some Properties of the Crude Exochitinase

The profile of the produced exochitinase at different pHs using a 0.2M acetate buffer and different temperatures is shown in figure 7. The results indicate that the enzyme was optimally active at pH 4.5 and 55°C using a 0.001g/mLsubstrate concentration. By incubation of the enzyme for different periods (up to 2h) without its substrate at pH ranging from 4 to 5 using a 0.2M acetate buffer, the enzyme retained 100 % of its activity for two hours at pH 4.5 and 5, but it lost 11.7 % of its activity after ninety minutes at pH 4. The thermal stability of the enzyme without the substrate at different temperatures ranging from 40 to 60°C was determined. The enzyme had a half-life time higher than two hours at temperature range from 40 to 55°C (figure 8).

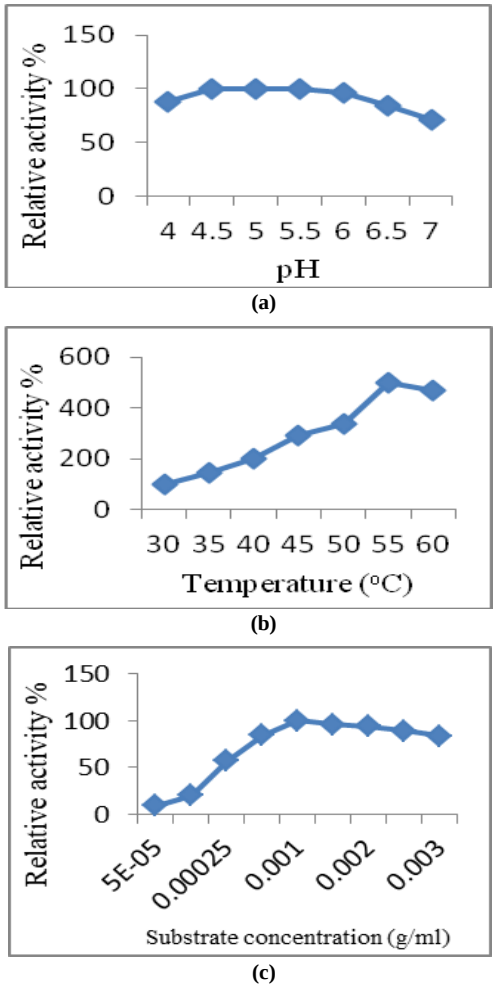

Figure 7. Effect of (A) the reaction pH (control is pH 5) (B) the reaction temperature (30°C is the control) (C) the substrate concentration (0.001g/mL is the control) on the activity of the crude exochitinase (the absence of error bars indicates that the errors are smaller than the symbols).

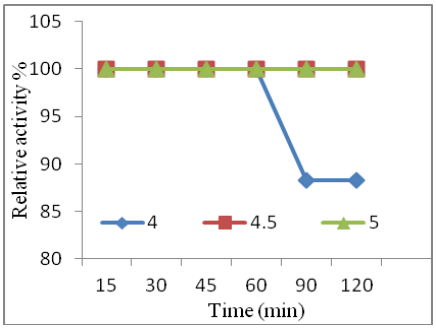

A

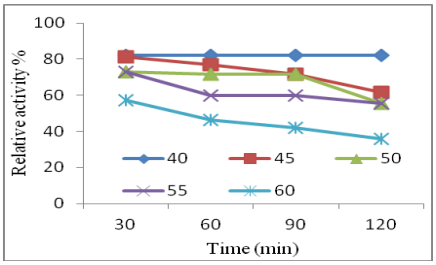

B

Figure 8. (A) The pH stability of the crude exochitinase at different time intervals. (B) The temperature stability of the crude exochitinase at different time intervals. The control in both experiments, is the activity of the enzyme at zero time (the absence of error bars indicates that the errors are smaller than the symbols).

3.3. Antifungal Activity of the Produced Exochitinase

The produced exochitinase showed antifungal activity against the phytopathogenic fungi *Rhizoctonia solani* and *Dothideomycetes* sp. as shown in figure 9.

A

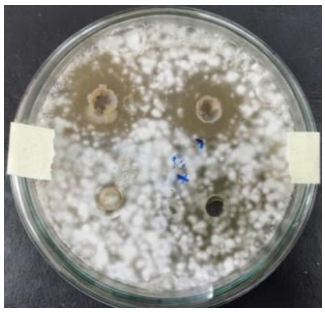

B

Figure 9. Antifungal activity of the produced exochitinase against A: *Rhizoctonia solani* B: *Dothideomycetes* sp. Strains.

4. Discussion

Exochitinases are chitinases capable of the hydrolysis of chitin from its terminal end; it has gained a great attention due to its various industrial, medical and agricultural applications (Sahaiand Manocha, 1993). Microorganisms are the highest chitinase producers as reported by Sridevi and Reddy, (2016). The environmental and the nutritional conditions required by the microorganisms have a crucial impact on the cost of the production process; for the use of agro-industrial residues is an economic approach (Sudhkar and Nagarajan, 2010 and Narendrakumar *et al*., 2015). Various agro-industrial residues as rice bran (Sudhakar and Nagarajan, 2010), wheat bran (De Freitas Soares *et al*., 2015), and sugarcane bagasse (Sudhakar and Nagarajan, 2011) have been used previously for the production of fungal chitinases. In this study the *Alternaria* sp. Sha strain isolated from marine organism wastes was used for the production of the enzyme by SSF using 5g of wheat bran supplemented with 1 % chitin as a substrate and moistened with 10mL of SR salt solution; the produced enzyme has an activity of 13.102U /g ds after a fourteen-day fermentation period. De Freitas Soares *et al*., (2015) reported the production of chitinase with the maximum activity of 6.2U/g ds by SSF of the same substrate using the fungus *Monacrosporium thaumasium*. The isolated microorganism was initially identified according to its cultural and morphological features then by the 18S rDNA technique. According to the 18S rDNA sequence, the evolutionary history of the isolated strain was inferred using the Maximum Likelihood method. The phylogenetic tree with the highest log likelihood indicated a 100 % similarity of the isolate with other *Alternaria* sp. strains. Evolutionary analyses have been conducted in MEGA6 (Molecular Evolutionary Genetics Analysis version 6.0) (Tamura *et al*., 2013). The production of chitinases using *Alternaria* sp. has been reported by other researchers (Abbasi *et al*., 2017; El-Shora *et al*., 2017; Ghanem *et al*., 2011).

The optimization of the nutritional and cultural conditions of the fermentation process is necessary to increase the yield of the enzyme production that consequently will decrease the cost. RSM is a popular statistical technique that has been used for the optimization of the production of various enzymes (Hashem *et al*., 2018). In the current study, sequential optimization of the exochitinase production was carried out in two phases. Firstly, seven variables were examined using the Plackett–Burman design in order to verify the significant factors. The results demonstrated a wide variation in the exochitinase productivity ranging from 2.901 to 16.521U/g ds. This reflects the importance of the initial enzyme production screening using statistical strategy for the selection of the fermentation medium components and the culture conditions that influence productivity. By calculating the main effect value of the examined variables, it was clear that the temperature, the addition of sugarcane bagasse and the volume of the moistening agent were the variables that exerted the highest main effect respectively and consequently were subjected to a further step of optimization. Additionally, from the calculated value of the main effect, it was evident that the temperature and the volume of the salt solution had

negative values. This confirms that positive effects on production were achieved when the temperature and the volume of the salt solution were adjusted to their low (-1) level values, while the opposite effect was shown with the other variables. The R^2value for the current applied model was 0.9919, suggesting that the variation of 99.19 % was due to the independent variables, while there was only a 0.81 % chance that the response was not due to the experimental model variables. The R^2 value (> o.9) indicates the accuracy of the model since it measures the degree of response exerted by the experimental variables (Edwards *et al*., 2008).

In the second step, the Box-Behnken design was applied to optimize the most significant variables. The optimization process increased the exochitinase productivity to reach 28.931U/g ds. Although the ANOVA results showed a high F value (10.197) and a low P value (7.01 E-07) of the model indicating the significant and the high potentiality impact of the model terms used in this design, but the R^2 value of the model was 0.76. RSM has been used successfully in the optimization of exochitinases (Kumar *et al*., 2012; Awad *et al*., 2017), but in this study, the R^2 value of the applied model indicated the lack of fitness of the model since it was less than 0.9. Therefore, the use of ANN has been examined in this study as an alternative tool in predicting the experimental results.

ANN has been considered as one of the most important methods used in modeling and optimization processes that have been applied in various fields (Astray *et al*., 2016; de Araujo Padilha *et al*., 2017; Cui *et al*., 2018). DANN is characterized by a larger number of hidden layers which is higher than the traditional ANN, and so the weight updates gradually moves toward the optimum solution with more accuracy (Serwa, 2017). In this study, the DANN module with three hidden layers (8, 7 and 8 neurons) was applied, and the analysis of the data presented better results than RSM in terms of the R^2 value which was 0.996.

The influence of pH on the enzyme activity was estimated using a 0.2M acetate buffer, and the results showed that the highest enzyme activity was achieved at acidic pHs ranging from 4.5 to 5, and the enzyme retained 100 % of its activity up to two hours in this range of pH. The former results agree with De Freitas Soares *et al*., (2015) who reported the production of fungal chitinase with the highest activity at pH 5.5.

In agriculture, the use of biocontrol agents as an alternative tool against pathogenic fungi can overcome the harmful effects of the current used strategies (A Veliz *et al*., 2017; Honari *et al*., 2018). *Rhizoctonia solani* is an important soil-borne fungus that causes difficult controllable diseases worldwide (Lahlali and Hijri, 2010; Woodhall *et al*., 2007; Yandigeri *et al*., 2015). In this study, the produced exochitinase showed antifungal activity against *Rhizoctonia solani.* The antifungal activity of chitinases against pathogenic fungi has been previously reported by Jankiewicz and Brzezinska, (2016), Velusamy and Kim, (2011) and Yandigeri *et al*., (2015).

5. Conclusion

DANN can be applied for the optimization of microbial enzymes as an alternative method to RSM. In the current study, DANN presented more accuracy in the prediction of the selected model with an R^2 value of 0.996 in comparison with the R^2 value of 0.76 using RSM. The produced exochitinase exhibited an antifungal activity against *Rhizoctonia solani.*

References

Abbasi K, Zafari D, Wick R. and Hamedan I. 2017. Evaluation of chitinase enzyme in fungal isolates obtained from golden potato cyst nematode (*Globodera rostochiensis*). *Žemdirbystė (Agriculture)*,**104(2):** 179-184.

Astray G, Gullón B, Labidi J. and Gullón P. 2016. Comparison between developed models using response surface methodology (RSM) and artificial neural networks (ANNs) with the purpose to optimize oligosaccharide mixtures production from sugar beet pulp. *Industrial Crops and Products*,**92:** 290-299.

Awad GE, Wahab WAA, Hussein M, El-diwany A and Esawy MA, 2017. Sequential optimizations of *Aspergillus awamori* EM66 exochitinase and its application as biopesticide. *J Appl Pharm Sci.*,**7(02):** 67-75.

Blaak H, Schnellmann J,WalterS, Henrissat B and Schermpf H. 1993. Characteristics of an exochitinase from *Streptomyces olivaceoviridis*, its corresponding gene, putative protein domains and relationship to other chitinases. *Euro J Biochem*, **214(3):** 659-669.

Box GE and Wilson KB. 1951. On the experimental attainment of optimum conditions. *J Royal Statistical Society: Series B (Methodological)*, **13(1),** 1-38.

Box GE and Behnken DW. 1960. Some new three level designs for the study of quantitative variables. *Technometrics*, **2(4):** 455-475.

Chavan SB and Deshpande MV., 2013. Chitinolytic enzymes: an appraisal as a product of commercial potential. *Biotechnol Progress*, **29(4):** 833-846.

Cui J, Li Y, Wang S, Chi Y, Hwang H and Wang P, 2018. Directional preparation of anticoagulant-active sulfated polysaccharides from *Enteromorpha prolifera* using artificial neural networks. *Sci Reports*, **8(1):** 3062.

de Araújo Padilha CE, de Araújo Padilha CA, de Santana Souza DF, de Oliveira, JA, de Macedo GR and dos Santos ES, 2017. Recurrent neural network modeling applied to expanded bed adsorption chromatography of chitosanases produced by *Paenibacillus ehimensis*. *Chem Eng Res and Des*, **117:**24-33.

de Freitas Soares FE, de Queiroz JH, Araújo JV, Queiroz PV, de Souza Gouveia A, Braga GMAM, De Morais SML and Braga FR. 2015. Statistical screening for the chitinase production by nematophagous fungi from *Monacrosporium* genu. *Afri J Microbiol Res*, **9(7):** 448-454.

Desai KM, Survase SA, Saudagar PS, Lele SS and Singhal RS. 2008. Comparison of artificial neural network (ANN) and response surface methodology (RSM) in fermentation media optimization: case study of fermentative production of scleroglucan. *Biochem Eng J*, **41(3):** 266-273.

Edupuganti S, Potumarthi R, Sathish T and Mangamoori LN. 2014. Role of feed forward neural networks coupled with genetic algorithm in capitalizing of intracellular alpha-galactosidase production by *Acinetobacter* sp. *BioMed Res int*, **214:** 361732-361740

Edwards LJ, Muller KE, Wolfinger RD, Qaqish BF and Schabenberger O. 2008. An R2 statistic for fixed effects in the linear mixed model. *Statis in Medicine*, **27(29):**6137-6157.

El-Shora HM, Khalaf SA and El-Sheshtawi SA. 2017. Biochemical characteristics of immobilized chitinase from *Alternaria infectoria*. *Microbiol Res J Int*,**22(1):** 1-10.

Ghanem KM, Al-Fassi FA and Farsi RM. 2011. Statistical optimization of cultural conditions for chitinase production from shrimp shellfish waste by *Alternaria alternata*. *Afric J Microbiol Res*, **5(13):** 1649-1659.

Gurunathan B, and Sahadevan R. 2011. Design of experiments and artificial neural network linked genetic algorithm for modeling and optimization of L-asparaginase production by *Aspergillus terreus* MTCC 1782. *Biotechnol and Biopro Eng*, **16(1):** 50-58.

Hamid R, Mahboob A, Ahmad MM, Abdin MZ and Javed S. 2013. Purification and characterization of thermostable chitinase from a novel *S. Maltophilia* strain. *Malaysian J Microbiol*, **9(1):** 7-12.

Hashem AM, Ismail SA, Hosny AE, Awad G. and Ismail SA. 2018. Optimization of *Dothideomycetes* sp. NrC-SSW chitosanase productivity and activity using response surface methodology. *Egy J Chem*,**61(6):** 973-987.

Honari H, Alborzian DA, Hosseini R, Akbari EM, Razavi SI and Etemad, ASM. 2018. The study of soil chitinolytic bacterial strains and their use against fungal pathogen *Alternaria alternata in vitro*. *Bio J Microorganism*,**25**: 63-74.

Hosny M.S., El-Shayeb N.A., Abood A. and Abdel-Fattah A.M. 2010. A potent chitinolytic activity of marine *Actinomycet*e sp. and enzymatic production of chitooligosaccharides. *Aust J Basic Appl Sci*, **4(4):** 615-623.

Jankiewicz U. and Swiontek-Brzezinska M. 2016. The role of exochitinase type A1 in the fungistatic activity of the rhizosphere bacterium *Paenibacillus* sp. M4. *Archives of Biol Sci*, **68(2):** 451-459.

Kumar DP, Singh RK, Anupama PD, Solanki MK, Kumar S, Srivastava AK. ans Arora DK. 2012. Studies on exo-chitinase production from *Trichoderma asperellum* UTP-16 and its characterization. *Ind J Microbiol*, **52(3):** 388-395.

Lahlali R and Hijri M. 2010. Screening, identification and evaluation of potential biocontrol fungal endophytes against *Rhizoctonia solani* AG3 on potato plants. *FEMS Microbiol Letters*, **311(2):** 152-159.

Mishraa SK, Kumarb S, and Singhd RK. 2016. Optimization of process parameters for α-amylase production using artificial neural network (ANN) on agricultural wastes. *Curr Trends Biotechnol Pharm*, **10(3**): 248-260.

Narendrakumar G, Namasivayam SKR and Singh RALS. 2015. Production and optimization of extracellular fungal chitinase produced by *Metarhizium anisopliae* (M.) Sorokin through submerged and solid state fermentation. *Res J of Pharm and Technol*, ***8*(3):** 280.

Neto Í, Andrade J, Fernandes AS, Pinto Reis C, Salunke JK, Priimagi A, Candeias NR and Rijo P. 2016. Multicomponent Petasis-borono Mannich preparation of alkylaminophenols and antimicrobial activity studies. *Chem Med Chem*, **11(18):** 2015-2023.

Plackett and Burman. 1946. The Design of optimum multifactorial experiments, *Biometrika*, **33 (4)**: 305–25.

Ramkumar A, Sivakumar N, Gujarathi AM, and Victor R. 2018. Production of thermotolerant, detergent stable alkaline protease using the gut waste of *Sardinella longiceps* as a substrate: Optimization and characterization. *Sci Reports*, **8(1):** 12442

Rustiguel CB, Jorge JA and Guimarães LHS. 2012. Optimization of the chitinase production by different *Metarhizium anisopliae* strains under solid-state fermentation with silkworm chrysalis as substrate using CCRD. *Adv Microbiol*, **2(03):** 268.

Sahai AS and ManochaMS. 1993. Chitinases of fungi and plants: their involvement in morphogenesis and host-parasite interaction. *FEMS Microbiol Rev*, **11(4):** 317-338.

Serwa A. 2017. Optimizing activation function in deep artificial neural networks approach for landcover fuzzy pixel-based classification. *Int J Remote Sensing Appl*, **7:**1-10.

Shivalee A, Lingappa K. and Mahesh D. 2018. Influence of bioprocess variables on the production of extracellular chitinase under submerged fermentation by *Streptomyces pratensis* strain KLSL55. *Genet Eng Biotechnol*, **16**:421-426.

Sridevi S. and Reddy DSR. 2016. Production of chitinase from aquatic using *Aspergillus oryzae* and *Streptomyces griseus* under solid state fermentation. *Indo Americ J Pharm Res*, **6(3).**

Sudhakar P. and Nagarajan P. 2010. Production of chitinase by solid state fermentation from rice bran. *Intl J Environ Sci Develop*, **1(5):** 435-440.

Sudhakar P. and Nagarajan P. 2011. Production of chitinase by solid state fermentation from sugar cane bagasse. *Int J Chem. Sci*.: **9(1).**

Tamura K, Stecher G, Peterson D, Filipski A and Kumar S. 2013. MEGA6: Molecular Evolutionary Genetics Analysis version 6.0. *Mol Bio Evol*, 30: 2725-2729.

Veliz E, Martínez-Hidalgo P and M Hirsch A. 2017. Chitinase-reducing bacteria and their role in biocontrol. *AIMS Microbiol*,**3(3):** 689-705.

Velusamy P and Kim KY. 2011. Chitinolytic activity of *Enterobacter* sp. KB3 antagonistic to *Rhizoctonia solani* and its role in the degradation of living fungal hyphae. *Int Res Microbiol*, **2(6)**: 206-214.

Woodhall JW, Lees AK, Edwards SG and Jenkinson P. 2007. Characterization of *Rhizoctonia solani* from potato in Great Britain. *Plant Pathol*, **56(2):** 286-295.

Yandigeri MS, Malviya N, Solanki MK, Shrivastava P and Sivakumar G. 2015. Chitinolytic *Streptomyces vinaceusdrappus* S5MW2 isolated from Chilika lake, India enhances plant growth and biocontrol efficacy through chitin supplementation against *Rhizoctonia solani*. *World J Microbiol Biotechnol*, **31(8):** 1217-1225.

Young VL, Simpson RM and Ward VK. 2005. Characterization of an exochitinase from *Epiphyas postvittana* nucleopolyhedrovirus (family Baculoviridae). *J General Virol*, **86(12):**3253-3261.

JJBS

Volume 12, Number 5,December 2019
ISSN 1995-6673
Pages 553 - 560

Jordan Journal of Biological Sciences

Reproductive Biology of Pacific Oyster (*Crassostrea gigas*): A Decade after the Tsunami Disaster in Aceh, Indonesia

Lili Kasmini[1], Ternala A. Barus [1*], M. Ali Sarong[2], Miswar Budi Mulya[1] and Agung Setia Batubara[3]

[1]*Faculty of Mathemathics and Science, Universitas Sumatera Utara, Medan 20155;* [2]*Faculty of Teacher Training and Education;* [3]*Department of Aquaculture, Faculty of Marine and Fisheries, Universitas Syiah Kuala, Banda Aceh 23111, Indonesia.*

Received January 6, 2019; Revised February 17, 2019; Accepted March 1, 2019

Abstract

The reproductive biology of pacific oysters (*Crassostrea gigas*) was studied in the coastal area of Banda Aceh City, Aceh Province, Indonesia. This study was conducted over six months from July to December, 2017. The samples were collected following the seasons. July to August represented the dry season, while September to October represented the transition season, and November to December had been within the rainy season. Surveys and observations were conducted at two locations, Tibang and Ulee Lheue, where samples were collected with a minimum of 150 samples per location per month. Data collection is done by the line transect method. The results of the analysis showed that the male oyster gonad first matured at a total length of 26.40 mm in Tibang and at the total length of 25.45 mm in Ulee Lheue. Furthermore, the female oyster gonad first matured at 20.46 mm of total length in Tibang and at a total length of 25.24 mm in Ulee Lheue. The range of oyster fecundity in Tibang is between 7,487,888-34,511,625 eggs/ind with an average fecundity reaching 17,360,821 eggs/ind, whereas the range of oyster fecundity in Ulee Lheue was between 9,237,258-40,575,863 eggs/ind with an average fecundity reaching 17,108,206 eggs/ind. The total number of the collected oyster samples was 1800 specimen, and all the samples were in the adult category. In addition to sex determination of the oysters into males and females, the oyster hermaphrodite sex is also found. The results of gonadal observation show that oysters are hermaphrodite synchronous (male and female gonads mature at the same time).

Keywords: Oyster, C*rassostrea*, Gonad, Reproductive, Fecundity, Hermaphrodite

1. Introduction

The tsunami in Aceh on December 26, 2004 occurred more than a decade ago (14 years ago). The earthquake in the Andaman Sea caused a tsunami in Aceh and claimed 130,000 human lives (Frankenberg *et al.*, 2008). In addition to causing human casualties, the tsunami also damaged the coastal environment which previously served as a habitat for both living flora and fauna organisms. It is known that the height of the tsunami waves in Aceh reached 30 m due to the 9.3SR earthquake which has damaged the coastal environment (Suppasri *et al.*, 2015).

Damage caused by tsunamis causes changes in coastal geomorphology, topography, and soil cover (Bayas *et al.*, 2011). Based on previous research, the effects of tsunami waves caused damage to corals in Aceh reaching up to 31 % in the low to medium category and 15 % in the heavily-damaged category (Hagan *et al.*, 2007). Furthermore, the tsunami also damaged 32,004 hectares of mangrove forests and coastal vegetation (Wibisono and Suryadiputra, 2006).

Tsunami waves that occurred in Aceh traveled up to a radius of 3-4 km from the coastline (Hagan *et al.*, 2007). This caused mudflows from the seabed to cover the surface of the land that was passed by the tsunami waves. Tsunami mud residues allowed changes in the ecology of the estuary area after the disaster occurred. One of the organisms that live in the estuary area is oysters.

Oysters are organisms that are very sensitive to environmental changes and can be indicators of pollution in an area (Sarong *et al.*, 2015; Astuti *et al.*, 2016). Based on previous studies that have been carried out in Aceh Province, oysters which are most commonly found consist of five species, included in two genera, namely the genus Ostrea and the genus Crassostrea, consisting of *C. virginica*, *C. gigas*, *C. iridescens*, C.*angulata*, and *O. edulis* (Octavina *et al.*, 2014). One of the mostly common species found is *C. gigas*. The *C. gigas* are reported to contribute to 80 % of the world's oyster trade and have been cultivated in sixty-six countries (Keightley *et al.*, 2015).

Research on oysters in Aceh, includes the analysis of heavy metal content in oysters (Sarong *et al.*, 2015; Astuti *et al.*, 2016), community structure of meat oysters (Fadli *et al.*, 2012; Octavina *et al.*, 2014), length-weight relationships, and oyster condition factors (Octavina *et al.*, 2015; Kasmini *et al.*, 2018). However, research on the reproductive biology of oysters after the tsunami phenomenon that struck in 2004 has not been carried out; thus this study would be an important contribution to the

* Corresponding author e-mail: ternala58@gmail.com.

development of Aceh oysters in the future, especially for oyster conservation or cultivation.

2. Methods

2.1. Time and Location

The current research was carried out in the coastal area of Banda Aceh City over the period of six months from July to December, 2017. The samples were collected following the seasons where July to August represented the dry season, while September to October represented the transition season, and November to December had been within the rainy season.

2.2. Data Collection

The samples were taken from two research locations, Tibang ($5^0$33'36.7" N, $95^0$17'22.8" E; $5^0$33'21.0" N, $95^0$17'11.7" E; $5^0$33'01.6" N, $95^0$17'09.5" E) and Ulee Lheue ($5^0$35'25.1" N, $95^0$21'03.5" E; $5^0$35'47.0" N, $95^0$20'50.8" E; $5^0$35'36.2" N, $95^0$20'44.4" E). Each location was divided into three research stations. The collection of the samples was carried out using a purposive sampling method, and a l ine transect method. Every month, 150 samples were collected randomly from each location consisting of fifty samples per station. The samples that have been obtained were taken to the Marine and Fisheries Faculty of the Marine Biology Laboratory for further analysis. The oyster samples were then identified based on Batista *et al.* (2008). The collected samples were then separated from each other to facilitate the measurements of length and weight. Length measurements were performed using a d igital caliper (Precision Measuring Error = 0.01 mm), and weight was taken for each individual using a d igital scale (Pocket Scale, MH-Series, Error = 0.01 g).

The preservation of the oyster's body was performed using 10 % NBF (Neutral Buffer Formalin). The analyses of oyster reproduction biology, including histology examination, gonad maturity level, and fecundity were carried out at the Pathology Laboratory, Brackishwater Aquaculture Station (BBAP) Ujong Batee, Ministry of Maritime Affairs and Fisheries, Indonesia.

2.3. Data Analysis

2.3.1. Gonad Maturity Level

The observation of the level of gonad maturity was done visually according to Fabioux *et al.* (2005). This observation aims at determining the maturity and seeing the female and male reproductive organs, so that the size of the oyster body when the gonad is mature can be estimated. For this purpose, oysters with various sizes have been distributed in several groups or classes based on body size. Data on gonadal maturity are then correlated with the length and weight of the oysters in each class. The stomach of the oyster, the gonad shape, size, color and texture were all observed in addition to the presence of sperms or oocytes. Then the gonads were preserved and examined histologically according to the procedure described earlier (Roberts, 2012). The maturity level of the gonads was also determined based on g onadal anatomy and morphology, weighing of gonads, determination of gonadosomatic index, and based on observations of histological preparations according to Roberts (2012).

2.3.2 Gonadosomatic Index

The measurement of the gonadosomatic index (GSI) was done by taking samples of the oysters that have been weighed and measured in length, on w hich surgery has been done to separate the gonads. They were finally weighed using a d igital scale. The GSI is calculated according to Gaughan and Mitchell (2000) by the formula:

$$\mathbf{GSI\ (\%) = \frac{Wg}{Wt}\ x\ 100}$$

Where the GSI = gonadosomatic index (%), Wg = weight of the gonad (g), and Wt = weight of the body (g).

2.3.3 Fecundity

Fecundity was measured with the formula by the gravimetrics method based on Adenike (2013) as follows:

$$F = \frac{Wg}{Ws} \times Fs$$

Where F = fecundity/number of eggs (grains), Wg = weight of the gonad (g), Wt = partial gonad weight (g), and Fs = number of eggs in parts of gonad (grains).

2.3.4 Sex Dimorphism

The observation of sex dimorphism was done to differentiate between the males and females of the oysters morphologically or by physical appearance. For this reason, the sampled oysters were observed visually regarding their body color and shape. The oysters taken were recorded morphologically, and the appearance of the shape and color of the gonads were observed. They were then grouped according to the same morphological appearance and sex that were confirmed on the basis of the histological examination under a microscope.

2.3.5 Histological Analysis and Reproductive Cycle

The sex and gonad maturity of each oyster was determined based on a histological examination. The procedures for making histology preparations using the slice method were done according to Roberts (2012).

2.3.6 Sex Ratio

The sex ratio analysis aims at comparing the numbers of male to the number of female individuals in a population. The observation of the level of gonad maturity and histology examination can help determine the sex of the oysters, thus the ratio of the numbers of females and males can be determined. Sex ratio is calculated by the formula of Adenike (2013) as follows:

$$\mathbf{Sex\ ratio = \frac{Number\ of\ male\ oyste}{Number\ of\ female\ oyster}}$$

2.4. Statistical Analysis

The statistic data analysis was subjected to the chi-square test followed by the Duncans multi-range test applied for cheking the oyster sex ratio and gonadosomatic index between the same and different locations using SPSS ver. 22.0.

3. Results

3.1. Sex Ratio and Gonadosomatic Index

Observations during the study showed that the size of the oysters was between the total lengths of 20.40-136.22 mm with an average size of 46.29 mm concerning the 1800 samples at both locations of the study (Tibang and Ulee Lheue). The results of male sex ratio (SR) analysis show that the highest value was in October (31.33 %) at the Tibang location and during September (36 %) at the Ulee Lheue location. The the highest value of female SR was found in December (75.33 %) at the Tibang location and in August (66.67 %) at the Ulee Lheue location. Furthermore, this study found oysters with hermaphrodite genitals, and their highest SR values were found in September (28.00 %) at Tibang and in October (28.67 %) at Ulee Lheue locations (Tables 1 and 2).

The results show that the sex ratio (SR) studied at two research sites (Tibang and Ulee Lheue) was dominated by the female ratio with a mean value of 65.11 % in Tibang area and 59.55 % at Ulee Lheue location. Male oysters have an SR value of 20.22 % at Tibang location and 28.11 % at Ulee Lheue location. This study also detected hermaphrodite oysters, where the average ratios were 14.67 % at Tibang location and 12.33 % at Ulee Lheue location. Based on the average SR results, female and hermaphroditic sexes at Tibang sites were higher than those at Ulee Lheue, but lower than the mean values of male SR.

Oyster SR values fluctuate every month, which is most significantly seen through the genitals of hermaphrodites. At the Tibang location, the value of hermaphrodite SR increased in July to September and decreased from October to December, whereas at the location of Ulee Lheue the value of hermaphrodite SR continued to decline in July to September and increased in October, but decreased again between November to December (Figure 2a and b).

An analysis of gonadosomatic index (GSI) of female oysters shows that the highest average value was found in October (4.53 %) in Tibang and in November (4.80 %) in Ulee Lheue. The highest mean male GSI score was found in October (3.81 %) in Tibang and in November (5.11 %) in Ulee Lheue. Furthermore, the highest mean hermaphrodite GSI values were found in October in Tibang (4.81 %) and in December (5.05 %) in Ulee Lheue (Tables 5 and 6).

3.2. Gonad Maturity Level

In this study, male oysters first gained gonad at the total length of 26.40 mm in Tibang and at 25.45 mm in Ulee Lheue. This suggests that the mature size of male oyster gonads does not significantly occur between the two different sites. Furthermore, over the period of six months, the study has found oysters with the highest gonadal maturity in two locations occurring in August 96.77 % (Tibang) and 92.31 % (Ulee Lheue) respectively (Table 3 and Figure 3).

Also, this study found female oysters' gonads that first matured at the size of 20.46 mm in Tibang and at 25.24 mm in Ulee Lheue. Furthermore, over the period of six months, the study found oysters in the highest mature gonad state in two locations (Tibang and Ulee Lheue) occurring in August with the same value reaching up to 96 % (Table 4 and Figure 4).

3.3. Gonad Histology and Fecundity

The histologic results of the gonads indicate that reproductive oysters are hermaphrodite (Figure 6). Furthermore, the gonad of mature female oysters has a maximum egg size of ± 50 µm which means that eggs cannot be seen visually without the aid of tools. The size of oysters with mature gonads in Tibang ranged from 20.46 to 94.30 mm with a fecundity range between 7,487,888 and 34,511,625 eggs/ind with an average of fecundity of 17,360,821 eggs/ind.

The size of oysters with ripe gonads in Ulee Lheue ranged from 25.24 to 110.87 mm with a fecundity range between 9,237,258 and 40,575,863 eggs/ind and a fecundity average of 17,108,206 eggs/ind. Regression results showed a very close relationship (Tibang r = 0.95% and Ulee Lheue r = 0.953%), in which the number of eggs increases with the increase of oyster size (Figure 5).

4. Discussion

Based on sex identification, hermaphrodite oysters were found in addition to male and female oysters at the time of the study. The sex ratio (SR) during the study found oysters dominated by the presence of females in two locations, where the mean value was 65.11 % in the Tibang area and 59.55 % in the Ulee Lheue location (Table 5). The SR values of oysters fluctuate each month, with the most significant fluctuation occurring in the hermaphrodites. At the Tibang site, the hermaphrodite SR value experienced an increase in July to September and decreased in October to December, while at the Ulee Lheue location, the SR hermaphrodite value continued to decline in July to September, and experienced an increase in October, but there was a further decline in November to December (Figure 2).

The results of gonadal observation show that oysters are hermaphrodite synchronous (male and female gonads mature at the same time) (Figure 6). However, other studies mention that in the reproductive cycle, oysters are protandrous hermaphrodites whose life begins with the male genitals turning into females several years later if the environment is good and when sufficient nutrition is available (Westphal *et al.,* 2015). According to Dheilly *et al*. (2012) oysters are generally protandrous hermaphrodites, but there are several cases of synchronous hermaphrodite oysters found because the gonads are labile. Thus, there are changes in the physiological properties of the oyster bodies in the study locations caused by environmental factors. Changes in physiological properties may occur due to tsunami disasters or other environmental factors such as global warming or pollution. However, the anthropogenic pressure of seawater can be a problem in the development of aquatic organisms (Hamdani and Soltani-Mazouni, 2011).

Analysis of the reproductive aspects of oysters showed spawning peaks occurring in August (Table 3 and Table 4). This is due to the fact that both male and female oysters are dominated by mature categories. In August, especially in Banda Aceh, the peak of the dry season occurred, when temperatures were relatively high and rain did not occur. The dry season that occurs in August causes an increase in

water salinity which then induces the spawning season of oysters. This is consistent with the results of research conducted by Dheilly *et al*. (2012) which states that oyster spawning peaks occur in the summer because the gametogenesis process occurs when the water temperature increases. This finding was also strengthened by the results of research conducted by Fabioux *et al*. (2005) which state that the gametogenesis process in *C. gigas* develops during summer with water temperatures being above 19 ^{0}C and salinity>30 ppt. In other studies, it was also mentioned that first-time oyster gonads develop in April and continue to grow until they become matured in August when the initial spawning process occurs and continues until September (Li *et al*., 2000).

In this study, the male oyster gonad was first ripe at 26.40 mm in Tibang and at 25.45 mm in Ulee Lheue. This shows that the size of first-time mature gonad of male oysters did not differ significantly between the two different locations. The gonads were first mature in female oysters at 20.46 mm in Tibang and at 25.24 mm in Ulee Lheue. According to Westphal *et al*. (2015), the genus *Crassostrea* first reproduced (spawning) at a size of 20 mm. Thus all of the oysters collected from the Tibang and Ulee Lheue estuaries are in the adult category.

Based on the results of the present study, it appears that the ability of oyster recruitment is very high. This is indicated by the high number of eggs (fecundity), at an average of 17,360,821eggs/ind in Tibang and 17,108,206 eggs/ind in Ulee Lheue. The study found a positive correlation (r) between the addition of length and egg production in oysters with a value reaching 95 % in both study locations, where the size of 110.87 mm (the highest size of female genital oysters) can produce more than 40,000,000 eggs (Figure 5). If an organism has a high recruitment ability, it c an maintain the stability of its population in nature (Bakun and Broad, 2003). Furthermore, there is no dispensatory dynamics in oysters similar to the phenomenon that often occurs in fish, where the recruitment ability is low due to the difficulty of finding a p artner or allee effect (Myers *et al*., 1995). In addition to that, the environment that often experiences eutrophication has a positive influence on oysters for the development of reproductive organs more often than the environment which is poor in organic content (Fabioux *et al*., 2005). It is known that oyster reproductive activity (recruitment) is done by random removing of eggs and sperm into the waters when stimuli for spawning are detected (Westphal *et al*., 2015).

The maximum size of *C. gigas* eggs with mature gonads during the study only reached ± 50 µm and that is why the eggs could not be seen visually. This is consistent with the results of research conducted by Lango-Reynoso *et al.* (2000) stating that the size of *C. gigas* eggs matured in gonads ranging from 31 to 60 µm. Furthermore, in other studies, it w as stated that the maximum size of *C. gigas* eggs in mature conditions reached 48.7 µm (Li *et al*., 2000).

Thus, the size of the oyster is very important as an indicator of egg-laying productivity. The measurement shows reproductive performance and its association with the process of recruiting new offspring of oysters. In male oysters the number is much less than in female oysters, so the ability of oyster regeneration will be very fast due to the fact that the role of female oysters are very significant because of the feature of egg production. Oysters with mature gonads can be found every month, which means that oysters can spawn throughout the year.

Table 1. Sex ratio (SR) and gonadosomatic index (GSI) *C. gigas* at Tibang

Month	Ind	Male Oyster		Female Oyster		Hermaprodite	
		SR (%)	GSI (%)	SR (%)	GSI (%)	SR (%)	GSI (%)
July	150	21.33	0.53-8.51 2.73±1.45	68.67	0.08-14.32 2.57±1.83	10.00	0.40-6.89 3.24±1.93
August	150	20.67	1.22-8.60 3.71±1.62	66.67	0.50-17.67 3.85±2.31	12.67	0.54-7.87 3.44±1.80
September	150	14.67	0.82-5.93 2.82±1.37	57.33	1.08-12.27 3.78±1.83	28.00	0.88-11.85 3.80±1.85
October	150	31.33	0.41-11.57 3.81±2.77	48.00	0.31-11.97 4.53±2.46	20.67	0.80-18.60 4.81±4.26
November	150	14.67	1.43-7.33 3.81±1.64	74.67	0.48-11.25 4.18±1.98	10.67	0.75-6.88 3.89±1.75
December	150	18.67	0.39-6.38 3.25±1.70	75.33	0.58-9.91 3.53±1.98	6.00	0.75-5.17 2.84±1.73

Table 2. Sex ratio (SR) and gonadosomatic index (GSI) *C. gigas* at Ulee Lheue

Month	Ind	Male Oyster		Female Oyster		Hermaprodite	
		SR (%)	GSI (%)	SR (%)	GSI (%)	SR (%)	GSI (%)
July	150	32.67	0.04-6.97 0.78±1.40	57.33	0.11-5.58 1.47±1.37	10.00	0.35-4.81 1.72±1.45
August	150	26	0.04-6.26 1.85±1.33	66.67	0.01-12.17 2.64±2.13	7.33	0.57-6.99 3.50±1.76
September	150	36	0.77-13.85 4.06±3.05	60	0.30-16.73 3.61±2.66	4	0.39-2.97 1.77±1.04
October	150	25.33	0.42-12.36 3.25±2.23	46.00	0.60-10.26 3.87±1.92	28.67	0.77-10.24 3.81±2.03
November	150	20.67	1.02-19.06 5.11±3.35	63.33	0.34-16.56 4.80±2.44	16.00	0.35-9.54 4.54±2.33
December	150	28.00	0.95-8.10 3.00±1.56	64.00	0.05-16.56 3.56±2.42	8.00	1.58-9.55 5.05±2.62

Table 3. Gonad maturity level of male oyster at Tibang and Ulee Lheue

Month	Tibang						Ulee Lheue				
	Ind	Gonad maturity level (%)					Ind	Gonad maturity level (%)				
		I	II	III	IV	V		I	II	III	IV	V
July	32	3.13	0.00	3.13	90.63	3.13	49	73.47	6.12	4.08	16.33	0.00
August	31	0.00	0.00	3.23	96.77	0.00	39	7.69	0.00	0.00	92.31	0.00
September	22	0.00	50.00	27.27	18.18	4.55	54	20.37	59.26	9.26	9.26	1.85
October	47	0.00	14.89	14.89	44.68	25.53	38	0.00	15.79	21.05	28.95	34.21
November	22	0.00	9.09	63.64	27.27	0.00	31	3.23	16.13	35.48	45.16	0.00
December	28	0.00	0.00	53.57	42.86	3.57	42	0.00	4.76	21.43	73.81	0.00

Table 4. Gonad maturity level of female oyster at Tibang and Ulee Lheue

Month	Tibang						Ulee Lheue				
	Ind	Gonad maturity level (%)					Ind	Gonad maturity level (%)				
		I	II	III	IV	V		I	II	III	IV	V
July	103	2.91	2.91	9.71	77.67	6.80	86	5.81	5.81	33.72	48.84	5.81
August	100	0.00	0.00	2.00	96.00	2.00	100	3.00	0.00	1.00	96.00	0.00
September	86	3.49	13.95	24.42	24.42	33.72	90	18.89	18.89	23.33	25.56	13.33
October	72	0.00	30.56	20.83	33.33	15.28	69	1.45	17.39	27.54	47.83	5.80
November	112	0.00	0.89	27.68	71.43	0.00	95	0.00	16.84	32.63	50.53	0.00
December	113	0.00	2.65	35.40	61.95	0.00	96	3.13	8.33	33.33	55.21	0.00

Table 5. The statistical analysis of SR and GSI according to each sampling location. The values in the same row followed by different superscripts are significantly different (P<0.05).

Location	Variable	Male	Female	Hermaprodite
Tibang	SR (%)	14.67-31.33 20.22±6.15^{a}	48-75.33 65.11±10.62^{b}	6-28 14.67±8.13^{a}
	GSI (%)	2.73-3.81 3.35±0.49^{a}	2.57-4.53 3.74±0.67^{a}	2.84-4.81 3.67±0.68^{a}
Ulee Lheue	SR (%)	20.67-36 28.11±5.49^{b}	46-66.67 59.55±7.39^{c}	4-28.67 12.33±8.93^{a}
	GSI (%)	0.78-5.11 3.00±1.54^{a}	1.47-4.8 3.32±1.14^{a}	1.72-5.05 3.39±1.39^{a}

Table 6. The comparative analysis of SR and GSI at the Tibang and Ulee Lheue locations. The values in the same row followed by different superscripts are significantly different (P<0.05).

Sex	SR (%)		GSI (%)	
	Tibang	Ulee Lheue	Tibang	Ulee Lheue
Male	14.67-31.33 20.22±6.15^{a}	20.67-36 28.11±5.49^{a}	2.73-3.81 3.35±0.49^{a}	0.78-5.11 3.00±1.54^{a}
Female	48-75.33 65.11±10.62^{a}	46-66.67 59.55±7.39^{a}	2.57-4.53 3.74±0.67^{a}	1.47-4.8 3.32±1.14^{a}
Hermaprodite	6-28 14.67±8.13^{a}	4-28.67 12.33±8.93^{a}	2.84-4.81 3.67±0.68^{a}	1.72-5.05 3.39±1.39^{a}

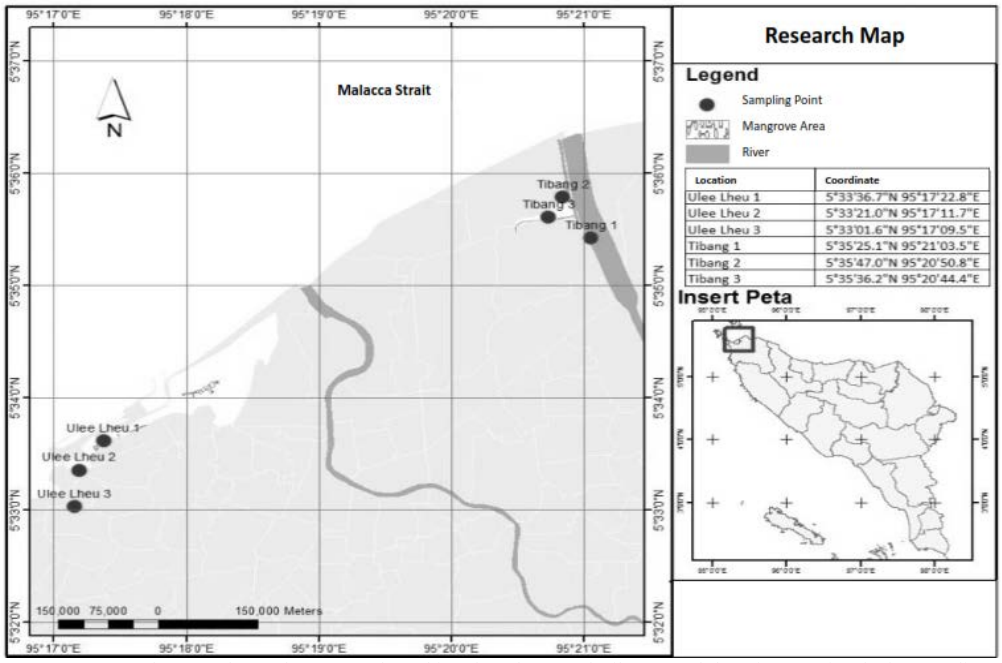

Figure 1. Research map. The study was conducted in Ulee Lheue and Tibang, each location consisted of 3 sampling points.

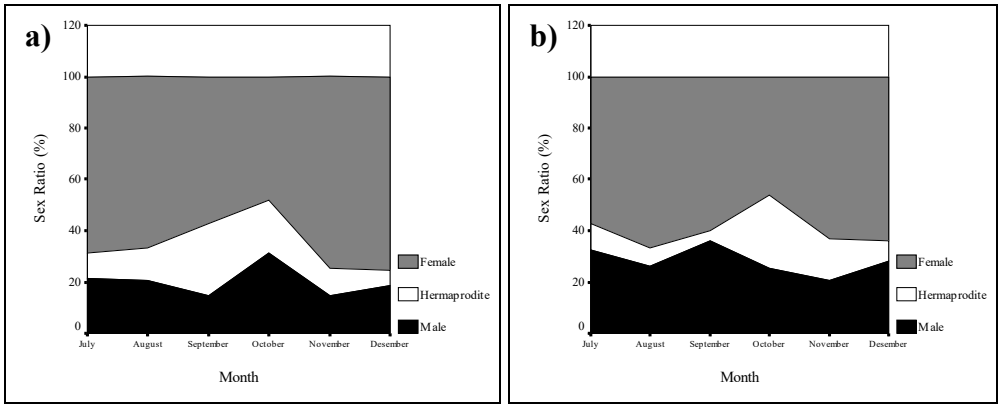

Figure 2. Sex ratio ratio (SR) oyster Crassostrea gigas, where a) Tibang location and b) the location of Ulee Lheue.

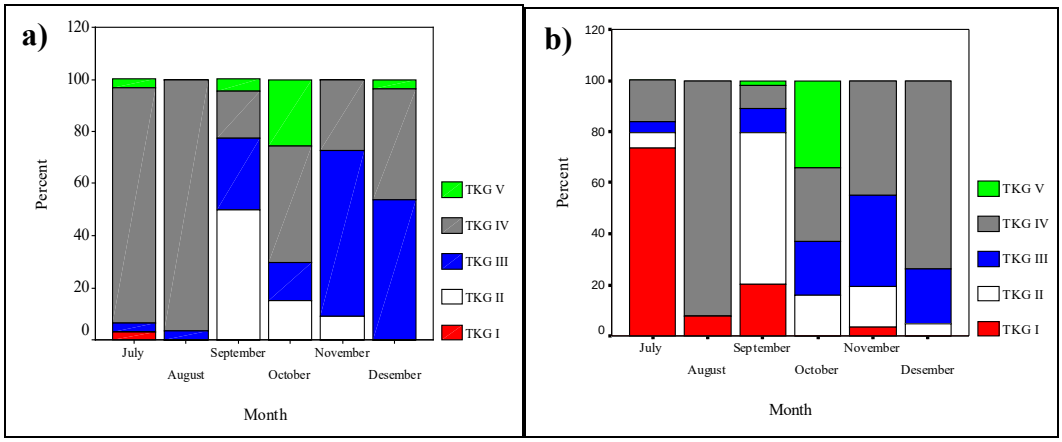

Figure 3. Percentage of mature male oyster gonad maturity levels (TKG) in a six-month study, where a) loaction of Tibang and b) Ulee Lheue.

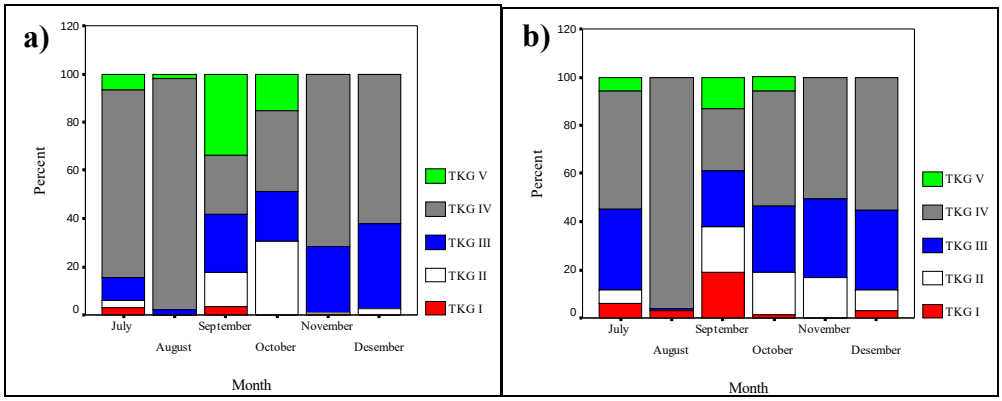

Figure 4. Percentage of mature female oyster gonad maturity levels (TKG) for 6 months of study, where a) loaction of Tibang and b) Ulee Lheue.

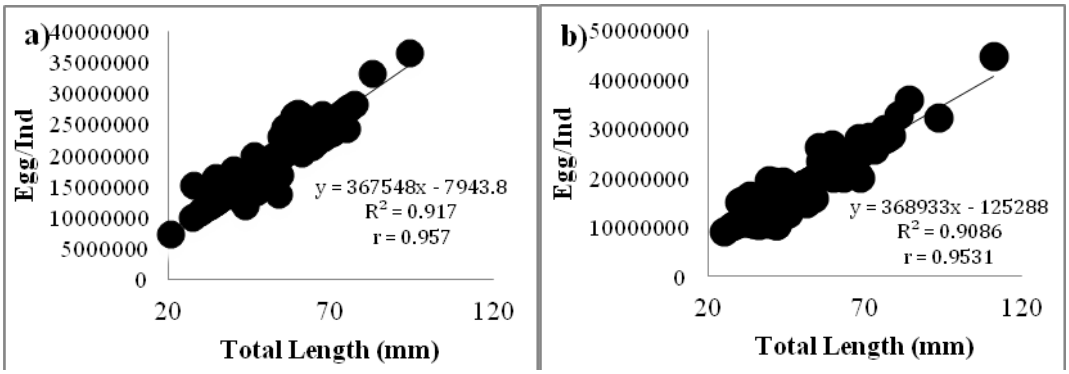

Figure 5. Regression of total length (mm) and oyster fecundity (egg/ind), where a) is Tibang and b) Ulee Lheue

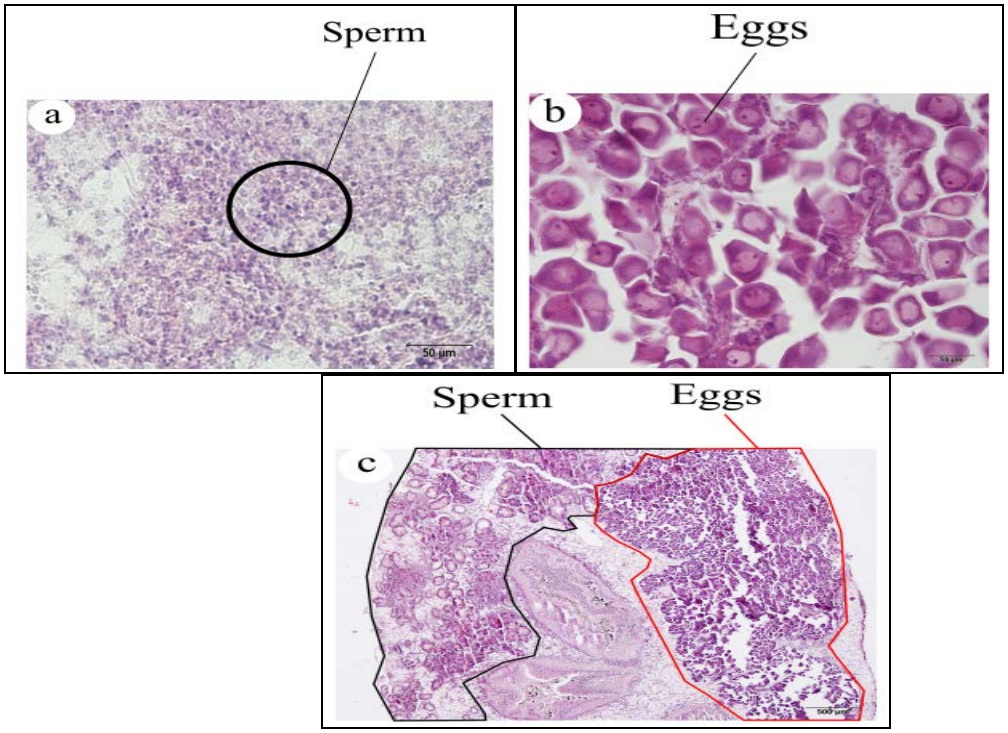

Figure 6. Histological appearance of oyster gonads, a) male, b) female, c) hermaphroditic.

5. Conclusion

The male oyster gonad first matured at 26.40 mm in Tibang and at 25.45 mm in Ulee Lheue. Furthermore, the female oyster gonad first matured at 20.46 mm in Tibang and at 25.24 mm in Ulee Lheue. The range of oyster fecundity in Tibang Village is between 7,487,888 and 34,511,625ggs/ind with an average fecundity reaching 17,360,821 eggs/ind; the range of oyster fecundity in Ulee Lheue was between 9,237,258 and 40,575,863eggs/ind with and average fecundity reaching 17,108,206 eggs/ind.

In addition to the male and female oysters, oysters of the hermaphrodite sex were also found.

Conflict of interest

The authors declare that there is no conflict of interest.

Acknowledgement

This study was supported by Kemenristek Dikti through "Penelitian Disertasi Doktor 2018" scheme. Therefore, the authors thank Kemenristek Dikti for supporting this study. The authors would like also to express appreciation for Mr. Muchlis, Ms. Nur Masyitah, and Ms. Roza Noviana for their assistance during field and laboratory works.

Author contribution

L.K.: the author is responsible for data collection, sample maintaining, data analysis, and manuscript drafting; T.A.B.: the author is responsible for developing of the study design, supervision, data validation, review and editing of the draft manuscript; M.A.S.: developing of the study design, supervision, data validation, review and editing the draft manuscript; M.B.M.: research supervision, data validation, review and editing of the draft manuscript; A.S.B.: data collection, sample maintaining, data analysis and validation. All authors read and approved the final manuscript.

References

Adenike FA. 2013. The sex ratio, gonadosomatic index, stages of gonadal developmentand fecundity of Sompat Grunt, *Pomadasys jubelini* (Cuvier, 1830). *Pakistan J Zool.*, **45(1)**: 41-46.

Astuti I, Karina S and Dewiyanti I. 2016. Analisis kandungan logam berat Pb pada tiram *Crassostrea cucullata* di pesisir Krueng Raya, Aceh Besar. *J Ilm Mah Kel Per Unsyiah*., **1(1)**: 104-113. (in Indonesian)

Bakun A and Broad K. 2003. Environmental 'loopholes' and fish population dynamics: comparative pattern recognition with focus on El Nin˜o effects in the Pacific. *Fish Oceanog.*, **12(4)**: 458-473.

Batista FM, Ben-Hamadou R, Fonseca VG, Taris N, Ruano F, Reis-Henriques MA and Boudry P. 2008. Comparative study of shell shape and muscle scar pigmentation in the closely related cupped oysters *Crassostrea angulata, C. gigas* and their reciprocal hybrids. *Aqua Liv Res.*, **21**: 31-38.

Bayas JCL, Marohn C, Dercon G, Dewi S, Piepho HP, Joshi L, Noordwijk MV and Cadisch G. 2011. Influence of coastal vegetation on the 2004 tsunami wave impact in west Aceh. *PNAS*, **108(46)**: 18612-18617.

Dheilly NM, Lelong C, Huvet A, Kellner K, Dubos MP, Riviere G, Boudry P and Favrel P. 2012. Gametogenesis in the pacific oyster *Crassostrea gigas*: A microarrays-based analysis identifies sex and stage specific genes. *PlosOne*, **7(5)**: 1-15.

Fabioux C, Huvet A, Souchu PL, Pennec ML and Pouvreau S. 2005.Temperature and photoperiod drive *Crassostrea gigas*reproductive internal clock. *Aqua.*, **250**: 458-470.

Fadli N, Setiawan I and Fadhilah N. 2012. Keragaman makrozoobenthos di perairan Kuala Gigieng, Kabupaten Aceh Besar. *Depik*, **1(1)**: 45-52. (in Indonesian)

Frankenberg E, Friedman J, Gillespie T, Ingwersen N, Pynoos R, Rifai LU, Sikoki B, Steinberg A, Sumantri C, Suriastini W and Thomas D. 2008. Mental health in Sumatra after the Tsunami. *Amer J Pub Health*, **98(9)**: 1671-1677.

Gaughan DJ and Mitchell RWD. 2000. **The biology and stock assessment of the tropical sardine, *Sardinella lemuru*, off the mid-west coast of Western Australia**. Fisheries Research Report. Published by Fisheries Western Australia, Perth.

Hagan AB, Foster R, Perera N, Gunawan CA, Silaban I, Yaha Y, Manuputty Y, Hazam I and Hodgson G. 2007. Tsunami impacts in Aceh Province and North Sumatra, Indonesia. *Atoll Res Bull.*, **544**: 37-54.

Hamdani A and Soltani-Mazouni N. 2011. Changes in biochemical composition of the gonads of *Donax trunculus* L. (Mollusca, Bivalvia) from the gulf of Annaba (Algeria) in relation to reproductive events and pollution. *Jordan J Biol Sci*., **4(3)**: 149-156.

Keightley J, Heyden SVD and Jackson S. 2015. Introduced Pacific oysters *Crassostrea gigas* in South Africa: demographicchange, genetic diversity and body condition. *African J Mar Sci.*, **37(1)**: 89-98.

Kasmini L, Barus TA, Sarong MA and Mulya MB. 2018. Length-weight relationships and condition factors of oyster (*Crassostrea gigas*) in the Tibang and Ulee Lheue Estuary, Banda Aceh City. *Depik*, **7(1)**: 60-68.

Lango-Reynoso F, Chavez-Villalba J, Cochard JC and Pennec ML. 2000. Oocyte size, a means to evaluate the gametogenic development of the Pacific oyster, *Crassostrea gigas* (Thunberg). *Aqua.*, **190**: 183-199.

Li Q, Osada M and Mori K. 2000. Seasonal biochemical variations in pacific oyster gonadal tissue during sexual maturation. *Fish Sci.*, **66**: 502-508.

Myers RA, Barrowman NJ, Hutchings JA and Rosenberg AA. 1995.Population dynamics of exploited fish stocks at low population levels. *Science*, **269**: 1106-1108.

Octavina C, Yulianda F and Krisanti M. 2014. Struktur komunitas tiram dagingdi perairan estuaria Kuala Gigieng, Kabupaten Aceh Besar, Provinsi Aceh. *Depik*, **3(2)**: 108-117. (in Indonesian)

Octavina C, Yulianda F, Krisanti M and Muchlisin ZA. 2015. Length-weight relationship of Ostreidae in the Kuala Gigieng estuary, Aceh Besar District, Indonesia. *AACL Bioflux*, **8(5)**: 817-823.

Roberts RJ. 2012. **Fish Pathology (4th E d.)**. Blackwell Publishing Ltd. Hoboken, New Jersey, USA.

SarongMA, Jiha C, Muchlisin ZA, Fadli N and Sugianto S. 2015. Cadmium, lead and zinc contamination on the oyster *Crassostrea gigas* muscle harvested from the estuary of Lamnyong River, Banda Aceh City, Indonesia. *AACL Bioflux*, **8(1)**: 1-6.

Suppasri A, Goto K, Muhari A, Ranasinghe P, Riyaz M, Affan M, Mas E, Yasuda M and Imamura F. 2015. A Decade after the 2004 Indian Ocean Tsunami: the progress in disaster preparedness and future challenges in Indonesia, Sri Lanka, Thailand and the Maldives. *Pure Appl Geoph.*, **172**: 3313-3341.

Westphal GGC, Magnani FP and Ostrensky A. 2015. Gonad morphology and reproductive cycle of the mangrove oyster *Crassostrea brasiliana* (Lamarck, 1819) in the Baia deGuaratuba, Parana, Brazil. *Acta Zool.*, **96**: 99-107.

Wibisono ITC and Suryadiputra IN. 2006. **Study of Lessons Learned from mangrove/coastal ecosystem restoration efforts in Aceh since the Tsunami**. Wetlands International, Bogor, Jawa Barat.

JJBS
Jordan Journal of Biological Sciences

Volume 12, Number 5,December 2019
ISSN 1995-6673
Pages 561 - 566

Morphometric and Meristic Characteristics of the Banded Gourami, *Trichogaster fasciata* (Bloch & Schneider, 1801) in a Wetland Ecosystem from Northwestern Bangladesh

Md. Ataur Rahman, Md. Shahinoor Islam, Md. Yeamin Hossain*, Md. Rabiul Hasan, Md. Akhtarul Islam, Dalia Khatun, Obaidur Rahman, Most. Farida Parvin, Zannatul Mawa and Asma Afroz Chowdhury

Department of Fisheries, Faculty of Agriculture, University of Rajshahi, Rajshahi 6205, Bangladesh

Received January 12, 2019; Revised March 3, 2019; Accepted March 12, 2019

Abstract

This study represents the morphometric and meristic characters of the least concern, *Trichogaster fasciata* (Bloch & Schneider, 1801) including length-weight relationships (LWRs) and length-length relationships (LLRs) using a total of six linear dimensions and various meristic counts from the Gajner *Beel*, a large wetland ecosystem of northwestern Bangladesh. Sums of 324 specimens of T. fasciata were occasionally collected from the Gajner *Beel* during the period from July 2017 to June 2018, using different traditional fishing gears. Fin rays were counted with the help of a magnifying glass. Moreover, a total of seven different lengths (e.g., TL, SL, PrDL etc.) were measured using digital slide calipers, and the total body weight (BW) was weighed by an electronic balance with a 0.01 g accuracy for each individual, respectively. Minimum and maximum sizes were 3.1-8.8 cm (Mean ± SD = 5.78 ± 1.50) in total length (TL) and 0.81- 13.15 g (Mean ± SD = 4.90 ± 3.30) in body weight (BW). All LWRs were highly significant ($p< 0.001$) with r^2 values ≥ 0.960. Based on the r^2 value, the LWRs by BW *vs.* TL constitute the finest fitted model among seven equations. In addition, the LLRs also had significance with r^2 values ≥ 0.993. Based on the r^2 values, the LLRs by TL *vs.* SL was the best fitted model among six equations. The fin formula of *T. fasciata* is: dorsal, D. XV-XVII/10-14; pectoral, Pc. 9-10; pelvic, Pv. 1; anal, A. XV-XVIII/15-19 and caudal, C. 18-20. This study will contribute to species identification and stock assessment of Gajner *Beel* and the adjacent ecosystems.

Keywords: *Trichogaster fasciata*, Morphometric, Meristic, Fin rays, Gajner *Beel*, Bangladesh

1. Introduction

The Banded gourami, *Trichogaster fasciata* (Bloch & Schneider, 1801) is a freshwater and estuaries tropical labyrinth fish belonging to the family of Osphronemidae (Romero, 2002; Froese and Pauly, 2018). It is an indigenous species and widely distributed throughout the Indian sub-continent: Bangladesh (Rahman, 1989; Menon, 1999), Bhutan (Petr, 1999), India, Nepal and Pakistan (Talwar and Jhingran, 1991; Gupta, 2015). This is well-known as Boro kholisha, Khailsha, Khalisha in Bangladesh, as Kholisha, Kholiana in India and as Katara, Khesara in Nepal (Froese and Pauly, 2018). The banded gourami is a benthopelagic, and generally prefer weedy environments such as estuaries, ponds, large rivers, ditches, and lakes (Menon, 1999). It is a carnivorous hardy fish and breeds in foul water (Bhuiyan, 1964). This species is considered as an important target species for small-scale fishers (Shafi and Quddus, 1982; Rahman, 2005), who use a variety of traditional fishing gears (Kibria and Ahmed, 2005). This fish species is used as a peaceful and beautiful aquarium fish, and traditionally people like its good taste (Talwar and Jhingran, 2001). Though this species is considered a minor in terms of commercial catches due to its small size, and is mostly captured as a b ycatch (Rahman *et al*., 2018; Hossain *et al.,* 2019; Hossen *et al.,* 2019a), it is regarded as a highly commercial fish species for the aquarium (Froese and Pauly, 2018). The conservational status of *T. fasciata* is listed as least concern both in Bangladesh (IUCN Bangladesh, 2015) and Worldwide (IUCN, 2017).

Morphometric and meristic characteristics are beneficial for species appreciation and classification (Bagenal and Tesch, 1978; Jayaram, 1999; Hossen *et al*., 2018). Morphometric characters constitute an important part of fisheries' research for comparing life history and morphological trends of fish populations (Hossain *et al*., 2014, 2016a; Elahi *et al.*, 2017). Morphometric and meristic characteristics, including length-weight relationships (LWRs) (Hossain *et al*., 2016b; Rahman *et al.,* 2019, Hossen *et al*., 2019), and length-length relationships (Hossain *et al*., 2006, 2016c; Hossen *et al*., 2019) of various threatened species of Bangladesh, are well-documented, but none covers a wide range of linear dimensions. However, a few studies have been conducted

* Corresponding author e-mail: hossainyeamin@gmail.com.

on *T. fasciata* i.e., length-weight relationships (LWRs) and condition factor (Sarkar *et al*., 2012; Kalita *et al*., 2016), biology and fishery (Mitra *et al*., 2007), morphometric study (Akter *et al*., 2016), captive breeding (Islam *et al*., 2017), some aspects of biology (Islam *et al*., 2016) etc. Therefore, the present study was intended to describe the morphometric and meristic characters of *T. fasciata* in the Gajner *Beel*, wetland ecosystem in NW Bangladesh via a number of specimens with various sizes over a study period of twelve months.

2. Materials and Methods

2.1. Study Area and Sampling

The current study was performed in the Gajner *Beel* (Lat. 23° 55□ N; Long. 89° 33□ E), NW Bangladesh. A total of 324 individuals of *T. fasciata* (Figure 1) were intermittently collected from the fishermen during July 2017 to June 2018. The specimens were caught using various conventional fishing gears, such as cast net (mesh size: 1.0-2.0 cm), gill net (mesh size: 1.5-2.5 cm), and square lift net (about 1.0 cm). The collected specimens were quickly kept in ice in the field, and were stored in the laboratory with a 10 % buffered formalin.

Figure 1. A photo of *Trichogaster fasciata* captured from the Gajner *Beel*, northwestern Bangladesh

2.2. Meristic Counts

The meristic counts of fin rays of *T. fasciata* in different body parts including dorsal, pectoral, pelvic and caudal fins were observed by a magnifying glass.

2.3. Fish Measurement

Different lengths such as Total length (TL), Standard length (SL), Pre-dorsal length (PrDL), Post-dorsal length (PoDL), Pre pectoral length (PcL), Pre Anal length (PrAnL), and Post Anal length (PoAnL) (Figure 2) were measured using a digital slide calipers. Body weight (BW) was weighed with an electronic balance with a 0.01 g accuracy for each individual, respectively.

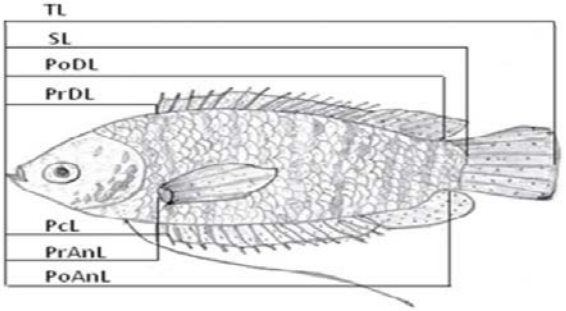

Figure 2. Showing the morphometric measurements of *Trichogaster fasciata* from the Gajner *Beel*, Northwestern Bangladesh (See Table 1 for abbreviation).

2.4. Growth Patterns

The growth pattern was recognized through LWRs with the equation: $BW = a \times (TL)^b$, where BW is the total body weight (g), and TL is the total length (cm). The parameter a and b were calculated by log-log linear regression analyses: $\ln(W) = \ln(a) + b \times \ln(L)$. Extreme outliers were deleted from the regression analysis according to Froese (2006). Furthermore, the 95 % confidence interval (CI) of a and b and the co-efficient of determination (r^2) were also estimated. In this study, a total of six LLRs were analyzed by linear regression analysis (Hossain *et al*., 2006). Based on the highest r^2 value, the best model was selected from the various models of both LWRs and LLRs.

2.5. Statistical analysis

Statistical analyses were conducted with GraphPad Prism 6.5 software. All statistical analyses were considered significant at the level of 5 % ($p < 0.05$).

3. Results

The body of *T. fasciata* is elevated and compressed. Its mouth is obliquely directed backwards. The nostrils lie at the anterior superior angle of eyes. Dorsal and abdominal profiles are equally convex. The dorsal is long with its softer portion pointed. Its pectoral extends up to 10 anal spines. Filamentous pelvic extends beyond the base of the caudal which is notched. The dorsal and caudal fins are speckled with orange. The lateral line is interrupted. Scales are present on head, body, and on the base of dorsal and anal fins. Body color is greenish above, dirty white bellow, pelvic with yellow-white bases and red tips (Figures 1-3).

In the total catch of 324 individuals, BW ranged from 0.81 g to 13.15 g (Mean ± SD = 4.90 ± 3.30) and TL varied from 3.1 cm to 8.8 cm (Mean ± SD = 5.78 ± 1.50). Standard length (76.47 %) showed the higher proportion of TL (Table 1).

Table 1. Morphometric measurements of the *Trichogaster fasciata* (Bloch & Schneider, 1801) (n = 324) captured from the Gajnar *Beel*, Pabna, Bangladesh

Measurements)	Min (cm)	Max (cm)	Mode	Mean ± SD	95% CI	%TL
TL (Total length)	3.1	8.8	4.4	5.78±1.50	5.62 to 5.95	
SL (Standard length)	2.3	6.8	3.4	4.42±1.13	4.30 to 4.55	76.47
PrDL (Pre-dorsal length)	0.9	2.3	1.1	1.57±0.37	1.52 to 1.61	27.16
PoDL(Post-dorsal length)	2.1	6.2	3.1	4.08±1.04	3.96 to 4.19	70.59
PcL (Pre pectoral length)	0.9	2.0	1.1	1.34±0.29	1.30 to 1.37	23.18
PrAnL (Pre-anal length)	1.0	2.3	1.2	1.54±0.36	1.50 to 1.58	26.64
PoAnL(Post-anal length)	2.1	6.6	3.3	4.26±1.09	4.14 to 4.38	73.70
BW(Body weight)	0.81	13.15	1.51	4.90±3.30	4.54 to 5.26	

Min, minimum; Max, maximum; SD, standard deviation; CI, confidence interval for mean values; TL, total length

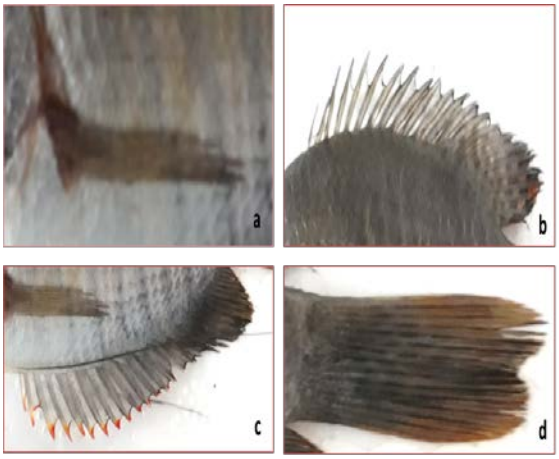

Figure 3. Different fins such as (a) Pectoral, (b) Dorsal, (c) Anal and (d) Caudal of *Trichogaster fasciata* from the Gajner *Beel*, Northwestern Bangladesh

3.1. Fin Formula

All meristic measurements are given in Table 2. The fin formula *T. fasciata* is: dorsal, D. XV-XVII/10-14; pectoral, Pc. 9-10; pelvic fin, Pv. 1; anal, A. XV-XVIII/ 15-19 and caudal, C. 18-20, respectively.

Table 2. Meristic measurements of the *Trichogaster fasciata* (Bloch & Schneider, 1801) (*n* = 324) captured from the Gajner *Beel*, Pabna, Bangladesh

Meristic data	Numbers	(Spine/ Branch)
Dorsal fin rays	22-24	XV-XVII/10-14
Pectoral fin rays	8-10	9-10
Pelvic fin rays	1	1
Anal fin rays	28-30	XV-XVIII/ 15-19
Caudal fin rays	18-20	18-20

3.2. Growth Pattern

The regression parameters (*a* and *b*) of the LWRs, the 95 % Confidence interval (CI) of *a* and *b*, the co-efficient of determination (r^2) of *T. fasciata* are given in Table 3 and **t**he regression parameters (*a* and *b*) of the LLRs, the 95 % confidence interval (CI) of *a* and *b*, the coefficient of determination (r^2) are given in Table 4. All LWRs were highly significant ($p< 0.001$) with r^2 values $\geq$ 0.997. Based on the maximum r^2 value, LWR by BW *vs.* TL constitutes the best fitted model among seven equations. Also, all LLRs, which are shown in Table 4, were highly correlated with the values of $r^2 \geq 0.993$. Based on the maximum r^2 value, LLR by TL *vs.* SL was the best fitted model among seven equations.

Table 3. Descriptive statistics and estimated parameters of the length-weight relationships of *Trichogaster fasciata* (Bloch & Schneider, 1801) (*n* = 324) captured from the Gajner *Beel*, Pabna, Bangladesh

Equation	Regression parameters		95% CL of *a*	95% CI of *b*	r^2
	a	*b*			
BW = a× TL^b	0.0356	2.72	0.0345 - 0.0367	2.703 - 2.738	0.997
BW= a× SL^b	0.0685	2.77	0.0656 - 0.0714	2.741 - 2.798	0.991
BW= a× $PrDL^b$	1.0859	3.00	1.0553 - 1.1173	2.939 - 3.058	0.969
BW= a× $PoDL^b$	0.0840	2.78	0.0800 - 0.0882	2.749 - 2.819	0.987
BW= a× PcL^b	1.5521	3.34	1.5129 - 1.5924	3.271 - 3.420	0.960
BW= a× $PrAnL^b$	1.1250	3.03	1.0972 - 1.1535	2.973 - 3.079	0.975
BW= a× $PoAnL^b$	0.0771	2.76	0.0736 - 0.0809	2.725 - 2.790	0.989

n, sample size; *a* and *b* are LWR parameters; CI, confidence intervals; r^2, coefficient of determination

Table 4. The estimated parameters of the length-length relationships (y = *a* + *b*×x) *Trichogaster fasciata* (Bloch & Schneider, 1801) (*n* = 324) captured from the Gajner *Beel*, Pabna, Bangladesh

Equation	Regression parameters		95% Cl of *a*	95% CI of *b*	r^2
	a	*b*			
TL = *a*+*b*× SL	-0.0574	1.32	-0.1147 to 9.8802	1.308 - 1.333	0.993
TL= *a*+*b*× PrDL	-0.506	4.01	-0.6213 to -0.3913	3.943 - 4.086	0.974
TL= *a*+*b*× PoDL	-0.086	1.44	-0.1585 to -0.0144	1.422 - 1.456	0.988
TL= *a*+*b*× PcL	-1.154	5.18	-1.3040 to -1.0043	5.066 - 5.285	0.964
TL= *a*+*b*× PrAnL	-0.484	4.06	-0.5943 to -0.3745	3.995 - 4.133	0.976
TL= *a*+*b*× PoAnL	-0.016	1.36	-0.0835 to 0.0516	1.345 - 1.375	0.990

n, sample size; *a*, intercept; *b*, slope; CI, confidence intervals; r^2, co-efficient of determination

4. Discussion

Information on morphometric and meristic characteristics of *T. fasciata* is very few in literature from Bangladesh and elsewhere. However, the current study reveals the morphometric characteristics of *T. fasciata*, including length-weight relationships using several length measurements (TL, SL, PcL, etc); length-length relationship and meristic counts.

The LWR is useful in differentiating populations as variations occur in populations of different localities (Le Cren, 1951; Chonder, 1972). In the present study, a total of 324 specimens from small to larger body sizes were sampled; however, the sampling of individuals smaller than 3.1 cm in TL was not possible, which can be

attributed to the selectivity of the fishing gear, but not to their nonappearance on the fishing grounds nor was it because fishermen were not fishing where the smaller sizes present (Rahman *et al*., 2012; Hossain *et al*., 2017a; 2017b; Parvin *et al*., 2018; Azad *et al*., 2018; Khatun *et al*., 2019).

In the current study, the observed maximum length of *T. fasciata* was 8.8 cm in TL which is higher than Nitai *beel* (TL=8.14) (Kalita *et al*., 2016) and Deepor Beel, India (TL= 8.10) (Borah *et al*., 2017), but lower than the maximum documented value of 12.5 cm in TL (Menon, 1999) and 9.6 cm TL (Sarkar *et al*., 2013) from the Ganga River, India. Information on maximum length is necessary for the estimation of growth parameters i.e., asymptotic length and growth co-efficient of fishes, which is significant for fisheries' resource planning and management (Hossain *et al.,* 2018, Khatun *et al*., 2018). In this study, the total number of fin rays of dorsal fin is XV-XVII/10-14, pectoral fin 9-10, pelvic fin 1, Anal fin XV-XVIII/ 15-19 and caudal fin 18-20 which is similar to what was reported by Rahman (2005); Talwar & Jhingran (2001) and Shafi & Quddus (1982).

The allometric co-efficient (*b*) values of LWRs may vary between 2.0- 4.0 (Carlander, 1969); however, values ranging from 2.5 to 3.5 are more frequent (Froese, 2006). In the present study, the *b* value was 2.72, which designates a negative allometric growth for *T. fasciata* in the Gajner *Beel*. Similar findings were also reported by Kalita *et al.* (2016) (*b*= 2.58) from the Nitai *Beel* and Borah *et al*. (2016) (*b*= 2.78) from the Deepor *Beel,* India. However, in an earlier study, Hossain *et al.* (2017a) reported a positive allometric growth (*b*= 3.29) in the Gajner *Beel,* which is inconsistent with what was reported by the current study. The *b* value of the same species may vary from one study to another due to the uses of different fishing gear with different mesh sizes, variations in number of specimen examined (Hossain *et al*., 2013; Ahamed *et al*., 2017), and the preservation technique of the samples (Tesch, 1971). Furthermore, such variations between studies may be influenced by the habituated, seasonal variation, sex and the health condition of fishes (Froese, 2006). The results of the present study are useful as baseline data for the species with no previous length-weight relationships as well as for comparisons for future studies; in majority of the cases, the value was not equal to 3.0. This difference was attributed to possible influence of sex and other internal and external factors on growth as described by Le Cren (1951) where generally *b* values equal to 3.0, which indicates that fish grow up isometrically; however, if the values are different from 3.0, this indicates an allometric growth (>3 positive allometry and <3 negative allometry) (Tesch, 1971).

The data of *T. fasciata* were collected over an extended period of time, not representative of any particular season. The LLRs of *T. fasciata* are highly correlated. In spite of the sufficient literature, the current study found the finest model amid equations using different lengths based on the coefficient of determination, which will offer a baseline for comparisons to future studies using any linear dimension.

5. Conclusion

The results of this study would be a tool for fishery managers, fish biologists to identify *T. fasciata* and initiate stock assessment of this least concern species in the wetland ecosystem of Bangladesh and neighboring countries.

Acknowledgements

The authors would like to extend their sincere appreciation to the PIU-BARC, NATP-2, Sub-Project ID: 484 for funding to work out the research in the Gajner *Beel* ecosystem and it is a partial work of this CRG (Competitive Research Grants) Project.

Conflicts of Interest

The authors announce that there is no conflict of interest regarding the publication of the present paper.

Reference

Ahmed, F., Saha, N., Jahan, S., Akter, S., Hossain, M.Y., Ahmed, Z. F., and Ohtomi, J. 2017. Length-weight and length-length relationships of two gobiid fishes *Eleotris fusca* (Foster, 1801) and *Odontamblyopus rubicundus* (Hamilton, 1822) from the Payra river, southern Bangladesh. *J Appl Ichthyol*, **34**: 227-229.

Akter S, Zaman MFU, Jaman MHU, Sithi IN, Yesmin D, and Asif AA. 2016. Morphometric study of banded gourami (*Colisa fasciata*) in Jessore, Bangladesh. *Asian J Med Biol Res*, **2**: 113-120.

Azad MAK, Hossain MY, Khatun D, Parvin MF, Nawer F, Rahman O and Hossen MA. 2018. Morphometric relationships of the Tank goby *Glossogobius giuris* (Hamilton, 1822) in the Gorai River using multi-linear dimensions. *Jordan J Biol Sci*, **11**: 81 -85.

Bagenal JB and Tesch FW. 1978. **Methods for assessment of fish production in freshwaters**. Blackwell Scientific publication, Oxford, p. 361.

Bhuiyan AL. 1964. **Fishes of Dacca.** Asiatic society, Pakistan, Pub.1, No. 13, Dacca, p. 71.

Borah S, Bhattacharjya BK, Saud BJ, Yadav AK, Debnath D, Yengkokpam S, Das P, Sharma N, Singh NS and Sarma KK. 2017. Length–weight relationship of six indigenous fish species from Deepor beel, a Ramsar site in Assam, India. *J Appl Ichthyol*, **33**: 655–657.

Chonder SL. 1972. Length–weight relationship of mature female *Labeo gonius* (Hamilton) fromthe Keetham Reservoir. *J Inland Fish Soc India,* **4**: 216-217.

Elahi N, Yousuf F, Tabassum S, Bahkali AH, El-Shikh M, Hossen MA, Rahman MM, Nawer F, Elgoban AM and Hossain MY. 2017. Life-history traits of the Blacktrip sardinella, *sardinella melamura (C*lupidae) in the Gwadar, Balochistan Coast, Pakistan. *Indian J Mar Sci,* **46**: 397-404.

Froese R and Pauly D. (Eds.) 2018. **Fish base 2018**, World Wide Web electronic publication. Available at: http://www.fishbase.org (accessed on 19 December, 2018).

Froese R. 2006. Cube law, condition factor and weight-length relationships: history, meta-analysis. *J Appl Ichthyol,* **22**: 241–253.

Gupta S. 2015. A note on feeding and reproductive biology of banded gourami, *Trichogaster fasciata* (Bloch and Schneider, 1801). *Int J Res Fish Aquacult*, **5**: 147-150.

Hossain MA, Hossain MY, Pramanik MNU, Khatun D, Nawer F, Parvin MF, Arabi A and Bashar MA. 2018. Population Parameters of the Minor carp *Labeo bata* (Hamilton, 1822) in the Ganges River of northwestern Bangladesh. *Jordan J Biol Sci*, **11**: 179- 186.

Hossain MA, Hossain, MY, Hossen MA, Rahman MA, Islam MA, Khatun D, Nawer F and Ohtomi J. 2019. Temporal variations of sex ratio and growth pattern of critically endangered catfish *Clupisoma garua* from the Ganges River of north-western Bangladesh. *Indian J Geo-Mar Sci*, **48**: 647-653.

Hossain MY, Ahmed ZF, Leunda PM, Jasmine S, Oscoz J, Miranda R and Ohtomi J. 2006. Condition, length-weight and length-length relationships of the Asian striped catfish *Mystus vittatus* (Bloch, 1794) (Siluriformes: Bagridae) in the Mathabhanga River, southwestern Bangladesh. *J Appl Ichthyol*, **22**: 304–307.

Hossain MY, Arefin MS, Mohmud MS, Hossain MI, Jewel MAS, Rahman MM, Othomi J. (2013). Length-weight relationships, condition factor, gonadosomatic index-based size at first sexual maturity, spawning season and fecundity of *Aspidoparia morar* (Cyprinidae) in the Jamuna River (Brahmaputra River distributary). Northern Bangladesh. *J Appl Ichthyol*, **29**: 1166-1169.

Hossain MY, Hossen MA, Ahmed ZF, Hossain MA, Pramanik MNU, Nawer F, Paul AK, Khatun D, Haque N, and Islam MA. 2017a. Length-weight relationships of 12 indigenous fish species in the Gajner Beel floodplain (NW Bangladesh). *J Appl Ichthyol*, **33**: 842-845.

Hossain MY, Hossen MA, Iitam MM, Pramanik MNU, Nawer F, Paul AK, Hammed HMA, Rahman MM, Kaushik G and Bardoloi S. 2016. Biometric indices and size at first sexual maturity of eight alien fish species from Bangladesh. *Egypt J Aquat Res*, **42**: 331-339.

Hossain MY, Hossen MA, Khatun D, Nawer F, Parvin MF, Rahman O and Hossain MA. 2017b. Growth, condition, maturity and mortality of the Gangetic leaf fish *Nandus nandus* (Hamilton, 1822) in the Ganges River (Northwestern Bangladesh). *Jordan J Biol Sci*, **10**: 57-62.

Hossain MY, Hossen MA, Pramanik MNU, Ahmed ZF, Hossain MA and Islam MM. 2016c. Length-weight and length-length relationships of three Ambassid fishes from the Ganges River (NW Bangladesh). *J Appl Ichthyol*, **32**: 1279-1281.

Hossain MY, Hossen MA, Pramanik MNU, Sharmin S, Nawer F, Naser SMA, Bahkali AH and Elgorban AM. 2016b. Length-weight and length-length relationships of five *Mystus* species from the Ganges and Rupsha River, Bangladesh. *J Appl Ichthyol*, **32**: 994-997.

Hossain MY, Pramanik MNU, Hossen MA, Nawer F, Khatun D, Parvin MF, Ahmed ZF and Ahamed F. 2018. Life-history traits of Pool barb *Puntius sophore* (Cyprinidae) in different Ecosystems of Bangladesh. *Indian J Geo-Mar Sci*, **47**: 1446-1454.

Hossain MY, Rahman MM, Ahamed F, Ahmed ZF and Ohtomi J. 2014. Length-weight and length-length relationships and form factor of three threatened fishes from the Ganges River (NW Bangladesh). *J Appl Ichthyol*, **30**: 221-224.

Hossen MA, Hossain MY, Pramanik, MNU, Rahman MA, Islam MA, Nawer F and Parvin MF. 2019. Biometry, sexual maturity, natural mortality and fecundity of endangered halfbeak Dermogenys pusilla (Zenarchopteridae) from the Ganges River in northwestern Bangladesh. *Indian J Geo- Mar Sci*, **48**:1548-1555.

Hossen MA, Paul AK, Hossain MY, Ohtomi J, Sabbir W, Rahman O, Jasmin J, Khan MN, Islam MA, Rahman MA, Khatun D and Kamaruzzaman S. 2019. Estimation of biometric indices for Snakehead *Channa punctata* (Bloch, 1793) through Multi-model Inferences. *Jordan J Biol Sci,* **12**: 197-202.

Hossen MA, Rahman MA, Hossain MY, Islam MA and Ohtomi J. 2019. Estimation of relative growth of Minor carp *Labeo bata* (Cyprinidae) through multi-linear dimensions. *Lake Res: res Manage,* **24**: 302-307.

Islam MS, Akter S, Hasan MR and Sheba SS. 2016. Some aspects of biology of banded gourami, *Colisa fasciata* (Bloch and schneider, 1801) in Jessore, Bangladesh. *Int J Bios*, **9**: 72-80.

Islam MS, Rikta S, and Ghosh S. 2017. Captive breeding of banded gourami, *Colisa fasciata* (Bloch And Schneider, 1801); considering the various hormonal responses. *Int J Pure App Zoo*, **5**: 109-114.

IUCN 2017. The IUCN red list of threatened species. Version 2017-1. Downloaded on 18 December 2018. https:// www.iucnredlist.org

IUCN Bangladesh. 2015. **Red List of Bangladesh. Volume 5: Freshwater Fishes.** IUCN, International Union for Conservation of Nature, Bangladesh Country Office, Dhaka, Bangladesh, xvi+360 p.

Jayaram KC.1999. **The Freshwater Fishes of the Indian Region**. Narendra Publishing House, Delhi.

Kalita B, Sarma SR, and Deka P, 2016. A comparison on length-weight relationship and relative condition factor of two species of *Trichogaster* of Nitai Beel of Kamrup district of Assam, India. *Int J of Zool Stud*, **1**: 9-12.

Khatun D, Hossain MY, Parvin MF, and Ohtomi J. 2018. Temporal variation of sex ratio, growth pattern and physiological status of *Eutropiichthys vacha* (Schilbeidae) in the Ganges River, NW Bangladesh. *Zool and Ecol*, **28**: 343-354.

Khatun D, Hossain MY, Rahman MA, Islam MA, Rahman O, Sharmin MS, Parvin MF, Haque ATU and Hossain MA. 2019. Life-history traits of the climbing perch *Anabas testeudineus* (Bloch, 1792) in a wetland ecosystem. *Jordan J Biol Sci,* **12:** 175-182.

Kibria G and Ahmed KKU. 2005. Diversity of selective and nonselective fishing gear and their impact on inland fisheries in Bangladesh. *NAGA*, **28**: 43-48.

Le Cren ED. 1951. The length-weight relationships and seasonal cycle in gonad weight and condition in the perch (*Perca fluviatilis*). *J Anim Ecol*, **20**: 201-219.

Menon AGK. 1999. Check list - **Fresh Water Fishes of India**. Rec. Zool. Surv. India, Misc. Publ., Occas. Pap. No. 175, 366 p.

Mitra K, Suresh Vr, Vinci Gk, Mazumdar N and Biswas Dk. 2007. Biology and Fishery of Banded Gourami, *Colisa fasciata* (Bloch and Schneider, 1801) in a Floodplain Wetland of Ganga River Basin. *Asian Fish Sci*, **20**:409-423

Parvin MF, Hossain MY, Sarmin MS, Khatun D, Rahman MA, Rahman O, Islam MA, and Sabbir W. 2018. Morphometric and meristic characteristics of *Salmostoma bacaila* (Hamilton, 1822) (Cyprinidae) from the Ganges River in northwestern Bangladesh. *Jordan J Biol Sci*, **11:** 533 - 536

Petr T. 1999. **Coldwater Fish and Fisheries in Bhutan.** p. 6-12. In T. Petr (ed.) Fish and fisheries at higher altitudes: Asia. FAO Fish. Tech. Pap. No. 385. FAO, Rome, p. 304.

Rahman AKA. 1989. **Freshwater Fishes of Bangladesh.** Zoological Society of Bangladesh, Department of Zoology, University of Dhaka, pp.364

Rahman AKA. 2005. **Freshwater Fishes of Bangladesh**, 2nd edition, *Zoological Society of Bangladesh*, Department of Zoology, University of Dhaka, Dhaka-1000, pp. 1-263.

Rahman MA, Hasan MR, Hossain MY, Islam MA, Khatun D, Rahman O, Mawa Z, Islam MS, Chowdhury AA, Parvin MF and Khatun H. 2019. Morphometric and meristic characteristics of the Asian stinging catfish *Heteropneustes fossilis* (Bloch, 1794): A key for its identification. *Jordan J Biol Sci,* **12**: 467-470.

Rahman MM, Hossain MY, Jewel MAS, Rahman MM, Jasmine S, Abdallah EM and Ohtomi J. 2012. Population structure, length-weight and length-length relationships, and condition- and form-factors of the Pool barb *Puntius sophore* (Hamilton, 1822) (Cyprinidae) from the Chalan *Beel*, North-Central Bangladesh. *Sain Malaysia,* **41**: 795–802.

Romero P. 2002. An Etymological Dictionary of Taxonomy. Madrid, unpublished.

Sarkar UK, Khan GE, Dabas A, Pathak AK, Mir JI, Rebello SC, Pal A and Singh SP. 2012. Length-weight relationship and condition factor of selected freshwater fish species found in River Ganga, Gomti and Rapti, India. *J Env Bio*, **34**: 0254-8704.

Shafi M and Quddus MMA. 1982. **Bangladesher Matshaw Sampad** (in Bengali). Bangla academy, Dhaka. pp. 307-308.

Talwar PK and Jhingran AG. 1991. **Inland Fishes of India and Adjacent Countries**, vol.2. A.A. Balkema, Rotterdam, p. 541.

Talwar PK and Jhingran AG. 2001. **Inland Fishes of India and Adjacent countries**. Oxford and IBH Publishing Co. Pvt. Ltd. New Dilhi. p. 288.

Tesch FW. 1971. Age and growth**.** In**:** Ricker WE (Ed), **Methods for Assessment of Fish Production in Fresh Waters**. Blackwell Scientific Publications, Oxford, pp.99–13.

JJBS

Volume 12, Number 5,December 2019
ISSN 1995-6673
Pages 567 - 571

Jordan Journal of Biological Sciences

A Botanical Study and Estimation of Certain Primary Metabolites of *Gymnocarpos decandrus* Forssk

Seham S. El-Hawary[1], Mona M. Okba[1], Rehab A. Lotfy[2] and Mahmoud M. Mubarek[2*]

[1]*Department of Pharmacognosy, Faculty of Pharmacy, Cairo University Kasr El-Ainy, 11562 Cairo ;* [2]*Department of Medicinal and Aromatic plants, Desert Research Center, 11753 Matariya, Egypt*

Received February 1, 2019; Revised March 2, 2019; Accepted March 12, 2019

Abstract

Gymnocarpos decandrus Forssk., of the family Caryophyllaceae, is a well-known grazing wild plant growing in the Middle East region and north of Africa. Recently several medicinal activities such as anti-inflammatory, analgesic, and diuretic were reported for *G. decandrus.* This study presents an investigation of the *G. decandrus'* macro and micro morphological features, to aid in the characterization and differentiation of such a commercially and medicinally important drug either in its entire or its powdered forms. The anatomical characters of the stem revealed the presence of cork cells, cortex, and pericycle traversed by patches of lignified pericyclic fibers. The epidermis of the leaf is characterized by the presence of anisocytic stomata, and absence of hairs. Druse crystals of calcium oxalate were found in the mesophyll. The total protein and lipid content were 10.5 % and 0.8 5% respectively. The analysis of protein revealed that leucine (6.27 %) and aspartic acid (12.87 %) were the major essential and non-essential amino acids respectively. A high level of glutamic acid (11.94 %) was also observed.

Keywords: Amino acids, Caryophyllaceae, Druse crystals, Gymnocarpos decandrus, Macro-Micromorphology.

1. Introduction

Gymnocarpos decandrus Forssk, of the family Caryophyllaceae, is the most extensively distributed species in the Gymnocarpos genus. It is found on t he Canary Islands, Morocco, Algeria, Tunisia, Libya, Egypt, Jordan, Syria, Saudi Arabia, Oman, Iran, Afghanistan, and Pakistan (Petrusson and Thulin, 1996).

The original spelling of this species by Forsskal was *Gymnocarpos decandrum.* According to the international code of botanical nomenclature, names with the suffix (carpos) are to be treated as masculine. So the accepted species name was modified to *G. decandrus*. *G. decandrus* is a shrublet with an erect stem, up to 45 cm tall. The bark is greyish or light brown. The leaves are sessile, slightly narrowed to the base, obtuse to subacute at the apex, and the seeds are brown in color (Petrusson and Thulin, 1996).

Traditionally, the aerial parts of the plant are used as food for grazing animals (El-Zanaty *et al.,* 2010). Recently, it has shown potent anti-inflammatory, analgesic, diuretic (Meselhy *et al*., 1994), and α-amylase inhibitory activities (Sallam and Galala, 2017). The *G. decandrus* aqueous extract exhibited antitumor activity against melanocyte cell lines (Sathiyamoorthy *et al*., 1999).

The plant has recently showed promising medicinal activities, in addition to being widely used as a grazing plant. The present study aims at the investigation of the *G. decandrus* macro and micro morphological features as well as at the estimation of its primary metabolite content to aid in characterization of such commercially and medicinally important drug either in its entire or powdered forms.

2. Materials and Methods

2.1. Plant Material

Collecting the aerial parts of *Gymnocarpos decandrus,* of the family Caryophyllaceae, was carried out during the flowering stage in April, 2016 from the western Mediterranean coastal region (Alexandria- Mersa Matrooh road 80- 140 km.). The plant was identified by Prof. Dr. Azza El Hadidy, Professor of Taxonomy and Flora-Herbarium, at the Faculty of Science, Cairo University. A voucher specimen of the plant under investigation was deposited with the code no. (7/12/15/1) at the Herbarium of Pharmacognosy Department, Faculty of Pharmacy, Cairo University.

2.2. Sample Preparation for Botanical Study

Fresh samples of stems and leaves were preserved in 70 % ethanol containing 5 % glycerol. Successive transverse sections (T.S), that are 10-15 µm thick, were performed with a manual microtome and were stained with Safranin

* Corresponding author e-mail: mahmoudmubarek88@gmail.com.

and Fast Green (Ruzin, 1999). The stems' and leaves' powder was stored in dark-colored, tightly closed vessels for the examination of the powdered organs. An optical microscope was used for taking the photographs combined with a digital camera Leica ICC50 HD (Okba *et al.,* 2013).

2.3. Determination of Total Lipid

Twenty grams of the dry plant powder were extracted with petroleum ether (40-60 ºC): ether (1:1 v/v) for twenty-four hours using the Soxhlet apparatus according to (Christie, 1982).

2.4. Determination of Total Nitrogen and Protein

The total nitrogen and total protein content were determined using the Kjeldahl method (James, 1995).

2.5. Methods for Amino-Acid Analysis

The defatted plant powder (0.1 g) was weighed in a tube and 10 mL of 6N hydrochloric acid was added. The tube was sealed and heated in an oven set at 110ºC for twenty-four hours. The solution was centrifuged to precipitate the insoluble components. The hydrolysate was evaporated to dryness on a rotary evaporator at the temperature of 40 ºC. Distilled water (5 mL) was added to the hydrolysate and evaporated to dryness. The residue was dissolved in citrate buffer (pH 2.2) and saved for analysis using an amino-acid analyzer (Arafat, *et al.*, 2009).

2.6. Apparatus and Conditions

Kjeldahl unit and Eppendrof-Germany LC3000 amino acid analyzer. Conditions: the mobile phase is citrate buffer (6.2 M, pH 2.2) with a flow rate at 0.25 mL/min for ninhydrin pump and 0.45 mL/min for eluent pump.

3. Results

Results of the macro and micro-morphological examination of the plant stems and leaves are illustrated in Figures (1-5). Dimensions in microns of the different elements are presented in Table (1)

3.1. Macroscopic Features

The *G. decandrus* Forssk under investigation is a heavily-branched erect shrublet (10-50 cm in height) with greyish or light brown stems (Figure 1A). The stem is erect, up to 45 cm tall and 1-1.5 cm in diameter. The bark is greyish or light brown in color, with glabrous internodes (0.5-3 cm) (Figure 1B). The leaves are fleshy, light green to light brown in color, and are fascicled on y ounger branches, sessile, linear-terete, slightly narrowed to the base, obtuse to subacute at the apex, oblanceolate. The leaf is 0.4-1 cm in length, and 1-2 mm in width (Figure 1C).

3.2. Microscopic Features

3.2.1. The Stem

The transverse section of stem **(**Figure 2) is almost circular in outline. It demonstrates a cork layer composed of four to five rows of compressed tangentially-elongated cells with suberized walls. The cortex consists of two to three rows of parenchymatous secondary cortex following one to two rows of collapsed parenchyma of the primary cortex. The pericycle is formed of seven to eleven rows of parenchyma traversed by patches of lignified pericyclic fibers.

The phloem is formed of sieve tubes, companion cells, and phloem parenchyma. The phloem parenchyma consists of a soft tissue, formed of ten to twelve rows of thin-walled cellulosic undifferentiated parenchymatous cells.

Xylem is composed of xylem vessels, wood fibers, and lignified wood parenchyma. The medullary rays are formed of lignified axially elongated cells. The pith represents about one third of the diameter of the stem, and is formed of thick lignified parenchymatous cells. The stem powder is brownish yellow in color with a characteristic taste. Microscopically, (Figure 3) it is characterized by the presence of cork fragments which are polygonal isodiametric thick suberized cells. Fragments of polygonal isodiametric epidermal cells with straight anticlinal walls and anisocytic stomata Fragments of lignified pericyclic fibers with wide and narrow lumen, tapering to pointed acute ends were found. Spiral and annular xylem vessels were also detected.

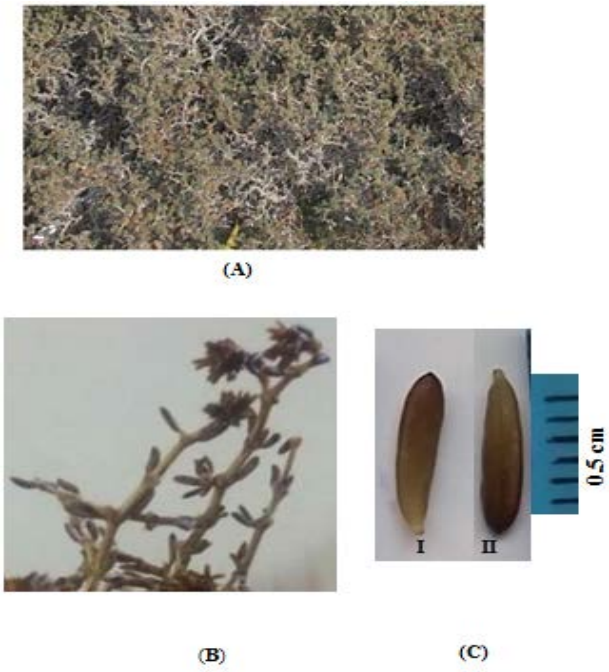

Figure 1. Macromorphology of the *G. decandrus* aerial parts. A: overview of the plant. B: stem carrying leaves. C: leaf (I: upper surface and II: lower surface).

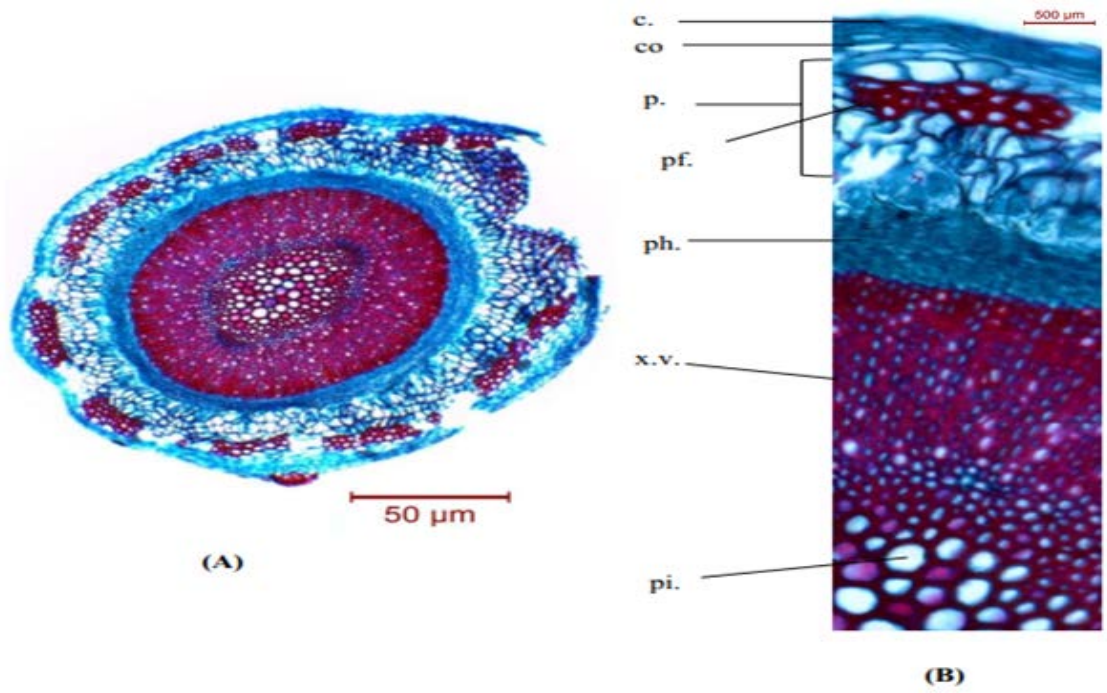

Figure 2. Micromorphology of *G. decandrus* stem. A: T.S. overview. B: T.S. detailed sector. c, cork cells; co, cortex; p, pericycle; pf, pericyclic fibers; ph, phloem; pi, pith; x.v, xylem vessels.

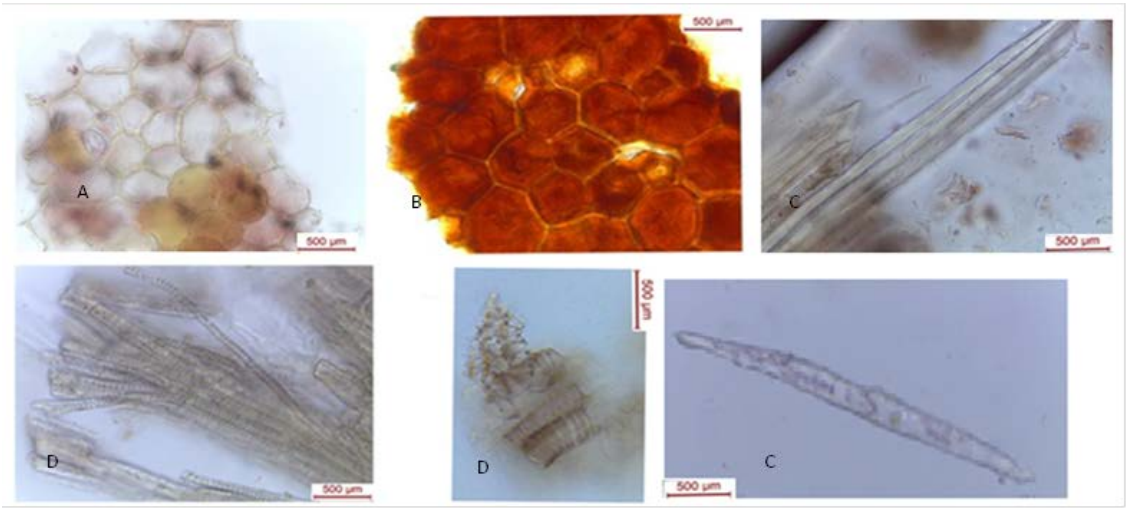

Figure 3. Micromorphology of *G. decandrus* powdered stem. (A) surface; (B) cork cells; (C) pericyclic fiber; (D) xylem vessels.

3.2.2. Leaves

A transverse section of the leaf lamina (Figure 4) shows the epidermis layer. It consists of one row of rectangular epidermal cells without intercellular spaces enclosing the mesophyll. The mesophyll is isobilateral. The palisade layer is formed of three to five rows of elongated columnar closely packed cells, with straight walls having green plastids inside. The palisade layer was extended overall the upper and lower surfaces. The parenchyma cells of the spongy tissue are irregular in shape and formed of five to seven rows of parenchyma cells with wide intercellular spaces containing druse crystals of calcium oxalate and small scattered vascular bundles embedded within. The midrib region consists of four to six rows of slightly thin walled irregular parenchyma cells. The vascular system is composed of a collateral vascular bundle. The phloem is formed of sieve tubes, companion cells and phloem parenchyma. The xylem is composed of spiral, pitted lignified xylem vessels, non-lignified wood parenchyma and wood fibers along with uniseriate medullary rays. The powdered leaf (Figure 5) is green in color, odorless with a characteristic - taste. Microscopically, it is characterized by the presence of fragments of the upper epidermis consisting of polygonal isodiametric straight-walled cells with anisocytic stomata. Fragments of the lower epidermis polygonal isodiametric cells with slightly wavy anticlinal walls and numerous anisocytic stomata were also found. Fragments of neural epidermis along with parenchyma cells containing druse crystals of calcium oxalate and fragments of palisade with columnar, thin-walled cells with green plastids inside were detected. In addition to fragments of wood fiber with wide lumen and blunt ends and tracheid fragments elongated with lignified pitted walls. Fragments of spiral xylem vessels were also observed.

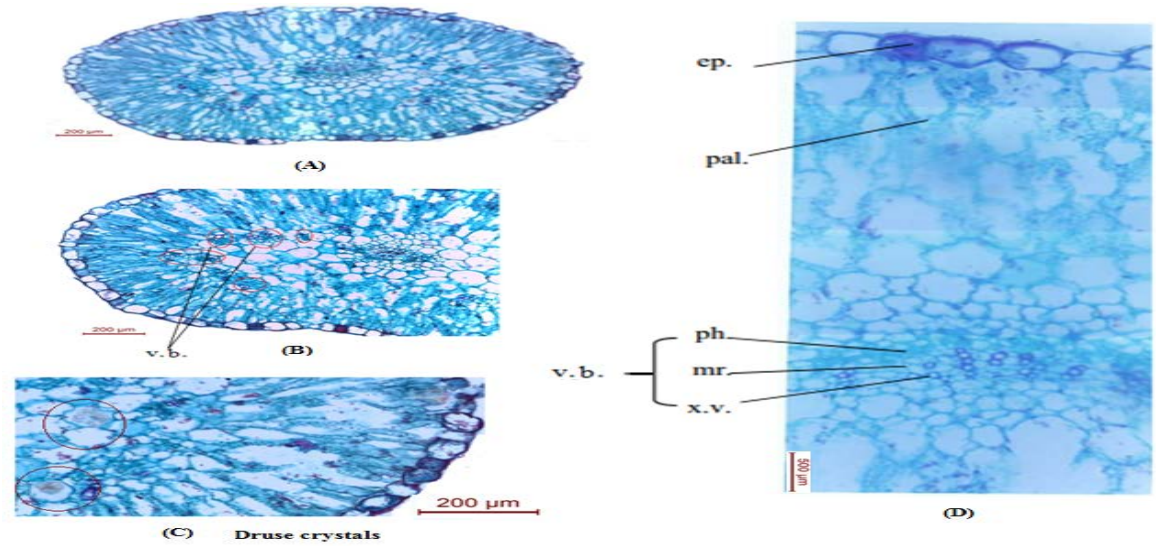

Figure 4. Micromorphology of *G. decandrus* leaf. (A) T.S. overview. (B) T.S. showing vascular bundles. (C) T.S. showing druse crystals. (D) detailed sector. ep, epidermis; mr, medullary rays; pal, palisade; ph, phloem; v.b, vascular bundle x.v, xylem vessels.

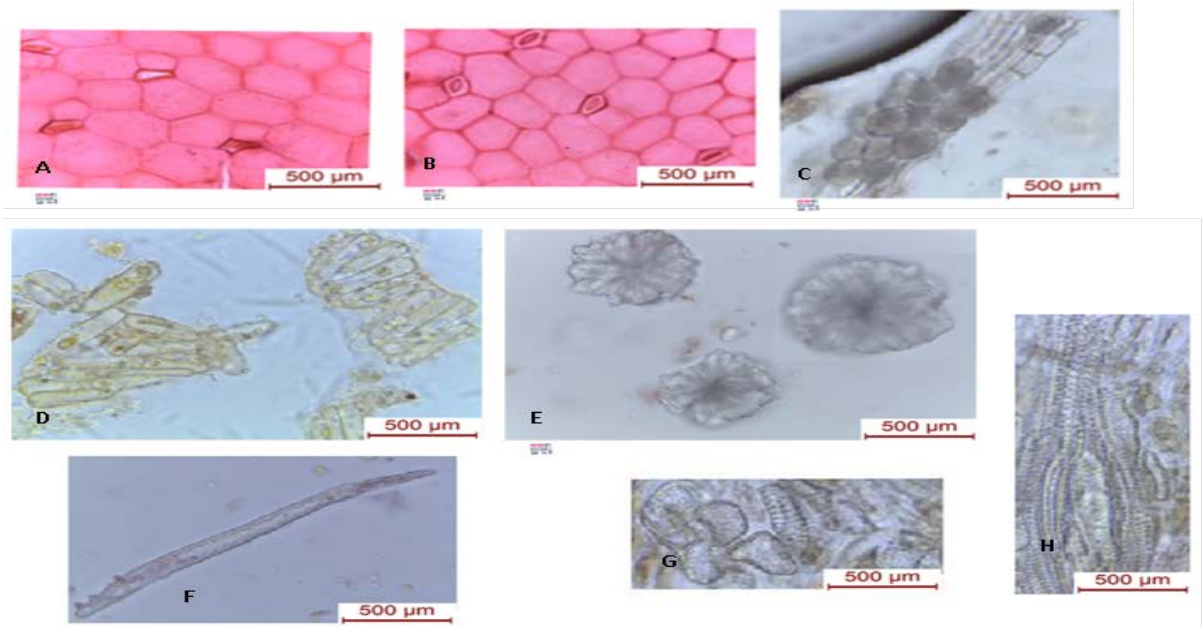

Figure 5. Micromorphology of a *G. decandrus* powdered leaf. (A) upper surface; (B) lower surface; (C) neural epidermis; (D) palisade cells; (E) druse crystals; (F) wood fiber; (G) tracheids; (H) xylem vessels.

Table 1. Dimensions of different elements of *G. decandrus* Forssk stems and leaves in microns.

Item	Length	Width	Diameter
	µm		
Stem			
Cork	20, 38.4, 51.4	22.4, 25.6, 38.4	
Pericyclic fiber	59, 62.5, 68.75	37.5, 50, 56.25	
Xylem vessels			16, 24, 28
Leaf			
Upper epidermis	65, 70, 80	30, 45, 55	
Lower epidermis	55, 90, 95	50, 55, 65	
Palisade	65, 70, 80	11, 15, 35	
Druse crystal			115, 120, 125
Xylem vessels			7.15, 8.19,8.5
Wood fibers	187 ,214, 216	10.5, 13.5,17	

3.3. Estimation of Certain Primary Metabolites

The percentage of total nitrogen, protein, and lipid were 1.68, 10.5 and 0.85 % respectively as tabulated in table (2). The results show that *G. decandrus* contains seventeen protein amino acids (table 3) with leucine (6.27 %) as the major essential amino acid, and aspartic acid (12.87 %) as the major non-essential amino acid. The percentage of the major protein amino acid was that of aspartic acid (12.87 %), followed by glutamic acid (11.94 %) respectively; meanwhile cysteine (0.49 %) was the minor identified protein amino acid.

Table 2. Quantitative estimation of certain primary metabolites in *G. decandrus* Forssk aerial parts.

Item	Percentage
Total nitrogen	1.68
Total protein	10.50
Total lipid	0.85

Table 3. Protein amino acid analysis of the *G. decandrus* Forssk aerial parts.

Essential Amino Acid	%	Non-essential Amino Acid	%
Cysteine	0.49	Arginine	5.07
Isoleucine	3.28	Proline	7.98
Leucine	6.27	Serine	6.41
Lysine	6.00	Glutamic acid	11.94
Methionine	0.94	Glycine	8.98
phenyl alanine	3.96	Alanine	5.61
Threonine	6.07	Aspartic	12.87
Tyrosine	2.49	Histidine	6.62
Valine	5.04		
Total	34.54	Total	65.48

4. Discussion

Different identification methods have been used throughout history including using morphological, anatomical, and chemical profiling. One of the easiest and most economic techniques for plant recognition is the microscopical examination (Singh, *et al.,* 2010). This study presents a complete macro and microscopically identification of the plant.

The current study is in consistence with findings of Metcalfe and Chalk, (1950) who reported the presence of druse crystals of calcium oxalate in this genus. In addition, the presence of anisocytic stomata and the absence of hairs were reported herein for the first time in *G. decandrus* which is not common in Caryophyllaceae.

Amino acids are the building blocks of all vegetable and animal proteins. The current study analyzed and identified the individual amino-acid composition of *G. decandrus*. It is worth noting that the salts of aspartic acid such as magnesium or potassium aspartate have an ergogenic activity either by increasing the metabolism of fatty acids and lowering the utilization of the glycogen in muscles or by reducing the cumulative effect of ammonia in exercise (Williams, 2005). Glutamic acid is necessary for sugar and fat metabolism, and also has a potent antiulcer activity (James and Phyllis, 1997). The high levels of aspartic acid and glutamic acid in *G. decandrus* call for more attention to this important grazing wild plant to explore its new medicinal activities.

References

Arafat MS, Gaafer MA, Amany MB and Shereen LN. 2009. Chufa tubers (*Cyperus esculentus* L.) as new source of food. *World Appl Sci J*. **7(2):** 151-156.

Christie WW. 1982. **Lipid analysis**. Pergamon Press, Oxford.

El-Zanaty RIA, Abdel-Hafez AA, Abdel-Gawad KI, El-Morsy MHM and Abusaief HMA. 2010. Effect of location and growth season on the productivity and quality of some range plants in Wadi Halazien in the North Western Coast in Egypt. *J Nat Sci*., **8(7):** 43-49.

James CS. 1995. **Analytical Chemistry of Foods**. Blackie academic and Professional press. Chemistry. 46: 4358-4362.

James FB and Phyllis AB. 1997. **Prescription for Nutritional Healing**. Avery Publishing Group, 2nd Ed. 38-41.

Meselhy MR, Aboutabl EA and Shoka AAE. 1994. Comparative phytochemical and pharmacological screening of *Polycarpon succulentum, Polycarpaea repens* and *Gymnocarpos decandrum* (Caryophyllaceae) growing in Egypt. Bulletin Faculty of Pharmacy (Cairo University), **32:** 399–405.

Metcalfe CR and Chalk L. 1950. **Anatomy of the Dicotyledons**. Clarendon Press, Oxford; London.

Okba MM, Soliman FM and Deeb K. 2013. Botanical study, DNA fingerprinting, nutritional values and certain proximates of *Entada rheedii* Spreng. *Int J Pharm Pharm Sci*, **5(3):** 311-329.

Petrusson L and Thulin M. 1996. Taxonomy and biogeography of Gymnocarpos (Caryophyllaceae). *Edinb. J. Bot.*, ***53*(1)**: 1-26.

Ruzin SE. 1999. **Plant Microtechnique and Microscopy**. New York: Oxford University Press.

Sallam A and Galala AA. 2017. Inhibition of alpha-amylase activity by *Gymnocarpos decandrus* Forssk Constituents. *Int J Pharm Phytochem Res*, **9:**.873-879.

Sathiyamoorthy P, Lugasi-Evgi H, Schlesinger P, Kedar I, Gopas J, Pollack Y and Golan-Goldhirsh A. 1999. Screening for cytotoxic and antimalarial activities in desert plants of the Negev and Bedouin market plant products. *Pharm Biol*, ***37*(3)**: 188-195.

Singh S, Machawal L and Chauhan MG. 2010. Pharmacognostic study of male leaves of *Trichosanthes dioica* Roxb. with special emphasis on microscopic technique. *Journal of Pharmacognosy and Phytotherapy*, ***2*(5):** 71-75.

Williams M. 2005. Dietary supplements and sports performance: amino acids. *J Int Soc Sports Nutr*. ***2*(2):** 63.

JJBS
Jordan Journal of Biological Sciences

Volume 12, Number 5,December 2019
ISSN 1995-6673
Pages 573 - 580

Microhabitat Selection of Ectoparasitic Monogenean Populations of the Nile Catfish, *Clarias gariepinus*

Mohamed I. Mashaly*, Ahmed M. El-Naggar, Ahmed E. Hagras and Haidi A. Alshafei

Zoology Department, Faculty of Science, Mansoura University, Egypt

Received January 6, 2019; Revised February 23, 2019; Accepted March 12, 2019

Abstract

The spatial fluctuations in the monogenean populations of the Nile catfish, *Clarias gariepinus* were investigated during the period from October 2015 to September 2016 in three different water quality environments in the Nile Delta, Egypt. A microhabitat specialization of different monogenean species was detected and showed considerable variations in their site selections from one locality to another. Some monogeneans attained significant preference for particular microhabitats on the gills; however, other monogeneans were randomly distributed on available microhabitats. The monogeneans, *Quadriacanthus aegypticus* and *Macrogyrodactylus clarii* preferred the proximal areas, while *Gyrodactylus rysavyi* preferred the distal area of the gill filaments of the *C. gariepinus* host in all investigated habitats except for *Q. kearni* that inhabited the ventral segment of the gill arches of the catfish host in the three localities. There was a noticeable locality-related variation in microhabitat distribution of the studied monogeneans on the dorsal, middle, and ventral segments of the catfish host. Gill arch II was the most favorable site of attachment for the three *Quadriacanthus* species in all three aquatic habitats and also for *G. rysavyi* in Ammar Drain. In this study, factors influencing population dynamics and those driving ecological interactions of the monogenean microfauna of the catfish host are discussed in detail.

Keywords: Monogenean populations, *Clarias gariepinus*, Aquatic ecosystems.

1. Introduction

Monogeneans are regarded as a highly specific group of fish parasites. These organisms are restricted to a particular host, definite organ, and specific tissue. The gills are vital organs for the survival of the fish and hospitable home for a variety of ectoparasitic monogeneans and ecological equivalents as well. According to Bychowsky (1957), monogeneans are a successful group for probing the adaptation of living organisms, their morphological variations, and association between cohabitants. This type of parasite shows a direct life cycle, and it is narrowly host-specific within species, genus, or family, and can occupy restricted microhabitat(s) on their favorable host(s). Many ecological investigations focused on the relationships of congener taxons (e.g. Kadlec *et al*., 2003, El-Tantawy *et al*., 2016 and 2018). However, there have been few studies on the ecological interaction between species belonging to two or more monogenean genera as well as between monogeneans and other parasite taxons (e.g. Ramasamy *et al*., 1985; El-Naggar and El-Tantawy, 2003).

The aim of the present study is to investigate and compare the microhabitats of cohabitant monogeneans on the catfish host, and to illustrate the ecological interactions (intraspecific aggregation) among different cohabitant monogeneans of *C. gariepinus*.

2. Materials and Methods

2.1. Area of Investigation

The investigated aquatic habitats are located in the Eastern region of the Nile Delta, Egypt. These ecosystems include:

1. The Damietta Branch of the Nile River in the vicinity of Kafr Al-Tawaila Village, Talkha City, Dakahlia Governorate (31° 7' 31" N, 31° 26' 2" E).
2. Ammar Drain (Drain No. 2): This is one of the largest agricultural drains in the Nile Delta. It terminates nearby the Mediterranean Coast at Gamasa City where waterway stores huge amount of waste released from suburban and agricultural areas (31° 22' 46" N, 31° 29' 23" E).
3. Telbanah Drain: This is a multi-polluted, man-made stream receiving considerable amounts of contaminated water discharged from Dakahlia Spin and Wear Company, Oil and Soap Company, agricultural

* Corresponding author e-mail: Dr.moh_mashaly@yahoo.com.

** Abbreviations:AS, adhesive sac; ASS, accessory sclerite; B, connecting bar; BP, body proper; CC, cluster of cells; CO, copulatory tube; D, diverticula; DB, dorsal bar; DH, dorsal hamulus; E1, first generation; H, haptor; HA, hamulus; MH, marginal hoohks; MS, massive sclerite; P, papilla; PH, pharynx; SS, supportive sclerites; U, uterus; VB, ventral bar; VH, ventral hamulus; VT, vaginal tube.

effluents, and domestic discharges. (1°05'00" N, 32°0'48" E).

2.2. Host Collection and Arbitrary Division of the Gills

A total of 989 *Clarias gariepinus* fish specimens were collected from November 2015 to October 2016. The fish was caught by special traps and were then immediately fixed in 10 % formaldehyde, and transferred to the laboratory in appropriate containers. The gill apparatus was dissected and individual gills were surveyed for monogenean parasites. The gill apparatus was divided into two gill sets, namely left and right. Gill arches were separated and numbered in an anteroposterior succession (I, II, III, and IV). Each gill arch was divided into three approximately equal segments in a dorsoventral succession (dorsal, middle and ventral). The gill filaments in each holobranch were divided longitudinally into approximately two equal halves, namely proximal and distal. The position of recorded monogeneans is shown as a schematic drawing of the gill arch in Figure1.

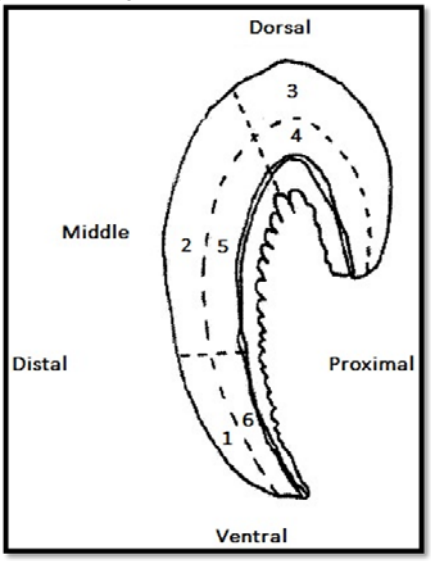

Figure 1. Illustration of gill arch showing its division into six arbitrary area: 1. distal-ventral, 2.distal-middle, 3.distal-dorsal, 4.proximal-dorsal, 5. proximal-middle, 6.proximal-ventral.

Each gill arch (holobranch) was divided into two hemibranchs, namely anterior and posterior. Each division was microscopically examined, and the detected monogenean parasites dislodged off from their attachment sites on the gills with the aid of a fine dissecting needle, and different species were discriminated according to their morphometric features. The isolated monogenean worms were identified using Leitz Laborlux 20 E B light microscope. The identification of the collected *Quadriacanthus* monogenean parasites was done according to Paperna (1961) and El-Naggar and Serag (1985, 1986). The monogeneans *Gyrodactylus rysavyi* were identified according to Ergens (1973) while *Macrogyrodactylus clarii* and *M. congolensis* were identified according to Gussev (1961) and Prudhoe (1957) respectively. Light micrographs showing some morphological features of *Q. aegypticus*, *Q. clariadis*, *Q. kearni*, *M. clarii, M. congolensis* and *G. rysavyi* are shown in Figures 2-7, respectively.

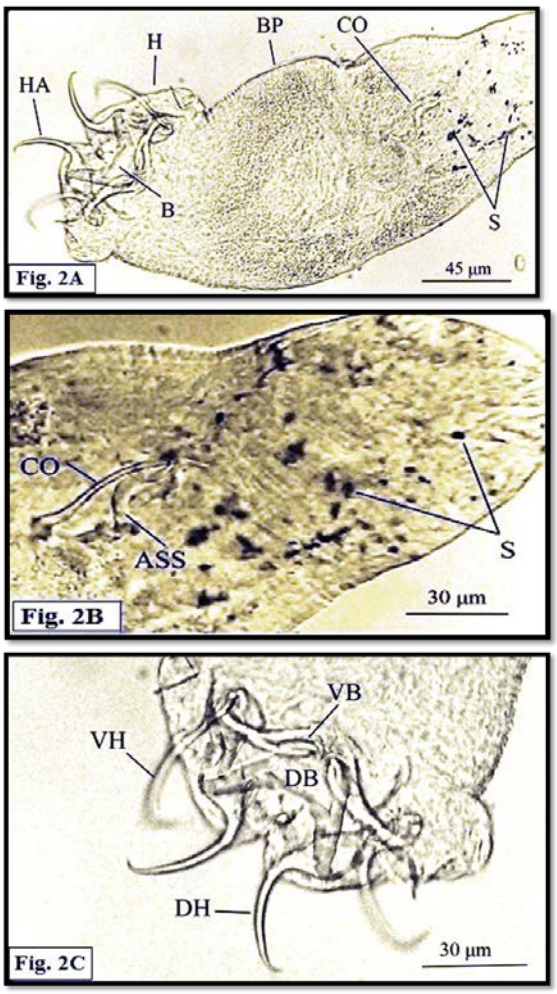

Figure 2.Light micrograph showing some morphological features of *Quadriacanthus aegypticus*. A) Whole mount. Scale bar = 45 µm. B) Copulatory organ. Scale bar = 30 µm. C) Haptoral sclerites. Scale bar = 30 µm.

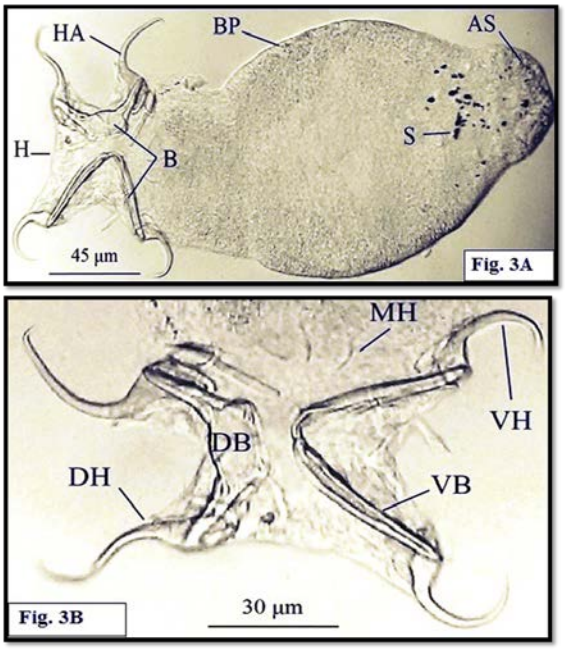

Figure3. Light micrograph showing some morphological features of *Quadriacanthus clariadis*. A) Whole mount. Scale bar = 45 µm. B) Haptoral sclerites. Scale bar = 30 µm.

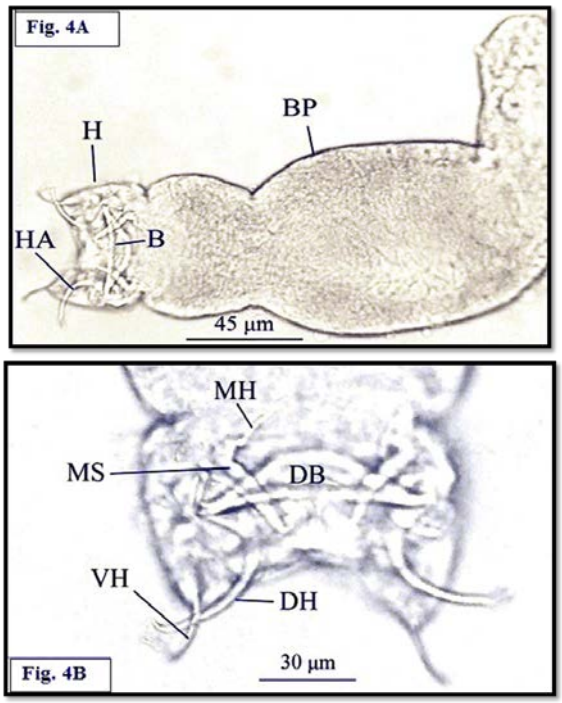

Figure 4. Light micrograph showing some morphological features of *Quadriacanthus kearni*. A) Whole mount. Scale bar = 45 µm. B) Haptoral sclerites. Scale bar = 30 µm.

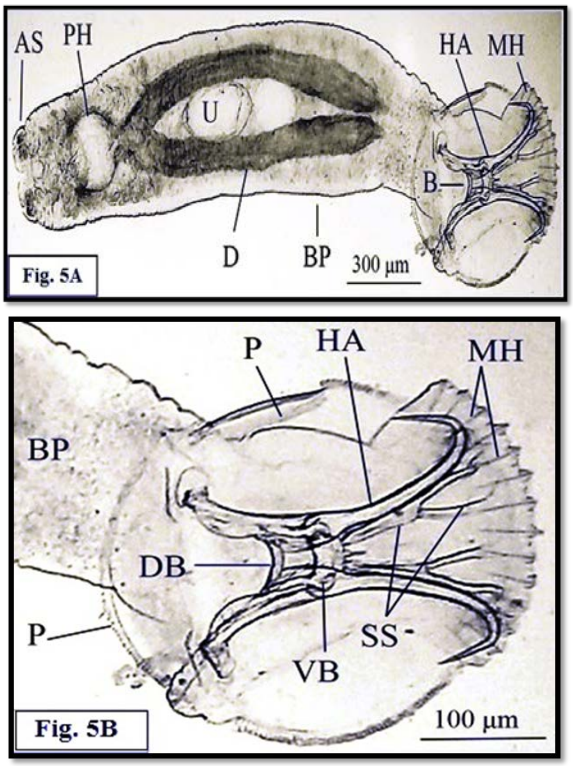

Figure 5. Light micrograph showing some morphological features of *Macrogyrodactylus congolensis*. A) Whole mount. Scale bar = 300 µm. B) Haptoral sclerites. Scale bar = 100 µm.

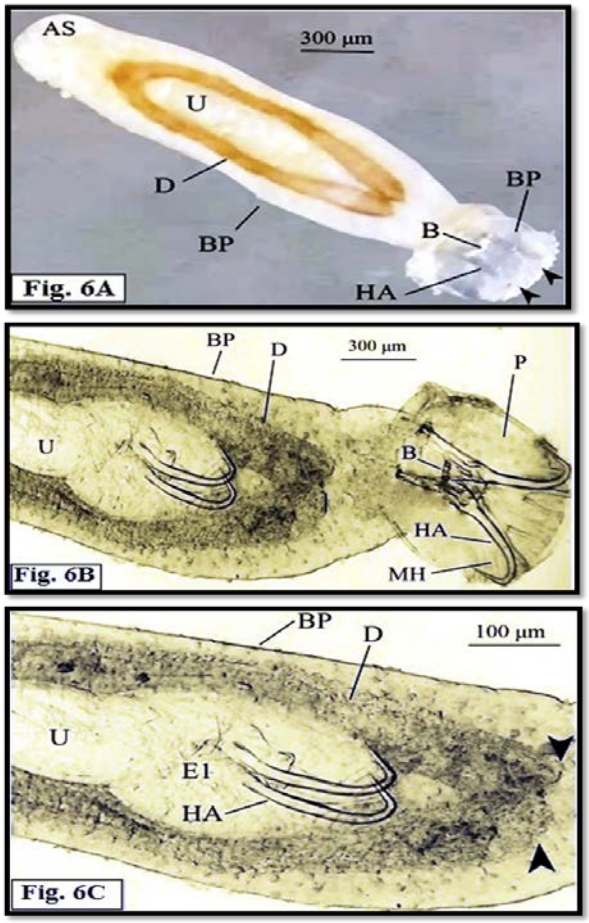

Figure 6. Light micrograph showing some morphological features of *Macrogyrodactylus clarii*. A) Whole mount. Scale bar = 300 µm. B) Posterior region. Scale bar = 300 µm. C) Embryonic load. Scale bar = 100 µm. The arrowheads point to the marginal hooks on the posteriorly projecting flap in Figure 6A and to the blind intestinal limbs (diverticulae) in Figure 6C.

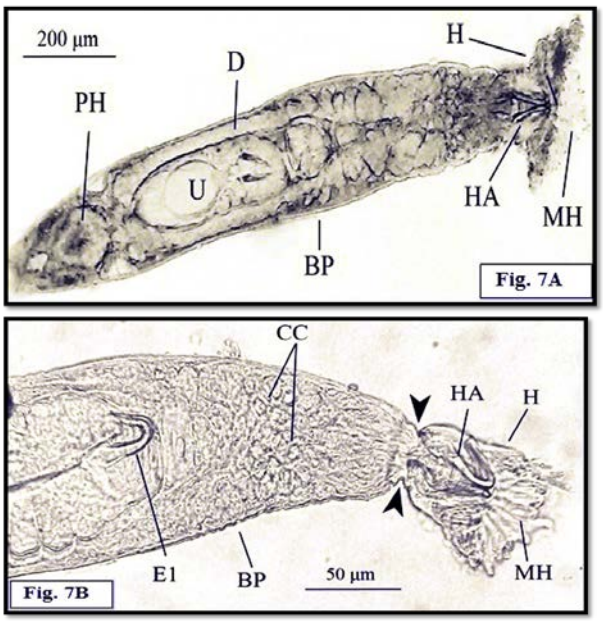

Figure 7. Light micrograph showing some morphological features of *Gyrodactylus rysavyi*. A) Whole mount. Scale bar = 200 µm. B) Posterior region. Scale bar = 50 µm. Note the marked constriction between the body proper and haptor (arrowheads).

The infestation variables (prevalence, intensity, and abundance) of the monogeneans under investigation were calculated according to Bush *et al*. (1997). To survey *Paraquadriacanthus nasalis* and *Gyrodactylus* sp. from the nasal cavities of the catfish host, the anterior dorsal sector of the mouth holding the nasal openings was dissected and kept in an appropriate container. This microhabitat was observed (searched) for monogeneans at the ventral, whitish side, where the internal opening was widened with the aid of a dissecting needle to expose its parasitic load. On the other hand, skin monogeneans on *C. gariepinus* were estimated as a t otal number on all examined fish/month/locality. Due to their superficial attachment to the surface epithelial layers, macrogyrodactylid and gyrodactylid monogeneans were easily detached during the direct fixation in the field in 10 % formaldehyde, and were transported to the laboratory; only the abundance of skin monogeneans was considered. To isolate the skin monogeneans in each monthly-collected host sample, impurities settled on the bottom of the container were filtered, and the precipitate was transferred to petri dishes containing water to be searched under a stereomicroscope for *M. congolensis* and *G. rysavyi*.

2.3. Ecological Interactions between the Monogeneans of Clarias gariepinus

To estimate the intraspecific aggregation among individuals of a particular monogenean species, a measure of intraspecific aggregation (I) was employed (Ives, 1988 and 1991):

$$I_r = \frac{\frac{v_r}{m_r} - 1}{m_r}$$

Where m_r is the mean number of parasite species, (*r*) individuals per an infested fish, and V_r is the variance in the numbers of parasite species (*r*). The index I_r shows the proportional increase in the number of conspecific competitors experienced by a random individual of species (*r*), relative to a random pattern of distribution.

2.4. Statistical Analysis

All records were represented as mean values. Differences in the distribution of the monogenean species between left and right gill sets, proximal and distal halves of the gill filaments as well as between outer and inner hemibranchs were tested statistically using the Student's *t*-Test on S PSS package (version: 20). On the other hand, differences in the distribution of the studied monogeneans among dorsal, middle, and ventral segments as well as among the four gill arches were tested by the same statistical software using One-Way ANOVA Test. The same test was employed to check for seasonal variations in the prevalence, mean intensity, and abundance of each monogenean species in each ecosystem. Further statistical analysis (PostHoc LSD) was selected to detect the differences between each pair of localities or seasons. Probability (*P*) values ≤ 0.05 were set as significant; those ≤ 0.01 as highly significant, and values ≤ 0.001 as very highly significant; however, *P* values > 0.05 were considered no significant.

3. Results

3.1. Seasonal Population Dynamics of the Monogeneans of Clarias gariepinus

The monogeneans *Quadriacanthus aegypticus (*El-Naggar and Serag, 1986), *Q. clariadis (*Paperna, 1961), *Q. kearni* (El-Naggar and Serag, 1985) and *Gyrodactylus rysavyi* (Ergens, 1973) were recorded throughout the year on catfish from the Nile River, Telbanah Drain, and Ammar Drain. Similarly, *Macrogyrodactylus clarii* (Gussev, 1961) was present on t he gills of *C. gariepinus* throughout the year in Ammar Drain; however, it was absent from the host in the Nile River during winter and spring. The congeneric *Macrogyrodactylus congolensis* (Prudhoe, 1957) was found on the skin of *C. gariepinus* at Ammar Drain throughout the year; however, it was not detected on the host during winter and summer at Telbanah Drain and during summer in the Nile River. *Gyrodactylus rysavyi* was only observed on the skin of *C. gariepinus* at Ammar and Telbanaah Drains throughout the year, and during summer in the Nile River. *Gyrodactylus* sp. was found in the nasal cavity of *C. gariepinus* only during autumn at Telbanah Drain and Ammar Drain; however, it was completely absent from the nasal cavity of the catfish host in the Nile River.

3.2. Microhabitat Distribution and Ecological Interactions (Intraspecific Aggregation) of the Gill monogeneans on Clarias Gariepinus

3.2.1. Microhabitat Distribution

Regarding the habitat of the detected monogenea species, the oviparous monogenean *Q. aegypticus, Q. clariadis* and *Q. kearni* were encountered only on the gill filaments and gill lamellae of *Clarias gariepinus*, whereas the viviparous *M. clarii* was found on the gill lamellae, gill rakers, and gill arch. The monogenean *G. rysavyi* occurred on the gills of the catfish host. Tables 1-5 show the percentage of the distribution of *Q. aegypticus, Q. clariadis, Q. kearni, M. clarii and G. rysavyi* respectively on the gills of *C. gariepinus* from the Nile River, Telbanah Drain, and Ammar Drain. As shown from Table 2, the monogeneans *G rysavyi*, *M. clarii* and *Q. kearni* prefer the left gill set than the right one. In contrast, the monogenean *Q. clariadis* showed a preference for the right gill set than the left one.

Quadriacanthus aegypticus occurred at a higher percentage on t he outer hemibranch than the inner one (Table 1), this monogenean preferred the proximal over the distal area of the gill filaments of the catfish at the three aquatic habitats (Table 3). *Q. aegypticus* preferred to exist on the middle segment of the gill filaments than the dorsal and ventral ones at Ammar Drain. However, this parasite preferred to exist on the dorsal segment of the gill filaments over the middle and ventral ones in the Nile River and Telbanah Drain (Table 4). This parasite was recorded at the highest percentage of distribution on the second gill arch (holobranch) (Table 5).

Quadriacanthus clariadis was recorded at a higher percentage of distribution on the outer than the inner hemibranch on t he gills of *C. gariepinus* inhabiting the Telbanah and Ammar Drains. However, the parasite

preferred the inner hemibranch over the outer ones in the Nile River (Table 1). The percentage of the distribution of *Q. clariadis* on the right gill set was higher than that on the left one (Table 2). The percentage of the distribution of this monogenean was higher on the proximal area than the distal one of *C. gariepinus* in the Nile River; however, at Telbanah Drain and Ammar Drain, the parasite exhibited a microhabitat shift and preferentially occupied the distal area. In contrast, *Q. kearni* showed no preference for the proximal over the distal area of the gill filaments of *C. gariepinus*. Similar marked preference for the distal over the proximal area of the gill filaments was obtained for *G. rysavyi* (Table 3).

Table 4 shows that *Q. clariadis* prefers to exist on the dorsal segment of gill holobranch than the middle and ventral ones in the Nile River, but prefers to exist on the middle segment at Ammar Drain and Telbanah Drain. The highest percentage of the distribution of *Q. clariadis* was estimated on the second gill arch in all studied environments (Table 5). A similar preference for the second gill arch was recorded for *Q. clariadis* and *Q. kearni* in all three habitats and for *G. rysavyi* at Ammar Drain. As shown in Table 1, *Q. kearni* tends to exist at a higher percentage on the outer than the inner hemibranch of the catfish in the Nile River, Ammar Drain, and Telbanah Drain. The percentage of the distribution of this monogenean on the left gill set was higher than that on the right set. *Q. kearni* prefers to attach to the proximal half of the gills than on the distal half at Ammar Drain, but the parasite showed no marked preference for the proximal or distal half of the gills in the Nile River and Telbanah Drain (Table 3). It is obvious that *Q. kearni* prefers to live on the ventral segment over the middle and dorsal ones of the gills of *C. gariepinus* at the three ecosystems. Similar to *Q. clariadis*, the highest percentage of distribution was found on the second gill arch of *C. gariepinus* in all investigated areas (Table 5).

Data obtained in Table 1 indicate that the viviparous monogenean *M. clarii* tends mainly to exist at higher proportions on the inner hemibranch of the gills than the outer one of the host at the majority of the studied habitats. The percentage of distribution on the left gill set was higher than that on the right one (Table 2). The parasite preferred to be attached to the proximal half of the gill filaments than the distal one (Table 3). It is clear that *M. clarii* prefers to live on the dorsal and middle over the ventral segment of the gills of *C. gariepinus* at the three ecosystems (Table 4).

As recorded in Table 1, the viviparous monogenean *G. rysavyi* tends to exist at a higher percentage of distribution on the outer hemibranch of the gills of *C. gariepinus* than the inner one at the three studied streams. The percentage of distribution on left gill set was higher than that on the right set (Table 2). The parasite preferred to attach itself to the distal half of the gills than proximal ones at the three investigated areas. Table 4 shows that *G. rysavyi* prefers to live on the middle segment of gill arch of the host in the Nile River and Ammar Drain, but prefers the ventral segment at Telbanah Drain. The highest percentage of the distribution of *G. rysavyi* was on the third gill arch in the Nile River (36.84 %), in the second gill arch at Ammar Drain (58.33 %) and on the first and fourth gill arch at Telbanah Drain (31.25 %).

Table 1. Percentage distribution (%) of Monogenean parasites on the outer and inner gill hemibranches of *Clarias gariepinus* from the River Nile, Telbanah Drain and Ammar Drain.

Monogenean species:	River Nile		Telbanah Drain		Ammar Drain	
	Outer	Inner	Outer	Inner	Outer	Inner
Quadriacanthus aegypticus	59.85	39.41	52.25	47.74	65.61	34.38
Quadriacanthus clariadis	40.00	60.00	53.23	46.76	55.94	44.05
Quadriacanthus kearni	62.00	38.00	57.30	42.69	55.00	45.00
Macrogyrodactylus clarii	50.00	50.00	47.61	52.38	46.00	54.00
Gyrodactylus rysayvi	8.00	2.00	8.00	2.00	8.00	2.00

Table 2. Percentage distribution (%) of Monogenean parasites on the left and right gill sets of *Clarias gariepinus* from the River Nile, Telbanah Drain and Ammar Drain.

Monogenean species:	River Nile		Telbanah Drain		Ammar Drain	
	Left	Right	Left	Right	Left	Right
Quadriacanthus aegypticus	51.82	48.17	56.46	43.53	49.92	48.56
Quadriacanthus clariadis	42.66	57.33	32.24	64.75	49.18	50.27
Quadriacanthus kearni	62.00	38.00	57.30	42.69	55.00	45.00
Macrogyrodactylus clarii	58.33	41.66	57.14	42.85	56.00	44.00
Gyrodactylus rysayvi	63.15	36.84	59.37	40.62	83.33	16.66

Table 3. Percentage distribution (%) of Monogenean parasites on the proximal and distal halves of the gills of *Clarias gariepinus* from the River Nile, Telbanah Drain and Ammar Drain.

Monogenean species:	River Nile		Telbanah Drain		Ammar Drain	
	Proximal	Distal	Proximal	Distal	Proximal	Distal
Quadriacanthus aegypticus	71.53	28.46	60.76	38.44	67.87	32.12
Quadriacanthus clariadis	52.00	48.00	29.02	70.97	22.97	77.02
Quadriacanthus kearni	50.00	50.00	50.29	49.70	57.85	47.50
Macrogyrodactylus clarii	75.00	25.00	71.42	28.57	60.00	40.00
Gyrodactylus rysayvi	15.78	84.21	28.12	71.87	41.66	58.33

Table 4. Percentage distribution (%) of Monogenean parasites on dorsal, middle and ventral gill segments of *Clarias gariepinus* from the River Nile, Telbanah Drain and Ammar Drain.

Monogenean species:	River Nile			Telbanah Drain			Ammar Drain		
	Dorsal	Middle	Ventral	Dorsal	Middle	Ventral	Dorsal	Middle	Ventral
Quadriacanthus aegypticus	48.17	29.92	4.52	39.32	34.05	26.61	27.75	42.38	29.86
Quadriacanthus clariadis	49.33	36.00	14.66	22.63	51.08	26.28	15.40	51.89	32.70
Quadriacanthus kearni	20.00	22.00	58.00	14.13	24.04	61.79	12.85	31.42	55.70
Macrogyrodactylus clarii	25.00	58.33	16.66	42.85	41.66	15.47	34.00	42.00	24.00
Gyrodactylus rysayvi	21.05	47.36	31.57	18.75	34.37	46.87	4.16	79.16	16.66

Table 5. Percentage distribution (%) of Monogenean parasites on the gills (I, II, III and IV) of *Clarias gariepinus* from the River Nile, Telbanah Drain and Ammar Drain.

Monogenean species:	River Nile				Telbanah Drain				Ammar Drain			
	I	II	III	IV	I	II	III	IV	I	II	III	IV
Quadriacanthus aegypticus	22.62	28.4	25.54	23.35	21.65	28.03	25.86	24.44	23.52	33.18	21.71	19.90
Quadriacanthus clariadis	28.88	29.77	20.88	20.44	19.81	23.46	21.55	21.55	20.81	35.13	24.05	20.00
Quadriacanthus kearni	32.00	32.00	24.00	12.00	20.56	36.45	22.22	20.76	22.85	31.78	23.21	25.71
Macrogyrodactylus clarii	0.00	33.33	41.66	25.00	27.38	20.23	25.00	27.38	18.00	36.00	32.00	14.00
Gyrodactylus rysayvi	21.05	31.57	36.84	10.52	31.25	28.12	9.37	31.25	8.33	58.33	12.5	20.83

3.2.2. Intraspecific Aggregation Index

Table 6 represents the intraspecific aggregation values of the gill monogeneans of the catfish host, *C. gariepinus* from the Nile River, Telbanah Drain and Ammar Drain. Except for the value recorded for the viviparous monogenean *M. clarii* from *C. gariepinus* in the Nile River (- 0.17), all the intraspecifc values recorded for all the studied monogenean from the three localities were above zero (Table 6). The maximum intraspecific aggregation value was estimated for *Q. kearni* in the Nile River (7.86). Moderate intraspecific aggregation values were obtained for *Q. clariadis* in the Nile River (2.27) and *G. rysavyi* at Telbanah Drain (2.74).

3.3. Statistical Analysis

Q. aegypticus significantly preferred the proximal area over the distal area of the gills of *Ç. gariepinus* in the Nile River and Ammar Drain (Student's t-Test: t = 2.186 and 2.340 $p \leq 0.05$, respectively). *Q. clariadis* showed a preference for the proximal half in the Nile River and Ammar Drain. In contrast, this monogenean preferred the distal half at Telbanah Drain. This distribution was significant at Ammar Drain (t = 2 .691, $p \leq 0.05$) and Telbanah Drain (t = -1.996, $p \leq 0.05$), but no significant in the Nile River ($p > 0.05$).

The congeneric *Q. kearni* exhibited a significant preference for the distal area in the Nile River (t=-2.696, $p \leq 0.05$) and Ammar Drain (t = - 2.749, $p \leq 0.05$) and Telbanah Drain (t = -2.830, $p \leq 0.01$). Unlike *M. clarii* which showed no preference between the proximal and the distal halves of the gill filaments, the viviparous monogenean *G. rysavyi* showed significant preference for the distal halves in the Nile River (t = -1.987, $p \leq 0.05$), high significant at Ammar Drain (t = - 3.010, $p \leq 0.01$) and very high significant at Telbanah Drain (t = - 4.553, $p \leq 0.001$).

All monogenean species showed no significant preference on the four gill arches, except for *G. rysavyi* at Ammar Drain (One- way ANOVA: F-ratio = 6.667, $p \leq 0.001$). Further statistical analysis (LSD) detected significant preference for the second gill arch over the first, third, or fourth gill arches.

The distribution of *Q. aegypticus* and *M. clarii* on the dorsal, middle, and ventral segments of the gill arches at all study sites was random. A similar distribution pattern was recorded for *Q. clariadis* and *G. rysavyi* in the Nile River and Telbanah Drain. There was a s ignificant preference for the middle segment over the dorsal one by *Q. clariadis* at Ammar Drain (One- way ANOVA: F-ratio = 13.824, $p \leq 0.001$). The oviparous monogenean *Q. kearni* significantly preferred the ventral segment over the dorsal and middle segments in the Nile River (F-ratio = 3.995, $p \leq 0.05$), Ammar Drain (F-ratio = 3.282, $p \leq 0.05$) and Telbanah Drain (F-ratio = 3.254, $p \leq 0.05$). Except for a high significant preference for the outer over the inner hemibranch of the catfish host by the mongenean *G. rysavyi* at the three study sites (Student's *t*-Test: t=3.679, $p \leq 0.001$), all monogenean species were randomly distributed between the outer and inner hemibranchs of the gills of *C. gariepinus* at all study sites.

4. Discussion

Microhabitat specialization and site selection in monogeneans may be influenced by habitat deterioration (e.g. Buchmann and Bresciani, 1998; Chapman *et al*., 2000; Raymond *et al*., 2006). Raymond *et al*. (2006) suggested that oxygen-poor aquatic environments may offer less competitive habitats especially when other gill dwellers are sensible to hypoxic environments. Olowo and Chapman (1996) proposed a higher gill ventilation rate in *Barbus neumayeri* under hypoxic conditions; this may facilitate the transmission and intromission of the monogeneans across the gill ventilation. According to Chapman *et al*. (2000), oxygen-deprived habitats can increase the opportunity of monogenean transmission. El-Naggar *et al*. (2001 and 2004) highlighted the significance of the swimming behavior in the bionomics of *G. rysavyi* from the skin and gill of *C. gariepinus.* The authors observed that *Gyrodactylus* worms displayed a v ariety of movement patterns including upside-down leech-like

movement, elongation, and shortening, searching movement, and self-cleaning acrobat-like displays. The determinants of narrow microhabitat specificity of many gill monogeneans are diverse. According to Holmes (1972), microhabitat specificity in helminth parasites may be ascribed to the direct competition or interactive site segregation among parasites living in the same host. Rohde (1979) demonstrated that monogeneans have highly confined microhabitats, even in the absence of competing species. Wootten (1974) suggested that microhabitat selection on/in the host may be related to physicochemical (abiotic) environments. *G. rysavyi* was found to prefer the second gill arch over others. Similar findings were recorded by Chapman *et al*. (2000) who found that *Afrodiplozoon polycotyleus* was highly site-specific on its host and constituted 78 % of the parasites on filaments of the second gill arch. The authors suggested that this monogenean may select the second gill arch to place itself in an area of maximal laminar flow in the gill. This may indicate that some monogenean species are rheophilic, i.e. favouring lotic streams over lentic ones.

El-Naggar (2012) made a preliminary investigation of the ecological interaction between two gyrodactylid monogeneans, namely *Gyrodactylus rysavyi* and *Macrogyrodactylus congolensis* from the skin of the Nile catfish, *C. gariepinus*, and found that these organisms exhibit significant morphological, ecological, and behavioural differences. Unlike *G. rysavyi*, which is fast-growing, small in size, and attains a high reproductive rate, the cohabitant *M. congolensis* is slow-growing, a large-sized species, and shows a co mparatively lower reproductive rate. The author also suggested that the attachment of *M. congolensis* is greatly damaging to the microhabitat, while the attachment of the rival *G. rysavyi* is comparatively less damaging. The output of all experimental infection trials revealed that *G. rysavyi* outnumbered *M. congolensis*, indicating that the former species is a superior competitor, while the latter is an inferior competitor.

The body dimensions of the viviparous monogenean *Macrogyrodactylus clarii* include the total length (2.330 mm), maximum breadth (400 µm), haptor length (460 µm), and haptor breadth (440 µm) (El-Naggar and Serag, 1987). On the other hand, the length of the gill filaments of the adult catfish host do not exceed a few centimeters. The following morphometric features may account for the optimal microhabitat selection by *M. clarii* for the proximal sector of the gill filaments of the catfish host. First, the bases of the gill filaments acquire an upstream location with respect to the hydrodynamic forces watering the gill apparatus and this seems likely to save the energy allocated to neutralize the sweeping action of the water current at the distal extremity of the filaments. Second, the proximal sector is supported and partially sheltered by the massive, cartilaginous plate (branchial arch) on which the gill filaments arrange; this may provide a more nursery living place for the newborn juveniles of *M. clarii*.

Third, comb-like gill rakers attached to the branchial arch act as a trap to suspend a variety of planktons and particulate matter, and prevent them from disturbing the functions of gill lamellae and routine activities of the resident monogenean worms as well. Fourth, the commencement of the movement from the base of gill filaments probably optimizes the opportunities of *M. clarii* to spend long distances whilst scanning the microhabitat and locating a mating partner or avoiding a hostile cohabitant. Fifth, residing in the vicinity of the branchial arch provides an advantage for *M. clarii* to migrate passively across the gill arches without challenging the violence imposed by gill inhabitants and to move, in a leech-like manner, on t he roof of the oral cavity of quiescent, nocturnal host in order to join a closely-spaced fish. Sixth, viviparous monogeneans of the catfish host are irritable, attaining permanent mobility and migration than the cohabitant monogeneans (El-Naggar *et al*., 2001) and crustacean copepods (El-Naggar, 2001) and it is wise to segregate their niche and partition the resources.

In the present study, the monogeneans *Q. aegypticus* and *M. clarii* preferred the proximal area, while *G. rysavyi* preferred the distal area of the gill filaments of the host in all investigated habitats. *Q. clariadis* showed no preference for the proximal or distal area of gill filaments of *C. gariepinus* in the Nile River, however it showed a marked preference for the distal area over the proximal in Telbanah Drain and Ammar Drain. Difference in microhabitat distribution may be correlated with the limnological features of aquatic ecosystem; the three investigated streams showed a marked variation in physicochemical and heavy-metal parameters of water. These variations may alter the behavioral and biological activities of fish, which in turn will modify the bionomics of monogeneans living on t hat host (El-Naggar *et al.,* 2017).

Except for *Q. kearni* that inhabited the ventral segment of the gill arches of the host in the three localities, there was a noticeable locality-related variation in the microhabitat distribution of the studied monogeneans on the dorsal, middle, and ventral segments of the catfish host. This may be correlated with the difference in the infestation levels of the monogeneans of the catfish inhabiting the three localities; it may also be related to the habitat characteristics in each locality. Higher infestation levels may obligate some species to conduct a microhabitat shift to avoid competition with other cohabitants with identical ecological requirements. However, differences in the sample size and quality (proportion of male and female host individuals, length and size classes of examined fish) may affect the obtained data.

The present observations indicated that no preference was conducted by *Q. aegypticus*, *Q. clariadis*, *Q. kearni*, *M. clarii* and *G. rysavyi*, for the left or right gill sets of *C. gariepinus*. Nonsignificant preferences for the left and right gill sets were recorded by several authors (Hagras *et al*., 2000; Raymond *et al*., 2006; Rubio-Godoi, 2008; Jeannette *et al*., 2010; Iannacone and Alvarino, 2012). These findings indicate that the fish hosts are symmetric and acquire equal amounts of water flowing on the left and right sides of the body.

The viviparous monogenean *M. clarii* from *C. gariepinus* in the Nile River recorded an intraspecific aggregation index below zero (- 0.17), indicating that the distribution pattern of this monogenean will be regular or uniformed. In contrast, all remaining monogeneans of *C. gariepinus* from the three localities were above zero, indicating that an increase in the number of conspecifics expected an aggregated or a cl umped distribution pattern. Studying the aggregation of nine congeneric monogenean species of the genus *Dactylogyrus* on the gills of the roach,

Rutilus rutilus by Simkova *et al*. (2001) indicated that at low infestation levels intraspecific competition may lead to a slight effect on the microhabitat distribution of the parasite.

References

Buchmann K and Bresciani J. 1998. Microenvironment of *Gyrodactylus derjavini* on rainbow trout *Oncorhynchus mykiss*: association between mucous cell density in skin and site selection. *Parasitol Res.,* **84**:17-24.

Bush AO, Lafferty KD, Lotz JM and Shostak AW. 1997. Parasitology meets ecology on its own terms. *J Parasitol.*, **83**: 575-583.

Bychowsky BE. 1957. **Monogenetic Trematodes, their Systematics and Phylogeny**. Izdatel'stvo Akademii Nauk SSSR, Moscow. (In Russian: English translation edited by Hargis, W.J. Jr., 1961), pp. 627.

Chapman LJ, Lanciani CA and Chapman CA. 2000. Ecology of a diplozoon parasite on the gills of the African cyprinid *Barbus neumayeri*. East African Wild Life Society. *Afri J Ecol.,* **38**: 312-320.

El-Naggar AM. 2001. The relationship of host sex and length with the infestation levels of nine Monogenean species on two cichlids fishes from the river Nile and Manzala lake, Egypt. *J Egyptian-German Soc Zool.,* **35(D)**: 109-127.

El-Naggar AM. 2012. A preliminary report on the ecological interaction between *Gyrodactylus rysavyi* and *Macrogyrodactylus congolensis*, viviparous Monogeneans from the skin and fins of the Nile catfish *Clarias gariepinus*. *Indian Streams Res J*., **2(11)**: 1-10.

El-Naggar AM and El-Tantawy SM. 2003. The dynamics of gill monogenean communities on cichlid fish hosts inhabiting Damiatta Branch of the River Nile: Long-term changes in species richness and community structure. *J Egyptian German Soc Zool.,* **41(D)**: 187-220.

El-Naggar AM, Mashaly MI, Hagras AM and Alshafei HA. 2017. Monogenean microfauna of the Nile catfish, *Clarias gariepinus* as biomonitors of environmental degradation in aquatic ecosystems at the Nile Delta, Egypt. Journal of Environmental Science, *Toxicol Food Technol.,* **8(1)**: 45-62.

El-Naggar MM and Serag HM. 1985. The monogenean *Quadriacanthus kearni* n. sp. and a report of Q. clariadis clariadis Paperna, 1979 on the gills of *Clarias lazera* in Nile delta. *J Egyptian Soc Parasitol.,* **15**: 479– 492.

El-Naggar MM and Serag HM. 1986. *Quadriacanthus aegypticus* n. sp., a monogenean gill parasite from the Egyptian teleost *Clarias lazera*. *Systematic Parasitol.,* **8(2)**: 129-140.

El-Naggar MM and Serag HM. 1987. Redescription of *Macrogyrodactylus clarii* Gussev 1961, a monogenean gill parasite of *Clarias lazera* in Egypt. *Arab Gulf J Sci Res.,* **5**: 257-271.

El-Naggar MM, El-Naggar AA and El-Abbassy SA. 2001. Microhabitat and movement of *Gyrodactylus alberti*, *Macrogyrodactylus clarii* and *M. congolensis* from the Nile catfish *Clarias gariepinus*. *J Egyptian German Soc Zool.,* **35(D)**: 169-187.

El-Naggar MM, El-Naggar AA and Kearn GC. 2004. Swimming in *Gyrodactylus rysavyi* (Monogenea: Gyrodactylidae) from the Nile catfish *Clarias gariepinus*. *Acta Parasitol.,* **49(2)**: 102-107.

El-Tantawy SA, Al-Habiby EM, Mashaly MI and El-Awady ME 2016. Ecological studies on water-borne parasites at Dakahlia Governorate, Egypt. *J Environ Sci.,* **45(1):** 63-73.

El-Tantawy SA, El-Naggar AM, Mashaly MI and Almagtuf HA. 2018. Relationship of physicochemical parameters of water to intestinal helminth fauna of *Clarias gariepinus* in Dakahlia Governorate, Egypt. *Wulfenia,* **25(8):** 101-121.

Ergens R. 1973. Two new species of *Gyrodactylus* from *Clarias lazera (Vermes, Trematoda, Monogenoidea), Revue de Zoologie et de Botanique Africaine,* **87**: 77-80.

Gussev AV. 1961. A viviparous monogenetic trematode from freshwater basins of Africa (In Russian). *Doklady Akademii Nauk,* **136(1-6)**: 177-179.

Hagras AE, El-Naggar MM, Ogawa K, Hussien AB, and El-Naggar AM. 2000. Effect of some ecological parameters of the monogenean gill parasites on the cichlid fish *Oreochromis niloticus* and *Tilapia zilli* from Manzala Lake and Mansouria Canal at east northern delta - Egypt. *J Egyptian- German Soc Zool.,* **32**: 205–221.

Holmes JC. 1972. Site selection by parasitic helminths: interspecific interactions, site segregation, and their importance to the development of helminth communities. *Canadian J Zool.,* **5**: 333-347.

Iannacone J. and Alvarino L. 2012. Microecology of the monogenean *Mexicana* sp. on the gills of *Anisotremus scapularis* (Tschudi, 1846) (Osteichthyes, Haemulidae) of the marine coast of Lima, Peru. *Neotropical Helminthol.,* **6**: 277-285.

Ives AR. 1988. Covariance, coexistence and the population dynamics of two competitors using a patchy resource. *J Theoritical Biol.,* **133**: 345-361.

Ives AR. 1991. Aggregation and coexistance in a carrion-fly community. *Ecological Monographs,* **61**: 75-94.

Jeannette T, Jacques N and Felix BC. 2010. Spatial distribution of Monogenean and Myxosporidian gill parasites of *Barbus martorelli*, Roman, 1971 (Teleostei: Cyprinidae): The role of intrinsic factors. *Afri J Agricul Res.,* **5(13)**: 1662-1669.

Kadlec D, Simkova A and Gelnar M. 2003. The microhabitat distribution of two *Dactylogyrus* species parasitizing the gills of the barbell, *Barbus barbus*. *Journal of Helminthol.,* **77**: 317-325.

Olowo JP and Chapman LJ. 1996. Papyrus swamps and variation in the respiratory behaviour of the African fish *Barbus neumayeri*. *Afri J Ecol.,* **34**: 211-222.

Paperna I. 1961. Studies on the monogenetic trematodes in Israel. 3. Monogenetic trematodes of the Cyprinidae and Claridae of the lake of Galilee. *Bamidgeh,* **13**: 14-29.

Prudhoe S. 1957. Trematoda. In: Exploration du Parc National de l'Upemba. I. Mission G. F. De Whitte en collaboration avec W. Adam, A. Janssens, L. *Van Meel et R. Verheyen,* **48**: 1-28.

Ramasamy PK, Ramalingam K, Hanna REB and Haleton DW. 1985. Microhabitats of gill parasites (Monogenea and Copepoda) of teleosts (*Scomberoids* Spp.). *Inter J Parasitol.,* **15**: 385-397.

Raymond KM, Chapman LL and Lanciani CA. 2006. Host, macrohabitat, and microhabitat specificity in the gill parasite *Afrodiplozoon polycotyleus* (Monogenea). *J Parasitol.,* **92(6)**: 1211-1217.

Rohde K. 1979. A critical evaluation of intrinsic and extrinsic factors responsible for niche restriction in parasites. *Amer Naturalist,* **114**: 648-671.

Rubio-Godoy M. 2008. Microhabitat selection of *Discocotyle sagittata* (Monogenea: Polyopisthocotylea) in farmed rainbow trout. *Folia Parasitol,* **55**: 270- 276.

Simkova A, Gelnar M and Sasal P. 2001. Aggregation of congeneric parasites (Monogenea: *Dactylogyrus*) among gill microhabitats within one host species (*Rutilus rutilus* L.). *Parasitol.,* **123(6)**: 599-607.

Wooten R. 1974. The spatial distribution of *Dactylogyrus amphibothrium* on the gills of ruffe *Gymnocephalus cernua* and its relation to the relative amounts of water passing over the parts of the gills. *J Helminthol,* **48**: 167-174.

JJBS
Jordan Journal of Biological Sciences

Volume 12, Number 5,December 2019
ISSN 1995-6673
Pages 581 - 588

An Evaluation of the Antioxidant Properties of Propolis against Fenvalerate-induced Hepatotoxicity in Wistar Rats

Wael M. Alamoudi*

Department of Biology, Faculty of Applied Sciences, Umm Al-Qura University, Saudi Arabia.

Received February 2, 2019; Revised March 1, 2019; Accepted March 16, 2019

Abstract

Fenvalerate is a synthetic pyrethroid pesticide used extensively in agriculture to protect a wide variety of crops. Propolis is a natural product produced by honey bees and is used widely in traditional medicines for its antioxidant properties. The present work evaluates the effects of fenvalerate administration on albino rats' liver and possible ameliorative roles played by propolis treatment. Fenvalerate treatment has induced histological changes in the liver of albino rats including the congestion of blood vessels, cytoplasmic vacuolization of the hepatocytes, necrosis and fatty degeneration. Biochemical analyses showed that fenvalerate caused a remarkable increase in the level of alanine aminotransferase (ALT), aspartate aminotransferase (AST), urea and creatinine, and a decrease in the total number of white blood cells (WBCs) and platelets. It also caused an increase in malondialdehyde (MDA) and depletion in the activity of the antioxidant enzymes, catalase (CAT), and superoxide dismutase (SOD) in the liver of rats. However, treating animals with fenvalerate followed by a propolis treatment led to an improvement in both histological and biochemical alterations induced by fenvalerate. The rats that were treated with fenv/propolis showed a dramatic improvement in the level of ALT, AST, urea and creatinine, WBCs, and platelets. Moreover, propolis was found to reduce the level of malondialdehyde and increase the activity level of antioxidant enzymes, SOD and CAT. In conclusion, propolis might be considered as a natural effective agent to eliminate the toxicity caused by fenvalerate, due to its antioxidant activity.

Keywords: Fenvalerate, Propolis, Hepatotoxicity, Transaminases, Antioxidants.

1. Introduction

The widespread utilization of insecticides in insect control has brought about the need for the evaluation of the hazards caused by such substances. Pyrethroids have been known as insecticides for many years, and are used as highly-active insecticides. The source of Pyrethroids is the flowers of the pyretherum plant *Chrysanthemum cinerariafolium* (Casida 1973). Due to the persistence of these insecticides in the environment, structures similar to Pyrethroids have been synthesized and proved to be effective against different insects (McEween and Stephenson, 1979). On the other hand, exposure to Pyrethroids was found to produce the serious side effects. It has been shown that animals exposed to these insecticides exhibited disturbances in their physiological activities in addition to other histopathological alterations (Amaravathi *et al.,* 2010; Giray *et al.,* 2011). Moreover, Fenvalerate is a cyanophenoxy-benzyl group of the synthetic pyrethroid pesticides used extensively in agriculture to protect a wide variety of crops; it also serves as an indoor pest control because of its high toxicity to insects (Kneko *et al.,* 1981).Moreover, it has been reported that fenvalerate can induce hepatotoxicity and alter the biochemical markers in experimental animals (Mani *et al*., 2004; Waheed *et al*., 2012) in addition to causing oxidative stress in rats (Prasanthi *et al.,* 2005).

Propolis is the substance that honey bees produce by mixing their own waxes with resins collected from plants. It has been widely used as a folk medicine since ancient times (Kumazawa 2018). Recently, propolis has gained popularity as healthy food in various parts of the world because it promotes health and prevents diseases (Gonzalez *et al*., 1994, Galeotti *et al*., 2018). Moreover, propolis has different biological effects and antibacterial activities including the inhibition of cell division, the inhibition of bacterial motility, disrupting the mechanism of cytoplasm cell membranes and cell walls, bacteriolysis, enzyme inactivation, and protein synthesis inhibition (AL-Ani *et al*., 2018; Sforcin *et al.,* 2000). It has also been reported as having anti-inflammatory (Khayyal *et al.,* 1993), anticarcinogenic (Bazo *et al*., 2002), antioxidative (Jasprica *et al*., 2007; Kanbur *et al*., 2009; Sobocanec *et al*., 2006) and hepatoprotective effects (Gonzalez *et al*., 1994). The components contained in propolis are more than 300, and these include sequiterpene quinines coumarins, phenolic aldehydes, steroids, polyphenol, inorganic compounds and amino acids (Khalil *et al.,* 2006). Earlier *in vivo* and *in vitro* studies indicated that there are numerous biological properties of propolis which include anti-inflammatory, immunomodulatory effects (Ivanovska *et al*., 1995), antitumor (Awale *et al*., 2008;

* Corresponding author e-mail: wmamoudi@uqu.edu.sa.

Ishihara *et al*., 2009; Aldemir *et al*., 2018), antioxidant (Jaiswal *et al.,* 1997) and free-radical scavenging effects (Pascual *et al.,* 1994). To the author's knowledge, literature and evidence on the protective effect of propolis on fenvalerate- induced alterations are not enough. Accordingly, the present investigation was designed to study the ameliorative effects and the protective role of propolis against fenvalerate hepatotoxicity in albino rats.

2. Materials and Methods

The experiment was performed according to the guidelines of the ethical committee of Umm Al-Qura University, Faculty of Applied Science, Makkah, KSA.

2.1. Chemicals

Fenvalerate was purchased from a commercial agricultural market at Jeddah city KSA, propolis was purchased from the local health food market at Jeddah city, KSA. Alanine aminotransferase (ALT), aspartate aminotransferase (AST), urea and creatinine kits were obtained from (Sigma-Aldrich, St. Louis, MO, USA).

2.2. Propolis Extraction

The Propolis extract was prepared in an ethanolic solution as described by Attalla and Ayman (2008). Propolis (10 g) was trimmed into small pieces and dissolved vigorously with 34.85 80 % (V/V) ethanol for forty-eight hours at 37 ± 1ºC. The resulted ethanolic solution was filtered through Whatman filter paper size No. 4. The obtained filtered solution was air-dried, and the extract was weighed and dissolved in a sterilized 0.9 % normal saline (PBS) for experimental processing.

2.3. Animals and Treatment

Male Wistar rats, aged three months and weighing (120 ± 5 g), were obtained from the animal house of King Abdel Aziz University, Jeddah, Saudi Arabia. They were housed and maintained under standard laboratory conditions (24 ± 2 ºC, natural light-dark cycle) in well-aerated chambers, and were given free access to drinking water and commercial pellet diet. The animals were acclimated in laboratory conditions for one week before treatment. The animals were randomly divided into four groups with ten rats each.

Group I: (G1) Control group: animals were injected intraperitoneally (i.p.) with a buffer saline solution (0.9 % PBS).

Group II: (G2) Positive control: The animals were injected intraperitoneally (i.p.) with propolis at a dose of 100 mg/kg b.w. (Boutabet *et al*., 2011).

Group III: (G3) The animals were injected intraperitoneally (i.p.) with 5 mg/kg of fenvalerate (1/10 LD_{50}) dissolved in PBS, three times a week for four weeks. (Boutabet *et al.,* 2011).

Group IV: (G4) The animals were injected intraperitoneally (i.p.) with fenvalerate (5 mg/kg) followed by propolis (100 mg/kg) after twenty-four hours of the fenvalerate treatment, three times a week for four weeks (Boutabet *et al.,* 2011).

2.4. Tissue Preparation for Histopathological and Histochemical Studies

At the end of the fourth week of treatment, all the rats were sacrificed by decapitation, and the liver pieces of each group were collected separately to be subjected to the histopathological, histochemical, and biochemical examinations. For the histopathological examination, small pieces of the liver were fixed in 10 % neutral formalin for twenty-four hours. Fixed materials were then processed and embedded in paraffin blocks. Sections that were 5 µm thick were cut and stained with Ehrlich's haematoxylin and eosin. For the histopathological examination, slides were later stained with Ehrlich's haematoxylin and eosin, whereas for the histochemical examination, the liver specimens were fixed in Carnoy's fluid for Periodic acid Schiff's reaction to demonstrate the content and distribution of polysaccharides as described by Kiernan (1999). The total protein contents were detected using the mercury bromophenol blue method as described by Pearse (1972).

2.5. Hematological and Biochemical Assays

2.5.1. Hematological Profile

Fresh blood samples were used for the measurement of the red blood cells count (RBCs), white blood cells count (WBCs), hemoglobin content (Hb g/dI), and total platelets counts. Blood was obtained from the tail veins of controls and the treated groups, and was collected separately using an electronic blood counter. Differential WBCs were measured from blood smears on day 0 and weeks 1, 2, 3, and 4, respectively.

2.5.2. Biochemical Assays

For the biochemical study, blood was also collected, and the serum was obtained by centrifugating the blood samples (1500 rpm for ten minutes at 4 ºC) and stored at -20º for biochemical analysis. The activity of ALT and AST enzymes were measured using a diagnostic kit (Diagnostic system, Medford, NY, USA) as described by Reitman and Frankel (1957). The urea and creatinine were determined in the serum using a diagnostic kit (Diagnostic system, Medford, NY, USA) as described by Trinder (1969). Fresh tissue samples of the rats' liver were homogenized in cold distilled water until a uniform suspension was obtained. The homogenate was centrifuged, and the clear supernatant was separated. The Catalase (CAT) activity was also measured according to the method adopted by Aebi (1983). The superoxide dismutase (SOD) activity was determined according to the method described by Minami and Yoshikawa (1979). Malondialdehyde (MDA) was determined according to the method used by (Ohkawa *et al*., 1979)

2.6. Statistical Analysis

The results were expressed as mean ± SD of different groups (n =10). The statistical differences between the mean values were evaluated by ANOVA. D ata were analyzed using the computer program SPSS/ version 15.0. Values were considered statistically significant when $p < 0.05$.

3. Results

3.1. Histopathological Observations

The histopathological examination of the livers of the control (G1) and the rats treated with propolis (G2) showed a normal hepatic architecture, and the cords of the hepatocytes radiated from the central vein to the periphery of the hepatic lobules. No histopathological alterations were observed from the normal and positive control groups (Figure 1A and B). However, the liver tissues of the rats treated with fenvalerate for four weeks (G3) showed apparent signs of pathological changes compared to the control group. The normal structural organization of the hepatic lobules was impaired with a cl ear hepatic degeneration; coagulative necrosis of many hepatocytes and blood vessels were congested (Figure 1C). Infiltration of inflammatory leucocytes was also noticed (Figure 1D). In addition, the hepatocytes revealed cytoplasmic vacuolation and the nuclei were pyknotic (Figure 2A). Moreover, impairment in the hepatocytes and necrosis signs with dense inflammatory cells and other debris were detected after four weeks of treatment with fenvalerate. In these tissues, a fatty degeneration composed of scattered fat droplets was clearly abundant (Figure 2B). On the other hand, in the animals treated with fenvalerate and propolis (G4), these histopathological changes became less. The hepatocytes regained normal architecture with normal achromatized central nuclei, and a noticeable reduction in the infiltration of inflammatory leucocytes was also noticed (arrow), (Figure 1E and F). Kupffer cells were activated and a large number of binucleated cells were noticed in these sections (arrows), (Figure 2C).

The histochemical observation of the livers of control rats (G1) showed a normal content of the total carbohydrates that appeared stained with a red or magenta colour with Schiff's reagent, and was not distributed in the cytoplasm of the hepatocytes, but appeared concentrated at one pole of the cells (Figure 3A). The examination of the livers of the rats treated with fenvalerate (G3) showed a diminution in their carbohydrates' content. The nuclei appeared negatively reacted (PAS-negative) confirming the absolute degradation of glycogen (Figure 3B). Figure 3C shows the remarkable increase in the carbohydrate content of the hepatocytes in the tissue of the rats treated with fenvalerate plus propolis (G4). Also, the total protein content of the hepatocytes of the control rats (G1) was positively reacted and stained with a blue color after being stained with a bromophenol blue. The protein content in the hepatocytes appeared to be distributed in the cytoplasm as fine granules (Figure 4A). Moreover, the chromatin bodies and nucleoli exhibiting deep coloration, Kupffer cells, and the endothelial lining cells of sinusoids showed a mild reactivity with a bromophenol blue. In addition, the walls of blood vessels revealed a strong stainability. The liver of the rats treated with fenvalerate (G3) showed a noticeable reduction in the total protein contents in the cytoplasm of the hepatocytes (Figure 4B). However, the liver cells of the rats treated with fenvalerate plus propolis regained a somewhat normal content of total protein (Figure 4C).

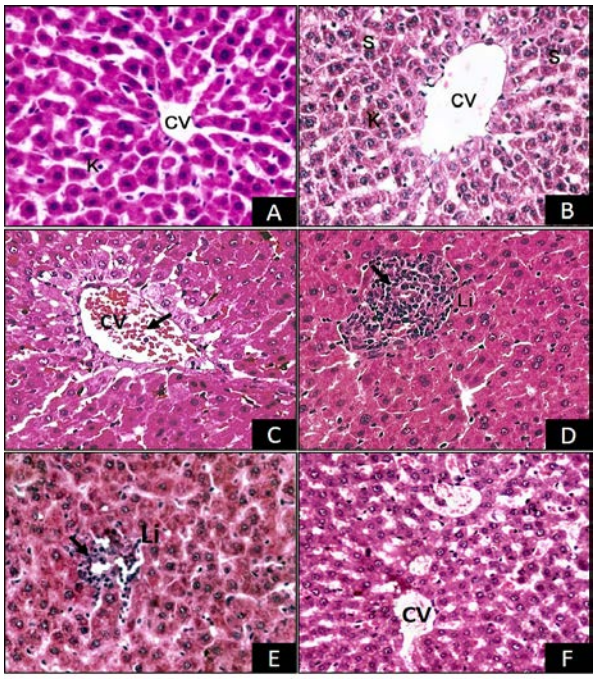

Figure 1. (A) Liver section of a control rat showing hepatic strands, kupffer cells (K), and central vein (CV). **(B)** Liver of a rat treated with propolis showing a normal hepatic architecture, kupffer cell (K) and sinusoids (S). **(C)** Liver of a rat treated with fenvalerate showing congestion of central vein (CV). **(D)** Liver of a rat treated with fenvalerate showing leucocytic infiltration (Li). **(E & F)** Sections of liver of rats treated with fenvalerate plus propolis showing a moderate degree of improvement in hepatocytes; few vacuolated hepatocytes exist with mild congestion in the central veins and lecocytic infiltration, (×400).

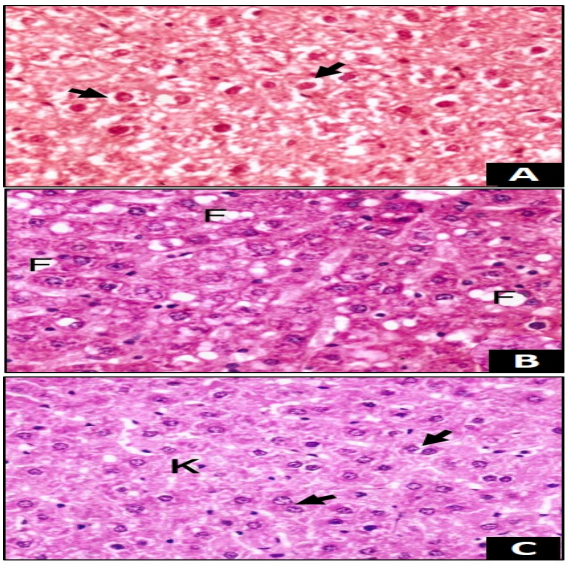

Figure 2. (A) Liver section of a rat treated with fenvalerate showing cytoplasmic vacuolizations of the hepatocytes and pyknotic nuclei (arrows). **(B)** Liver section of a t reated rat showing fat droplets (F). **(C)** Liver section of a rat treated with fenvalerate and propolis showing an advanced degree of improvement in the hepatocytes which regained normal architecture with binucleated cells (arrow head) and activated kupffer cells (K), (×400).

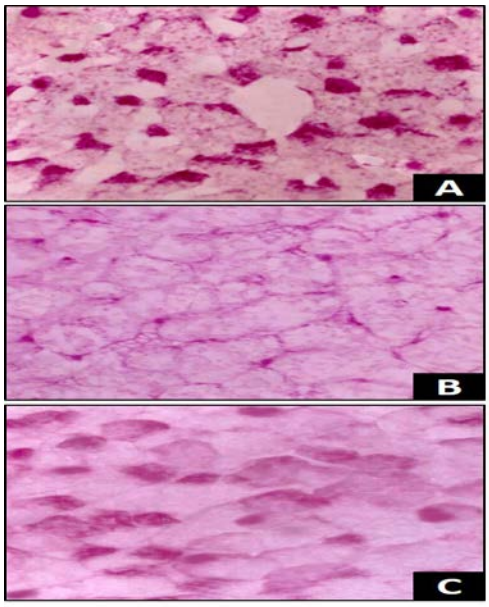

Figure 3. (A) Liver section of a control rat showing the distribution of carbohydrates in the cytoplasm of the hepatocytes. **(B)** Section of a rat treated with fenvalerate showing a noticeable decrease of carbohydrate in the hepatocytes. **(C)** Liver section of a rat treated with fenvalerate plus propolis showing a marked increase in the carbohydrate content in the hepatocytes, (×400).

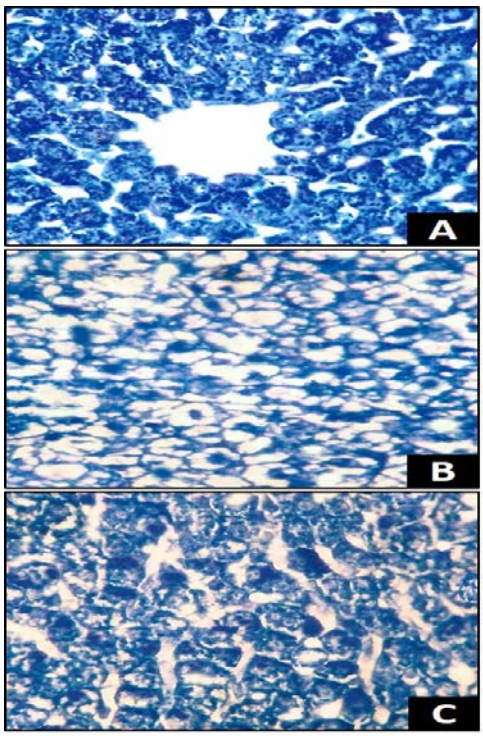

Figure 4. (A) Section of a liver showing the normal protein content of a control rat. **(B)** Section of liver showing a reduction of the protein content after treatment with fenvalerate. **(C)** Liver of a rat treated with fenvalerate plus propolis showing a noticeable increase in the protein content of hepatocytes, (×400).

3.2. Biochemical Parameters

3.2.1. Effect of Propolis on Fenvalerate-induced Changes in Serum Biochemical Parameters

According to the results of the study, it was found that there is no significant change ($p \geq 0.05$) in the level of serum ALT, AST, urea and creatinine in the rats of the control (G1) and positive control (G2) groups. Treating rats with fenvalerate (G3) caused a significant increment ($p \leq 0.05$) in serum ALT, AST, urea and creatinine levels following a month of treatment in comparison with their levels in the serum of the (G1 and G2) groups. In other words, animals infused with fenvalerate alongside propolis (G4) demonstrated a significant decrease ($p \leq 0.05$) in the ALT, AST, urea and creatinine values compared with fenvalerate-infused group (G3). Importantly, they are still significantly higher ($p \leq 0.05$) compared with the control groups (G1 and G2) (Table. 1).

Table 1. Effect of propolis on fenvalerate-induced changes in serum biochemical parameters of liver in rats.

	Control	Propolis	Fenvalerate	Fenv + Prop
ALT (IU/L)	77 ± 0.4	72 ± 0.55	107 ± 1.7	81 ± 0.8
AST (IU/L)	115 ± 1.6	116.8 ± 4.1	194.6 ± 2.6	143.2 ± 0.9
Urea (mmol/L)	15.4 ± 0.6	17.3 ± 1.4	49.5 ± 0.8	28.9 ± 0.5
Creatinine(µmol/L)	1.4 ± 0.06	1.97 ± 0.31	3.16 ± 0.05	2.13 ± 0.06

Values are expressed as mean ± SD, *n*=10

3.2.2. Effect of Propolis on Fenvalerate-induced Changes in Antioxidant Enzyme Levels

Table 2 presents the biochemical results which showed that treatments on M alondialdehyde (MDA) (index of tissue lipid peroxidation), superoxide dismutase (SOD) and catalase (CAT) activity in the livers of animals examined after treatment for four weeks did not have any noticeable effects. There is no significant change ($p \geq 0.05$) in the enzyme levels of the control groups (G1 and G2). The MDA level was significantly increased ($p \leq 0.05$) in the rats infused with fenvalerate (G3), whereas the activity of SOD and CAT were significantly decreased ($p \leq 0.05$). However, treating the animals with fenvalerate alongside propolis (G4) demonstrated a significant decrease ($p \leq 0.05$) in the MDA level and significant increase in the SOD and CAT activity, compared to those of the control (G1) and positive control (G2) groups.

Table 2. Effect of propolis on fenvalerate-induced changes in MDA,CAT and SOD levels in the liver in rats.

	Control	Propolis	Fenvalerate	Fenv + Prop
MDA (u mole/g tissue)	133.5 ± 5.2	135 ± 6.3	192 ± 5.5	140.5 ± 2.3
SOD (Units/g tissue)	45.6 ± 2.8	44.7 ± 1.5	28.4 ± 2.5	36.5 ± 3.4
CAT (mole/min/g tissue)	0.33 ± 0.01	0.30 ± 0.02	0.12 ± 0.01	0.23 ± 0.01

Values are expressed as mean ± SD, *n*=10

3.3. Hematological Parameters

3.3.1. Total Number of White Blood Cells (WBCs)

The present outcomes demonstrate that there is no significant change ($p \geq 0.05$) in the total number of WBCs in both control groups (G1 and G2) during the experiment period.

Nevertheless, there is a significant reduction ($p \leq 0.05$) in the aggregate number of WBCs in fenvalerate group (G3) and in the fenvalerate- and propolis-infused group (G4) in contrast with the (G1 and G2) groups until week

three and week four of treatment. The outcomes additionally demonstrate that there is no significant difference ($p \geq 0.05$) in the total number of WBCs in the fenvalerate and propolis group (G4) in contrast with the fenvalerate group (G3) until week three of treatment, (Table 3). During the fourth week of the experiment, the group treated with fenvalerate (G3) showed that they still have a significant drop in the total number of WBCs compared with the control groups (G1 and G2). Essentially, the group (G4) demonstrated a significant increase ($p \geq 0.05$) in the total number of WBCs in comparison with groups (G3 and G1). However, there was a nonsignificant increase ($p \geq 0.05$) in the total number of WBCs in comparison with the positive control (G2) (Table 3).

Table. 3. Effect of propolis on fenvalerate-induced changes in WBCs number in the serum of rats

	Control	Propolis	Fenvalerate	Fenv + Prop
Day 0	7.2 ± 0.7	7.5 ± 0.5	7.65 ± 0.35	7.73 ± 0.2
Week 1	7.12 ± 0.6	7.21± 0.7	3.51 ± 0.4	3.98 ± 0.9
Week 2	7.25 ± 0.5	7.0 ± 0.6	3.87 ± 0.8	4.17 ± 0.3
Week 3	7.20 ± 0.6	6.82 ± 0.35	3.69 ± 0.9	6.21 ± 1.14
Week 4	7.1 ± 1.12	7.7 ± 1.31	6.13 ± 0.4	8.9 ± 0.8

Values are expressed as mean ± SD, *n*=10

3.3.2. Total Number of Red Blood Cells and Hemoglobin Level

The fndings demonstrate that there are no significant differnces ($p \geq 0.05$) in the aggregate number of RBCs and hemoglobin levels in the positive control (G2), control (G1) and the fenvalerate-infused group (G3). In contrast, the rats treated with fenvalerate plus propolis (G4) demonstrated a s ignificant decrease ($p \leq 0.05$) in the aggregate of RBCs and Hb levels in comparison with the (G1, G2 and G3) groups respectively (Table 4).

Table 4. Effect of propolis on fenvalerate-induced changes in the RBCs number, Hb content and dential leucocytes in the serum of rats.

	Control	Propolis	Fenvalerate	Fenv + Prop
RBCs (10^6 /ml)	7.4 ± 0.5	7.6 ± 0.3	6.9 ± 0.4	5.8 ± 0.1
HGB (g/dl)	14.2 ± 1.0	13.1 ± 1.1	12.8 ± 0.6	10.6 ± 0.45
PLT (10^3 /ml)	346 ± 2.0	785 ± 2.5	575 ± 4.6	1235 ± 8.2
% Lymphocytes	68	66	63	7.1
% Monocytes	3.2	2.9	3.1	1.96
% Granulocytes	35.5	37.3	38.9	39.7

Values are expressed as mean ± SD, *n*=10

3.3.3. Total Number of Blood Platelets

The findings demonstrate that the rats infused with propolis (G2) demonstrated a significant increase ($p \leq 0.05$) in the aggregate of platelets compared with the control group (G1). Furthermore, there was a s ignificant increase ($p \leq 0.05$) in the platelets' number in the groups G1 and G2 compared with the rats treated with fenvalerate (G3). In addition, the rats treated with fenvalerate and propolis (G4) showed a significant increase ($p \leq 0.05$) in the platelets' counts compared with the control (G1) and the fenvalerate-infused (G3) groups (Table 4).

3.3.4. The Percentage of Differential Leucocytes

Nonsignificant differences ($p \geq 0.05$) in the differential leucocytes in the control (G1, G2) and fenvalerate-infused (G3) groups were found in this study. Moreover, the group treated with fenvalerate plus propolis (G4) demonstrated a little increase in the percentage of lymphocytes and a decrease in the percentage of monocytes and granulocytes compared with the control (G1, G2) and the fenvalerate-infused (G3) groups (Table 4).

4. Discussion

Synthetic pyrethroids account for more than 30 % of insecticide use worldwide through household and agricultural applications. Nevertheless, exposure to these chemicals has been accompanied by several toxicities and health issues. This study is aimed at investigating the possible ameliorative effects of propolis after treatment with fenvalerate. The results indicate that the administration of fenvalerate to rats resulted in many histopathological, histochemical, and biochemical parameters including ALT, AST, urea and creatinine levels in the liver. The results show that there are no significant changes in the histological observation and biochemical analysis in the rats of the control group injected with PBS and the rats of the positive control group injected with propolis. The histopathological and histochemical observations of the rats treated with fenvalerate caused hepatotoxicity and noticeable changes in the hepatocytes architecture which appeared as hepatic degeneration and coagulative necrosis of many hepatocytes, cellular degeneration of some hepatocytes and cellular leucocytic infiltration.

The results also show a r emarkable reduction in cytoplasmic carbohydrates and a degradation of protein contents in the hepatocytes of liver. This histological and histochemical change was significantly ameliorated following the propolis injection. These findings confirmed the toxic effects of fenvalerate on liver functions, and are similar with previous studies which indicate that the therapeutic dose of fenvalerate may cause liver toxicity in freshwater fish *Cirrhinus mrigala* and zebrafish (Velmurugan *et al*., 2007; Han *et al*., 2017). It has been reported that fenvalerate causes histopathological damage to the liver tissues, and alters the architecture of the organ cells in female rats (Jayachitra *et al*., 2016). In agreement with this result, Amaravathi has reported that treating rats with fenvalerate caused degenerative changes in the liver, haemorrhages, and mild fatty changes, infiltration of mono nuclear cells, and proliferation of bile duct (Kanbur *et al*., 2009). The inhalation of fenvalerate resulted in liver necrosis and fatty degeneration in rats (Mani *et al*., 2004). It was also observed that fenvalerate caused histopathological changes in the liver of rats, such as the degeneration and proliferation of hepatocytes forming acinar and pseudoglandular patterns (Ali, 2013). On the other hand, treatment with propolis could ameliorate the side effects caused by fenvalerate treatment, even though it could not return the changes to the normal levels. It has been reported by Ates *et al*., (2006) and Bhadauria *et al.,* (2007) that the major compound, caffeic acid phenethyl ester (CAPE), found in the propolis may be responsible for the regulation of the antioxidant enzymes, the inhibition of lipid peroxidation, and the reduction of hepatic damage.

The propolis extract was shown to have a protective effect on hepatocytes against carbon tetrachloride (CCl)-induced injuries *in vitro* and *in vivo* (El-Khatib *et al.,* 2002 and Mahran *et al*., 1996). Kolankaya has reported that the treatment with propolis significantly prevented the release of transaminases, and significantly enhanced protein towards control, suggesting its hepatoprotective potential (Kolankaya *et al*., 2002).

In the current study, a significant increase in the levels of ALT, AST, urea, and creatinine in the serum of fenvalerate-injected rats was noticed compared with the normal and positive control groups. Also, a marked reduction in the level of SOD and CAT was observed in the fenvalerate-treated rats, while the MDA level has significantly increased compared with the control group. However, rats that were treated with propolis along with fenvalerate showed a significant decrease in the level of ALT, AST, urea, creatinine, and MDA, while the activities of SOD and CAT were significantly increased compared to the fenvalerate-treated rats; they were still higher than the control groups. The effects of fenvalerate on ALT and AST had been recorded by many researchers. It has been found that fenvalerate caused a significant increase in the activities of hepatic transaminases, ALP and LDH. (Prasanthi *et al*., 2005). It was confirmed in a previous study that the administration of fenvalerate to rats causes acceptance of toxicity to the liver as a result of the rise of liver-damage marker enzymes such as aspartate transaminase, alanine transaminase, Gamma Glutamyl transferase, and lactate dehydrogenase (Waheed and Mohamed, 2012). This study found that fenvalerate causes increment in the lipid peroxidation marker, MDA and the reduction of the antioxidant enzymes SOD and CAT. Similarly, it was maintained that the fenvalerate-treated rats demonstrated a reduced activity levels of SOD, CAT, GSHPx, and GSH in the liver homogenates, while the quantity of lipid peroxidation was high as a result of the increment in the level of MDA (Waheed and Mohamed, 2012). Thus, a rise in MDA and a decrease in the content of SOD and CAT might be identified with the oxidative pressure created in the hepatocytes of rats treated with fenvalerate.

Propolis is known to have antioxidant effects and free radical scavengers. It detoxifies a variety of free radicals and reactive oxygen intermediates (AL-Ani *et al*., 2018; Galeotti *et al.,* 2018). The antioxidant activities of propolis and its polyphenolic flavonoid components including flavonoids, aromatic acids, and their esters are related to their ability to chelate metal ions and scavenge singlet oxygen, superoxide anions, proxy radicals, hydroxyl radicals and peroxynitrite (Ferrali *et al*., 1997; AL-Ani *et al*., 2018, Galeotti *et al*., 2018). Also, propolis instigates the decrease of the expanded movement of AST, ALT, urea and creatinine values in the plasma of rats treated with $AlCl_3$ The present findings demonstrate that propolis diminished the lipid peroxidation conceivably by its antioxidant activity (Ferrali *et al.,* 2009). It was found that propolis also modulates the antioxidant enzymes and reduces lipid peroxidation processes in plasma, lungs, liver, and the brains of mice in a dose- and tissue-dependent manner (Shinohara *et al*., 2002). Luan stated in his work that propolis enhances the lipid profile, MDA and SOD activity in mice (Luan *et al*., 2000). Propolis can likewise lessen the levels of ROS, for example, H2O2 and NO, that may be in charge of its anti-inflammatory effects (Tan-No *et al*., 2006) in addition to the scavenging impact of propolis on free radicals delivered by liver in light of octylphenol toxicity (Saleh, 2012; Aldemir *et al*., 2018) revealed a discovery by Benguedouar who stated that propolis reduced superoxide anion radicals and restrained the lipid peroxidation in rats given doxorubicin and vinblastin (Benguedouar *et al*., 2008). The findings of the present study confirm the antioxidative properties of propolis and its ability to prevent damage induced by fenvalerate in albino rats.

The greater part of various classes of pesticides and chemotherapeutic medications have resistant suppressive symptoms, brought about by the division of the hematopoietic cells that are affected, leading to neutropenia and lymphopenia which weaken the immunity system (Saleh, 2012). The findings demonstrate that there is a nonsignificant difference in the aggregate number of RBCs or in the Hb level in the fenvalerate-infused rats. Moreover, rats that were infused with fenvalerate plus propolis demonstrated a significant reduction in their values in comparison with the control groups. Also, it was shown that the rats which were infused with propolis only or with propolis alongside fenvalerate demonstrated a significant increment in the aggregate number of the platelets in comparison with the normal and positive control groups. These findings demonstrate that propolis may display intense antiplatelet activities. Recent studies have demonstrated that propolis plays an essential part in improving oxidative stress, apoptosis and necrosis induced by chemotherapeutic drugs, pesticide chemicals, and heavy metal elements (Kocot *et al*., 2018). Moreover, propolis was found to have significant anti-inflammatory, antioxidant, antioroliferative, cytostatic, antibacterial properties due to the major compound, caffeic acid phenethyl ester (CAPE), that is extracted from propolis (Akyol *et al*., 2012; Kocot *et al*., 2018). Moreover, it has been demonstrated that propolis is a promising adjuvant with chemotherapy (Padmavathi, *et al*., 2006) and with immunization (Chu *et al.,* 2006)

5. Conclusion

In conclusion, the results presented in this investigation indicate that propolis may be considered as a potential natural product that can be used to ameliorate and prevent the adverse side effects, such as toxicity and immunosuppression, due to its anti-inflammatory and antioxidant properties.

References

Aebi, H.E. 1983. Catalase. In: Bergmeyer HU., (Ed.), **Methods of Enzymatic Analysis,** Verlag Chemie, Weinhem, pp 273- 286.

Akyol S, Ginis Z, Armutcu F, Ozturk G, Yigitoglu MR and Akyol O. 2012. The potential usage of caffeic acid phenethyl ester (CAPE) against chemotherapy-induced and radiotherapy-induced toxicity. *Cell Biochem Funct* **30**: 438-443.

AL-Ani I, Zimmermann S, Reichling J and Wink M. 2018. Antimicrobial activities of European propolis collected from various geographic origins alone and in combination with antibiotics. *Medicines* **5(2):** 1-17.

Aldemir O, Yildirim HK and Sözmen EY. 2018. Antioxidant and anti-inflammatory effects of biotechnologically transformed propolis. *J Food Processing Preserv.,* **42(6):** 25-33.

Ali AM. 2013. The Effect of antioxidant nutrition against fenvalerate toxicity in rat liver (Histological and immunohistochemical studies). *Ann Rev Res Biol.,* **3(4):** 636-648.

Amaravathi P, Srilatha CH, Kumari RV, Suresh Ramadevi V and Sujatha K. 2010. H istopathological changes in induced fenvalerate toxicity in rats and its amelioration with *Withania somnifera*. *Indian J Vet Pathol.,* **34(1):** 65-86.

Ates B, Dogru MI, Gul M, Erdogan A, Dogru AK, Yilmaz I and Esrefoglu M 2006. Protective role of caffeic acid phenethyl ester in the liver of rats exposed to cold stress. *Fund Clin Pharm* **20**: 283-289.

Attalla F and Ayman A. 2008. Protective effects of propolis against the amitraz hepatotoxicity in mice. *J Pharmacol Toxicol* **3**: 402-408.

Awale S, Li F, Onozuka H, Esumi H, Tezuka Y and Kadota S. 2008. Constituents of Brazilian red propolis and their preferential cytotoxic activity against human pancreatic PANC-1 cancer cell line in nutrient-deprived condition. *Bioorg Med Chem* **16**: 181-189.

Bazo AP, Rodrigues MA, Sforcin JM, de Camargo JL, Ribeiro LR and Salvadori DM. 2002. Protective action of propolis on the rat colon carcinogenesis. *Teratog Carcinog Mutagen* **22(3):** 183-194.

Benguedouar L, Boussenane HN, Kebsa W, Alyane M, Rouibah H and Lahoouel M. 2008. Efficiency of propolis extract against mitochondrial stress induced by antineoplastic agents (doxorubicin and vinblastin) in rats. *Indian J Exper Biol.,* **46**: 112-119.

Bhadauria M, Nirala SK and Shukla S. 2007. Propolis protects CYP2E1enzymatic activity and oxidative stress induced by carbon tetrachloride. *Mol Cell Biochem* 3**02**: 215-224.

Boutabet K, Kebsa W, Alyane M and Lahouel M. 2011. Polyphenolic fraction of Algerian propolis protects rat kidney against acute oxidative stress induced by doxorubicin. *Indian J Nephrol* **21**: 101-106.

Casida JE. 2006. **Pyrethrum, the Natural Insecticide**. Academic Press. London, N.Y, 329pp.

Chu WH. 2006. Adjuvant effect of propolis on immunization by inactivated Aeromonas hydrophila in carp (Carassius auratus gibelio). *Fish Shelfish Immunol* **21**: 113-117.

El-Khatib AS, Agha AM, Mahran LG and Khayyal MT. 2002. Prophylactic Effect of Aqueous Propolis Extract against Acute Experimental Hepatotoxicity *in vivo*. *Z Naturforsch C* **57(3-4):** 379-385.

Ferrali M, Signorini C, Caciotti B, Sugherini L, Ciccoli L, Giachetti D and Comporti M. 1997. Protection against oxidative damage of erythrocyte membrane by the flavonoid quercetin and its relation to iron chelating activity. *FEBS Lett* **416(2**): 123-129.

Galeotti F, Maccari F, Fachini A and Volpi N. 2018. Chemical composition and antioxidant activity of propolis prepared in different forms and in different solvents useful for finished products. *Food* **7(41):** 1-10.

Giray B and Hincal F. 2011. Fenvalerate induced hepatic oxidative stress in selenium- and/or iodine-deficient rats. *Hum Exp Toxicol* **30(10):** 1575-1583.

Gonzalez R, Rernirez. D and Rodriguez S. 1994. Hepatoprotective effects of propolis extract on paracetamol-induced liver damage in mice. *Phytother Res.,* **8(4)**: 229-232.

Han J, Ji C, Guo Y, Yan R, Hong T, Dou Y and An Y 2017. Mechanisms underlying melatonin-mediated prevention of fenvalerate-induced behavioral and oxidative toxicity in zebrafish. *J Toxicol Environ Health A* **80(23-24):** 1331-1341.

Ishihara M, Na K, Hashita M, Itoh Y and Suzui M. 2009. Growth inhibitory activity of ethanol extracts of Chinese and Brazilian propolis in four human colon carcinoma cell lines. *Oncol Rep* **22**: 349-354.

Ivanovska N, Nechev H, Stefanova Z, Bankova V and Popov S. 1995. Influence of cinammic acid on lymphatic proliferation, cytokine release and *Klebsiella* infection in mice. *Apidologie* **26**: 73-81.

Jaiswal AK, Venugopal R, Mucha J, Carothers AM and Grunberger D. 1997. Caffeic acid phenethyl ester stimulates human antioxidant response element-mediated expression of the NAD(P)H: Quinone oxidoreductase (NQO1) gene. *Cancer Res* **57:** 440-446.

Jasprica I, Mornar A, Debeljak Z, Smolcić-Bubalo A, Medić-Sarić M, Mayer L, Romić Z, Bućan K, Balog T, Sobocanec S and Sverko V. 2007. In vivo study of propolis supplementation effects on antioxidative status and red blood cells. *J Ethnopharmacol* **110(3):** 548-554.

Jayachitra G, Ponmanickam P, Vijaya Kumar J, Sevarkodiyone SP and Rajagopal T. 2016. The effects of fenvalerate on production of pheromone, hormone and histopathological changes in endocrine glands of female albino rats. *ANJAC J Sci* **15(2):** 61-74.

Kanbur M, Eraslan G and Silici S. 2009. Antioxidant effect of propolis against exposure to propetamphos in rats. *Ecotoxicol Environ Saf* **72(3):** 909-915.

Khalil ML. 2006. Biological activity of bee propolis in health and disease. *Asian Pac J Cancer Prev* **7(1):** 22-31.

Khayyal MT, el-Ghazaly MA and el-Khatib AS. 1993. Mechanisms involved in the antiinflammatory effect of propolis extract. *Drugs Exp Clin Res* **19(5):** 197-203.

Kneko H, Ohkawa H and Miyamaota J. 1981. Comparative metabolism of fenvalerate and the [2s, as]-isomer in rats and mice. *J. Pesticide Sci* **6**: 317-326.

Kiernan JA. 1999. **Histological and Histochemical Methods**. Theory and Practice, Pergamon Press, New York, 12(6), pp 479.

Kocot J, Kiełczykowska M, Luchowska-Kocot D, Kurzepa J and Musik I. 2018. Antioxidant potential of propolis, bee pollen, and royal jelly: possible medical application. *Oxidative Med Cellular Longevity* **3**: 1-29.

Kolankaya D, Selmanoglu G, Sorkun K and Salih B. 2002. Protective effects of Turkish propolis on alcohol-induced serum lipid changes and liver injury in male rats. *Food Chem.,* **78(2**): 213-217.

Kumazawa S. 2018. Bioactive compounds in bee propolis for drug discovery. *AIP Conference Proceedings* **1933(1):** 030001-5.

Luan J, Wang N and Tian L. 2000. Study on the pharmacologic effect of propolis. *J Chinese Medl Materials* **23(6):** 346-348.

Mahran LG, El-Khatib AS, Agha AM and Khayyal MT. 1996. The protective effect of aqueous propolis extract on isolated rat hepatocytes against carbon tetrachloride toxicity. *Drugs under Exper Clin Res.,* **22(6):** 309-316.

Mani U, Prasad AK, Sureshikumar V, Kumar P, Kewel LAL and Maji BK. 2004. Hepatotoxic alterations induced by subchronic exposure of rats to formulated fenvalerate (20% EC) by nose only inhalation. *Biomed Environ Sci* **17(3**) 309-314.

McEween FL and Stephenson GR. 1979. **The use and Significance of Pesticides in the Environment**. John Wiley and Sons. NY, pp538.

Minami M and Yoshikawa HA. 1979. Simplified assay method of superoxide dismutase activity for clinical use. *Clinica Chimica Acta* **92(3**): 337-342.

Newairy AA, Salama AF, Hussien HM and Yousef MI. 2009. Propolis alleviates aluminium-induced lipid peroxidation and biochemical parameters in male rats. *Food Chem Toxicol.,* **47(6)**: 1093-1098.

Ohkawa H, Ohishi N and Yagi K. 1979. Assay for lipid peroxides in animal tissues by thiobarbituric acid reaction. *Analytical Biochem.,* **95(2)**: 351-358.

Padmavathi R. Senthilnathan P, Chodon D and Sakthisekaran D. 2006. Therapeutic effect of paclitaxel and propolis on lipid peroxidation and antioxidant system in 7,12 dimethylbenz(a)anthracene-induced breast cancer in female Sprague Dawley rats. *Life Sci* **24**: 2820-2825.

Pearse AGE. 1972. **Histochemistry, Theoretical and Applied**, Churchill Livingstone, London. 23rd Edition.

Pascual C, Gonzalez R and Torricella RG. 1994. Scavenging action of propolis extract against oxygen radicals. *J Ethnopharmacol* **41**: 9-13.

Prasanthi K, Muralidhara and Rajini PS. 2005. Fenvalerate-induced oxidative damage in rat tissues and its attenuation by dietary sesame oil. *Food Chem Toxicol*., **43(2):** 299-306.

Reitman S and Frankel S. 1957. A colorimetric method for the determination of serum glutamic oxalacetic and glutamic pyruvic transaminases. *Am J Clin Pathol* **28(1):** 56-63.

Saleh EM. 2012. Antioxidant effect of aqueous extract of propolis on hepatotoxicity induced by octylphenol in male rats. *Acta Toxicol. Argent* **20(2):** 68-81.

Sforcin JM, Fernandes A, Lopes CAM, Bankova V and Funari SRC. 2000. Seasonal effect on Brazilian propolis antibacterial activity. *J Ethnopharmacol.,* **73(1-2**): 243–249.

Shinohara R, Ohta Y, Hayashi T and Ikeno T. 2002. Evaluation of antilipid peroxidative action of propolis ethanol extract. *Phytother Res.,* **16(4)**: 340-347.

Sobocanec S, Sverko V, Balog T, Saric A, Rusak G, Likic S, Kusic B, K atalinic V, Radic S and Marotti T. 2006. Oxidant/antioxidant properties of Croatian native propolis. *J Agric Food Chem.,* **54**: 8018-8026.

Tan-No K, Nakajima T, Shoji T, Nakagawasai O, Niijima F, Ishikawa M, Endo Y, Sato T Satoh S and Tadano T. 2006. Anti-inflammatory effect of propolis through inhibition of nitric oxide production on carrageenin-induced mouse paw edema. *Biol Pharma Bull.,* **29**: 96-99.

Trinder P. 1969. Determination of glucose in blood using glucose oxidase with an alternative oxygen acceptor. *Ann Clin Biochem.,* **6**: 24-27.

Velmurugan B, Selvanayagam M, Cengiz EI and Unlu E. 2007. The effects of fenvalerate on different tissues of freshwater fish *Cirrhinus mrigala*. *J Environ Sci Health, Part B* **42(2):** 157-163.

Waheed MP and Mohamed HS. 2012. Fenvalerate induced hepatotoxicity and its amelioration by Quercetin. *Inter J Pharm Tech Res.,* **4(4):** 1391-1400.

JJBS
Jordan Journal of Biological Sciences

Volume 12, Number 5,December 2019
ISSN 1995-6673
Pages 589 - 594

In silico Detection of Acquired Antimicrobial Resistance Genes in 110 Complete Genome Sequences of *Acinetobacter baumannii*

Talal S. Salih* and Raghad R. Shafeek

Department of Biophysics, College of Science, University of Mosul, Mosul, Iraq

Received February 21, 2019; Revised March 14, 2019; Accepted March 24, 2019

Abstract

Multidrug-resistant (MDR) *Acinetobacter baumannii* is one of the most common nosocomial pathogens posing a serious health threats to patients around the world. The present study aims at the in silico detection of the acquired antimicrobial resistance (AMR) genes in *A. baumannii*. In this study,110 complete whole genome sequences (WGS) of *A. baumannii* obtained from the NCBI database are analyzed. The comprehensive ResFinder 3.1 tool is used to identify the AMR genes among the *A. baumannii* sequences. The core genome of *A. baumannii* in fasta format was created using Spine program. Furthermore, the Pasteur MLST scheme was performed for the 110 complete WGS of *A. baumannii* using the MLST 2.0 web server. Resistance genes against beta-lactam antimicrobial agents were detected in all *A. baumannii* strains (n=110; 100%), followed by resistance genes against aminoglycoside (n=87; 79 %), sulphonamide (n=84 ; 76%), phenicol (n=52; 47 %), tetracycline (n=52; 47 %), fluoroquinolone (n=42; 38 %), MLS (n=43; 39 %), trimethoprim (n=4; 3.6 %), and rifampicin (n=2; 1.8%). Moreover, the blaADC-25 gene encoding beta-lactam resistance was found in all of the *A. baumannii* strains (n=110; 100 %), followed by blaOXA-66 (n=61; 55.4%), blaOXA-23 (n=50; 45%) and blaTEM-1D (n=36; 32 %) as the most predominant genes. These results suggest that bioinformatics tools such as ResFinder can be utilized for the detection of AMR genes in *A. baumannii* and other pathogens.

Keywords: *In silico*, Resistance genes, Genome sequences, *Acinetobacter baumannii*

1. Introduction

The current emergence of multidrug-resistant (MDR) pathogens is a major area of concern. The World Health Organisation (WHO) has published its first list ever of antibiotic-resistant "priority pathogens" which includes twelve families of bacteria that pose serious threats to human health (WHO, 2017). Among these families *Acinetobacter baumannii* is an organism of serious concern due to the increased emergence of carbapenems-resistant isolates. Hence, *A. baumannii* has been designated as "critical" and occupies the top of the list (WHO, 2017). In the 1970s, it was thought that *A. baumannii* strains were sensitive to most antimicrobial agents. Today *A. baumannii* strains have been found resistant to most antibiotic classes, including beta-lactams, aminoglycosides, fluoroquinolones, and tetracyclines (Perez *et al*., 2007; Pleg *et al*., 2008; Wong *et al*., 2016). Many recent studies have shown that *A. baumannii* strains are still considered emerging health threats to patients around the world, due to their ability to develop multidrug-resistance (MDR) (Fang *et al*., 2015; Michiels *et al*., 2016; Almaghrabi *et al.,* 2018; Nasser *et al*, 2018).

The disk diffusion test and the broth micro-dilution test are the routine methods utilized in diagnostic laboratories to probe for antibiotic susceptibility of bacterial clinical isolates (Rolinson and Russell 1972; Diene and Rolain 2013). These techniques are markedly influenced by a number of variables including inoculum size, depth of agar, conditions of incubation, and medium composition. Although these parameters may influence antibacterial susceptibility testing results, these parameters have been standardized; hence, they are no longer an area of concern. Furthermore, the obtained results usually cannot be replicated among different laboratories for the same antimicrobial susceptibility test (Huys *et al*., 2005; Baltekin *et al*., 2017).

In several recent studies, the whole genome sequencing technology has been applied to identify bacteria and their antimicrobial gene patterns from different sources (Stoesser *et al.,* 2013; Tyson *et al*., 2015; Ruppé *et al*., 2017). The presence of antimicrobial resistance (AMR) genes within the bacterial whole genome sequences can be detected using dedicated databases of antibiotic gene sequences such as ResFinder (Zankari *et al*., 2012), CARD (McArthur *et al.,* 2013), and ARG-ANNOT (Gupta *et al*. 2014). The ResFinder reference gene database has been developed by the Centre for Genomic Epidemiology (CGE) (www.genomice pidemiology.org) for *in silico* analysis of bacterial whole genome sequences (WGS) including *A. baumannii*. ResFinder is based on a database of more than 2,000 resistance genes covering twelve types of antimicrobial agents (aminoglycosides, beta-lactams, fluoroquinolones, fosfomycin, fusidic acid, glycopeptides,

* Corresponding author e-mail: talal.salih@uomosul.edu.iq.

macrolide-lincosamide-streptogramin B (MLS), phenicol, rifampicin, sulphonamide, tetracycline, and trimethoprim).

In the present study, 110 complete WGS of *A. baumannii* that were deposited in the National Centre for Biotechnology Information (NCBI) were utilized for the detection of the antimicrobial resistance (AMR) genes and agents for each isolate using the ResFinder tool. Additionally, the multiple locus sequence typing (MLST) was performed for the 110 *A. baumannii* genome sequences to classify the strains based on their antimicrobial profiles.

2. Materials and Methods

2.1. The Complete Whole Genome Sequences of A. baumannii

Because the main goal of this study is to identify acquired AMR genes in *A. baumannii*, only the 110 complete WGS of *A. baumannii* (https://www.ncbi. nlm.nih. gov/genome/? term= acinetobacter) were used for *in silico* AMR genes identification. The WGS of *A. baumannii* were obtained from the National Center for Biotechnology Information (NCBI) public database as of December, 2018. Draft genomes, scaffolds, and contigs were excluded from this study.

2.2. Detection of Antimicrobial Resistance Agents and Genes in the Genomes of A. baumannii

A web version of the ResFinder 3.1 tool (Zankari *et al*., 2012) was used to identify AMR agents and genes in the 110 *A. baumannii* sequences. The ResFinder tool uses BLAST (Basic Local Alignment Search Tool) (Altschul *et al*., 1990) for the detection of acquired AMR genes in the whole genome database. The fasta (.fasta) format of the input genome sequences was used. The threshold for reporting a m atch between a gene in the ResFinder database and the input sequence was set at a 50 % identity with a minimum length of 60 %.

2.3. Detection of Antimicrobial Resistance Genes in the Core Genome of A. baumannii

The core genome of *A. baumannii* was constructed from the 110 complete WGS of *A. baumannii* used in this study. Spine software program (Ozer *et al.,* 2014) was used to create the core genome of *A. baumannii* in a fasta format file. For the detection of AMR genes in the core genome of *A. baumannii*, the constructed sequence file was uploaded on the ResFinder database and the input sequence was set at a 50 % identity with the minimum length of 60 %.

2.4. Multiple Locus Sequence Typing (MLST)

MLST was performed from the 110 complete WGS of *A. baumannii* using the MLST 2.0 web server (www.genomicepidemiology.org). The Pasteur MLST Scheme (Jolley *et al*., 2010) which is based on s even housekeeping genes (*cpn60, fusA, gltA, pyrG, recA, rplB* and *rpoB*) of *A. baumannii* (http://pubmlst.org/ abaumannii) was used to classify the strains based on the sequence types.

3. Results

3.1. Detection of Antimicrobial Resistance Agents

The RestFinder 3.1 analysis of the 110 *A. baumannii* strains indicate that the strains harboured genes mediating resistance to nine antimicrobial agent groups, namely aminoglycosides, beta-lactams, fluoroquinolone, macro-lide-lincosamide-streptogramin B (MLS), phenicol, rifampicin, sulphonamide, tetracycline, and trimethoprim (Figure 1). The AMR genes against beta-lactams w ere found in all strains (n=110; 100 %), followed by those against aminoglycosides (n=87; 79 %), sulphonamide (n=84 ; 76 %), phenicol (n=52; 47 %), tetracycline (n=52; 47 %), fluoroquinolones (n=42; 38 %), MLS (n=43; 39 %), trimethoprim (n=4; 3.6 %), and rifampicin (n=2; 1.8 %).

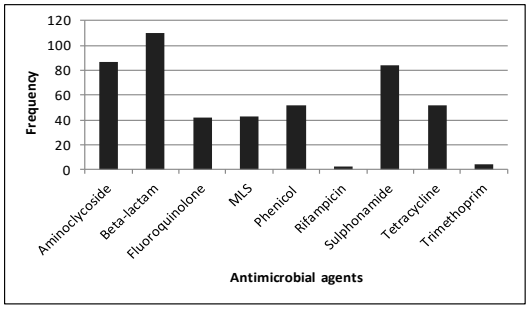

Figure 1. Antimicrobials' resistance genes harboured within the 110 WGS of *A. baumannii* strains obtained from the NCBI database as of December 2018, as detected by the ResFinder 3.1 tool.

3.2. Detection of Antimicrobial Resistance (AMR) Genes

A total of fifty-six unique resistance genes were identified in the 110 *A. baumannii* sequences (Table 1), most of which are genes encoding beta-lactam and aminoglycoside resistance. The blaADC-25 gene encoding beta-lactam resistance was found in all *A. baumannii* strains (n=110; 100 %), followed by blaOXA-66 (n=61; 55.4 %), blaOXA-23 (n=50; 45 %) and blaTEM-1D (n=36; 32 %), as the most predominant genes (Table 1). The BlaOXA-66 and blaADC-25 genes were also found in the predicted core genome of the 110 *A. baumannii* sequences used in this study, with identities of 100 % and 99.9 %, respectively. In addition to that, twenty-six genes encoding beta-lactam resistance were also detected in *A. baumannii* using ResFinder (Table 1).

As for the aminoglycoside resistance, fourteen distinct aminoglycoside resistance genes were detected, with twelve different gene types. The most predominant aminoglycoside resistance genes in the 110 *A. baumannii* strains were aadA1 (n=63; 57 %), aph (3")-Ib (n=59; 53 %) and aph (6)-Id (n=57; 52 %), followed by aph (3')-Ia (46; 42%) and aac (6')-Ib3 (40; 36 %) (Table 1).

As for fluoroquinolone, only the aac (6')-Ib-cr resistance gene was detected in *A. baumannii* (n=40; 36 %). As for MLS resistance, msr (E) (n=43; 39 %) and mph (E) (n=43; 39 %) resistance genes were detected. As for phenicol resistance, three resistance genes were detected, with the most common being catB8 (n=37; 33.6 %), followed by catA1 (n=7; 6 %) and cmlA1 (n=2; 1.8 %) (Table 1).

Sulphonamide resistance was predominantly encoded by sul1 (n=64; 58 %) and sul2 (n=43; 39 %) (Table 1).

Tetracycline resistance was encoded predominantly by tet(B) (n=42; 38 %), followed by tet(A) (n=7; 6.3 %) and tet(G) (n=3; 2.7 %).

Rifampicin resistance was encoded by ARR-2 (n=; 1.8 %). Trimethoprim resistance was encoded by dfrB1, dfrA1, dfrA10 and dfrA12 which were encountered at less than 2 % of the strains, each (Table 1).

Table 1. Resistance genes detected in the 110 whole genome sequences of *A. baumannii* by ResFinder with ID ≥99.00 %.

Resistance gene	Frequency (N=110)	Percentage (100%)	Predicted Phenotype	Accession No.
*aad*A1	63	57	Aminoglycoside resistance	JQ414041
*arm*A	48	43		AY220558
aph(3")-Ib	59	53		AF321550
aph(6)-Id	57	52		M28829
aac(6')-Ian	8	7.2		AP014611
aph(3')-Ia	46	42		X62115
aph(3')-Via	10	9		X07753
aac(6')-Ib3	40	36		X60321
aac(3)-IIa	6	5.4		X51534
*aad*A11	1	0.9		AY144590
ant(2")-Ia	2	1.8		X04555
*aad*A2	1	0.9		JQ364967
*bla*TEM-1D	36	32	Beta-lactam resistance	AF188200
*bla*OXA-23	50	45		AY795964
*bla*OXA-66	61	55.4		AY750909
*bla*OXA-65	8	7.2		AY750908
*bla*OXA-239	1	0.9		JQ837239
*bla*OXA-109	1	0.9		EF650035
*bla*PER-1	6	5.4		GU944725
*bla*OXA-94	1	0.9		DQ519088
*bla*OXA-64	7	6.3		AY750907
*bla*OXA-235	4	3.6		JQ820240
*bla*OXA-69	13	11.8		AY859527
*bla*TEM-1B	4	3.6		AY458016
*bla*OXA-2	1	0.9		DQ112222
*bla*OXA-68	6	5.4		AY750910
*bla*OXA-92	1	0.9		DQ335566
*bla*OXA-70	1	0.9		AY750912
*bla*ADC-25	110	100		EF016355
*bla*OXA-51	1	0.9		DQ385606
*bla*OXA-20	1	0.9		AY307114
*bla*OXA-100	1	0.9		AM231720
*bla*PER-7	1	0.9		HQ713678
*bla*OXA-259	1	0.9		KF057028
*bla*OXA-10	1	0.9		J03427
*bla*OXA-106	1	0.9		EF650032
*bla*OXA-68	6	5.4		AY750910
*bla*OXA-180	2	1.8		HM570036
*bla*NDM-1	4	3.6		FN396876
*bla*VEB-1	1	0.9		DQ393569
aac(6')-Ib-cr	40	36	Fluoroquinolone resistance	EF636461
msr(E)	43	39	MLS resistance	EU294228
mph(E)	43	39		DQ839391
*cat*B8	37	33.6	Phenicol resistance	AF227506
*cat*A1	7	6.3		V00622
*cml*A1	2	1.8		AB212941
*sul*1	64	58	Sulphonamide resistance	U12338
*sul*2	43	39		AY034138
tet(B)	42	38	Tetracycline resistance	AP000342
tet(G)	3	2.7		AF133140
tet(A)	7	6.3		AJ517790
ARR-2	2	1.8	Rifampicin resistance	HQ141279
*dfr*B1	1	0.9	Trimethoprim resistance	U36276
*dfr*A1	2	1.8		X00926
*dfr*A10	1	0.9		L06418
*dfr*A12	1	0.9		AM040708

3.3. Multilocus Sequence Typing (MLST)

Using Pasteur MLST scheme, twenty-five different MLST types and one unknown ST were observed in the 110 *A. baumannii* strains (Table 2). The most prevalent MLST types were ST2 (n=56; 51 %) with a resistance profile against aminoglycosides, beta-lactams, fluoroquinolones, MLS, phenicol, sulphonamide and tetracycline, and ST1 (n=12; 11 %) having a r esistance profile against aminoglycosides, beta-lactams, fluoroquinolones, MLS, phenicol, rifampicin, sulphonamide, tetracycline and trimethoprim. The remaining MLST types were represented by less than 5 % of the strains, and had different resistance profiles (Table 2).

Table 2. Multilocus Sequence Typing (MLST) of the 110 *A. baumannii* complete whole genome sequences according to the Pasteur MLST Scheme.

MLST (Pas)	Frequency	Resistance agents profile
ST1	12	Aminoglycoside, Beta-lactam, Fluoroquinolone, MLS, Phenicol, Rifampicin, Sulphonamide, Tetracycline, Trimethoprim
ST2	56	Aminoglycoside, Beta-lactam, Fluoroquinolone, MLS, Phenicol, Sulphonamide, Tetracycline
ST10	4	Aminoglycoside, Beta-lactam, Sulphonamide, Tetracycline
ST20	1	Aminoglycoside, Beta-lactam, MLS, Phenicol, Sulphonamide, Tetracycline, Trimethoprim
ST23	2	Aminoglycoside, Beta-lactam, Sulphonamide, Tetracycline
ST25	3	Aminoglycoside, Beta-lactam,
ST32	1	Beta-lactam, Sulphonamide
ST52	1	Beta-lactam, Sulphonamide
ST79	5	Aminoglycoside, Beta-lactam, Phenicol, Sulphonamide,
ST81	1	Beta-lactam
ST126	2	Beta-lactam
ST138	1	Beta-lactam

MLST (Pas)	Frequency	Resistance agents profile
ST156	1	Aminoglycoside, Beta-lactam, Phenicol, Sulphonamide,
ST187	1	Aminoglycoside, Beta-lactam, Fluoroquinolone, MLS, Phenicol, Sulphonamide,
ST215	1	Aminoglycoside, Beta-lactam, Fluoroquinolone, MLS, Phenicol, Sulphonamide, Tetracycline
ST229	1	Aminoglycoside, Beta-lactam, Fluoroquinolone, MLS, Sulphonamide, Trimethoprim
ST267	2	Beta-lactam
ST422	2	Aminoglycoside, Beta-lactam, Phenicol, Sulphonamide, Tetracycline
ST437	2	Beta-lactam, Sulphonamide
ST464	1	Beta-lactam
ST622	1	Beta-lactam
ST638	1	Aminoglycoside, Beta-lactam, Sulphonamide
ST639	1	Beta-lactam, Sulphonamide, Tetracycline
ST880	1	Aminoglycoside, Beta-lactam, Fluoroquinolone, MLS, Phenicol, Sulphonamide, Tetracycline
ST922	1	Aminoglycoside, Beta-lactam, MLS, Sulphonamide, Tetracycline
STUnknown	5	Aminoglycoside, Beta-lactam, Fluoroquinolone, MLS, Phenicol, Sulphonamide

4. Discussion

This study is focused on t he detection of resistance genes and antimicrobial resistance profiles of 110 WGS of *A. baumannii* strains submitted to the NCBI from different laboratories across the world. Several studies have assessed the power of WGS to detect antimicrobial resistance genes in several bacterial genomes (Ruppé *et al*., 2017; Almaghrabi *et al*., 2018; Kagambèga *et al*., 2018). The results of this study have shown that the 110 *A. baumannii* strains were resistant to more than one antimicrobial agent. Among these antimicrobial agents nine were detected using the ResFinder tool; they included: aminoglycosides, beta-lactams, fluoroquinolone, macrolide-lincosamide-streptogramin B (MLS), phenicol, rifampicin, sulphonamide, tetracycline, and trimethoprim (Zankari *et al*., 2012). However, the wide spectrum of multidrug-resistance of *A. baumannii* can be mediated by all of the major resistance mechanisms known to exist in bacteria (Peleg *et al*., 2008; Mihu and Martinez 2011).

Analysing the core genome of the 110 A. *baumannii* WGS revealed that *bla*ADC-25 gene (GenBank accession number EF016355 with 99.9 % identity) is an intrinsic gene in *A. baumannii*. The presence of *bla*ADC-25 gene in *A. baumannii* genome can be correlated with resistance to cephalosporins (Srinivasan *et al*., 2008). However, only isolates having an insertion sequence (IS), such as IS*Aba1* or IS*Aba9*, upstream from *blaADC-25*, can display a high-level β-lactamase resistance to cephalosporins (Périchon *et al*., 2014; Evans and Amyes 2014).

Within the large diversity of OXA-type carbapenemase genes identified by the ResFinder tool, the genes for *bla*OXA-66 and *bla*OXA-23 types were the most predominant. Studies have shown that *A. baumannii* strains harbouring one or both of these genes are resistant to all β-lactam antibiotics, including carbapenems (Woodford *et al*., 2006; Figueiredo *et al*., 2009; Diene and Rolain 2013). Moreover, multidrug-resistant *A. baumannii* strains, showing resistance to carbapenems, have emerged worldwide, which raises serious concerns about the limited number or antimicrobial treatment options available (Pogue *et al*., 2013; WHO, 2017). Furthermore, the *bla*OXA-66 and *bla*OXA-23 genes have been associated with IS*Aba1* or IS*Aba4* upstream sequences that enhance their expression (Corvec *et al*. 2007).

Other resistance genes attributed to cephalosporin-resistant isolates, including those encoding extended-spectrum β-lactamases (ESBLs) (*bla*TEM, *bla*PER and *bla*VEB) (Diene and Rolain 2013), and carbapenemase-encoding gene (*blaNDM*) (Cornaglia *et al*., 2011), were also detected in this study. *Bla*NDM is the newest metallo-β-lactamase. *Bla*-NDM-1 gene, first reported in an MDR *Klebsiella pneumoniae* clinical isolate from a patient of an Indian origin, confers resistance to all β-lactams, including carbapenems (Yong *et al*., 2009). However, *Bla*NDM-1 was also identified in clinical isolates of *A. baumannii* in several continents including Asia, North America, and Australia (Cornaglia *et al*., 2011).

Various genes encoding aminoglycoside-modifying enzymes and 16S rRNA methylases that confer resistance to aminoglycosides were detected in this study. These genes are known to contribute to resistance to streptomycin, gentamycin, kanamycin and amikacin (Ramirez and Tolmasky 2010). However, among the aminoglycosides, amikacin and tobramycin are genes having the greatest activity against many *A. baumannii* isolates (Fishbain and Peleg 2010).

The presence of *aac* (6')-Ib-cr gene in forty (36 %) of the strains confers resistance to fluoroquinolones. Moreover, genes confering MLS *(msr*(E) and *mph*(E)), phenicol (*cat*B8, *cat*A1 and *cml*A1), sulphonamide (*sul*1 and *sul*2) and t etracycline (*tet*(B), *tet*(G) and *tet*(A)) resistances were detected in ≥33.6 % of isolates. These results are in agreement with other findings (Ramirez and Tolmasky 2010; Diene and Rolain 2013; Nowak *et al*., 2014; Wong *et al.,* 2016; Wang *et al*., 2017), which indicate that *A. baumannii* has a wide variety of genes contributing to resistance against a wide variety of antimicrobials.

Notably, only two (1.8 %) and four (3.4 %) of the isolates were found to carry genes that confer resistance to rifampicin and trimethoprim, respectively. Interestingly, rifampicin has been used successfully in combination with colistin for the treatment of *A. baumannii* (Lee *et al.,* 2013). Also, trimethoprim-sulfamethoxazole in combination with colistin has shown synergistic activity against *A. baumannii* clinical isolates (Nepka *et al*., 2016).

No genes mediating colistin resistance were identified in the current study. Colistin, alone or in combination with other agents, has been used as a p otential therapeutic option for the treatment of MDR Gram-negative bacteria (Fishbain and Peleg 2010) including carbapenem-resistant *A. baumannii* (Gounden *et al*., 2009; Velkov *et al.,* 2013). However, colistin resistance in the *A. baumannii* isolates has been recently reported in many parts of the world (Lee *et al*., 2014; Choi *et al*., 2016; Dortet *et al*., 2018).

Among the 110 strains, the ST2 was the most dominant sequence type followed by ST1. Studies have shown that isolates having these two sequence types are associated with *A. baumannii* nosocomial outbreaks and antimicrobial MDR phenotypes (Diancourt *et al*., 2010; Matsui *et al*., 2014) according to a scheme developed by the Pasteur

Institute (Jolley *et al*., 2010). Moreover, ST1 and ST2 are known to be endemic clinical strains that have emerged worldwide (Rafei *et al*., 2014; Kim *et al*., 2016).

5. Conclusions

This study has shown that the RestFinder bioinformatics tool can serve as accurate *in silico* genetic analysis tool to identify acquired AMR genes in the genomes of *A. baumannii*. In this study, fifty-six known resistance genes were identified in the 110 complete WGS of *A. baumannii* available in the NCBI database. Most detected genes were associated with resistance to beta-lactam and aminoglycoside agents. Furthermore, the *bla*OXA-66 and *bla*ADC-25 genes were found in all *A. baumannii* sequences which suggest that these two genes are within the intrinsic genes in *A. baumannii*. Also, no genes contributing to colistin resistance were detected in this study. Finally, the current study demonstrates that ST2 has been the most dominant sequence type in *A. baumannii* according to the Pasteur MLST scheme.

References

Almaghrabi MK, Joseph MR, Assiry MM and Hamid ME . 2018. Multidrug-resistant *Acinetobacter baumannii*: An emerging health threat in Aseer Region, Kingdom of Saudi Arabia. *Canadian J Infect Dis Med Microbiol*, Article ID 9182747: 1-4.

Altschul P, Gish W, Miller W, Myers EW and Lipman DJ. 1990. Basic local alignment search tool. *J. Mol Biol*, **215**: 403-410.

Baltekin O, Boucharin A, Tano E, Andersson DI and Elf J. 2017. Antibiotic susceptibility testing in less than 30 min using direct single-cell imaging. PNAS, **34**: 9170-9175

Choi IS, Lee YJ, Wi YM, Kwan BS, Jung KH, Hong WP and Kim JM. 2016. Predictors of mortality in patients with extensively drug-resistant *Acinetobacter baumannii* pneumonia receiving colistin therapy. *Int J Antimicrob Agents*, **48**: 175–180.

Cornaglia G, Giamarellou H and Rossolini, GM. 2011. Metallo-β-lactamases: a last frontier for β-lactams?. *The Lancet Infect Dis.*, **11**: 381–93.

Corvec S, Poirel L, Naas T, Drugeon H and Nordmann P. 2007. Genetics and expression of the carbapenem-hydrolyzing oxacillinase gene blaOXA-23 in *Acinetobacter baumannii*. *Antimicrob Agents Chemother*, **51**: 1530-1533.

Diene SM and Rolain JM. 2013. Investigation of antibiotic resistance in the genomic era of multidrug-resistant Gram-negative bacilli, especially *Enterobacteriaceae*, *Pseudomonas* and *Acinetobacter*, *Expert Rev. Anti Infect Ther*, **11**: 277–296.

Dortet L, Potron A, Bonnin RA, Plesiat P, Nass T, Filloux A and Larrouy-Maumus G. 2018. Rapid detection of colistin resistance in *Acinetobacter baumannii* using MALDI-TOF-based lipidomics on intact bacteria. *Sci Rep*, **8**: 16910.

Evans BA and Amyes SG. 2014. OXA β-Lactamases. *Clin Microbiol Rev.*, **27**: 241–263.

Fang Y, Quan J, Hua X, Feng Y, Li X, Wang J, Ruan Z, Shang S and Yu Y. 2015. Complete genome sequence of *Acinetobacter baumannii* XH386 (ST208), a multi-drug resistant bacteria isolated from pediatric hospital in China. *Genomics Data*, **7**: 269 – 274.

Figueiredo S, Poirel L, Croize J, Recule C and Nordmann P. 2009. In Vivo Selection of Reduced Susceptibility to Carbapenems in *Acinetobacter baumannii* Related to ISAba1-Mediated Overexpression of the Natural blaOXA-66 Oxacillinase Gene. *Antimicrob Agents Chemother*, **6**: 2657–2659.

Fishbain J and Peleg AY. 2010. Treatment of *Acinetobacter* infections. *Clin Infect Dis*, **51**: 79–84.

Gounden R, Bamford C, Zyl-Smit R, Cohen K, and Maartens G. 2009. Safety and effectiveness of colistin compared with tobramycin for multi-drug resistant *Acinetobacter baumannii* infections. *BMC Infectious Diseases*, **9**: 26.

Gupta SK, Padmanabhan BR, Diene SM, Lopez-Rojas R, Kempf M, Landraud L and Rolain JM. 2104. ARG-ANNOT, a new bioinformatic tool to discover antibiotic resistance genes in bacterial genomes. *Antimicrob. Agents Chemother*, **58**: 212–220.

Huys G, Cnockaert M, Bartie K, Oanh DT, Phuong NT, Somsiri T, Chinabut S, Yussoff FM, Shariff M, Giacomini M, Bertone S, Swings J and Teale A. 2005. Intra- and interlaboratory performance of antibiotic disk-diffusion-susceptibility testing of bacterial control strains of relevance for monitoring aquaculture environments. *Dis Aquat Organ*, **66**: 197-204

Jolley KA, Bray JE and Maiden MC. 2010. Open-access bacterial population genomics: BIGSdb software, the PubMLST.org website and their applications. *Wellcome Open Res*, **3**: 124.

Kagambèga A, Lienemann T, Frye JG, Barro N and Haukka K. 2018. Whole genome sequencing of multidrugresistant *Salmonella enterica* serovar Typhimurium isolated from humans and poultry in Burkina Faso. *Tropical Med Health*, **46**: 4.

Kim DH, Jung S, Kwon KT and Ko KS. 2016. Occurrence of Diverse AbGRI1-Type Genomic Islands in *Acinetobacter baumannii* Global Clone 2 Isolates from South Korea. *Antimicrob Agents Chemother*, **61**: e01972-16.

Lee HJ, Bergen PJ, Bulitta JB, Tsuji B, Forrest A, Nation RL and Li J. 2013. Synergistic Activity of Colistin and Rifampin Combination against Multidrug-Resistant *Acinetobacter baumannii* in an In Vitro Pharmacokinetic/Pharmacodynamic Model. *Antimicrob Agents Chemother.*, **57**: 3738–3745.

Lee HY, Chen CL, Wu SR, Huang CW and Chiu CH. 2014. Risk factors and outcome analysis of *Acinetobacter baumannii* complex bacteremia in critical patients. *Crit Care Med*, **42**: 1081–1088.

Liu F, Zhu Y, Yi Y, Lu N, Zhu B and Hu Y. 2014. Comparative genomic analysis of *Acinetobacter baumannii* clinical isolates reveals extensive genomic variation and diverse antibiotic resistance determinants. *BMC Genomics*, **15**: 1163-1177.

Matsui M, Suzuki S, Yamane K, Suzuki M, Konda T, Arakawa Y and Shibayama K. 2014. Distribution of carbapenem resistance determinants among epidemic and non-epidemic types of *Acinetobacter* species in Japan. *J Med Microbiol.*, **63**: 870–877.

McArthur AG, Waglechner N, Nizam F, Yan A, Azad MA, Baylay AJ, Bhullar K, Canova MJ, De Pascale G, Ejim L, Kalan L, King AM, Koteva K, Morar M, Mulvey MR, O'Brien JS, Pawlowski AC, Piddock LJ, Spanogiannopoulos P, Sutherland AD, Tang I, Taylor PL, Thaker M, Wang W, Yan M, Yu T and Wright GD. 2013. The comprehensive antibiotic resistance database. *Antimicrob. Agents Chemother*, **57**: 3348–3357.

Michiels JE, Van den Bergh B, Fauvart M and Michiels J. 2016. Draft genome sequence of *Acinetobacter baumannii* strain NCTC 13423, a multidrug-resistant clinical isolate. *Standards in Genomic Sci*, **11**: 57.

Mihu MR and Martinez LR. 2011. Novel therapies for treatment of multidrug-resistant *Acinetobacter baumannii* skin infections. *Virulence*, **2**: 97-102.

Nasser K, Mustafa AS, Khan MW, Purohit P, Al-Obaid I, Dhar R, and Al-Fouzan W. 2018. Draft genome sequences of six multidrug-resistant clinical strains of *Acinetobacter baumannii*, isolated at two major hospitals in Kuwait. *Genome Announcements*, **6**: e00264-18.

Nepka M, Perivolioti E, Kraniotaki E, Politi L, Tsakris A, and Pournaras S . 2016. In Vitro Bactericidal activity of trimethoprim-sulfamethoxazole alone and in combination with colistin against carbapenem-resistant *Acinetobacter baumannii* clinical isolates. *Antimicrob Agents Chemother*, **60**: 6903-6906.

Nowak P, Paluchowska P and Budak A. 2014. Co-occurrence of carbapenem and aminoglycoside resistance genes among multidrug-resistant clinical isolates of *Acinetobacter baumannii* from Cracow, Poland. *Med Sci Monit Basic Res*, **20**: 9-14.

Ozer EA, Allen JP, and Hauser AR. 2014. Characterization of the core and accessory genomes of *Pseudomonas aeruginosa* using bioinformatic tools Spine and AGEnt. *BMC Genomics*, **15**: 737.

Peleg AY, Seifert H and Paterson DL. 2008. *Acinetobacter baumannii*: Emergence of a Successful Pathogen. *Clin Microbiol Rev*., **7**: 538–582.

Perez F, Hujer AM, Hujer KM, Decker BK, Rather PN, and Bonomo RA. 2007. Global challenge of multidrug-resistant *Acinetobacter baumannii*. *Antimicrob Agents Chemother*, **51**: 3471–3484.

Périchon B, Goussard S, Walewski V, Krizova L, Cerqueira G, Murphy C, Feldgarden M, Wortman J, Clermont D, Nemec A, and Courvalin P . 2014. Identification of 50 Class D β-Lactamases and 65 *Acinetobacter*-Derived Cephalosporinases in Acinetobacter spp. *Antimicrob Agents and Chemother*., **58**: 936–949.

Pleg AY, Seifert H and Paterson DL. 2008. *Acinetobacter baumannii*: Emergence of a Successful Pathogen. *Clin Microbiol Rev*., **21**: 538-582.

Pogue JM, Mann T, Barber KE and Kaye KS. 2013. Carbapenem-resistant *Acinetobacter baumannii*: epidemiology, surveillance and management. *Expert Rev Anti Infect Ther*, **11**: 383–393.

Rafei R, Dabboussi F, Hamze M, Eveillard M, Lemarié C, Gaultier MP, Mallat H, Moghnieh R, Husni-Samaha R, Joly-Guillou ML and Kempf M. 2014. Molecular analysis of *Acinetobacter baumannii* strains isolated in Lebanon using four different typing methods. *PLoS One*, **9**:e115969.

Ramirez M S and Tolmasky M E. 2010. A minoglycoside modifying enzymes. *Drug Resist Updat*, **13**: 151–71.

Rolinson GN and Russell EJ. 1972. New Method for Antibiotic Susceptibility Testing. *Antimicrob Agents Chemother*, **2**: 51-56.

Ruppé E, Cherkaoui A, Lazarevic V, Emonet S and Schrenzel J. 2017. Establishing Genotype-to-Phenotype Relationships in Bacteria Causing Hospital-Acquired Pneumonia: A Prelude to the Application of Clinical Metagenomics. *Antibiotics*, **6**(4): 30.

Stoesser N, Batty EM, Eyre DW, Morgan M, Wyllie DH, Del Ojo Elias C, Johnson JR, Walker AS, Peto TE and Crook DW. 2013. Predicting antimicrobial susceptibilities for Escherichia coli and *Klebsiella pneumoniae* isolates using whole genomic sequence data. *J Antimicrob Chemother*, **68**: 2234–2244.

Srinivasan VB, Rajamohan G, Pancholi P, Stevenson K, Tadesse D, Patchanee P, Marcon M and Gebreyes WA. 2008. Genetic relatedness and molecular characterization of multidrug resistant *Acinetobacter baumannii* isolated in central Ohio, USA. *Ann Clin Microbiol Antimicrob.*, **8**:21.

Tyson GH, McDermott PF, Li C, Chen Y1, Tadesse DA1, Mukherjee S1, Bodeis-Jones S, Kabera C, Gaines SA, Loneragan GH, Edrington TS, Torrence M, Harhay DM and Zhao S . 2015. WGS accurately predicts antimicrobial resistance in *Escherichia coli*. *J Antimicrob Chemother*, **70**: 2763–2769.

Velkov T, Roberts KD, Nation RL Thompson PE and Li J. 2013. Pharmacology of polymyxins: new insights into an 'old' class of antibiotics. *Future Microbiol*, **8**:711–24.

Wang H, Wang J, Yu P, Ge P, Jiang Y, Xu R, Chen R and Liu X . 2017. Identification of antibiotic resistance genes in the multidrug-resistant *Acinetobacter baumannii* strain, MDR-SHH02, using whole-genome sequencing. *Inter J Mol Med*, **39**: 364-372.

WHO. (2017). Global priority list of antibiotic-resistant bacteria to guide research, discovery, and development of new antibiotics, https://www.who.int/medicines/publications/global-priority-list-antibiotic-resistant-bacteria/en/ (Des. 6, 2018).

Wong D, Nielsen TB, Bonomo RA, Pantapalangkoor P, Luna B and Spellberg B. 2017. Clinical and Pathophysiological Overview of *Acinetobacter* Infections: a Century of Challenges. *Clin Microbiol Rev*, **30**:409–447.

Woodford N, Ellington MJ, Coelho JM, Turton JF, Ward ME, Brown S, Amyes SG and Livermore DM. 2006. Multiplex PCR for genes encoding prevalent OXA carbapenemases in *Acinetobacter* spp. *Inter J Antimicrob Agents*, **27**: 351–353.

Yong D, Toleman MA, Giske CG, Cho HS, Sundman K, Lee K and Walsh TR. 2009. Characterization of a new metallo-beta-lactamase gene, blaNDM-1, and a n ovel erythromycin esterase gene carried on a unique genetic structure in *Klebsiella pneumoniae* sequence type 14 from India. *Antimicrob Agents Chemother*., **53**:5046–5054.

Zankari E, Hasman H, Cosentino S, Vestergaard M, Rasmussen S, Lund O, Aarestrup FM and Larsen MV. 2012. Identification of acquired antimicrobial resistance genes. *J Antimicrob Chemother*, **67**: 2640–2644.

Zhu L, Yan Z, Zhang Z, Zhou Q, Zhou J, Wakeland EK, Fang X, Xuan Z, Shen D and Li QZ.. 2013. Complete Genome Analysis of Three *Acinetobacter baumannii* Clinical Isolates in China for Insight into the Diversification of Drug Resistance Elements. *PLoS ONE*, **8**(6).

JJBS

Volume 12, Number 5,December 2019
ISSN 1995-6673
Pages 595 - 601

Jordan Journal of Biological Sciences

Thermal Manipulation during Broiler Chicken Embryogenesis Modulates the Splenic Cytokines' mRNA Expression

Khaled M. Saleh[1] and Mohammad B. Al-Zghoul[2*]

[1] Department of Applied Biological Sciences, Faculty of Science and Art, [2] Department of Basic Medical Veterinary Sciences, Faculty of Veterinary Medicine, Jordan University of Science and Technology, P.O. Box 3030, Irbid 22110, Jordan

Received January 12, 2019; Revised March 14, 2019; Accepted March 26, 2019

Abstract

The increased incubation temperature has several impacts on the physiology and development of broiler chicken embryos. However, the impact of these conditions on embryonic immunity is unclear. The aim of this study is to evaluate the effect of intermittent thermal manipulation during embryogenesis (TM) on the mRNA expression of cytokines in the spleen of chicken embryos. In this study, the IL-4, IL-6, IL-8, IL-15, IL-16, IL-17, IL-18, IFN-γ, IFN-β, IFN-α, TNF-α and IL-1β genes are evaluated. The eggs of the TM group were subjected to thermal manipulation at 39^{o}C and 65 % relative humidity for eighteen hours/day during embryonic days (ED) 10-18, whereas the eggs of the control group were kept at 37.8^{o}C and 56 % RH throughout the incubation period. On ED 18, the spleen was collected from the embryos in order to evaluate the mRNA levels of cytokines by relative quantitation real time RT-PCR. On the day of hatching, the hatchability rate, body weight, and cloacal temperature (T^{c}) of the hatched chicks were recorded. TM significantly increased the mRNA expression of IL-6, IL-8, IL-4, IL15, IL-16, IL-17, IL-18, IFN-γ, IFN-β, IFN-α, TNF-α and IL-1β in the spleen of broiler chicken embryos on ED eighteen. However, TM did not significantly affect the hatchability rate, T^{c} and the body weight of chicks on the day of hatching. In conclusion, results of the present study suggest that TM modulates the cytokine expression in broiler embryos, but did not lead to significant impacts on the hatchability rate and hatchling body weights, and cloacal temperatures.

Keywords: Broilers, Thermal manipulation, Interleukins, Interferons, Cytokines

1. Introduction

The incubation temperature is an essential factor for a normal development of broiler chicken embryos (*Gallus gallus domesticus*) (Nakage *et al*. 2003, Lourens *et al*. 2005, Lourens *et al.* 2006, Wineland *et al*. 2006, Brand *et al*. 2007, Yalçin *et al*. 2007). Eggs incubated at temperatures higher than the standard conditions have severe effects on the physiology and development of broiler chicken embryos (French 1997). It was found that increased incubation temperatures have deleterious effects on the immune organs and immune system (Thaxton *et al*. 1968, Heller *et al*. 1979, Mashaly *et al*. 2004, Oznurlu *et al*. 2010).

On the other hand, intermittent increased incubation temperature, also called thermal manipulation (TM), was suggested to enhance post-hatch heat tolerance in broiler chickens (Al-Zghoul *et al*. 2013, Loyau *et al*. 2014, Al-Zghoul *et al*. 2015, Al-Zghoul *et al*. 2015, Al-Zghoul *et al*. 2015, Morita *et al*. 2016, Al-Rukibat *et al*. 2017). Furthermore, in pekin ducklings, TM during periods after the incubation day ten led to beneficial effects on the immune system during embryogenesis and during post-hatch lipopolysaccharide-challenge (Shanmugasundaram *et al*. 2018, Shanmugasundaram *et al.* 2019). TM led to increased IL-6, IFN-γ and IL-10 cytokines, and to increased MHCI and MHCII gene expression in pekin duck embryos (Shanmugasundaram *et al*. 2018). However, Liu *et al*. (2013) reported that increased incubation temperature during the middle stage of pekin ducks embryogenesis led to repressive effects on immunity and the development of immune organs.

Cytokines are extracellular, small, signaling proteins that have a critical role in immunity, both during the development of immune system and in the cases of immune response to pathogens or to certain stimulus (Giansanti *et al*. 2006, Kaiser 2010, Davison *et al*. 2011). Cytokines could be secreted by every cell type in vertebrates (Kaiser 2010, Davison *et al*. 2011). They were classified depending on their function, the cells that secret them, or on the cells that they act upon (Giansanti *et al*. 2006). Cytokines include interleukins (IL), tumor necrosis factors (TNF), interferons (IFN), chemokines, transforming growth factor beta family (TGF-β) and colony stimulating factors (CSF) (Davison *et al.* 2011). In birds, TNF-α, IL-1β, IL-18, IL-17, IL-6, IL-16 and IL-8 are known to act as pro-inflammatory cytokines. Chicken IL-15 promotes T-cells proliferation, and IFN-γ is a signal for the cell mediated immune response, while IL-4 activates the antibody-mediated immunity. Chicken type I –interferons (IFN-α and IFN-β) possess antiviral activity

* Corresponding author e-mail: alzghoul@just.edu.jo.

(Kaiser and Stäheli 2014). Abdul-Careem *et al*. (2007) reported that cytokines have a function in the maturation and shaping of spleen in chicken embryos.

In broiler chickens, the effect of TM on mRNA expression of proinflammatory cytokines during post hatch heat stress exposure had been evaluated (Al-Zghoul *et al.* 2019), however, the impact of high incubation temperatures on the embryonic development and immune status of broiler chicken embryos still needs further investigations. Therefore, the aim of this study is to evaluate the influence of intermittent thermal manipulation during embryogenesis (TM) on the mRNA levels of the cytokines (signaling molecules that are important in immune response and have roles in embryonic development) in the spleen of broiler embryos. The evaluated cytokines were: IL-4, 6, 8, 15, 16, 17, 18, IFN-γ, IFN-α, IFN-β, IL-1β and TNF-α.

2. Materials and Methods

2.1. Ethical Statement

All experimental procedures that are followed in this study were approved by the Jordan University of Science and technology Animal Care and Use Committee (JUST-ACUC).

2.2. Incubation Management and Sampling

A total of six-hundred fertile eggs of the Indian River broiler breed with a uniform weight were obtained from an Indian River breeder (Irbid, Jordan). The abnormal and broken eggs were excluded, and the approved eggs were incubated in commercial Type-I HS-SF incubators (Masalles, Barcelona, Spain). The eggs were subdivided into two treatment groups: the control group and the thermal manipulation (TM) group. The eggs of the control group were maintained at 37.8 °C and 56 % relative humidity (RH) throughout the embryogenesis period, while those of the TM group were subjected to 39°C and 65 % RH for eighteen hours/day during days ten to eighteen of embryogenesis. On day seven of incubation, the eggs were examined by candling and the infertile eggs, and the eggs containing dead embryos were removed.

On embryonic day (ED) eighteen, six eggs were randomly selected from each group, and the spleen samples were collected for the purpose of evaluating the mRNA expression of cytokines by real time RT-PCR analysis. On hatching day, the number of hatched chicks and their cloacal temperatures (T^c) and body weights were recorded.

2.3. Total RNA Extraction and Reverse Transcription

Splenic total RNA was isolated using Direct-Zol™ RNA MiniPrep (Zymo Research, Irvine, USA) with TRI Reagent® (Zymo Research, Irvine, USA) according to the manufacturer's procedures. RNA concentrations were determined using XS2 Spectrophotometer (BioTek Instruments, Inc., USA). 2 µg total RNA from each sample was used for the cDNA synthesis (reverse transcription) using a Power cDNA Synthesis Kit (Intron Biotechnology، Kyungki-Do, Korea).

2.4. Real-Time PCR and mRNA Relative-Quantitation

QuantiFast SYBR® Green PCR Kit (Qiagen corp., CA, USA) was used on a Rotor-Gene Q MDx5 plex instrument (Qiagen corp., CA, USA). Briefly, the 20 µL reaction mix was prepared from 10 µL of master mix, 1.2 µL forward primer (12 pmol), 1.2 µL reverse primer (12 pmol), 1 µL cDNA from the sample, and 6.6 µL of nuclease-free water. The PCR cycles employed the following parameters: 95°C for five minutes; forty cycles of 95°C for ten seconds followed by thirty seconds at 55°C; and 72°C for ten seconds with final melting at 95°C for twenty seconds. The fluorescence emission detection was during the extension step. The fold changes in the gene expression were normalized to the 28S ribosomal RNA, which was utilized in this study as an internal control. The single target amplification specificity was checked using the melting curve. The fold changes in gene expression were calculated automatically. Table 1 presents the primers' sequences that were used in the real time PCR analysis.

2.5. Statistical Analysis

All Statistical analyses were conducted using the IBM SPSS statistics 23 software (IBM software, Chicago, USA). The data of cloacal temperature, body weight, and relative mRNA levels of IL-1β, TNF-α, IL-6, IL-8, IFN-α, IFN-β, IFN-γ, IL-4, IL-15, IL-16, IL-17 and IL-18 were expressed as means ± SD. An independent t-test was used to compare the difference between the controls vs. the TM treatment groups. The hatchability was assessed using the Chi-square statistical test. Parametric differences were considered statistically significant when $P < 0.05$.

Table 1. Primer sequences of genes used in the real time RT-PCR analysis.

The gene	Forward	Reverse
IL-6	GCGAGAACAGCATGGAGATG	GTAGGTCTGAAAGGCGAACAG
IL-4	GAGAGCATCCGGATAGTGAATG	TGTGGAGGCTTTGCATAAGAG
IL-8	CTGCGGTGCCAGTGCATTA	AGCACACCTCTCTTCCATCC
IL-15	GTGGTCAGACGTTCTGAAAGAT	CAGGTTCCTGGCATTCTATATCC
IL-16	GGAACAAAGCAGCCCAGTTC	GGCTGTGGTGTGCACCTGTA
IL-17	CTCCGATCCCTTATTCTCCTC	AAGCGGTTGTGGTCCTCAT
IL-18	AGGTGAAATCTGGCAGTGGAAT	TGAAGGCGCGGTGGTTT
IFN-γ	CAAGTCAAAGCCGCACATC	CGCTGGATTCTCAAGTCGTT
IFN-α	ATGCCACCTTCTCTCACGAC	AGGCGCTGTAATCGTTGTCT
IFN-β	CCTCAACCAGATCCAGCATTA	TAGTTGTTGTGCCGTAGGAAG
IL-1β	GGGCATCAAGGGCTACAA	CTGTCCAGGCGGTAGAAGA
TNF-α	GACAGCCTATGCCAACAAGTA	GAATTAAGCAACAGCCAGCTATG
28S rRNA	CCTGAATCCCGAGGTTAACTATT	GAGGTGCGGCTTATCATCTATC

3. Results

3.1. Effect of Intermittent TM on The Splenic mRNA Levels of Cytokines in Broiler Chicken Embryos

The effect of intermittent TM at 39°C for 18 h/day during EDs 10-18 on the splenic mRNA expression of cytokines in the broiler embryos is shown in Figure 1 (A-L). Intermittent TM significantly increased the mRNA expression of IL-6, IL-8, IL-4, IL15, IL-16, IL-17, IL-18, IFN-γ, IFN-β, IFN-α, TNF-α and IL-1β in the spleen of broiler chicken embryos on ED 18 (*P*-value< 0.05).

3.2. Effect of Intermittent TM on Hatchability Rate, Hatchling Tc and Hatchling Body Weight of Broiler Chicks

Figure 2 (A-D) presents the effect of intermittent TM at 39°C for 18 h/day during EDs 10-18 on the number of hatched chicks, hatchability, cloacal temperature, and the body weight on the day of hatch. No significant difference was observed in the hatchability rate, hatchling T^c, and hatchling body weight between the TM and control groups (*P*-value > 0.05).

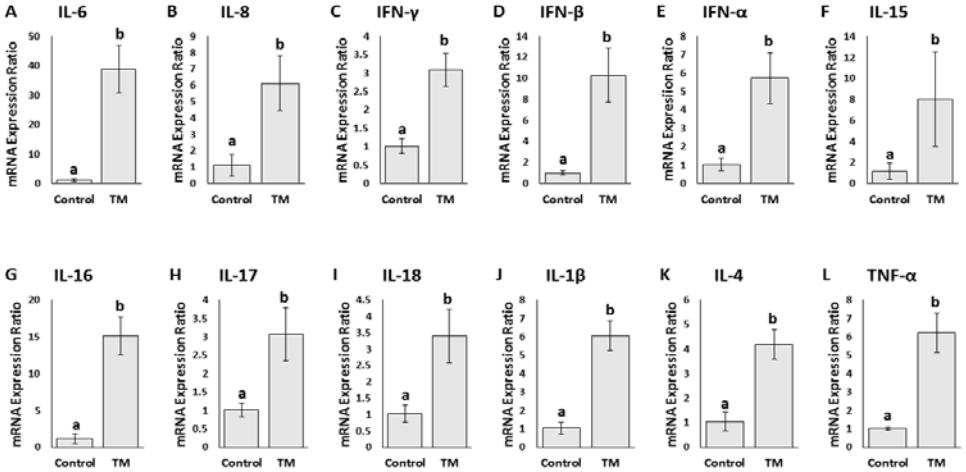

Figure 1. Effect of intermittent TM on the mRNA levels of cytokines, (A) IL-6, (B) IL-8, (C) IFN-γ, (D) IFN-β, (E) IFN-α, (F) IL-15, (G) IL-16, (H) IL-17, (I) IL-18, (J) IL-1β, (K) IL-4, (L) TNF-α, in the spleen of broiler chicken embryos on embryonic day eighteen .

a-b means ± SD with different superscripts differ significantly ($p < 0.05$).

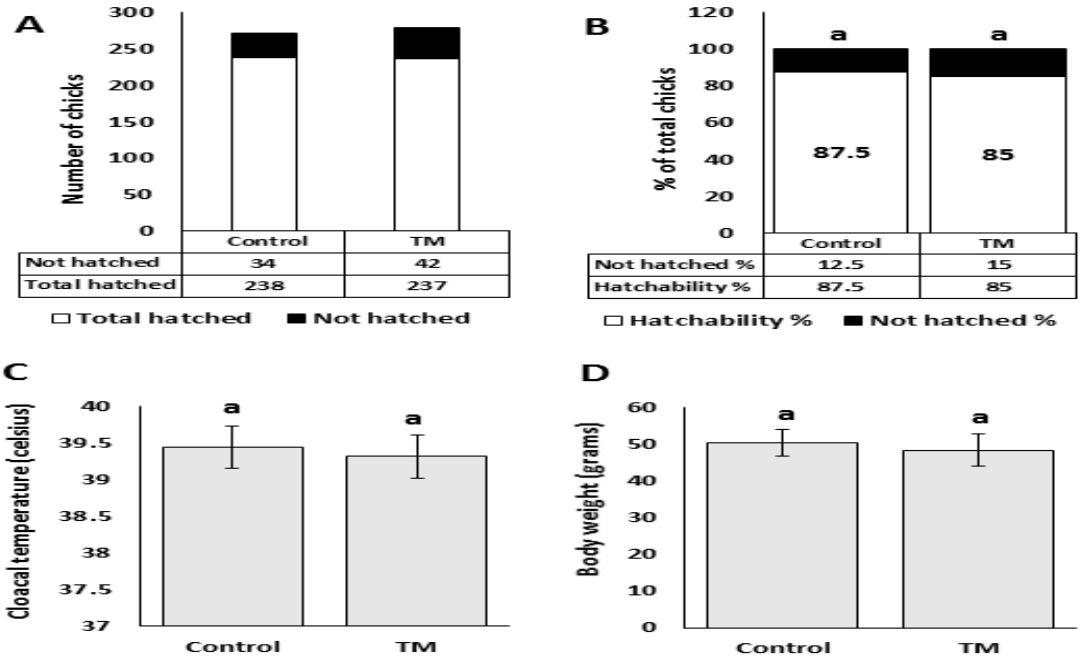

Figure 2: Effect of intermittent TM on the number of hatched chicks (A), the hatchability rate (B), hatchling T^c (C), and hatchling body weights (D) of broiler chicks. $^{a-b}$ values with different superscripts differ significantly.

4. Discussion

The incubation conditions of broiler chickens, especially the incubation temperature, had been proven to affect embryonic development, leading to significant impacts on hatched chicks' quality and post-hatch physiology and performance (Decuypere and Michels 1992, Lourens *et al*. 2005, Lourens *et al*. 2007). The aim of the present study is to evaluate the effect of TM at 39°C and 65 % RH for 18 h/day during incubation days 10 to 18 on the splenic mRNA levels of cytokines (IFN-α, IFN-β,

IFN-γ, IL-4, IL-8, IL-15, IL-16, IL-17 and IL-18) in broiler chicken embryos, as well as on the hatchability, hatchling body weights, and cloacal temperatures.

Cytokines are small proteins that have a function in signaling and immunoregulation. Their major function is during the immune response against pathogens, however, they are also important in the regeneration and healing of injured tissues (Wigley and Kaiser 2003, Eming *et al*. 2009).

In this study, TM increased the IFN-α, IFN-β, IFN-γ, IL-4 and IL-15 mRNA levels in the spleen of broiler embryos. IFNs are mainly upregulated in response to viral infections (Wigley and Kaiser 2003, Giansanti *et al*. 2006), and IL-15 has a function in lymphocytes proliferation, intestinal epithelium growth, as well as stimulating cytokines' expression (Wigley and Kaiser 2003).The role of interferons and IL-15 in the response to heat stress is not clear and no previous studies were found in the literature describing IFN-α, IFN-β and IL-15 expression during heat stress in broilers. In humans, the IFN-α level was reported to be elevated during a heat stroke (Leon 2007). Previously, IFN-γ expression was found to be increased in chickens exposed to heat stress (Song *et al*. 2017, Xie *et al*. 2017). However, Ohtsu *et al*. (2015) had shown that heat stress decreased the IFN-γ expression in broiler chickens. In Pekin duck embryos, TM led to increased IFN-γ expression (Shanmugasundaram *et al.* 2018). IFN-γ is mainly upregulated during cell-mediated immune response through Th1 cells (Wigley and Kaiser 2003, Giansanti *et al*. 2006). In contrast, IL-4 is a Th2 cytokine that plays a role in the humoral (antibody) immune response (Giansanti *et al*. 2006). Ohtsu, *et al*. (2015) had found that broilers exposed to heat stress had upregulated the IL-4 expression. The immune response is functionally polarized into either cell-mediated or into the antibody-mediated response (Mosmann *et al.* 1986, Degen *et al*. 2005). Cytokines were reported to be expressed in minute amounts during standard embryonic conditions (Abdul-Careem *et al.* 2007); thus, the current results suggest that TM chicks were under stress due to the non-standard incubation condition. Previously, heat stress was reported to disturb the normal levels of cytokines and the Th1 - Th2 polarization signals in broiler chickens (Ohtsu *et al*. 2015).

In the current study, TM increased the splenic mRNA levels of the IL-1β, TNF-α, IL-6, IL-8, IL-16, IL-17 and IL-18 in broiler embryos.IL-1β, TNF-α, IL-6, IL-8, IL-16, IL-17 and IL-18 are pro-inflammatory cytokines, that have a major function in native immunity and the activation of acute phase response (Wigley and Kaiser 2003, Giansanti *et al.* 2006). Pro-inflammatory cytokines play a critical role in the regeneration and repair of damaged and stressed tissues, especially IL-8 and IL-6 (Rennekampff *et al*. 2000, Streetz *et al*. 2000, Bosch *et al*. 2002, Wigley and Kaiser 2003, Eming *et al*. 2007, Crouser *et al*. 2009, Eming *et al*. 2009, McFarland-Mancini *et al*. 2010, Welc *et al*. 2013, Cheng *et al*. 2015, Phillips *et al*. 2015). Previously, heat stress was found to increase the expression of IL-1β, IL-6, IL-8 and TNF-α in broiler chickens and mammals, and to reduce IL-8 plasma level in chickens (Leon 2007, Heled *et al*. 2013, Varasteh *et al.* 2015, Lan *et al*. 2016, Al-Zghoul *et al*. 2019). Recently, it has been found that chickens' IL-6 functions as a heat-shock gene, since its transcription is induced by HSF3 during heat stress (Prakasam *et al*. 2013). In Pekin duck embryos, TM was found to increase the IL-6 expression (Shanmugasundaram *et al*. 2018). Moreover, it was reported that the IL-18 expression was not changed during heat stress in broiler chickens (Ohtsu *et al*. 2015); however, its level was modulated in mammals (Heled *et al.* 2013). Furthermore, artificial stress induced by corticosterone administration resulted in increased IL-1β, IL-6, IL-8 and IL-18 expression in chickens (Shini and Kaiser 2009, Shini *et al*. 2010). To the authors' knowledge, no previous studies could be found in the literature about the impact of heat stress on the expression of IL-16 and IL-17. Since stress conditions induce proinflammatory cytokines' expression, the present results could be described as the stress response in the broiler embryos.

In the current study, TM did not affect the hatchability rate of broiler chicks. This finding is consistent with two previous studies (Lourens *et al.* 2005, Zaboli *et al*. 2016); however, TM at 39.5^{o}C for 12 h/day during ED 7-16 was reported to decrease the hatchability rate, and TM at 39.5^{o}C for 3 h/day during ED 8-10 and at 38.8^{o}C for 18 h/d during ED 10-18 was found to increase the hatchability rate (Collin *et al*. 2007, Piestun *et al.* 2008, Piestun *et al.* 2008, Al-Zhgoul *et al*. 2013). These contradicting results may be attributed to the strain type, age factors, or incubation conditions (relative humidity and temperature).

The present study shows that TM did not change the hatchling weights and cloacal temperatures. The findings concerning hatchling weights in the previous studies were contradictory; different studies had shown that TM increased, decreased, or did not affect the hatchling weights (Hulet *et al*. 2007, Yalçin *et al*. 2007, Narinç *et al.* 2016, Zaboli *et al.* 2016, Al-Rukibat *et al*. 2017). The present results of the hatchling T^{c} are consistent with two previous studies (Soren *et al.* 2012, Al-Rukibat *et al.* 2017); however, other studies had shown that TM decreased (Collin *et al*. 2005, Collin *et al.* 2007, Al-Zghoul *et al*. 2013, Piestun *et al.* 2013), or increased the hatchling T^{c} in broiler chicks (Al-Zghoul *et al*. 2015). The present findings suggest that although TM increased the cytokines mRNA expression, it did not lead to deleterious impacts on the hatchability rate, weight, and T^{c} of the hatched chicks. The increased cytokines' expression in the thermally- manipulated chicks might be attributed to the fact that TM stimulated an immune response in the embryos, thus, leading to an improved immune response during post-hatch life. Previously, it was found that TM increased the cytokines' expression in Pekin duck embryos, and led to an enhanced post-hatch immune response to a lipopolysaccharide injection (Shanmugasundaram *et al*. 2018, Shanmugasundaram *et al.* 2019). Further studies are required to evaluate the effect of TM on post-hatch immune challenges. On the other hand, the modulation of cytokines' expression during embryogenesis might affect the development of embryos and differentiation of different types of tissues, since cytokines are important players in the differentiation of embryonic stem cells (Chadwick *et al*. 2003, Kristensen *et al.* 2005, Zhou *et al*. 2010). However, this impact on differentiation might be beneficial for the post-hatch performance, as shown in several studies, or might have deleterious effects on the development and post-hatch

health status (Loyau *et al.* 2014, Morita *et al*. 2016, Narinç *et al*. 2016, Al-Zghoul *et al.* 2019).

5. Conclusion

In conclusion, the results of the present study suggest that intermittent thermal manipulation modulates the cytokines' expression in broiler embryos, but does not lead to significant impacts on the hatchability rate, hatchling body weights, and cloacal temperatures. Further studies are required to evaluate the impacts of thermal manipulation on the immune challenges during post-hatch life.

Conflict of Interest

The authors declare that they have no conflict of interest.

Acknowledgments

The authors would like to thank Eng. Ibrahim Alsukhni and Miss Amneh Tarkhan for their excellent technical assistance and valuable comments. The authors would like to express deep appreciation and thanks to the Deanship of Research/ Jordan University of Science & Technology for its financial support of this work (Grant#: 44/2019).

References

Abdul-Careem M, Hunter D, Lambourne M, Barta J and Sharif S.2007. Ontogeny of cytokine gene expression in the chicken spleen. *Poultry Sci.*, **86**(7): 1351-1355.

Al-Rukibat RK, Al-Zghoul MB, Hananeh WM, Al-Natour MQ and Abu-Basha EA.2017. Thermal manipulation during late embryogenesis: Effect on body weight and temperature, thyroid hormones, and differential white blood cell counts in broiler chickens. *Poultry Sci*., **96**(1): 234-240.

Al-Zghoul MB, Dalab AE, Ababneh MM, Jawasreh KI, Al Busadah KA and Ismail ZB.2013. Thermal manipulation during chicken embryogenesis results in enhanced Hsp70 gene expression and the acquisition of thermotolerance. *ResVet Sci.*, **95**(2): 502-507.

Al-Zghoul MB, Dalab AE, Yahya IE, Althnaian TA, Al-Ramadan SY, Ali AM, Albokhadaim IF, El-Bahr SM, Al Busadah KA and Hannon KM.2015. Thermal manipulation during broiler chicken embryogenesis: Effect on mRNA expressions of Hsp108, Hsp70, Hsp47 and Hsf-3 during subsequent post-hatch thermal challenge. *Res Vet Sci*., **103**: 211-217.

Al-Zghoul MB, El-Bahr SM, Al-Rukibat RK, Dalab AE, Althnaian TA and Al-Ramadan SY.2015. Biochemical and molecular investigation of thermal manipulation protocols during broiler embryogenesis and subsequent thermal challenge. *BMC Vet Res.*, **11**: 292.

Al-Zghoul MB, Ismail ZB, Dalab AE, Al-Ramadan A, Althnaian TA, Al-Ramadan SY, Ali AM, Albokhadaim IF, Al Busadah KA, Eljarah A, Jawasreh KI and Hannon KM.2015. Hsp90, Hsp60 and HSF-1 genes expression in muscle, heart and brain of thermally manipulated broiler chicken. *Res Vet Sci*. **99**: 105-111.

Al-Zghoul MB, Saleh KM and Ababneh MMK.2019. Effects of pre-hatch thermal manipulation and post-hatch acute heat stress on the mRNA expression of interleukin-6 and genes involved in its induction pathways in 2 broiler chicken breeds. *Poultry Sci*., **98**(4): 1805-1819.

Al-Zhgoul MB, Dalab AES, Ababneh MM, Jawasreh KI, Al Busadah KA and Ismail ZB.2013. Thermal manipulation during chicken embryogenesis results in enhanced Hsp70 gene expression and the acquisition of thermotolerance. *Res Vet Sci*., **95**(2): 502-507.

Bosch I, Xhaja K, Estevez L, Raines G, Melichar H, Warke RV, Fournier MV, Ennis FA and Rothman AL.2002. Increased production of interleukin-8 in primary human monocytes and in human epithelial and endothelial cell lines after dengue virus challenge. *J Virol*., **76**(11): 5588-5597.

Brand H, Lourens A, Meijerhof R, Heetkamp M and Kemp B.2007. Incubation circumstances affect energy metabolism in avian embryos. *In*: Miraux N, Brand-Williams W and Ortigues-Marty I. (Eds.),**Energy and Protein Metabolism and Nutrition,** Eaap 124, Vichy, France, 9-13 September, 2007 (pp. 511-512). Wageningen: Wageningen Academic Publishers.

Chadwick K, Wang L, Li L, Menendez P, Murdoch B, Rouleau A and Bhatia M.2003. Cytokines and BMP-4 promote hematopoietic differentiation of human embryonic stem cells. *Blood*, **102**(3): 906-915.

Cheng C-Y, Tu W-L, Wang S-H, Tang P-C, Chen C-F, Chen H-H, Lee Y-P, Chen S-E and Huang S-Y.2015. Annotation of differential gene expression in small yellow follicles of a broiler-type strain of taiwan country chickens in response to acute heat stress. *PloS one*, **10**(11): e0143418.

Collin A, Berri C, Tesseraud S, Rodon FER, Skiba-Cassy S, Crochet S, Duclos MJ, Rideau N, Tona K and Buyse J.2007. Effects of thermal manipulation during early and late embryogenesis on thermotolerance and breast muscle characteristics in broiler chickens. *Poultry Sci.*, **86**(5): 795-800.

Collin A, Berri C, Tesseraud S, Rodon FR, Skiba-Cassy S, Crochet S, Duclos M, Rideau N, Tona K and Buyse J.2007. Effects of thermal manipulation during early and late embryogenesis on thermotolerance and breast muscle characteristics in broiler chickens. *Poultry Sci.*, **86**(5): 795-800.

Collin A, Picard M and Yahav S.2005. The effect of duration of thermal manipulation during broiler chick embryogenesis on body weight and body temperature of post-hatched chicks. *Animal Res*., **54**(2): 105-111.

Crouser ED, Shao G, Julian MW, Macre JE, Shadel GS, Tridandapani S, Huang Q and Wewers MD.2009. Monocyte activation by necrotic cells is promoted by mitochondrial proteins and formyl peptide receptors. *Critical Care Med.*, **37**(6): 2000.

Davison F, Kaspers B, Schat KA and Kaiser P. 2011. **Avian Immunology,** Academic Press.

Decuypere E and Michels H.1992. Incubation temperature as a management tool: a review. *World's Poultry Sci. J*., **48**(1): 28-38.

Degen WG, van Daal N, Rothwell L, Kaiser P and Schijns VE.2005. Th1/Th2 polarization by viral and helminth infection in birds. *Vet Microbiol*., **105**(3-4): 163-167.

Eming SA, Hammerschmidt M, Krieg T and Roers A. 2009. Interrelation of immunity and tissue repair or regeneration. **Seminars in Cell and Developmental Biology**, Elsevier.

Eming SA, Krieg T and Davidson JM.2007. Inflammation in wound repair: molecular and cellular mechanisms. *J Invest Dermatol*., **127**(3): 514-525.

French N.1997. Modeling incubation temperature: the effects of incubator design, embryonic development, and egg size. *Poultry Sci*., **76**(1): 124-133.

Giansanti F, Giardi M and Botti D.2006. Avian cytokines-an overview. *Current Pharma Design*, **12**(24): 3083-3099.

Heled Y, Fleischmann C and Epstein Y.2013. Cytokines and their role in hyperthermia and heat stroke. *J Basic Clin Physiol Pharmacol*., **24**(2): 85-96.

Heller E, Nathan DB and Perek M.1979. Short heat stress as an immunostimulant in chicks. *Avian Pathol*., **8**(3): 195-203.

Hulet R, Gladys G, Hill D, Meijerhof R and El-Shiekh T.2007. Influence of egg shell embryonic incubation temperature and broiler breeder flock age on posthatch growth performance and carcass characteristics. *Poultry Sci*., **86**(2): 408-412.

Kaiser P. 2010. Advances in avian immunology—prospects for disease control: a review. *Avian Pathol*., **39**(5): 309-324.

Kaiser P and Stäheli P. 2014. Avian cytokines and chemokines. **Avian Immunology** (Second Edition), Elsevier**:** 189-204.

Kristensen DM, Kalisz M and Nielsen JH.2005. Cytokine signalling in embryonic stem cells. *APMIS*, **113**(11 - 12): 756-772.

Lan X, Hsieh JC, Schmidt CJ, Zhu Q and Lamont SJ.2016. Liver transcriptome response to hyperthermic stress in three distinct chicken lines. *BMC Genomics*, **17**(1): 955.

Leon LR.2007. Heat stroke and cytokines. *Progress Brain Res*., **162**: 481-524.

Liu J, Yan X, Li Q, Wang G, Liu H, Wang J, Li L, Du X, Han C and He H.2013. Thermal manipulation during the middle incubation stage has a repressive effect on the immune organ development of Peking ducklings. *J Thermal Biol.*, **38**(8): 520-523.

Lourens A, Van den Brand H, Heetkamp M, Meijerhof R and Kemp B.2006. Metabolic responses of chick embryos to short-term temperature fluctuations. *Poultry Sci.*, **85**(6): 1081-1086.

Lourens A, Van den Brand H, Heetkamp MJW, Meijerhof R and Kemp B.2007. Effects of eggshell temperature and oxygen concentration on embryo growth and metabolism during incubation. *Poultry Sci*., **86**(10): 2194-2199.

Lourens A, Van den Brand H, Meijerhof R and Kemp B.2005. Effect of eggshell temperature during incubation on embryo development, hatchability, and posthatch development. *Poultry Sci.*, **84**(6): 914-920.

Lourens A, Van den Brand H, Meijerhof R and Kemp B.2005. Effect of eggshell temperature during incubation on embryo development, hatchability, and posthatch development. *Poultry Sci*., **84**(6): 914-920.

Loyau T, Metayer-Coustard S, Berri C, Crochet S, Cailleau-Audouin E, Sannier M, Chartrin P, Praud C, Hennequet-Antier C, Rideau N, Courousse N, Mignon-Grasteau S, Everaert N, Duclos MJ, Yahav S, Tesseraud S and Collin A.2014. Thermal manipulation during embryogenesis has long-term effects on muscle and liver metabolism in fast-growing chickens. *PLoS One*, **9**(9): e105339.

Mashaly M, Hendricks 3rd G, Kalama M, Gehad A, Abbas A and Patterson P.2004. Effect of heat stress on production parameters and immune responses of commercial laying hens. *Poultry Sci*., **83**(6): 889-894.

McFarland-Mancini MM, Funk HM, Paluch AM, Zhou M, Giridhar PV, Mercer CA, Kozma SC and Drew AF.2010. Differences in wound healing in mice with deficiency of IL-6 versus IL-6 receptor. *J Immunol*., **184**(12): 7219-7228.

Morita VS, Almeida VR, Matos Junior JB, Vicentini TI, van den Brand H and Boleli IC.2016. Incubation temperature alters thermal preference and response to heat stress of broiler chickens along the rearing phase. *Poultry Sci.*, **95**(8): 1795-1804.

Mosmann TR, Cherwinski H, Bond MW, Giedlin MA and Coffman RL.1986. Two types of murine helper T cell clone. I. Definition according to profiles of lymphokine activities and secreted proteins. *J Immunol*., **136**(7): 2348-2357.

Nakage E, Cardozo J, Pereira G and Boleli I.2003. Effect of temperature on incubation period, embryonic mortality, hatch rate, egg water loss and partridge chick weight (Rhynchotus rufescens). *Revista Brasileira de Ciência Avícola*, **5**(2): 131-135.

Narinç D, Erdoğan S, Tahtabiçen E and Aksoy T.2016. Effects of thermal manipulations during embryogenesis of broiler chickens on developmental stability, hatchability and chick quality. *Animal*, **10**(8): 1328-1335.

Ohtsu H, Yamazaki M, Abe H, Murakami H and Toyomizu M.2015. Heat Stress Modulates Cytokine Gene Expression in the Spleen of Broiler Chickens. *J Poultry Sci.*, **52**(4): 282-287.

Oznurlu Y, Celik I, Telatar T and Sur E.2010. Histochemical and histological evaluations of the effects of high incubation temperature on embryonic development of thymus and bursa of Fabricius in broiler chickens. *British Poultry Sci.*, **51**(1): 43-51.

Phillips NA, Welc SS, Wallet SM, King MA and Clanton TL.2015. Protection of intestinal injury during heat stroke in mice by interleukin - 6 pretreatment. *J Physiol*., **593**(3): 739-753.

Piestun Y, Druyan S, Brake J and Yahav S.2013. Thermal manipulations during broiler incubation alter performance of broilers to 70 days of age. *Poultry Sci*., **92**(5): 1155-1163.

Piestun Y, Shinder D, Ruzal M, Halevy O, Brake J and Yahav S.2008. Thermal manipulations during broiler embryogenesis: effect on the acquisition of thermotolerance. *Poultry Sci.*, **87**(8): 1516-1525.

Piestun Y, Shinder D, Ruzal M, Halevy O and Yahav S.2008. The effect of thermal manipulations during the development of the thyroid and adrenal axes on in-hatch and post-hatch thermoregulation. *J Thermal Biol*., **33**(7): 413-418.

Prakasam R, Fujimoto M, Takii R, Hayashida N, Takaki E, Tan K, Wu F, Inouye S and Nakai A.2013. Chicken IL - 6 is a heat - shock gene. *FEBS letters*, **587**(21): 3541-3547.

Rennekampff H-O, Hansbrough JF, Kiessig V, Doré C, Sticherling M and Schröder J-M.2000. Bioactive interleukin-8 is expressed in wounds and enhances wound healing. *J Surgical Res*., **93**(1): 41-54.

Shanmugasundaram R, Wick M and Lilburn M.2019. Effect of embryonic thermal manipulation on heat shock protein 70 (HSP70) expression and subsequent immune response to post-hatch lipopolysaccharide challenge in Pekin ducklings. *Poultry Sci.*, **98**(2): 722-733.

Shanmugasundaram R, Wick M and Lilburn MS.2018. Effect of embryonic thermal manipulation on heat shock protein 70 expression and immune system development in Pekin duck embryos. *Poultry Sci*., **97**(12): 4200-4210.

Shini S and Kaiser P.2009. Effects of stress, mimicked by administration of corticosterone in drinking water, on the expression of chicken cytokine and chemokine genes in lymphocytes. *Stress*, **12**(5): 388-399.

Shini S, Shini A and Kaiser P.2010. Cytokine and chemokine gene expression profiles in heterophils from chickens treated with corticosterone. *Stress*, **13**(3): 185-194.

Song Z, Cheng K, Zhang L and Wang T.2017. Dietary supplementation of enzymatically treated Artemisia annua could alleviate the intestinal inflammatory response in heat-stressed broilers. *J Thermal Biol*., **69**: 184-190.

Soren S, Bhanja S, Mandal A, Mehra M and Goel A.2012. Effect of incubational thermal manipulation on the embryonic and early post-hatch growth in layer chickens. *Indian J Poultry Sci*., **47**(3): 263-268.

Streetz K, Luedde T, Manns M and Trautwein C.2000. Interleukin 6 and liver regeneration. *Gut*, **47**(2): 309-312.

Thaxton P, Sadler C and Glick B.1968. Immune response of chickens following heat exposure or injections with ACTH. *Poultry Sci*., **47**(1): 264-266.

Varasteh S, Braber S, Akbari P, Garssen J and Fink-Gremmels J.2015. Differences in Susceptibility to Heat Stress along the Chicken Intestine and the Protective Effects of Galacto-Oligosaccharides. *PLoS One*, **10**(9): e0138975.

Welc SS, Clanton TL, Dineen SM and Leon LR.2013. Heat stroke activates a stress-induced cytokine response in skeletal muscle. *J Applied Physiol*., **115**(8): 1126-1137.

Wigley P and Kaiser P.2003. Avian cytokines in health and disease. *Revista Brasileira de Ciência Avícola*, **5**(1): 1-14.

Wineland M, Christensen V, Yildrum I, Fairchild B, Mann K and Ort D.2006. Incubator temperature and oxygen concentration at the plateau stage in oxygen consumption affects intestinal maturation of broiler chicks. *Inter J Poultry Sci*., **5**(3): 229-240.

Xie X, Liang C, Li M and Chen Z.2017. Effects of Gaba on the Thymus Cytokines of Wenchang Chickens Submitted to Heat Stress. *Revista Brasileira de Ciência Avícola,* **19**(1): 143-150.

Yalçin S, Molayoğlu H, Baka M, Genin O and Pines M.2007. Effect of temperature during the incubation period on tibial growth plate chondrocyte differentiation and the incidence of tibial dyschondroplasia. *Poultry Sci.,* **86**(8): 1772-1783.

Zaboli GR, Rahimi S, Shariatmadari F, Torshizi MAK, Baghbanzadeh A and Mehri M.2016. Thermal manipulation during Pre and Post-Hatch on thermotolerance of male broiler chickens exposed to chronic heat stress. *Poultry Sci*., **96**(2): 478-485.

Zhou M, Li P, Tan L, Qu S, Ying QL and Song H.2010. Differentiation of mouse embryonic stem cells into hepatocytes induced by a combination of cytokines and sodium butyrate. *J Cellular Biochem.*, **109**(3): 606-614.

JJBS
Jordan Journal of Biological Sciences

Volume 12, Number 5,December 2019
ISSN 1995-6673
Pages 603 - 608

Lack of Association of Human Prostate Cancer with Exon 1 and -116 C/G Promoter Polymorphism on the X-Box DNA Binding Protein-1 Gene

Ahmad M. Khalil[1*], Lulu H. Alsheikh Hussien[1], Ahmad Y. Alghadi[1], Rami S. Alazab[2], Ahmad Y. Alwuhoush[2], Mohammad A. Al-Ghazo[2] and Najla H. Aldaoud[3]

[1] *Department of Biological Sciences, Yarmouk University,* [2] *Department of General Surgery and Urology,* [3] *Department of Pathology and Microbiology, Jordan University of Science and Technology, King Abdullah University Hospital, Irbid, Jordan.*

Received March 2, 2019; Revised March 20, 2019; Accepted March 27, 2019

Abstract

The X-box binding protein-1 (XBP1), a critical gene in the endoplasmic reticulum stress response, has been linked to many cancers in several studies. Recent studies indicate that the upregulation of XBP1 promotes cell proliferation and invasion of prostate cancer (PC). This research is aimed at the measurement of the frequencies of Exon 1 and -116 C/G promoter polymorphism on the XBP1 gene as well as the investigation of this polymorphism as a predisposing genetic marker to assess possible strategies for screening families at the risk of developing PC. Blood samples of seventy patients with PC and seventy healthy individuals were evaluated using TaqMan genotyping technique and direct DNA sequencing analysis. Overall, the sequencing of exon1 of the XBP1 showed that there was no mutation, neither in PC subjects nor in the control. Additionally, there was no significant statistical difference between the PC cases with -116C/G polymorphism of XBP1 and the control subjects in the genotype (P = 0.674) and allele frequencies (P = 0.436). The present study is the first report to discuss the risk factors associated with mutations in XBP1 in PC progression. The results suggest no significant relevance between -116C/G and exon 1 (rs5762809 and rs2228260), and PC susceptibility in the Jordanian population.

Keywords: DNA sequencing, Polymorphism, Prostate cancer, X-box binding protein-1 gene.

1. Introduction

Prostate cancer (PC) is one of the most commonly diagnosed cancers and the second leading cause of cancer-related deaths among men, representing ~9 % of all cancer deaths in men worldwide with > 29,430 deaths in 2018 (Tao *et al.,* 2015; Siegel *et al*., 2018). Worldwide, a distinct geographical variation in the incidence of PC has been reported (Benafif *et al*., 2018). According to the latest WHO data published in 2017, PC deaths in Jordan reached 191 or 0.72% of total deaths (WHO, 2017). Although PC mortality rate is decreasing in high income countries, the incidence and burden of the disease are steadily increasing globally, resulting in further challenges in the allocation of limited health care resources (Pishgar *et al*., 2018). Information is limited concerning the efficacy of available screening tests in men predisposed to developing PC (Giri *et al*., 2018). The pathogenesis underlying PC remains out of reach. However, the epidemiologic observations have revealed that pathogenesis of PC reflects both genetic and environmental factors. For example, familial PC studies suggested that PC has a substantial inherited predisposition; they have found that the risk tends to increase with the increased numbers of affected relatives (Alberti, 2010; Kral *et al*., 2011; Al Olama *et al*., 2014). In addition, the study of cohort twins between 44,788 pairs of Sweden, Denmark, and Finland indicated that more than 40 % of the cases of the PC disease were attributed to inheritance (Lichtenstein *et al*., 2000).

Previous research has revealed that both endoplasmic reticulum stress (ERS) and the unfolded protein response (UPR) activation are implicated in tumorigenesis (Corazzari *et al*., 2017; Doultsinos *et al*., 017). UPR involves three main signaling pathways: protein kinase RNA-like ER kinase (PERK), inositol requiring kinase1α (IRE1α), and activating transcription factor 6 (ATF6) (Corazzari *et al*., 2017; Doultsinos *et al*., 017). The activated IRE1 α sensor is responsible for the non-conventional splicing of unspliced XBP1 (XBP1u) mRNA to the active form spliced XBP1 (XBP1s) through its endoribonuclase activity (Moore and Hollien, 2015). XBP-1s enters the nucleus and induces the transcription of genes correlated with the protein-folding capacity and the ER-associated degradation. XBP1s is a central UPR effector, and previous studies indicate that the up- regulation of

* Corresponding author email: kahmad76@yahoo.com.

** Abbreviations: ER, endoplasmic reticulum; GWAS, genome wide association studies; OR, odds ratio; PCR, polymerase chain reaction; PC, prostate cancer; PSA, prostate-specific antigen; SNPs, single nucleotide polymorphisms; UPR, unfolded protein response; XBP1, X-box binding protein-1

XBP1s promotes cell proliferation and invasion of cancerous cells. To the authors' knowledge, no independent study has yet assessed the potential of mutations on the XBP1 gene of human PC cell lines or clinical samples as useful markers in prostate oncology. For this goal the present study was carried out.

Over the past decade and with the emergence of new technologies, identifying genetic variations, such as Single Nucleotide Polymorphisms (SNPs) offered the possibility of developing a novel biomarker (Botstein *et al*., 1980; Daly *et al*., 2017). Moreover, previous studies found that approximately 30 % of the estimated heritability of PC can be attributed to SNPs and more than 100 of them have been genotyped (Al Olama *et al*., 2014; Broeck *et al.,* 2014; Benafif *et al*., 2018).

2. Materials and Methods

2.1. Patients and Control Subjects

This study consisted of two hospital-based case-control groups: seventy Jordanian patients with PC from the Department of Pathology at the King Abdullah University Hospital (KAUH) (Irbid, Jordan) (mean age = 69.9 ± 9 years) and age-matched (mean age = 6 1.6 ± 12.0 years). The subjects were recruited between September 2017 and February 2018. The histopathological diagnosis was conducted by specialized pathologists according to the TNM staging system (stage I-IV) by the American Joint Committee on C ancer (AJCC). The study protocols were approved by the Jordanian Ministry of Health (CODE: MOH REC 170106) and the Institutional Review Board of the KAUH (IRB number 130/1/2902). A written informed consent was obtained from each recruited participant before enrollment. Information on age, PSA level, Gleason score at diagnosis and other sociodemographic characteristics of the study subjects were obtained through a direct questionnaire survey.

2.2. Cell Lines and Cell Culture

The human PC cell lines (PC3, DU145 and LNCaP) were purchased from American Type Culture Collection (ATCC, Manassas, VA, USA). The cells were maintained and cultured in a DMEM (Dulbecco's modified Eagle's medium; Hyclone, Logan, UT, USA) medium supplemented with a 10 % heat-inactivated fetal bovine serum (FBS), 100 u nits/mL of penicillin, 100µg/mL of streptomycin and 1 % amphotericin B (25µg/mL) (Wel GENE Inc.). The cells were cultured in a humidified atmosphere with 5 % CO_2 at 37°C.

2.3. SNP Selection and Genotyping

DNA was extracted from the blood samples and the cultured cells using a Wizard Genomic DNA Purification Kit (Promega, USA) according to the manufacturer's instructions. All the primers and restriction enzyme used in this study were designed manually. The location and fidelity of restriction enzyme and primers' sequence were checked using the following software:

- http://primer3.ut.ee/,https://genome.ucsc.edu/,
- http://ensembl.org/Homo_sapiens/Gene,
- and http://www.labtools.us/nebcutter-v2-0/.

Primers for rs2269577 SNP were designed: 5′-GTTTCAGGACCGTGGCTATG-3′ (forward primer) and 5′-TCAGTCTGGAAAGCTCTCGG-3′ (reversed primer). A total of 50 ng of genomic DNA was amplified in a 25 µL of a final volume PCR reaction containing 0.4 µM of each primer and 12.5µL of the green master mix (GoTaq®Green Master Mix, Promega, USA). The amplification was performed at 95°C for five minutes with an initial denaturation, followed by thirty-five cycles of 95°C for thirty seconds, 52°C for thirty seconds, and 72°C for thirty seconds, and a final extension of five minutes at 72°C. The amplified fragments of 190 bp of PCR products were digested with the *BstEII* restriction enzyme.

2.4. Sequence Analysis

Primers for Exon1 were designed: 5′-GTTTCAGGACCGTGGCTATG-3′ (forward primer) and 5′-TCAGTCTGGAAAGCTCTCGG-3′ (reversed primer). These primers were designed for flanking the exon 1, as well as 186 bp upstream (containing putative regulatory elements) and 48 bp from intron 1 s equences of XBP1 gene. The products were amplified by polymerase chain reactions (PCR) with a touchdown program (95°C for 5 min; 40 cycles of 95°C for 30 s, 52°C for 30s, 72°C for 30 s, 72°C for 5 min). After amplification, the products were purified using a MEGA quick-spin Total Fragment DNA Purification Kit (Intron, Korea) and directly sequenced on ABI 3730XL DNA Analyzer (Applied Biosystems). All the variants identified by sequence analysis were checked against the dbSNP data (version 129) for determining the novelty of variants, and the novel variants.

2.5. Statistical Analysis

Statistical analyses were conducted using the Statistical Package of the Social Sciences software version 15.0 (SPSS, Inc., Chicago, IL). Comparisons between-group differences in continuous variables were evaluated using the Pearson Chi square and goodness of fit test (P 0 ≤ .05). The association between -116C/G and exon 1 polymorphisms on XBP1and the risk of PC were estimated by odds ratio (OR) with a 95 % confidence interval (95 % CI). Hardy–Weinberg allele frequency percentages for the prostate cancer patients and the control group and allele frequency were calculated according to the following equation: (A) is the major allele and (a) is the minor allele

Frequency of allele A= p = f (AA) + 1/2 (Aa)

Frequency of allele a= q = f (aa) + 1/2 (Aa).

The observed and expected numbers for the healthy control and patients for the -116 C→G mutant genotype (GG) were as follows: (31 and 28.5) and (26 and 28.5), respectively. For the heterozygous genotype (GC), the values were (35 and 35.5) and (36 and 35.5), respectively. For the wild-type genotype (CC), the observed and expected numbers were (4 and 6) as well as (8 and 6) for the control and PC patients, respectively. No significant difference was observed between the actual and expected distributions of the -116 C→G SNP between the PC patients and control (P-value > 0.05).

3. Results

Table 1 s hows the frequencies of the -116 of XBP1 genotypes in patients and controls, and the corresponding odds ratios. Neither the GC, nor the GG genotypes were significantly more frequent in early onset prostate cases than in the controls (OR= 0.514, 95% = CI 0.14-1.86 and 0.419, 95% CI= 0.11-1.55, respectively), while the lowest frequency was for homozygous (CC) genotype (11.43 %)

in PC patients, and (5.7 %) in controls. In this study, possible interactions between the various XBP1 polymorphisms and PC risk have been investigated. There was no evidence of any interaction between the XBP1 genotypes (OR= 0.514, 95 % CI= 0.014-1.86, *P*=0.31).

Table 1. Distribution of genotypes and allelic frequencies among PC patients and control.

XBP1 (-116 G→C) Genotypes	Prostate Cancer Number (%)	Control Number (%)(1)	OR(2)	95% CI(3)	*p*-Value
GG	26 (37.14%)	31 (44.3%)	0.419	0.11 - 1.55	0.193
GC	36 (51.43%)	35 (50%)	0.514	0.14- 1.86	0.311
CC	8 (11.43%)	4 (5.7%)	1.01	0.42 - 2.75	0.099
Allele Frequencies					
G	88 (62.9%)	97 (69.3%)	0.750	0.46 - 1.32	0.26

% (1) = Hardy–Weinberg allele frequency percentages for prostate cancer patients and control group, OR (2) = odd ratio, C.I (3) = confidence interval at 95%.

To explore potential interactions between genes and the environment, the relationship between genotype and the risk of PC at different levels depending on the selected properties was examined. The risk of developing prostate cancer according to the PC patients' variables (age, Gleason score, PSA level, metastasis and treatment) was studied. Results shown in Table 2 reveal that there were no significant differences between the frequencies of genotypes and alleles of XBP1 -116C→G polymorphism and PC patients' variables. Furthermore, no significant difference between the patients' age and genotypes and alleles' frequencies was recorded with p-values of 0.31 and 0.27, respectively. Data presented in Table 2 indicate that the stratification analysis of the PC group on the basis of Gleason score frequencies of the CC+CG genotype and alleles of XBP1 (-116 C→G) polymorphism was not associated with significant increases in Gleason score (*P*-values = 0.14 and 0.99, respectively). Similarly, there was no significant association between the PC patients' PSA level and genotypes and alleles of XBP1 (-116 C→G) frequencies with *P*- values of 0.44 and 0.19, respectively. Chi square analysis for association showed nonsignificant association between the presence or absence of metastasis of PC in patient and the genotypes and alleles of XBP1 (-116 C→G) polymorphism frequencies (*P*-values 0.86 and 0.65, respectively). There was no significant difference between GG, GC and CC genotypes and C, G allele frequencies according to the treatment type in the PC patients and control group with *P*- values of 0.58 and 0.32, respectively

Table 2 Association between the frequencies of genotypes and alleles of XBP1 -116C→G polymorphisms and prostate patients' variables.

	rs2269577 Genotypes				rs2269577 Allele Frequencies		
Variable	GG Number (%)	GC Number (%)	CC Number (%)	*p*-value	C (%)	G (%)	*p*-value
PC Patient's Age							
40-60	4 (15.4%)	9 (25%)	1 (12.5%)		11 (39.3%)	17 (60.7%)	
61-80	22 (84.6%)	23 (63.9%)	6 (75%)	0.31	35 (34.3%)	67 (65.7%)	0.27
>80	0 (0%)	4 (11.1%)	1 (12.5%)		6 (60%)	4(40%)	
PC Patient's Gleason Score							
5-6	5 (22.7%)	14 (38.9%)	1 (12.5%)		16 (40%)	24 (60%)	
7-8	12 (54.6%)	11 (30.6%)	6 (75%)	0.14	23 (39.7%)	35 (60.3%)	0.99
9-10	5 (22.7%)	11 (30.6%)	1 (12.5%)		13 (38.3%)	21 (61.7%)	
PC Patients' PSA Level							
0.0-4.0	10 (40%)	17 (51.5%)	5 (62.5%)		27(55.1%)	37 (44.6%)	
4.1-10.0	7 (28%)	5 (15.2%)	0 (0%)	0.44	5 (10.2%)	19 (22.9%)	0.19
>10.0	8 (32%)	11 (33.3%)	3 (37.5%)		17 (34.7%)	27 (32.5%)	
PC Patient's Metastasis Status							
Yes	5 (20.8%)	6 (17.7%)	1 (12.5%)	0.86	8 (33.3%)	16 (66.7%)	0.65
No	19 (79.2%)	28 (82.3%)	7 (87.5%)		42 (38.9%)	66 (61.1%)	
PC Patients' Treatment							
Hormonal Therapy	15(62.5%)	23(67.6%)	6 (75%)		35 (39.8%)	53 (60.2%)	
Hormonal & Chemo/ Radiotherapy	6 (25%)	6 (17.7%)	0 (0%)	0.58	6 (25%)	18 (75%)	0.32
Radical Prostatectomy	3 (12.5%)	5 (14.7%)	2 (25%)		9 (45%)	11 (55%)	

Figures 1and 2 show the *BstEII*-digested products of the DNA from the subjects and cell lines, respectively, electrophoresed on 3 % high-resolution agarose gel. Three types of bands, namely 190 bp, 103 bp and 87 bp are resolved. The two bands of 103 bp and 87 bp signify the normal CC genotype; three bands of 190 bp, 103 bp and 87 bp indicate the heterozygous CG genotype, while the 190 bp indicates the mutant GG genotype.

To identify prostate susceptibility-related genetic variants, sixty-six of the PC subjects and control subjects were screened for mutations in XBP1 exon1 by direct nucleotide sequencing. The sequencing analysis revealed no noteworthy mutation.

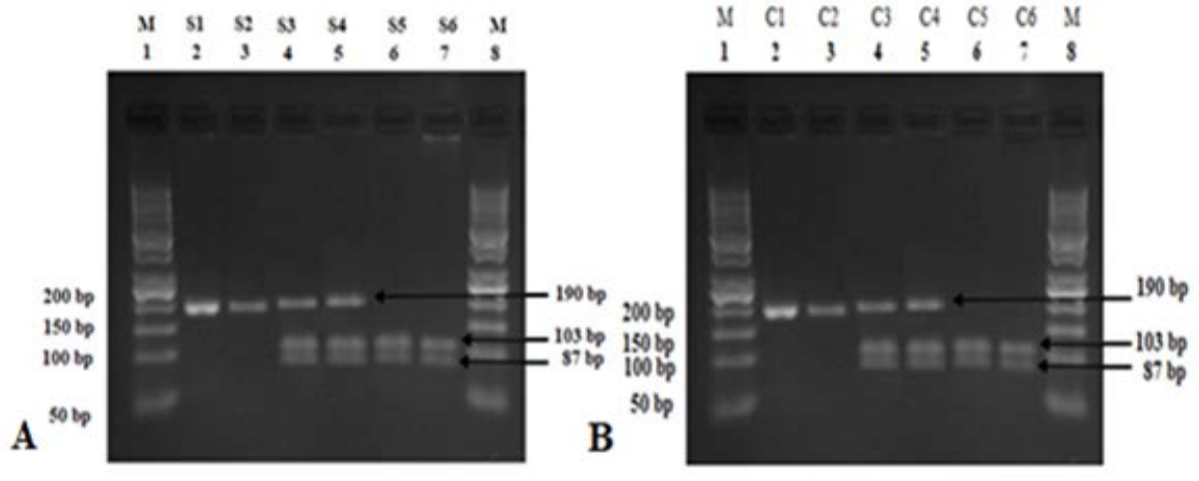

Figure 1. PCR-RFLP analysis of XBP1 (-116C→G) SNP. A. The *BstEII*-digested products of the DNA from Prostate cancer subjects (PC). Samples separated by 3 % agarose gel electrophoresis. Lane 1:50 bp DNA ladder. The remaining lanes (S1 through S6) represent the *BstEII* digested PCR products of PC samples. B. Control samples separated by 3 % agarose gel electrophoresis. Lane 1:50 bp DNA ladder. The remaining lanes (C1 through C6) represent the digested PCR products of control samples. The two bands of 103 bp and 87 bp signify the normal CC genotype; three bands of 190 bp, 103 bp and 87 bp indicate the heterozygous CG genotype, while the 190 bp indicates the mutant GG genotype.

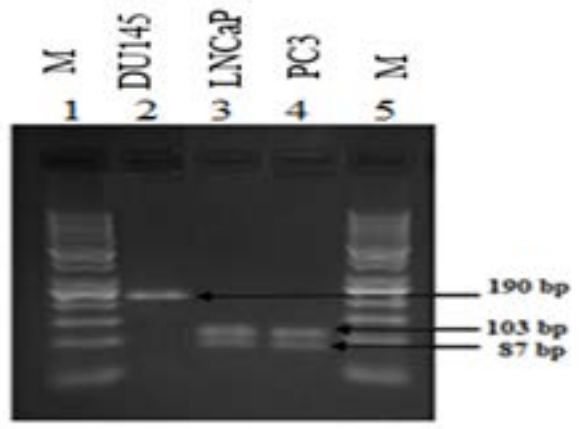

Figure 2. PCR-RFLP analysis of XBP1 (-116C→G) SNP of PC cell lines. The *BstEII*-digested products of the DNA from cell lines were separated by 3% agarose gel electrophoresis. Lane 1:50 bp DNA ladder. Lane 2: DU145 cell line. Lane 3: LNCaP cell line. Lane 4: PC3 cell line. The genotypic analysis of the three cell lines shows that the genotype of the DU145 was GG, while the genotype CC appeared in both LNCaP and PC3 cell lines.

4. Discussion

This study is an attempt to identify PC susceptibility genes and variants as reliable biomarkers associated with the increased cancer risk that has been challenging and unsuccessful (Wallis and Nam, 2015; Alvarez-Cubero *et al.,* 2016; Lynch *et al*., 2016).

An increasing number of SNPs had been suggested to be implicated in the development and progression of PC (Broeck *et al*., 2014). However, studies are not directly comparable because of the different classifications of the disease risk and different Prostate specific antigen (PSA) levels used (Colicchia *et al*., 2017).

rs2269577 (C→G) is a promoter variant and a disease-causing mutation of XBP1 that exerts functional effects on XBP1 activity itself therefore resulting in an abnormal XBP1 expression, which can be involved in an abnormal splicing and DNA damage that might affect the clinical outcome in PC patients (Knight, 2003). Recently, association studies in cancer have focused on several candidate genes. The present study is focused upon the XBP1 gene. It could not prove any statistically significant difference in the genotypic frequency of the (−116 C/G) polymorphism between the PC patients and control group. Moreover, the results of the current study did not find any significant association between rs2269577 genetic variations on the XBP1 gene and patients' age, presence or absence of metastasis, Gleason score, PSA level and treatment type. XBP1 is a cr itical transcription factor induced by ER stress as a major regulator of the unfolded protein response (UPR). There are few reports about the incidence of promoter mutations in several diseases including Alzheimer (Liu *et al*., 2013), the bipolar disorder (Masui *et al*., 2006), diabetes (Liu *et al*., 2015), inflammatory bowel diseases (Kaser *et al*., 2008), psychiatric illnesses (Cheng *et al*., 2014), multiple myeloma (Carrasco *et al*., 2007), and schizophrenia (Jonsson *et al*., 2006). A previous study (Hou *et al*., 2004) which is consistent with the results of the present study, observed no r elationship between XBP1 (-116C→G) polymorphism and the bipolar disorder when normal controls were compared with bipolar disorder patients. These results support many studies on various populations with different disorders who could not find a strong correlation of this polymorphism. One possible explanation for the inconsistencies among different population groups is the ethnic characteristics. In addition, they are likely to be due to a number of factors including social and environmental factors as well as hereditary genetics. (Tanaka *et al*., 2001; Benafif *et al*., 2018).

To the best of the authors' knowledge, this is the first study to be conducted on men using SNPS in the XBP1 gene. It does not provide evidence that (C-116G) polymorphism in this gene is significantly associated with a high risk of PC. However, this study has the advantage of being conducted on a homogeneous population of the same ethnicity. This excludes the influences on allele sequences that may arise from different ethnic groups.

However, there are several limitations to be considered in the interpretation of the results of this study. First, it is limited by time and geographical factors: all subjects were recruited from a single institution, and the sample size was relatively moderate, which has limited the study to the common variants. The authors have been faced with several instrumental and administrative routine applications and reluctance in collaboration from a number of public and private hospitals. Thus, the investigated population may not be representative because the issue of selection bias cannot be ruled out due to hospital-based controls. To limit the potential selection bias, the authors recruited samples by matching the controls to the cases based on age. The use of blood donors as population controls has been criticized on the grounds that blood donors differ from the general population in several factors, including their medical history and the medical histories of their parents (Golding *et al*., 2013). This might introduce a bias in the interpretation of the results and lead to spurious disease associations. It is true that in Jordan, male blood donors have not been screened for PC, and their family history of the disease also is unknown. Therefore, these donors may be affected with PC later in life or carry variants with reduced penetrance that is associated with the disease. The collection of control samples from people with an assessed medical history is often not feasible for individual research groups, as it is both time-consuming and expensive. While blood donors may not optimally represent the genomic constitution of the general population, they do, however, provide a set of controls that is readily available. To reduce the bias for accuracy, sufficiently large numbers of controls should be analyzed. Second, no information on other factors such as occupational exposure and certain dietary components was available in our research; these variables might interact with XBP1 genotypes or act as potential confounding factors.

5. Conclusions

This is the first study to be conducted on men using SNPS in the XBP1 gene. It does not provide evidence that (– C-116G) allele in this gene is significantly associated with a high risk of PC. Although no mutations in the exon1 of the XBP1 were found, there may be other mutations in XBP1 that may have beneficial, deleterious, or neutral effects, depending on their location in the gene. However, since this study does not include the whole gene, further studies should be conducted to analyze the whole gene in order to identify other genetic alterations that can help determine an effective treatment plan.

Acknowledgments

We thank all the participants who took part in this research. This work was financially supported by the Deanship of Scientific Research and Graduate Studies at Yarmouk University under grant number (28/2015).

Conflict of Interest

The authors declare that they have no c onflicts of interest.

References

Alberti C. 2010. Hereditary/familial versus sporadic prostate cancer: Few indisputable genetic differences and many similar clinicopathological features. *Eur Rev Med Pharmacol Sci.* **14**: 31-41.

Al Olama AA, Kote-Jarai Z, Berndt SI, Conti DV, Schumacher F, Han Y, *et al.* 2014. A meta-analysis of 87,040 individuals identifies 23 new susceptibility loci for prostate cancer. *Nat Genet.* **46**:1103–1109.

Alvarez-Cubero MJ, Pascual-Geler M, Martinez-Gonzalez LJ, Alvarez JC, Lorente JA and Cozar JM . 2016. Association between RNASEL, MSR1, and ELAC2 single nucleotide polymorphisms and gene expression in prostate cancer risk. *Urol Oncol*. **34**:431.e1-8.

Benafif S, Kote-Jarai Z and Eeles R. 2018. A Review of prostate cancer Genome-Wide association studies (GWAS). *Cancer Epidemiol Biomarkers Prev*. doi:10.1158/1055-9965.EPI-16-1046.

Botstein D, White RL, Skolnick M and Davis RW. 1980. Construction of a genetic linkage map in man using restriction fragment length polymorphisms. *Am J Hum Genet*. **32**:314-331.

Broeck T, Joniau S, Clinckemalie L, Helsen C, Prekovic S, Lien Spans L, et al. 2014.The role of single nucleotide polymorphisms in predicting prostate cancer risk and therapeutic decision making. *Biomed Res Int*. **2014**: 16 pages.

Carrasco DR, Sukhdeo K, Protopopova M, Sinha R, Enos M, Carrasco DE, *et al*. 2007. The differentiation and stress response factor XBP-1 drives multiple myeloma pathogenesis. *Cancer Cell*. **11**: 349-360.

Cheng D, Zhang K, Zhen G, and Xue Z. 2014. The -116C/G polymorphism in XBP1 gene is associated with psychiatric illness in Asian population: A meta-analysis. *Am J Med Genet B Neuropsychiatr Genet.* **165 B**: 665-672.

Colicchia M, Morlacco A, Cheville JC and Karnes RJ. 2017. Genomic tests to guide prostate cancer management following diagnosis. *Expert Rev Mol Diagn*. **17**:367–377.

Corazzari M, Gagliardi M, Fimia GM and Piacentini M. 2017. Endoplasmic reticulum stress, unfolded protein response, and cancer cell fate. *Front Oncol*. **7**: 78.

Daly MB, Pilarski R, Berry M, Buys SS, Farmer M, Friedman S, *et al.* 2017. NCCN Guidelines Insights: Genetic familial high-risk assessment: Breast and ovarian (Version2.2017). *J Natl Compr Canc Netw*. **15**:9-20.

Doultsinos D, Avril T, Lhomond S, Dejeans N, Guédat P and Chevet E. 2017. Control of the unfolded protein response in health and disease. *SLAS Discov*. **22** (7): 787-800.

Giri VN, Knudsen KE, Kelly WK, Abida W, Andriole GL, Bangm, CH, *et al*. 2018. Role of genetic testing for inherited prostate cancer risk: Philadelphia Prostate Cancer Consensus Conference 2017. *J Clin Oncol*. **36** (4):414-424.

Golding J, Northstone K, Miller LL, Davey Smith G and Pembrey M. 2013. Differences between blood donors and a population sample: implications for case-control studies. *Int J Epidemiol*. **42**:1145-1156.

Hou SJ, Feng-Chang Y, Cheng CY, Tsai SJ and Hong CJ. 2004. X-box binding protein 1 (XBP1) C-116G polymorphisms in bipolar disorders and age of onset. *Neurosci. Let*. **367**: 232–234.

Jonsson EG, Cichon S, Schumacher J, Jamra RA, Schulze TG, Deschner M, *et al.* 2006. Association study of a functional promoter polymorphism in the XBP1 gene and schizophrenia. *Am J Med Genet*. **141B**: 71–75.

Kaser A, Lee AH, Franke A, Glickman JN, Zeissig S, Tilg H, *et al*. 2008. XBP1 links ER stress to intestinal inflammation and confers genetic risk for human inflammatory bowel disease. *Cell.* **134**: 743-756.

Knight JC. 2003. Functional implications of genetic variation in non-coding DNA for disease susceptibility and gene regulation. *Clin Sci*. **104**: 493-501.

Kral M, Rosinska V, Student V, Grepl M, Hrabec M and Bouchal J. 2011. Genetic determinants of prostate cancer: Areview. *Biomed Pap Med Fac Univ Palacky Olomouc Czech Repub*. **155**:3-9

Lichtenstein P, Holm NV, Verkasalo PK, Iliadou A, Kaprio J, Koskenvuo M, *et al*. 2000. Environmental and heritable factors in the causation of cancer—Analyses of cohorts of twins from Sweden, Denmark, and Finland. *N Engl J Med*. **343**:78-85.

Liu S, Ma G, Yao S, Chen Z, Wang C, Zhao B, *et al*. 2015. Polymorphism - 116C/G of the human X box binding protein 1 gene is associated with risk of type 2 diabetes in a Chinese Han population. *Gene*. **575**:71-74.

Liu S, Wang W, Cai ZY, Yao LF, Chen ZW, Wang CY, *et al*. 2013. Polymorphism -116C/G of human X-box-binding protein 1 promoter is associated with risk of Alzheimer's disease. *CNS Neurosci Ther*. **19**:229-234.

Lynch HT, Kosoko-Lasaki O, Leslie SW, Rendell M, Shaw T, Snyder C, *et al*. 2016. Screening for familial and hereditary prostate cancer. *Int J Cancer*. **138**: 2579–2591.

Masui T, Hashimoto R, Kusumi I, Suzuki K, Tanaka T, Nakagawa S, *et al*. 2006. A possible association between the− 116C/G single nucleotide polymorphism of the XBP1 gene and lithium prophylaxis in bipolar disorder. *Int J Neuropsychopharmacol*. **9**: 83-88.

Moore K and Hollien J. 2015. Ire1-mediated decay in mammalian cells relies on mRNA sequence, structure, and translational status. *Mol Biol Cell*. **26**(16):2873-2884.

Pishgar F, Ebrahimi H, Moghaddam SS, Fitzmaurice C and Amini E. 2018. Global, regional and national burden of Prostate cancer, 1990 to 2015: Results from the global burden of disease study 2015. *J Urol*. **199** (5):1224-1232.

Siegel RL, Miller KD and Jemal A. 2018. Cancer statistics, 2018. *CA Cancer J Clin*. **68**:7-30.

Tanaka K, Sugiura H, Uehara M, Hashimoto Y, Donnelly C and Montgomery DS. 2001. Lack of association between atopic eczema and the genetic variants of interleukin-4 and the interleukin-4 receptor α chain gene: heterogeneity of genetic backgrounds on immunoglobulin E production in atopic eczema patients. *Clin Exp Allergy*. **31:** 1522-1527.

Tao ZQ, Shi AM, Wang KX and Zhang WD. 2015. Epidemiology of prostate cancer: Status. *Eur Rev Med Pharmacol Sci*. **19**: 805-812.

Wallis CJD and Nam RK. 2017. Prostate cancer genetics: A Review. *EJIFCC.* 2015; **26**: 79–91.

World Health Organization (WHO). Age Adjusted Death Rate Estimates.

JJBS

Volume 12, Number 5,December 2019
ISSN 1995-6673
Pages 609 - 616

Jordan Journal of Biological Sciences

Molecular Identification and Inter-Simple Sequence Repeat (ISSR) Differentiation of Toxigenic *Aspergillus* Strains

Rasha G. Salim[1*], Soher E-S. Aly[2], Nivien A. Abo-Sereh[1], Amal S. Hathout[2] and Bassem A. Sabry[2]

[1]*Department of Microbial Genetics,* [2]*Department of Food Toxicology and Contaminants, National Research Centre, 33El Bohouth St, Dokki, P.O.Box12622, Giza, Egypt*

Received February 3, 2019; Revised March 27, 2019; Accepted April 1, 2019

Abstract

The *Aspergillus* genera are one of the most abundant and widely distributed fungi. Among the *Aspergillus* genera are *A. parasiticus*, *A. flavus*, which produces aflatoxins, *A. ochraceus*, and *A. niger* that can produce ochratoxin A. Therefore, the aim of this study is to perform molecular identification and differentiation using the ISSR technique to the *Aspergillus* species, and study the ability of fungal isolates to produce mycotoxins. The ISSR markers are used in the analysis of the genetic similarity of *Aspergillus* isolated from peanuts. Data show the ability of the isolated *A. flavus*, and *A. parasiticus* to produce aflatoxins, whereas *A. ochraceus* produced ochratoxin A. To analyze the genetic similarity among the different fungal isolates, a total of 165 full bands were scored from the amplified products with the ten ISSR primers; 116 bands were polymorphic, and forty-one were unique bands with an average range size of (143-1939) bp. The similarity matrix between the isolated fungi revealed that the isolates *A. parasiticus* and *A. niger* showed the highest similarity (59 %). The ISSR molecular markers are an extremely valuable means to characterize the genetic similarity of the *Aspergillus* genera.

Keywords: *Aspergillus* fungi, Mycotoxins, PCR, ISSR , Internal transcribed spacer

1. Introduction

The growth of several fungi in different agricultural crops leads to a decrease in the yield and quality with major economic losses (Richard, 2007; Adejumo and Adejoro, 2014). Among these fungi is *Aspergillus,* which is one of the most economically important genera, as foods, plants, and soils are commonly inhabited by the majority of these species (Yu *et al*., 2005). The excessive occurrence of *Aspergillus* isolates is considered significant since these species are well-known to produce several mycotoxins (Sahab *et al*., 2014).

Aflatoxins (AFs) are among the most potent mycotoxins produced by the toxigenic strains of *Aspergillus flavus* and *A. parasiticus* (Ashiq, 2015). Meanwhile, ochratoxin A (OTA) is produced by several genera of the *Penicillium* and *Aspergillus* species including *A. ochraceus* (Aly *et al*., 2012). Aflatoxins have been classified as group one human carcinogen (IARC, 2012). Moreover, OTA is classified as group 2B, that is possible human carcinogens (IARC, 2002). Territrems produced by *A. terreus*, induce acute toxicities such as tremor, as well as hepatocellular and nephrotoxic damage in rats and mice (Abdalla *et al*., 1998).

Morphological parameters including colony diameter, color and texture, size, and texture of conidia and hypha structure are traditional strategies for fungal species identification. Nevertheless, due to the intensive divergence of the morphological characters created by a high level of genetic variability, each inter-and intraspecific fungal species classification may be difficult (Kumeda and Asao, 2001). In spite of numerous investigations, the taxonomy of fungi is still highly complex. To minimize the problem, the genetic methods help determine the level of polymorphism and similarity amongst fungal strains.

From their DNA sequences, taxonomy, population structure, and the epidemiology associated with fungi, molecular biology have presented numerous insights into the detection and genetic relationships of fungal isolates (Paplomatas, 2004). The 18S rRNA gene, mitochondrial DNA, the intergenic spacer region, and the internal transcribed spacer (ITS) regions are targets for the genus level detection of *Aspergillus*. For the appropriate detection of pathogens at the species level, the ribosomal RNA (rRNA) genes in ribosomal DNA possess the characteristics (O´Donnell, 1992). These rDNA sequences show a variety of conserved and different regions within the genome that are highly stable (Bruns *et al*., 1991). They each consist of the 18S small subunit (SSU), the 5.8S, and the 28S large subunit (LSU) genes, and occur in multiple copies with up to 200 copies per haploid genome arranged in tandem repeats (Paplomatas, 2004). To amplify the entire 5.8S rRNA gene, ITS primers 1 and 4, ITS regions I and II, and a portion of the 18S small-subunit rRNA gene have been used.

* Corresponding author e-mail: rasha_gomma@yahoo.com.

Recently, the development of molecular biology tools and technologies has enormously progressed (Frankham *et al*., 2002). Consisting of several simple sequence repeats, the inter-simple sequence repeat (ISSR) is established on closely-spaced microsatellites by primers (25-30 bp) and the amplification of regions (100-3000 bp) between inversely-oriented microsatellites (Reischl and Lohmann, 1997). These primers that are abundant throughout the eukaryotic genome and grow fast are annealed to simple-sequence repeats (microsatellites) (Morgante *et al*., 2002). However, primers that work for one may not work for another, since there is a l ot of diversity among fungi. Therefore, the ISSR primers need to be enhanced for each fungal species (Klaassen, 2009).

The ISSR technology has been used to characterize gene tagging (Ratnaparkhe *et al*., 1998), phylogenetic studies (Dutech *et al*., 2007), population genetic structure (Hadrich *et al*., 2010), genome mapping (Chakravarty, 2011), genetic structure (Rampersad, 2013; Gramaje *et al*., 2014), genetic diversity (Mahmoud *et al*., 2014), and fingerprinting (Priyanka *et al*., 2014) in plant-pathogenic fungi. Therefore, the aim of this study is to perform molecular identification and differentiation using the ISSR technique to *Aspergillus* species, and to study the ability of fungal isolates to produce mycotoxins.

2. Materials and Methods

2.1. Fungal Strains

Aspergillus flavus, *A. parasiticus*, *A. niger*, *A. ochraceus* and *A. terreus* were used in this study. They were isolated from peanut (*Arachis hypogaea*) samples as mentioned previously (Aly *et al*., 2018).

2.2. Ability of Fungal Isolates to Produce Mycotoxins

One mL of each of the fungal spore suspensions were transferred into a 250 mL flask containing 100 mL of yeast extract broth (yeast extract 2 %-Sucrose 20 %). The cultures were incubated for seven days at 28°C. Aflatoxins, ochratoxin A, and territrems were extracted using chloroform. The chloroform extracts were evaporated under nitrogen gas, and the residue was dissolved in methanol and passed at a r ate of about 1-2 drops/second through immunoaffinity column (C_{18}). The immunoaffinity column was washed twice with 10 mL of purified water at a r ate of about two drops/second. Using 1.0 mL of methanol, elution was performed and analyzed by HPLC.

The HPLC system used for mycotoxin analyses is an Agilent 1200 series system (Agilent, Berks, UK) with a fluorescence detector (FLD G1321A), an autosampler ALS G1329A, FC/ALS thermal G1330B, Degasser G1379B, Bin Bump G1312A,and a C_{18} (Phenomenex, Luna 5 m icron, 150 × 4.6 mm) column joined to a pre-column (security guard, 4 × 3-mm cartridge, Phenomenex Luna). The acetonitrile/water/methanol (1/6/3 v/v/v) mobile phase was used for the separation of AFs at a flow rate of 1.0 mL/min, and at ambient temperature. The cetonitrile/water/acetic acid (99/99/2 v/v/v) mobile phase was used for the separation of ochratoxin A(OTA).

Spots were applied on T hin Layer Chromatography plates (Aluminum plate of silica gel $60F_{254}$, Merck No. 5554) for the determination of territrems, and benzene-ethyl acetate (65:35 v/v) was used for the development of plates.

2.3. Molecular Identification of Toxigenic Fungi

2.3.1. Extraction of Genomic DNA

Using the Qiagen Kit (Qiagen Sciences, Maryland, USA), the extraction of genomic DNA was performed by following the manufacturer's instruction manual cat. No 69104.

2.3.2. PCR Amplification of ITS Region

To amplify the ITS gene from the fungal isolates, the PCR reactions were done. Using the primer set; ITS1 (5-CTTGGTCATTTAGAGGAAGTAA-3) and ITS4 (5-GCTGCGTTCTTCATCGATGC-3), the ITS region was amplified with some modification (White *et al*., 1990). The PCR cycles consisted of an initial denaturation step for five minutes at 94°C followed by thirty-five cycles of denaturation for thirty seconds at 94°C, annealing for one minute at 55°C, and amplification for two minutes at 72°C, with a final extension step for five minutes at 72°C. On a 1 % agarose gel by electrophoresis in 1X TBE buffer (Tris-borate EDTA, pH 8.0), the amplification products for the ITS locus were separated using a 100-bp ladder DNA marker (Invitrogen, California, USA). The gel was visualized and photographed using ™XR + Gel Documentation System (Bio-Rad, California 94547, USA).

2.4. Molecular Differentiation of Isolated Fungi Using ISSR Technique

Ten ISSR primers were used in the detection of polymorphism among five isolated fungi. These primers were synthesized by Metabion Corporation, Germany. The primers' code and nucleotide sequences are presented in Table 1. With some modifications, the PCR amplification reactions were carried out (Williams *et al*., 1990). Reactions were performed in a 25 µL volume composed of 1x reaction buffer, 0.2 mM of dNTPs, 1.5 mM $MgCl_2$, 0.2 µM of primer, 0.5 unit of Taq polymerase (Qiagen Sciences, Maryland, USA), and 50 ng of template DNA, in sterile distilled water.

Table 1. Name and Sequence of the Primers used in the ISSR analysis

Primer	Sequence
ISSR- 1	5'-AGAGAGAGAGAGAGAGYC-3'
ISSR- 2	5'-AGAGAGAGAGAGAGAGYG-3'
ISSR- 3	5'-ACACACACACACACACYT-3'
ISSR- 4	5'-ACACACACACACACACYG-3'
ISSR- 8	5'-ACACACACACACACACYA-3'
ISSR- 11	5'-ACACACACACACACACYC-3'
ISSR- 12	5'-AGAGAGAGAGAGAGAGYT-3'
ISSR- 13	5'-CTCCTCCTCCTCCTCTT-3'
ISSR- 15	5'-CTCTCTCTCTCTCTCTRG-3'
ISSR- 16	5'-TCTCTCTCTCTCTCTCA-3'

The ISSR-thermocycling profile and the PCR amplification of the DNA have been performed in a Perkin Elmer thermal cycler 9700. The temperature profile in the different cycles was as follows: an initial strand separation cycle for five minutes at 94°C followed by forty cycles comprised of a denaturation step for one minute at 94°C, an annealing step for one minute at 45°C and an extension

step for 1.5 minute at 72°C. The final cycle was a polymerization cycle for ten minutes at 72°C.

PCR products were mixed with a 5 µL gel loading dye and resolved by electrophoresis in a 1.5 % agarose gel containing ethidium bromide (0.5 mg/mL in 1 x TBE buffer at 120 v olts). A 100bp DNA ladder was used as molecular-size standard. The PCR products were visualized under UV light, and documented using a ™XR+ Gel Documentation System (Bio-Rad, California 94547, USA).

2.4.1. PCR Fragment Purification

According to the manufacturer's instructions, the PCR products were eluted from agarose gels using Promega®'s Wizard® SV Gel and PCR Clean-Up System.

2.4.2. Data Analysis

The amplified fragments were scored as present (1) or absent (0). Ladder 100 bp DNA was used to identify the molecular weights of fragments. Among the fungal isolates, the similarity matrix was calculated according to Coelho (2001). According to Rohlf (1993), the Unweighted Pair-Group Method with Arithmetical average (UPGMA) were used to design the dendrogram for the similarity coefficient.

3. Results and Discussion

3.1. Ability of Fungal Isolates to Produce Mycotoxins

Fifty fungal isolates, mainly (25) *Aspergillus flavus*, (8) *A. parasiticus*, (8) *A. niger*, (5) *A. ochraceus*, and (4) *A. terreus* were isolated from peanut (*Arachis hypogaea*) samples as mentioned previously (Aly *et al*., 2018). Data in Table 2 show that six out of twenty-five *A. flavus* isolates and four out of eight *A. parasiticus* isolates produced AFs with a percentage of contamination reaching 24.00 and 50.00 % respectively. It was noticed that *A. parasiticus* produced higher concentrations of four types of aflatoxins i.e. AFB_1, AFB_2, ABG_1, and AFG_2 at the concentrations of 53.329, 5.442. 31.746 and 8.408 ppb respectively (Table3). Similarly, *Aspergillus flavus* produced the four types of aflatoxins i.e. AFB_1, AFB_2, AFG_1 and AFG_2 at the concentrations of 1.499, 0.428, 0.806, and 0.452 ppb respectively. *A. ochraceus* produced ochratoxin A at the concentration of 2.775 ppb. Table 3 also shows that *A. niger* and *A. terreus* were not able to produce OTA or territrems, respectively.

The results of this study are in agreement with Sahab *et al*. (2011) who determined that both *A. flavus* and *A. parasiticus* produced AFB_1. Similar observations were reported by Sabry *et al*. (2016) who found that out of fifty *A. parasiticus* isolates, fourteen isolates were able to produce AFB_1. Recently, Al-Hindi *et al*. (2017) reported that 15.4 % of *A. flavus* and 55.0 % of the *A. parasiticus* isolates produced AFB_1 in concentrations ranging from 1.6 to 12.4 and from 3.4 to 7.9µg/L respectively. The production of high concentrations of AFB_1 by *A. parasiticus* is highly dangerous as it is considered the most potent carcinogen that causes mycotoxicoses to human and animals (Pildain *et al*., 2008).

Table 2. The ability of isolated fungi to produce mycotoxins.

Fungal Isolates	Mycotoxins	No. of fungal isolates	No. of positive isolates	%
A.flavus	Aflatoxins	25	6	24.00
A.parasiticus	Aflatoxins	8	4	50.00
A.niger	Ochratoxin A	8	0	0.00
A.ochraceus	Ochratoxin A	5	2	40.00
A terreus	Territrems	4	0	0.00

Table 3. Mycotoxin concentration (ppb)**.**

Fungi	Mycotoxin concentration (ppb)						
	AFB_1	AFB_2	AFG_1	AFG_2	OTA	TRA	TRB
Aspergillus flavus	1.499±0.758	0.428±0.342	0.806±0.530	0.452±0.426	-	-	-
Aspergillus parasiticus	53.329±3.173	5.442±3.295	31.746±1.560	8.408±1.486	-	-	-
Aspergillus ochraceus	-	-	-	-	2.775±0.264	-	-
Aspergillus niger	-	-	-	-	ND	-	-
Aspergillus terreus	-	-	-	-	-	ND	ND

AFB_1: Aflatoxin B_1; AFB_2: Aflatoxin B_2; AFG_1: Aflatoxin G_1; AFG_2: Aflatoxin G_2; OTA: Ochratoxin A; TRA: Territrems A; TRB: Territrems B. Results are mean ±SD;ND: Not detected

3.2. Molecular Identification of Toxigenic Fungi

For the species-level identification of fungi, the ITS region is the official DNA barcoding marker. To identify fungal species, DNA barcoding systems employ a short standardized region (between 400 and 800 base pairs). For all the isolated fungal strains, the ITS amplification products using the ITS1 and ITS4 primers with a unique band ranging from 500-600 bp were obtained (Figure 1). The amplicons of ITS regions were column-purified and sequenced using a set of primers. The ITS region sequences were aligned using blast algorithm (http://www.ncbi.nlm.nih.gov/ blast/Blast.cgi) and compared with the published sequences of the ITS region gene of several fungi (Table 4). The first fungal isolate of the sequenced 18S rRNA gene was identified as *Aspergillus ochraceus* with a (98 %) similarity with the *Aspergillus ochraceus* isolate Nitaf 24 (Figure 2). The second fungal isolate of the sequenced 18S rRNA gene was identified as *Aspergillus flavus* with a (99 %) similarity with the *Aspergillus flavus* strain UOA/HCPF 5774 (Figure 3). The high similarity between the fungal strains and their closest phylogenetic relatives indicates that the 18S rRNA gene sequence data are helpful for the identification of fungi. The gene sequence was deposited in GenBank database as *Aspergillus ochraceus* Egy2 (Accession No. LC360803.1) and *Aspergillus flavus* Egy3. (Accession No. LC368455.1). Data in Figures 2 and 3 display the phylogenetic tree based on t he ITS region sequences, showing the relationship between fungal

isolates and other species. The tree was constructed using the neighbor-joining method.

The results of this study confirm the importance of using molecular methods such as DNA barcoding systems (ITS region) for typing newly-isolated microorganisms. The phenotypic and genotypic methods are part of the first step of the identifications and selection of potential fungal isolates. These results are in agreement with Henry *et al*. (2000) who identified *Aspergillus* at the species level using the 18S and 28S rRNA genes for primer binding sites, to differentiate it from other true pathogenic and opportunistic molds.

The connected ITS region, ITS 1-5.8S-ITS 2, from documented strains and clinical isolates of Aspergilli and different fungi, were amplified, sequenced, and compared with non-reference strain sequences in GenBank. The ITS amplification of the genus *Aspergillus* species ranged from 565 to 613 bp. Similarly, Okoth *et al*. (2018) used ITS to identify and analyze polymorphism in the *A. flavus* ITS region.

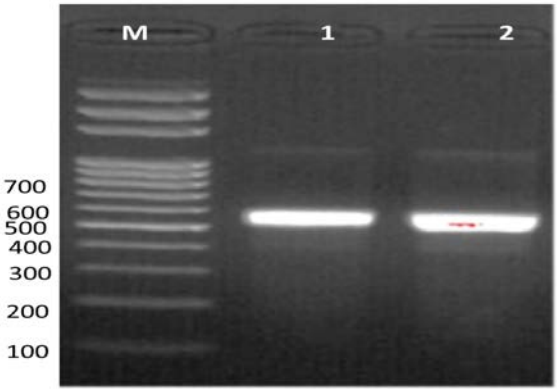

Figure 1. PCR amplification of 18S *rRNA* gene and ITS region ; Lane M: Gene Ruler DNA Ladder 100 bp, Lane 1: 18S *rRNA* gene and ITS region of the isolate *Aspergillus ochraceus*, Lane 2: 18S *rRNA* gene and ITS region of the isolate *Aspergillus flavus*.

Table 4. The nucleotide sequence of two fungal isolates.

Strain	Aligned Sequence Data
Aspergillus ochraceus	CGCGGCGCGCCCCCCCCCCGCCCCCCCGATTCACCCATTTATACCTCCAAACACCCCTTGACCCAAAAAATGC GCGCCTTTGTTCCGGGGGGGTGCGCGCGCTCAACTTTCCTTTCCTTAAGGGGAAACCCTGCGGAAGGATCATT ACTGAGTGAGGGTCCCTCGGGGCCCCAAACCTCCCCACCCCGTGGTATACCGTACCTTGTTGCTTCGGGCGAG CCCCGCCCCCTTTTTTCTTTTAGGGGGCACAGCGCTCGCCGGAGACACCAACGTGAACACTGTCTGAAGTTTT GTCGTCTGAGTCGATTGTATCGCAATCAGTTAAAACTTTCAACAATGGATCTCTTGGTTCCGGCATCGATGAA GAACGCAGCGAAATGCGATAATTAATGTGAATTGCAGAATTCAGTGAATCATCGAGTCTTTGAACGCACATT GCACCCCCTGGTATTCCGGGGGGTATGCCTGTCCGAGCGTCATTGCTGCCCTCAAGCACGGCTTGTGTGTTGG GTCGTCGTCCCCCCCCCAGGGGGACGGGCCCGAAAGGCAGCGGCGGCACCGCGTCCGGTCCTCGAGCGTATGG GGCTTTGTCACCCGCTCTTGTAGCCCGGCCGGCTGCTGGCCGACGCTGAAAAGCAACCAACTATTTTCCAGGG GACCTCGGATCAGGTAGGATACCCGCTGAATTAGG
Aspergillus flavus	GTGTAACCTGCAGCATGATTCATTACCGAGTGGTAGGGTTCCTTAGCGAGCCCAACCCTCCCCACCCCGTGTT TACTGTACTTTAATTGCTTCGGCGGGCCCCGCCCATTCATGGCCGCCCGGGGGTTTCAGCCCCGGGCCCCGCG CCCCGCCGGAGACACCACGAACTCTGTCTGATCTAGTGAAGTCTGAGTTGATTGTATCGCAATCAGTTAAAAC TTTCAACAATGGATCTCTTGGTTCCGGCATCGATGAAGAACGCAGCGAAATGCGATAACTAGTGTGAATTGCA GAATTCCGTGAATCATCGAGTCTTTGAACGCACATTGCGCCCCCTGGTATTCCGGGGGGCATGCCTGTCCGAG CGTCATTGCTGCCCATCAAGCACGGCTTGTGTGTTGGGTCGTCGTCCCCTCTCCGGGGGGGACGGGCCCCAAA GGCAGCGGCGGCACCGCGTCCGATCCTCGAGCGTATGGGGCTTGTCACCCGCTCTGTAGGCCCGGCCGGCGCT TGCCGAACGCAAATCAACTTTCCAGGTTGACCTCGGATCAGGTAGGGAACCCGTGATTAGG

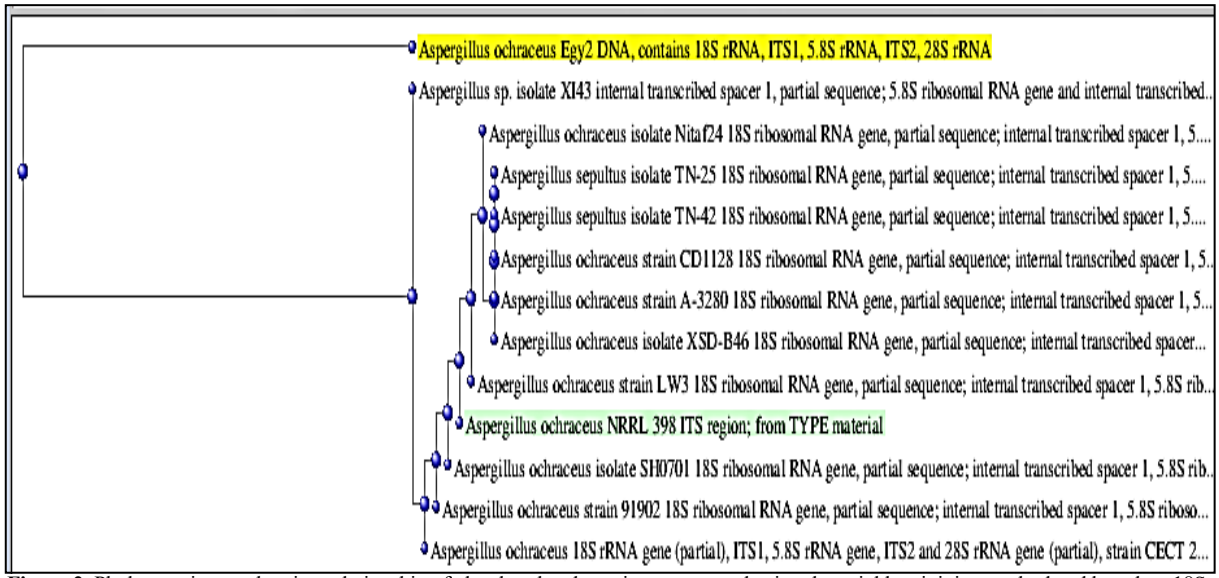

Figure 2. Phylogenetic tree showing relationship of closely related species constructed using the neighbor-joining method and based on 18S *rRNA* gene and ITS region sequences. Isolate is closely related to *Aspergillus ochraceus*

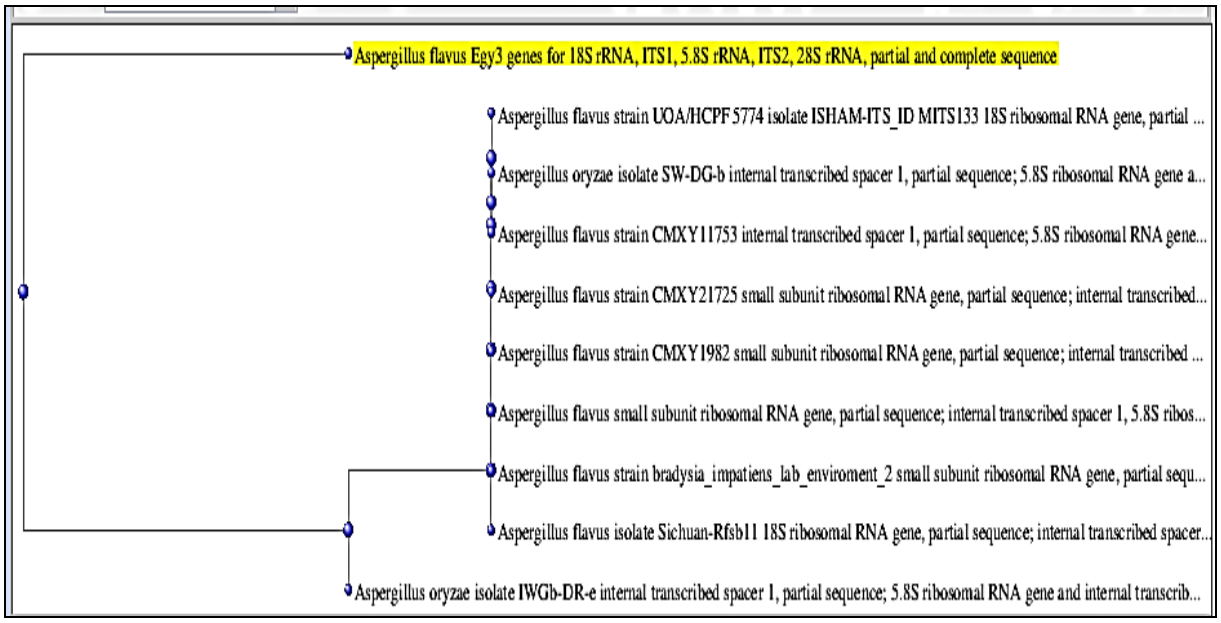

Figure 3. Phylogenetic tree showing the relationship of closely-related species constructed using the neighbor-joining method and based on 18S rRNA gene and ITSregion sequences. The isolate is closely-related to *Aspergillus flavus*

3.3. Molecular Differentiation of Isolated Fungi Using the ISSR Technique

The Inter Simple Sequence Repeat (ISSR) represents genome regions between microsatellite loci. Sequences amplified by ISSR-PCR can be used for delimiting species. ISSR-PCR is a simple, inexpensive, robust, multi-locus marker system which has been used to examine genetic variability among fungal pathogens. The resultant PCR response intensifies the arrangement between two SSRs, yielding a multilocus marker framework helpful for fingerprinting and genome mapping (Chadha and Gopalakrishna, 2007).

In this study, the ISSR PCR technique is used to reveal the genetic diversity between different fungal isolates. Ten ISSR primers produced scorable and reproducible banding patterns. The majority of the primers which produced polymorphic bands had been AC or AG repeats and AT or TC repeats.

A total of 165 full bands were scored from the amplified products with the ten Inter-Simple Sequence Repeat (ISSR) primer; 116 bands were polymorphic, forty-one unique bands with an average range size of (143-1939) bp (Table 5). All primers generated 100 % polymorphism except primers ISSR-14 and ISSR-15 which generated 76.923, and 78.571 % respectively. The obtained results reveal that the primers ISSR-1, ISSR-3 have amplified the maximum number of bands 21-23 respectively. On the other hand primers, ISSR-8 and ISSR-14, have amplified the lowest number of bands (13) (Figure 4). These results indicate that the primers ISSR-1 and ISSR-3 are the most repeated sequences in these fungal isolates compared to other primers. On the other hand, the forty-one unique bands that were detected among the total bands could be considered for marker-assisted selection. The maximum number of unique bands were amplified by primer ISSR-3 which recorded eleven bands, whereas the lowest number of unique bands (two bands) was amplified by ISSR-2, ISSR-8, ISSR-14, and ISSR-15.

These results show that the ISSR primers are robust, informative makers and would be a better tool for genetic divergence and phylogenetic studies. For the production of dendrogram using the UPGMA system, the ISSR primers were used to create a similarity matrix. Mahmoud *et al.* (2016) evaluated the genetic similarity of 30 % among *A. flavus* strains from agricultural crops and air using ISSR markers and proposed that ISSR is an extremely valuable tool for illustrating the genetic similarity of *A. flavus* isolated from several sources.

Nowadays, the advanced performance of the isolates' characterization is used for the ITS species identification as a result of both traditional techniques combined with molecular markers. For the sake of genetically characterizing the *Aspergillus* species, the internal transcribed spacer, the inter-simple sequence repeats (ISSR), and molecular markers are used.

The similarity matrix between isolated fungi reveals that isolates *A. parasiticus* and *A. niger* showed a 59 % similarity (Table 6). The results also show that both *A. terreus* and *A. niger* had a similarity of 56 %, followed by *A. flavus* and *A. niger* showing a similarity of 54 %. Lower similarities were recorded between *A. flavus* and *A. ochraceus* (34 %), and between *A. flavus* and *A. terreus* (44 %). Similar observations were reported by Rassin *et al.* (2015) who used ISSR to study the genetic diversity between different *A. fumigatus* isolates. Similarly, Yugander *et al.* (2015) also used the ISSR markers to examine the genetic variability of twenty-four strains of *Aspergillus* species isolated from paddy. Recently, Adss *et al.* (2017) used RAPD and ISSR to differentiate between seven isolates of *A.solani* and their pathogenic capability.

Table 5. The ISSR primer names and specific character of the ISSR analysis

NO.	Name of primer	Monomorphic bands*	Polymorphic bands**		Total bands	Polymorphism(%) = (polymorphic bands /total bands)* 100	MW range(bp)	Mean of frequency
			Non- unique bands	unique bands				
1	ISSR-1	0	16	5	21	100	214-1939	0.4
2	ISSR-2	0	17	2	19	100	323-997	0.5
3	ISSR-3	0	12	11	23	100	143-1730	0.4
4	ISSR-4	2	9	6	17	88.235	182-1338	0.5
5	ISSR-8	0	11	2	13	100	227-958	0.5
6	ISSR-11	0	11	3	14	100	145-1365	0.4
7	ISSR-12	0	9	5	14	100	182-1577	0.5
8	ISSR-13	0	14	3	17	100	197-1815	0.4
9	ISSR-14	3	8	2	13	76.923	278-1434	0.6
10	ISSR-15	3	9	2	14	78.571	905-1714	0.6
	Total	8	116	41	165	95.152		

*Monomorphic bands= similar band **polymorphicbands= different band

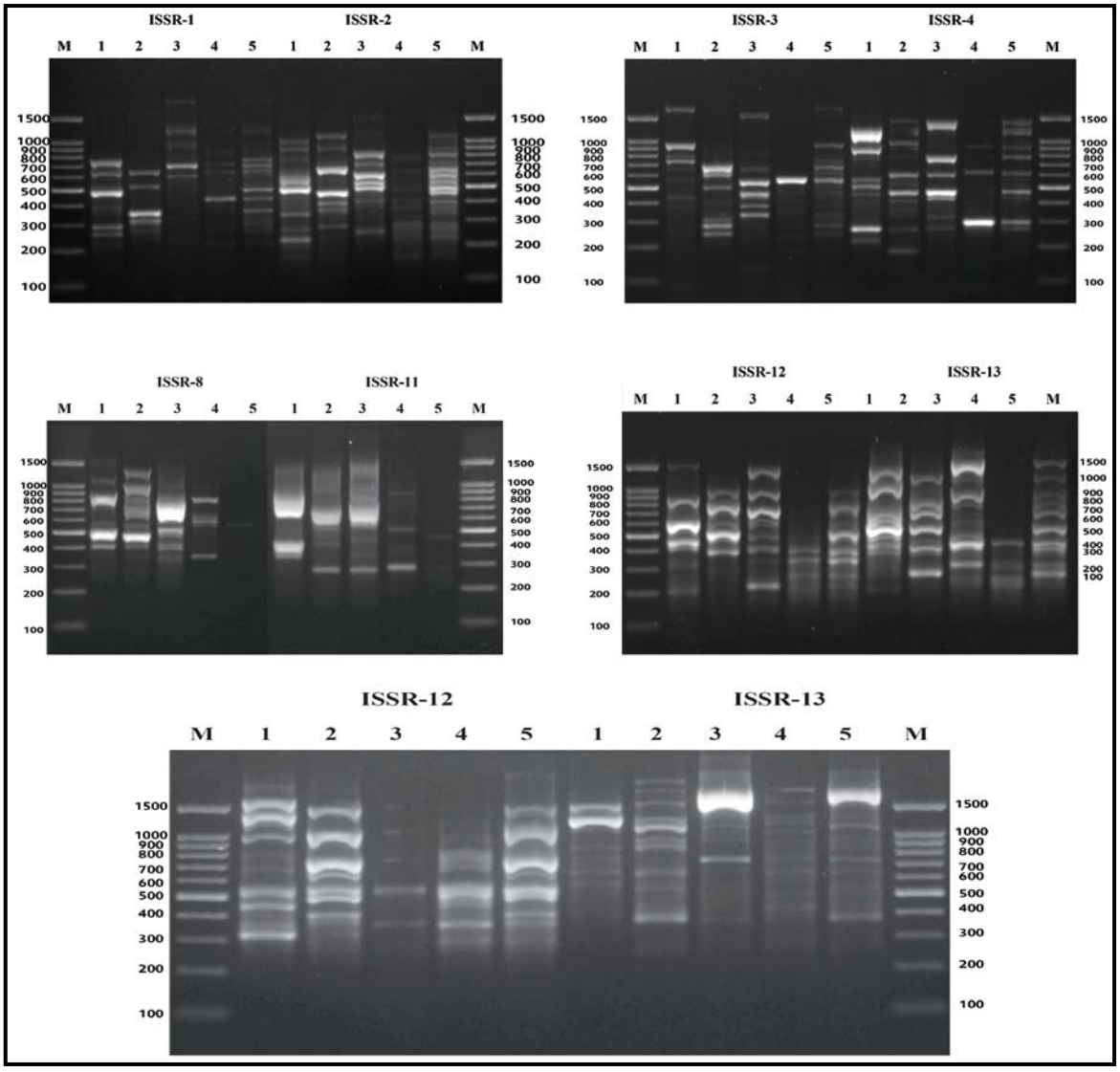

Figure 4. ISSR profile for five isolates of Aspergillus species. Lane 1: Aspergillus flavus; Lane 2: Aspergillus parasiticus; Lane 3: Aspergillus terreus; Lane 4: Aspergillus ochraceus; Lane 5: Aspergillus niger.

Table 6. Similarity matrix of isolated fungi based on ISSR analysis

	Matrix				
Isolates	1	2	3	4	5
1	1				
2	45	1			
3	44	47	1		
4	34	46	45	1	
5	54	59	56	48	1

Isolate 1: Aspergillus flavus; Isolate 2: Aspergillus parasiticus; Isolate 3: Aspergillus terreus; Isolate 4: Aspergillus ochraceus; Isolate 5: Aspergillus niger.

3.4. Cluster Analysis

Dendrogram was constructed using the UPGMA cluster analysis to reveal the genetic relationships among five fungal isolates based on similarity matrix between the isolates. Figure (5) shows three major clusters. The first cluster included the *A. flavus* isolate separate group (1), the second cluster (interposed group) contained the *A. terreus* isolate (3), divided into two subclusters *A. parasiticus* (2) and the *A. niger* isolates (5), and the third group contained A. *ochraceus* isolate (4). Similar observations were reported by Abdulateef *et al*. (2014) who used an ISSR-PCR based technology to document genetic diversity among some local Iraqi isolates through the determination of the ability *A.flavus* isolates to produce aflatoxin B_1.

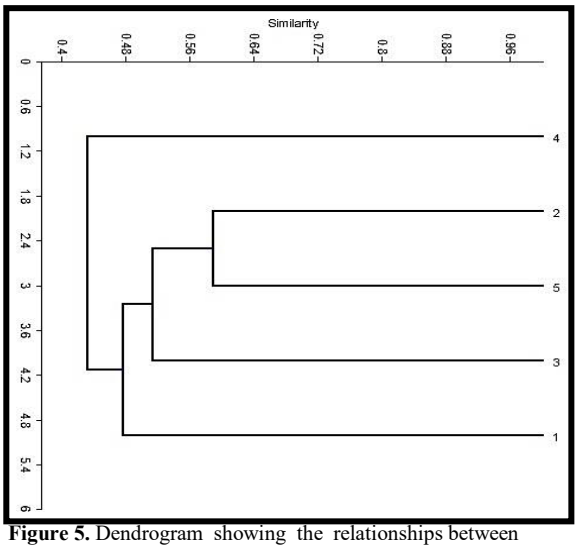

Figure 5. Dendrogram showing the relationships between isolated fungi based on ISSR analysis. Isolate 1: *Aspergillus flavus*; Isolate 2: *Aspergillus parasiticus*; Isolate 3: *Aspergillus terreus*; Isolate 4: *Aspergillus ochraceus*; Isolate 5: *Aspergillus niger*.

4. Conclusion

In this study, results demonstrate the role of ISSR markers, which estimated the genetic diversity for *Aspergillus* genera. In this work, ISSR analysis has provided information on the genetic similarity within selected *Aspergillus* genera. Thus, the present study shows that ISSR is an appropriate and efficient means to estimate genetic similarity amongst the *Aspergillus* genera.

Acknowledgment

This work has been funded by the National Research Centre, Cairo, Egypt, under grant No. 11090342.

References

Abdalla EAM, Kheiralla ZMH, Sahab AF and Hathout AS. 1998. *Aspergillus terreus* and its toxic metabolites as a food contaminant in some Egyptian bakery products and grains.*Mycotoxin Res*,**14**:83-91.

Abdulateef SM, Aljubori MH and Abdulbaqi NJ. 2014. Genetic Diversity Among Some *Aspergillus flavus* Isolates by Using Inter-simple sequence repeats (ISSR). *Iraqi J Sci*,**55**: 986-993.

Adejumo TO and Adejoro DO. 2014. Incidence of aflatoxins, fumonisins, trichothecenes,and ochratoxins in Nigerian foods and possible intervention strategies. *Food Sci.Quality Manag*,**31**: 127-146.

Adss AA, Abdel-Gayed MA, Botros W and Hafez E E. 2017.Multilocus Genetic Techniques, RAPD-PCR,and ISSR-PCR Markers and Polygalacturonase Activity as Tools for Differentiation Among Alternaria solani Isolates on Tomato Fruits and Relation to their Pathogenicity in Egypt. *Asian J Plant Pathol*,**11**: 18-27.

Al-Hindi RR, Aly SE, Hathout AS, Alharbi MG, Al-Masaudi S and Al-Jaouni SK, Harakeh SM. 2017. Isolation and molecular characterization of mycotoxigenic fungi in agarwood. *Saudi J. Biol. Sci*, doi.org/10.1016/j.sjbs.2017.07.008

Aly SE, Abo-Sereih NA, Salim, R G and Hathout A S. 2018. Isolation and molecular identification of food grade lactic acid bacteria and their antifungal activity. *J. Biol Sci*,**18**: 260-269.

Aly SE, Hathout AS and Ibrahim MIM. 2012. The stability of some *Lactobacillus* species to remove ochratoxin A from aqueous medium. *J Food Industries Nutr Sci*,**2**: 65-75.

Ashiq S. 2015. Natural occurrence of mycotoxins in food and feed: Pakistan perspective. *Comprehensive Rev. Food Sci Food Safety*,**14**:159-175.

Bruns TD, White TJ and Talyor JW. 1991. Fungal molecular systematics. *Annu Rev Ecol Sys*,**22**: 525-564

Chadha S and Gopalakrishna T. 2007. Comparative assessment of REMAP and ISSR marker assays for genetic polymorphism studies in Magnaporthe grisea. *Curr Sci*,**93**: 688-692.

Chakravarty B. 2011. Trends in Mushroom cultivation and breeding. *Am. J. Agric. Econ*,**2**: 102-109.

Coelho ASG. 2001. Software: Dboot-Evaluation of dendrograms based on estimates of distances / genetic similarities through the bootstrap procedure, version 3.0. Federal University of Goiás, Goiânia.

Dutech C, Enjalbert J, Fournier E, Delmotte F,Barre`s B, Carlier J, Tharreau D and Giraud T. 2007. Challenges of microsatellite isolation in fungi. *Fungal Genet. Biol,* **44**: 933-949.

Frankham R, Ballou JD and Briscoe DA. 2002. **Introduction to Conservation Genetics**. First Edition published by Cambridge University Press, pp. 642

Gramaje D, León M, Santana M, Crous PW and Armengol J . 2014. Multilocus ISSR markers reveal two major genetic groups in Spanish and South African populations of the grapevine fungal pathogen Cadophora luteo-olivacea. *PLoS One*,**9** (10) : e110417.

Hadrich I, Makni F, Ayadi A and Ranque S. 2010. Microsatellite typing to trace *Aspergillus flavus* infections in a hematology unit. *J. Clin. Microbiol*,**48**: 2396-2401.

Henry T, Iwen PC and Hinrichs SH. 2000. Identification of *Aspergillus* species using internal transcribed spacer regions 1 and 2. *J. Clin. Microbiol*,**38**: 1510-1515.

IARC. 2002. Some traditional herbal medicines, some mycotoxins, naphthalene, and styrene. Monograph on the evaluation of carcinogenic risk to humans, **82** (Lyon: IARC).

IARC.2012. Monographs on the evaluation of carcinogenic risks to humans: chemical agents and related occupations. A review of human carcinogens. Lyon, France: Inter Agency for Res Cancer **100F**:224-248

Klaassen CH. 2009. MLST versus microsatellites for typing *Aspergillus fumigatus* isolates. *Med Mycol*,**47**:S27-33.

Kumeda Y and Asao T. 2001. Heteroduplex panel analysis, a novel method for genetic identification of *Aspergillus* section *Flavi* strains. *Appl. Environ.Microbiol*,**67**: 4084-4090.

Mahmoud MA, Ali HM, El-Aziz ARM, Al-Othman MR and Al-Wadai SA. 2014. Molecular characterization of aflatoxigenic and nonaflatoxigenic*Aspergillus flavus* isolates collected from corn grains. *Genet. Mol. Res*,**13**: 9352-9370.

Mahmoud MA, EL-Samawaty AMA,Yassin MA and Abd EL-Aziz ARM. 2016. Genetic diversity analysis of *Aspergillus flavus* isolates from plants and air by ISSR Markers. Genet. *Molecul. Res*,**15**: 15028-081.

Morgante M, Hanafey M and Powell W. 2002. Microsatellites are preferentially associated with nonrepetitive DNA in plant genomes. *Nature Genet*,**30**: 194-200.

O´Donnell K. 1992. Ribosomal DNA internal transcribed spacers are highly divergent in the phytopathogenic ascomycete *Fusarium sambucinum* (Gibberella pulicaris*). Curr. Genet*, **22**: 213-220.

Okoth S, De Boevre M, Vidal A, Diana D M J, Landschoot S, Kyallo M, Njuguna J, Harvey J and De Saeger S. 2018.Genetic and toxigenic variability within *Aspergillus flavus* population isolated from maize in two diverse environments in Kenya. *Front. Microbiol*,**9**: 57.

Paplomatas EJ. 2004. Molecular diagnostics for soil-borne fungal pathogens. *Phytopathol. Mediterr*,**43**: 213-220.

Pildain MB, Frisvad JC, Vaamonde G, Cabral D. Varga J and Samson RA. 2008. Two novel aflatoxin-producing *Aspergillus* species from Argentinean peanuts. *Int. J. Syst. Evol. Microbiol*,**58**: 725-735.

Priyanka SR, Uppalapati SR, Kingston JJ, Murali HS and Batra HV. 2014. Development of ISSR-derived SCAR marker-targeted PCR for identification of *Aspergillus* section Flavi members. *Lett. Appl. Microbiol*,**58**: 414-42.

Rampersad SN. 2013. Genetic structure of Colletotrichum gloeosporioidessensulato isolates infecting papaya inferred by multilocus ISSR markers. *Phytopathol*,**103**: 182-189.

Rassin NK, Al- Judy NJ and Dheeb BI. 2015. Molecular Identification of *Aspergillus fumigatus* Using ISSR and RAPD Markers. *Iraqi J. Sci*,**56**: 2788-2797.

Ratnaparkhe MB, Tekeoglu M and Muehlbauer FJ. 1998. Inter-simple-sequence-repeat (ISSR) polymorphisms are useful for finding markers associated with disease resistance gene clusters. *Theor. Appl. Genet*,**97:** 515-519.

Reischl U and Lohmann C P. 1997. Die Polymerase-Kettenreaktion (PCR) und ihre Anwendungsmöglichkeiten zur infektiologischen Diagnsotik in der Opthalmologie. Klin. Monatsbl. *Augenheilkd*,**211**: 227-234.

Richard JL. 2007. Some major mycotoxins and their mycotoxicoses-An overview. *Int. J. Food Microbiol*,**119**: 3-10.

Rohlf FJ. 1993. NTSYS-pc: Numerical taxonomy and multivariate system. Version 2.9. New York. *Applied Biostatistics.*

Sabry BA, Hathout AS, Nooh A, Aly SE and Shehata M. 2016. The prevalence of aflatoxin and *Aspergillus parasiticus* in Egyptian sesame seeds. *Int. J. ChemTech Res*,**9:** 308-319.

SahabAF, Aly SE, Nawar LS and El-Faham SY. 2011. Fungal occurrence in physic nut (*Jatropha curcas*) seeds during storage and possibility aflatoxin production by *Aspergillus flavus* and *Aspergillus parasiticus* isolates. *J. Am. Sci*,**7**:511-516.

Sahab AF, Hathout AS, Sabry BA and Aly SE. 2014. Application of some plant essential oils to control *Fusarium* isolates associated with freshly harvested maize in Egypt. *J. Essential Oil Bearing Plants*,**17**:1146-1155.

White TJ, Bruns T, Lee S and Taylor JW. 1990. Amplification and direct sequencing of fungal ribosomal RNA genes for phylogenetics. In: Innis MA, Gelfand DH, Sninsky JJ, and White TJ, (Eds.), **PCR Protocols: A Guide to Methods and Applications**. Academic Press Inc., New York, pp. 315-322.

Williams JG, Kubelik AR, Livak KJ, Rafalski, JA, and Tingey SV.1990. DNA polymorphisms amplified by arbitrary primers are useful as genetic markers. *Nucleic Acids Res*,**18**: 6531-6535.

Yu J, Cleveland TE, NiermanWC and Bennett JW. 2005. *Aspergillus flavus* genomics: gateway to human and animal health, food safety, and crop resistance to diseases. *Rev. Iberoam. Micol*,**22**: 194-202.

Yugander A, Kiran S, Surekha M, babupK, LahaGS, Madhav M S and Reddy S M. 2015. determination of genetic variation by using ISSR markers in toxigenic strains of *Aspergillus* in paddy from Telangana state India. *Int. J. Agricult. Sci. Res,* **5**:193-202.

JJBS

Volume 12, Number 5,December 2019
ISSN 1995-6673
Pages 617 - 624

Jordan Journal of Biological Sciences

Biosorption Analysis and Penoxsulam Herbicide Removal Efficiency by Transgenic *Chlamydomonas reinhardtii* Overexpression the Cyanobacterial Enzyme Glutathione-*s*-transferase

Mostafa M. S. Ismaiel, Yassin M. El-Ayouty and Asmaa H. Al-Badwy*

Plant Biotechnology Laboratory (PBL), Botany and Microbiology Department, Faculty of Science, Zagazig University, El-Gamaa Street 1, 44519 Zagazig- Sharkia- Egypt.

Received February 26, 2019; Revised March 30, 2019; Accepted April 7, 2019

Abstract

Penoxsulam, a new post-emergent rice herbicide, is widely used in rice fields in Egypt. Penoxsulam has been shown to have adverse effects on plant growth; hence, it prevents plants from producing an important enzyme, acetolactate synthase**.** Glutathione-*s*-transferase (GST) plays a vital role in the detoxification of xenobiotics including Herbicides. Genetically-engineered algae can provide feasible and environmentally safe approaches for the phycoremediation of herbicides. In the current study, Cyanobacterial GST was transferred to *Chlamydomonas reinhardtii*, a model unicellular alga, via the *Agrobacterium tumefaciens*-mediated transformation method. The GST enzyme activity was confirmed in three transgenic *C. reinhardtii* lines. To evaluate the removal capacity of penoxsulam by transgenic *C. reinhardtii*, the microalgae were treated with penoxsulam at 5, 10, and 20 µg ml^{-1} for twenty-four hours. The percentage of the herbicide removal from 5 and 20 µg ml^{-1} reached maximally 93.6 % and 54 % in the case of transgenic alga, whereas in the case of the wild type, the percentage of removal reached 52 % and 21 %, respectively. Langmuir and Freundlich adsorption isotherm models and the sorption kinetics have been applied to the experimental data to check the effectiveness of the removal process. The equilibrium data were well-fitted with the Langmuir isotherm model. The results showed that GST transgenic microalgae are effective in the removal of penoxsulam from aqueous solutions and it can be used in phycoremediation systems of herbicides.

Keywords: Penoxsulam- phycoremediation- Glutathione-*s*-transferase (GST) - Isotherm- Langmuir

1. Introduction

Xenobiotics are naturally-occurring compounds (animal poisons, toxins, antibiotics, drugs, and toxic products from plants) or synthetic compounds (insecticides, pesticides, herbicides, and inorganic fertilizers) (Bulucea *et al*., 2012). These compounds may cause damage to living organisms resulting in deformities, DNA damage, poisoning or at the very least, a feeling of discomfort (Shamaan, 2005; Bulucea *et al*., 2012). Nowadays, pollution and soil contamination are among the major concerns, and biofertilizers play a very significant role in that pollution. These contaminants limit the growth and development of many microorganisms that play a role in mineralization process (Mishra *et al*., 2013).

Herbicides are considered as pollutants in aquatic environments, including ground water, estuaries, rivers, lakes, and coastal marine waters (Prado *et al*., 2009). The different types of herbicides are designed to kill plant tissues. However, this is accomplished through two basic methods referred to as selective (Systemic) and non-selective (contact) herbicides. Penoxsulam is a new post-emergent rice herbicide in Egypt. Penoxsulam is a member of the triazolopyrimidine sulfonamide family of herbicides. It is considered to be a systemic herbicide. It moves throughout the plant tissues and prevents plants from producing an important enzyme, called acetolactate synthase (ALS) (Whitcomb, 1999). Microalgae are essential to provide energy and primary substances for survival in most aquatic ecosystems (Ma *et al*., 2002; Prado *et al*., 2009). Hence, there is a need to estimate the effect of the toxic herbicide on microalgae. *Chlamydomonas reinhardtii* has attracted more attention as a model for studying biological systems because this organism is the most biologically characterized one (Harris, 2001). The genomes in *C. reinhardtii* (chloroplast, nuclear and mitochondrion) are well characterized (Merchant, 2007; Popescu and Lee, 2007), and provide wealth of information for genetic manipulation and studies of this microalgae. New strategies have been established for developing algae or plants that are highly tolerant to herbicides through biotechnological tools. In this context, glutathione-*s*-transferases (GSTs) are members of the transferases family that quench reactive molecules and catalyze the conjugation of GSH to an array of

* Corresponding author e-mail: bio_asmaa88@yahoo.com.

hydrophobic and electrophilic substrates, protecting the cells from oxidative burst. Members of this family were first discovered for their potential of metabolizing an array of toxic exogenous compounds, that is xenobiotics via GSH conjugation (Cummins *et al*., 2011). GSTs have been implicated in several cellular processes (Nianiou- Obeidat *et al*., 2017). Studies suggest that GSTs could protect the plants from different abiotic stresses (Ding *et al*., 2017), heavy metal stress (Zhang *et al*., 2013), damage of ultra-violet light (UV) and radiations (Liu and Li, 2002). Studies suggest that GSTs safeguard the cells against chemical-induced toxicity and provide tolerance by catalyzing S-conjugation between the reduced thiol group of GSH and electrophilic moiety in the hydrophobic and toxic substrate (Deavall *et al*., 2012). After conjugation, the new molecules are sequestered into the vacuoles or are exported from the cells by putative membrane ATP-dependent pump systems. Although the involvement of members of GST family has been reported in plant development and biotic stresses (Nianiou- Obeidat *et al*., 2017), limited information is available regarding the involvement of this family in combating stress. Among the different classes of GSTs, the role of Lambda class GSTs has been reported in stress responses (Kumar *et al*., 2013a, 2013b) as well as in plant growth and development. Thus, functional characterization and analysis of regulatory aspects of gene expression of the GST gene family members can help enhance the understanding of their role in detoxification. Apart from herbicide detoxification, the involvement of GSTs in hormone biosynthesis, tyrosine degradation, and peroxide breakdown (Oakley, 2011), stress-signaling proteins (Loyall *et al*., 2000), and non-catalytically acting as flavonoid-binding proteins (Mueller *et al*., 2000) has been reported. In the current study, the cyanobacterial glutathione-*s*-transferase gene (GST, gi451779298, sll0067)) was genetically cloned and transferred into *C. reinhardtii* cells. The overexpression of GST in transgenic *C. reinhardtii* showed an enhanced tolerance to the penoxsulam herbicide compared to wild types.

2. Materials and Methods

2.1. Chemicals.

All chemicals used were of the analytical grade and were obtained from Sigma-Aldrich (Munich, Germany). Th stock solution of penoxsulam was freshly-prepared daily with deionized water throughout the tests.

2.2. Chlamydomonas reinhardtii Culture Conditions.

Chlamydomonas reinhardtii, was obtained from Prof. Mohammed Ismaeil (Botany Department, Faculty of Science, Mansoura University, Egypt). *C. reinhardtii* was aseptically grown in a Tris Acetate Phosphate (TAP) medium (Gorman and Levine, 1965). The pH of the medium was adjusted to 7.4. For kanamycin (5 mg/mL) selection of transformed *C. reinhardtii* colonies, solid TAP medium supplemented with 1.5 % (w/v) agar was used. The algal cultures were incubated in growth chamber at 25±2 ˚C under long day conditions (16 h light/8 h dark), and were kept under a light intensity of 80 µmol m^{-2} s^{-1} with continuous shaking (75 rpm) in case of liquid cultures.

2.3. Experimental Procedures

2.3.1. Gene Cloning and Plasmid Constructs

The Glutathione-S-transeferase gene (GST) coding sequence (gi451779298, sll0067) was amplified by PCR using genomic DNA isolated from *Synechoccous elongatus PCC6803* (kindly provided by Botany Department, Faculty of Science, Cairo University, Giza, Egypt) as template. A forward primer with extension for *Nco*I site (5′-ACTGCCATGGGTATCAAACTATACG-GTGC-3′), and a r everse primer (5′-AATTTCTAGAT-CAGCGGGCACCGATG-3′) with extensions for *Xba*I site were used. The amplified GST PCR fragments were column-purified and then ligated into the binary expression vector pTRAK, a derivative of pPAM (gi13508478). This cloning step results in a single-plant expression construct (pTRAK-GST) for GST (Figure 1). The GST gene expression cassette was flanked by the scaffold attachment region (SAR) of the tobacco RB7 gene (gi3522871). The nptII cassette of pPCV002 was used for the transgenic *C. reinhardtii* selection on kanamycin (Koncz and Schell, 1986). The GST gene expression is designed to be under the control of CaMV-35S promoter (Reichel *et al*., 1996).

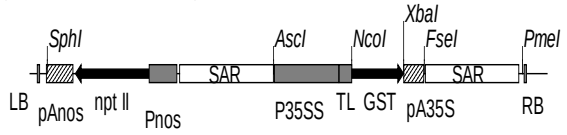

Figure 1. Schematic representation of the binary expression vector pTRAK-GST. P35SS/PA35S; promoter/Terminator sequence of Cauliflower Mosaic virus. TL (Cab22L); 5'UTR of the tobacco leader peptide. LB and RB; Left and Right border sequences of Nopalin-Tiplasmids. NptII; Neomycin phosphor-transferase type II that confers resistance to kanamycin. Pnos/PAnos; Promoter/Terminator of Nopaline synthase gene from *Agrobacterium tumefaciens*. GST gene is flanked by the scaffold attachment region (SAR) of the tobacco RB7 gene (gi3522871).

2.3.2. Transformation and Generation of Transgenic C. reinhardtii

The pTRAK-GST construct was transformed into *C. reinhardtii* following the *Agrobacterium tumefaciens* (GV3101)-mediated co-cultivation transformation protocol as previously described (Kumar *et al*., 2004). A single colony of *C. reinhardtii* was inoculated into a liquid TAP medium and was allowed to grow till reaching a log phase of growth. Cells were then plated on a solid TAP medium and incubated under continuous light for forty-eight hours until forming a lawn of cells. An *Agrobacterium* culture transformed with pTRAK-GST plasmid was grown in a liquid LB medium containing appropriate antibiotics (25 mg/l rifampicin and 50 mg/l kanamycin) at 28 ˚C till OD_{600} reaches 0.6. The *A. tumefaciens* cells were then spun down (4000 × g for 5 min at 4 ˚C) and resuspended in a 250 µl liquid TAP medium containing 100 µM acetosyringone. The bacterial suspension was then co-cultivated with *C. reinhardtii* cells grown on the agar plates for two hours at 28 ˚C followed by overnight incubation at 25 ˚C in dark. The *C. reinhardtii* cells were harvested and washed twice with a liquid TAP medium supplemented with 500 m g/l cefotaxime in order to completely kill and/or remove the *Agrobacterium* cells. For the selection of the transformed *C. reinhardtii* cells,

the washed cells were cultivated on solid TAP agar plates containing 500 mg/l cefotaxime and 5 mg/ml kanamycin, and were incubated at 25 °C in growth chamber for eight days until the appearance of the transformed colonies. The presence of the GST transgene in the selected *Chlamydomonas* colonies was confirmed by the colony PCR test using GST gene specific primers.

2.3.3. Quantitative Real-time RT-PCR Analysis

The quantitative real-time RT-PCR was performed as described previously (Kebeish *et al*., 2015). RNA was extracted from the *C. reinhardtii* cells following the 1-bromo-3-chlorpropane (BCP protocol) of Chomczynski and Mackey (1995). First-strand complementary DNA (cDNA) was synthesized as described by Niessen *et al.* (2007). An ABI PRISM1 7300 Sequence Detection System (Applied Biosystems, Darmstadt, Germany) was used following the manufacturer's instructions. PCR amplifications were performed using SYBR Green Reagents (SYBR1 GreenERTM qPCR Super Mixes; Karlsruhe, Germany). Primers were purchased from Intron Biotechnology Inc. (Kyungki-Do, South Korea). For the detection of GST transcripts, primers 5′-GCGATCGCCATTTATCCTC-3′/5′-ACCGCAGGATA-GTCGTCAAA-3′ were used. Primers 5′GCGATGTGGA-CATCCGCAAG-3′ and 5′-GGGCCGTGATCTCCT-TGCTC-3′ were used for the detection of ACTIN transcripts. Primer concentration in the reaction mixture was adjusted to 200 nM. The amplification program used for the amplification of both of the GST and ACTIN fragments was a ten-minute primary denaturation at 95 ˚C, followed by forty cycles consisting of fifteen seconds of denaturation at 95 ˚C and one minute of combined annealing and extension at 60 ˚C.

2.3.4. Growth Assay of Transgenic and Wild C. reinhardtii

The algal strains were aseptically grown in a TAP medium according to Gorman and Levine (1965). The wild type (WT) as well as transgenic strain were allowed to grow in a TAP medium under a photoperiod of light: dark (16:8 hrs) for twenty-six days. The optimum light intensity (80 µmol m^{-2} s^{-1}) was supplied with cool white fluorescent tubes. The growth curves of both WT and transgenic were spectrophotometrically estimated at different intervals (2 days) at 650 nm according to Robert (1979) through the incubation periods. As the incubation period reached a mid-log phase (12 days), the algal cells of either WT or transgenic strains (C.GST3) were harvested by centrifugation at 5000 xg for five minutes and were double-washed thoroughly with 10 mM Na_2-EDTA, and then by sterile distilled water. The algal tissue was used for further analyses.

2.3.5. Estimation of Glutathione-s-Transferase

A determined amount of each treatment was ground to a fine powder in liquid N_2 and was then homogenized in 1 ml of an extraction buffer (50 mM potassium phosphate buffer (pH 7.4) containing 10 mM EDTA, 0.1 % Triton X-100, 20 % sorbitol and 2 % Polyvinyl pyrrolidone). The homogenate was centrifuged for fifteen minutes at (8000 xg /4˚C). The supernatant was collected and made up to a known volume and used to estimate the enzymes activity.

The GST activity was determined according to Habig *et al*. (1974), using 1-chloro -2, 4-dinitrobenzene (CDNB) as substrate. Assay of GST activity, 3 mL of the reaction mixture (100 mM Potassium phosphate buffer (pH 7.0), 0.03 % Reduced glutathione (GSH), 0.02 % CDNB and 0.0372 % Na-EDTA) were mixed with 100 µL of the enzyme extract. The enzyme activity was calculated by monitoring the reaction mixture for 120 m inutes (20 minutes intervals) at 340 nm in a spectrophotometer.

2.3.6. Analysis of Adsorption Equilibrium Isotherm

2.3.6.1. Isotherm Process

To Erlenmeyer flask, 100 mL containing 25 m L of sterilized TAP medium, a suitable volume of penoxsulsm 2.5 % stock was taken and inoculated to reach the final concentration (5, 10 and 20 µg mL^{-1}). Three flasks for each concentration were prepared. All the flasks were inoculated with 5 ml of healthy algae under aseptic conditions. (1 mL = 0.6 optical density) and incubated at 25±2 °C under a photoperiod 16 light: 8 dark for twenty-four hours. At the end of the incubation period, different samples were taken from both treated and untreated alga. The algal cells were separated by centrifugation at 10000 rpm, and the clear solutions were used to estimate the herbicide residue according to Nour El-Dien *et al*. (2010).

2.3.6.2. Determination of Penoxsulam Residue

2 mL of 2 % (w/v) of an ammonium molybdate solution was added to 6 m L of 4M H_2SO_4, 0.75 mL of ammonium thiocyanate (10%, w/v) and 0.1 mL of ascorbic acid (10%, (w/v)). The solutions were placed in a 100 mL separating funnel. The mixtures were left for fifteen minutes at room temperature (25±5 ˚C). 1 mL of the herbicide solution was added, and the reaction mixture was left for another fifteen minutes. The ion-pairs were extracted with dichloromethane twice with 5 mL portions after shaking for one minute. The ion-pairs were collected in a 10 mL measuring flask and methylene chloride was dried over anhydrous sodium sulphate. The absorbance of the filtered extract was measured at 470 nm, against a reagent blank, prepared similarly without the herbicide (Nour El-Dien *et al*., 2010).

The removal percentage was determinated by the following equation

$$\text{Removal \%} = (C_0 - C) \times 100/C_0$$

Where C_0 is the initial concentration of penoxsulam (µg mL^{-1}) in the solution, and C is the final concentration of penoxsulam (µg mL^{-1}).

2.3.6.3. Adsorption Isotherm

Studies of the adsorption equilibrium isotherm were conducted using varying concentrations of the penoxsulam herbicide (5, 10, and 20 µg mL^{-1}) for twenty-four hours at room temperature. These data were evaluated by Langmuir and Freundlich adsorption isotherm equations to interpret the efficiency of the bioremediation of the penoxsulam sorption (Freundlich, 1906; Langmuir, 1918).

Langmuir's isotherm model assumes monolayer adsorption, and is presented by the following equation.

Langmuir model: $qe = Q_{max} * K_L * Ce/(1+K_L * Ce)$

Langmuir model in linear form: $Ce/qe = 1/(Qmax*KL) + 1/ Qmax *Ce$

Where qe is the penoxsulam amount adsorbed per unit mass of adsorbent (mg g^{-1}), Ce is the equilibrium concentration of penoxsulam in the solution (mg mL^{-1}), Q_{max} is the maximum adsorption capacity (mg g^{-1}), and K_L is the constant related to the free energy of adsorption. A straight line is obtained by plotting

Ce/qe against Ce and the slope and intercept are used to calculate the Q_{max} and K_L, respectively.

The Freundlich model is presented by the following equation, which indicates that the surface of the adsorbent is heterogeneous (Freundlich, 1906).

Freundlich model: $qe = K_F * Ce\ 1/n$

Freundlich model in linear form: $\log qe = \log K_F + 1/n * \log Ce$

Where K_F is a parameter of the relative adsorption capacity of the the adsorbent related to the temperature, and n is a characteristic constant for the adsorption system. A plot of log qe against log Ce gives a straight line; the slope and intercept correspond to 1/n and log K_F, respectively.

2.4. Statistical Analysis

The data were represented in figures as mean ± stander error (SE) of three independent samples for each genotype. The obtained data were analyzed statistically using Student's *t*-test to determine the significant differences among the data. Differences were considered significant when (* $p < 0.05$, ** $p < 0.01$, *** $p < 0.001$). All statistical analyses were carried out using Microsoft Excel software (Microsoft corporation, USA).

3. Results

3.1. Gene Cloning and Generation of Transgenic C. reinhardtii.

GST plays a vital role in various detoxification processes of xenobiotics under biotic and abiotic stresses. The over-expression of cytosolic GST in algae enhances the tolerance to herbicide. Therefore, glutathione-*s*-transferase was genetically cloned and transferred into the nuclear genome of the model microalga, *C. reinhardtii.* The binary expression vector, pTRAK-GST (Figure 1) was used for the t ransformation of the green microalga, *C. reinhardtii* via the *Agrobacterium tumefaciens*-mediated co-cultivation method (Kumar *et al.*, 2004) in order to test the efficacy of the transformed alga in the removal of herbicide. Transgenic *Chlamydomonas* lines were selected on a solid TAP medium supplemented with kanamycin antibiotic (Figure 2). Three independent lines of *Chlamydomonas reinhardtii* transgenic for GST, named C.GST-1, C.GST-2, and C.GST-3, were generated and used for further molecular and biochemical analyses.

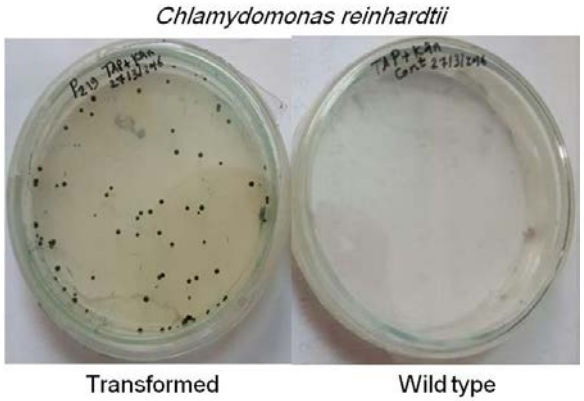

Figure 2. Photograph representing the selection of the transformed colonies of *C. reinhardtii* and the wild type cells on solid TAP medium supplemented with kanamycin.

3.2. RT-PCR and Glutathione-S-Transeferase Enzymatic Assays.

Quantitative real-time polymerase chain reaction (qRT-PCR) systems for the screening of GST gene expression level using TaqMan 7300 series were established. Primer systems for GST and Actin (as a house-keeping gene) were designed and optimized for the RT-PCR analysis using serial dilutions of plasmid DNA. This test was used for testing the expression level of GST. The results of the qRT-PCR analysis for the expression of the GST gene in transgenic *C. reindardtii* are shown in Figure 3A. Three transgenic *C. reinhardtii* lines of GST were tested. Variable expression levels for the GST gene were observed in all of the tested lines. All the tested lines revealed a high expression level of the mRNA transcript accumulation of both GST compared with Actin. C.GST-3 and C.GST-2 show a high expression level for both transgenes compared to the other tested algae.

In vitro, the biochemical reaction was prepared to determine the activity of GST in the case of the transgenic and wild types. The results in Figure 3B show that the different transgenic lines under investigation have a more or less similar increase with a highly significant response with respect to the wild type. The previous increases reaching about 5x fold over the WT. C.GST-2 and C.GST-3 lines show more a GST activity compared to GST-1 line. C. GST-3 exhibited the highest expression level for GST, thus this line was chosen for the herbicide biosorption and removal analyses.

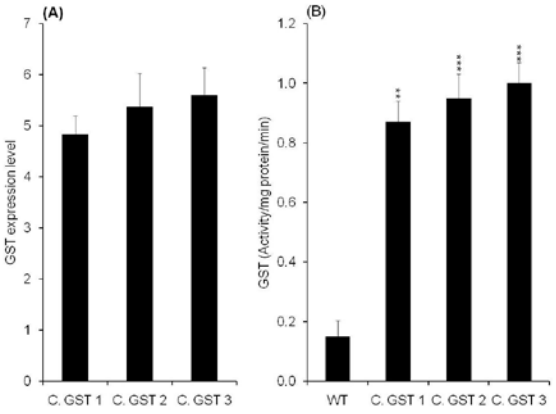

Figure 3. (A) Accumulation of GST mRNA transcripts in the GST transgenic *C. reinhardtii* alga. (B) Activity of glutathione-*s*-transferase.

3.3. Growth Assay of Transgenic and Wild-Type C. reinhardtii.

The growth of transgenic (C.GST-3) and wild-type *C. reinhardtii* was varied (Figure 4). Short-lag phases were observed, which indicates that the algae have a good adaptability to these growth conditions. The growth patterns of both algae have log phases extended for eighteen days followed by the stationary phase. There were significant differences in the cell density of the transgenic and wild-type *C. reinhardtii* due to the overexpression of GST in the transgenic line.

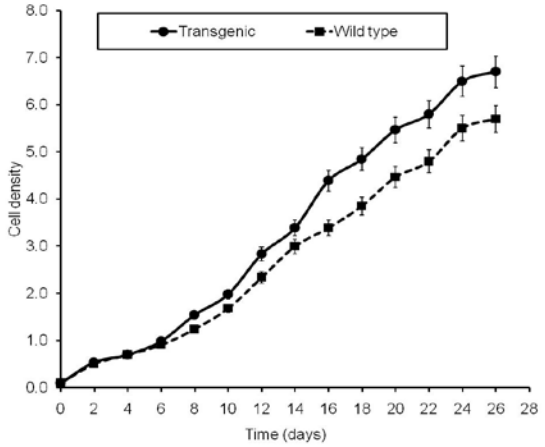

Figure 4. Growth curve of transgenic (C. GST3) and wild type *C. reinhardtii*.

3.4. Sorption and Desorption Efficiency of Penoxsulam

The Penoxsulam (Triazopyrimidine sulfonamide) herbicide removal was checked by transgenic *C. reinhardtii* for the GST gene against the wild type. Two sets of different concentrations of penoxsulam each comprised of (5, 10, 20 µg mL^{-1}) were prepared. Each concentration inoculated by 50 mg fresh weight of transgenic and wild cells, and all sets were maintained for twenty-four hours at room temperature. The results in Table 1 reveal that transgenic alga has a promising efficiency to remove the herbicide compared to the wild type. The percentage of herbicide removal attained from the culture was maximally 93.6 % as the transgenic alga treated with 5 µg mL^{-1}, whereas, in the case of the wild type, the percentage of removal reached 52 %. As the concentration of penoxsulam increased, the rate of its removal decreased to reach 54 % and 21 % for the transgenic and wild type, respectively.

Table 1. Percentage of removal of penoxsulam by transgenic (C. GST3) *Chlamydomonas* against wild type.

Concentration of penoxsulam (µg mL^{-1})	Residual concentrations of penoxsulam (µg mL^{-1})		Removal percentage of penoxsulam (%)	
	C.GST	WT	C.GST	WT
5	0.32	2.4	93.6	52.0
10	4.26	6.5	57.4	35.00
20	9.2	15.7	54.00	21.50

Table 2 shows that the adsorption co-efficient isotherm for penoxsulam fitted the Langmuir equation quite well. The values of Langmuir constants, q_{max} and k_L obtained from the linear plot of C_e/q_e against C_e, and their correlation coefficient (R^2), k_L and q_{max} revealed that the Langmuir isotherm model best fitted the experimental data for the sorption of herbicide by both the wild and transgenic alga (Figure 5A and 6A). This is because the experimental q_{max} in the case of transgenic type was 10.8 µg mg^{-1} and the calculated value was 12.5 µg mg^{-1} and R^2 reached 0.80. Meanwhile, in the case of the wild type, the calculated q_{max} (4.8 µg mg^{-1}) was also coincident with the experimental one (q_{max}= 4.89 µg mg^{-1}); R^2 also reached 0.96 and the Langmuir constant was 3.52. The major difference between the sorption capacities of both the transgenic and wild type was due to the difference in their overexpression of GST.

Table 2. Langmiur and Frundlich isotherm constants for penoxsulam adsorption by *C. reinhardtii.*

Species	Langmuir Isotherm				Freundlich Isotherm		
	R^2	K_L	Q_{max} Experimental (µg mg^{-1})	Q_{max} Calculated (µg mg^{-1})	R^2	K_F	1/n
C. GST3	0.88	0.05	11.7	12.5	0.69	0.89	4.87
WT	0.98	3.52	4.38	4.8	0.44	0.342	4.27

On the other hand, the Freundlich isotherm model did not fit the experimental data for the biosorption of the penoxsulam due to slope n<1 and other parameters (R^2 and K_F) was also low (Figure 5B and 6B). So, the overexpression of glutathione-*s*-transferase enables the transgenic alga to remove the herbicide compared with the wild type. In the future, phycoremediation would be a promising and eco-friendly process to reduce the risks of xenobiotics.

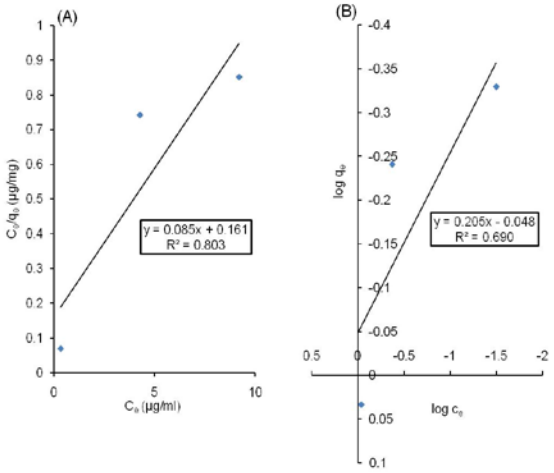

Figure 5. The amount of penoxulam adsorbed onto the trasnsgenic *C. reinhardtii* (C. GST3) at various equilibrium penoxsulam concentrations, (A) Langmuir adsorption isotherm, (B) Freundlich adsorption isotherm. *P*-value <0.05 for transgenic line (C. GST3) compared to wild type.

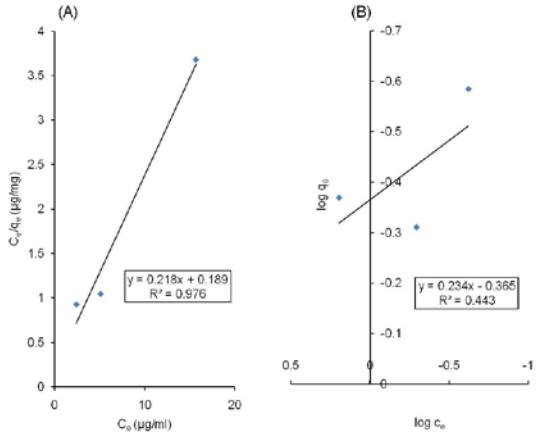

Figure 6. The amount of penoxulam adsorbed onto the Wild *Chlamydomonas* at various equilibrium penoxulam concentrations, (A) Langmuir adsorption isotherm, (B) Freundlich adsorption isotherm

4. Discussion

4.1. Gene Cloning and Generation of Transgenic C. reinhardtii Lines.

This study presented the overexpression of the antioxidant enzyme, glutathione-*s*-transferase, (GST, from *Synechococcus elongatus*) in *C. reinhardtii*. *C. reinhardtii* was shown to accumulate a large quantity of penoxsulam. Such uptake and decay of penoxsulam resulted in the rapid removal of penoxsulam from the medium due to the overexpression of GST in transgenic alga. This observation suggests that *C. reinhardtii* may be useful in molecular breeding designed to improve the environmental stress tolerance to the herbicide or remediation of contaminated aquatic ecosystems. To achieve this purpose, the gene- encoding GST was cloned into a binary expression construct in the current study. The construct was transferred into *Chlamydomonas* via an *Agrobacterium tumefaciens*-mediated transformation (Kumar *et al*., 2004). GST was overexpressed in *Arabidopsis* to increase tolerance to salt (Qi *et al*., 2004). It was also overexpressed in tobacco separately or in combination with CYND to maintain the redox homeostasis and improve the cyanide remediation capacity of tobacco (Kebeish *et al*., 2017).

4.2. RT-PCR and Enzymatic Assay.

The activity of the GST enzyme was tested in the algal extract isolated from the GST transgenic algal cells. As control, an extract from the wild-type (WT) *Chlamydomonas* was used. There was a 5x fold increase in GST expressing *Chlamydomonas* lines over WT (Fig. 3B). This indicates that GST is functionally active in the GST lines. The background activity observed for the GST enzyme in the wild-type alga may be related to the endogenous *Chlamydomonas* glutathione-*s*-transferase activity. The results of this study are in accordance with Kebeish *et al*. (2017) who found a three- fold (GST) to a four-fold (CYND) increase in the activity over background in GST and CYND expressing tobacco lines when GST was cloned separately or in combination with CYND. Similarly, about a 5x-fold GST expression level over actin was observed for the GST transgenic algae (Figure 3A). The data obtained from the qRT-PCR analysis (Figure 3A) and the GST enzymatic activity (Figure 3B) indicate that GST is functionally active in the transgenic lines.

There are three phases of biotransformation. Phase I consists of enzymes that catalyze reactions which modify the functional groups of the pollutant. In phase II, those enzymes catalyze transfer reactions of whole groups or biomolecules to pollutants. Phase III includes translocation processes that render pollutants or their metabolites non bioavailable. For bioremediation purposes, biotransformation enzymes mainly belong to four biochemical types: oxidoreductases, hydrolases, transferases and translocases (or pumps). Among all known transferases, Glutathione *S*-transferase (GST) is mainly involved in biodegradation for bioremediation purposes. GST includes a superfamily of enzymes that have been found in bacteria, fungi, algae, plants and animals (Herve *et al*., 2008; Toribio *et al*., 1996). Even though they catalyze the transference of glutathione to electrophillic pesticides, they can also show hydrolytic and peroxidase activities (Toribio *et al*., 1996). Interestingly, GST can also catalyze the dehalogenation of rings e.g. Lindan (Habig *et al*., 1974). In addition, there is evidence that GST has a role in the regulation of plant growth and development (Jiang *et al*., 2010).

4.3. Sorption and Desorption Efficiency of C. reinhardtii to Penoxsulam

The biosorption isotherm models (Figure 5 and 6) are extensively used to evaluate the maximum biosorption capacity, the concentration of treated effluent, the distribution of polluted agents in the bulk solution and on the biomass, which could all be described by one or more isotherms such as the Langmuior model and Freundlich that are the most commonly used.

The Langmuir's isotherm model describing the Adsorption of Adsorbate onto the surface of the Adsorbent requires three assumptions (Langmuir, 1981):

1. The surface of the adsorbent is in contact with a solution containing an adsorbate which is strongly attracted to the surface.
2. The surface has a specific number of sites where the solute molecules can be adsorbed.
3. The adsorption involves the attachment of only one layer of molecules to the surface, i.e. monolayer adsorption.

The Langmuir model assumes a monolayer adsorption with a homogenous distribution of the adsorption sites and adsorption energies without interaction between the adsorbed molecules. The Langmuir adsorption isotherm model describes quantitatively the formation of a monolayer adsorbate on the outer surface of the adsorbent; hence, no f urther adsorption takes place. On the other hand, in the Freundlich model, the energetic distribution at the sites is heterogeneous due to diversity of adsorption sites and the diverse nature of the adsorbate.

The Langmuir isotherm model best fitted the experimental data for the sorption of herbicide by both the wild and transgenic alga. The results in the current study are concomitant with Ramadoss and Subramaniam (2018) who found out that the Langmuir isotherm model shows clear data about the experimental adsorption of chromium on blue green marine algae with an R^2 value of 0.90. R^2 values of Langmuir are highly significant with the experimental data. In the present study, the value of the Langmuir adsorption equilibrium constant k_L is 0.05 for transgenic alga. This shows quantitatively the clear affinity between the herbicide and transgenic alga. These results are also in accordance with Ramadoss and Subramaniam (2018) who observed that the Langmuir adsorption equilibrium constant k_L was 0.0354. Suwannahong *et al.* (2014) found out that fly ash may possess a homogeneous as well as a heterogeneous surface energy distribution that describes the formation of monolayer and heterolayer solute (Herbicide; Paraquat, Alachlor) coverage on the surface of the adsorbent (fly ash). Ho Kyong Shon (2008) has found that the adsorption of metsulfuron-methyl onto titanium oxide and powdered activated carbon fitted the Langmuir isotherm model with a r easonable degree of accuracy with higher R^2 values than those of the Freundlich isotherm model.

In conclusion, transgenic alga C. GST3 plays an effective role in the biosorption and bioremediation of the herbicide penoxsulam. The overexpression of GST improved the phycoremediation capacity of transgenic alga

through the reduction of the stress generated by xenobiotics.

References

Bulucea CA, Rosen MA, Mastorakis NE, Bulucea CA and Brindusa CC. 2012. Approaching Resonant Absorption of Environmental Xenobiotics Harmonic Oscillation by Linear Structures. *Sustainability*, **4**: 561-573.

Chomczynski P and Mackey K. 1995. Substitution of chloroform by bromo-chloropropane in the single-step method of RNA isolation. *Anal Biochem*, **225**:163-164.

Cummins I, Dixon DP, Freitag-Pohl S, Skipsey M and Edwards R. 2011. Multiple roles for plant glutathione transferases in xenobiotic detoxification. *Drug Metab Rev*, **43**: 266-280.

Deavall DG, Martin EA, Horner JM and Roberts R. 2012. Drug-induced oxidative stress and toxicity. *J Toxicol*, **64**: 54-60.

Ding N, Wang A, Zhang X, Wu Y, Wang R and Cui H. 2017. Identification and analysis of glutathione-*s*-transferase gene family in sweet potato reveal divergent GST-mediated networks in aboveground and underground tissues in response to a biotic stresses. *BMC Plant Biol*, **17**: e225.

Freundlich H. 1906. Adsorption in solution. *Phy Chem Soc*, **40**:1361-1368.

Gorman DS and Levine RP. 1965. Cytochrome f and plastocyanin: their sequence in the photosynthetic electron transport chain of *Chlamydomonas reinhardt*i. *Proc Natl Acad Sci USA*, **54**:1665-1669.

Habig WH, Pabst MJ and Jakoby WB. 1974. Glutathione-*s*-transferases. The first enzymatic step in mercapturic acid formation. *J Biol Chem*; **249**(22): 7130-7139.

Harris E H. 2001. *Chlamydomonas* as a Model Organism. *Annu. Rev. Plant Physiol. Plant Mol Biol*, **52**: 363-406.

Herve C, de Franco PO, Groisillier A, Tonon T and Boyen C. 2008. New members of the glutathione transferase family discovered in red and brown algae. *Biochem J*, **412**(3): 535-44.

Ho Kyong S, Seoung-Hyun K, Hao Ngo H and Vigneswaran S. 2008. Adsorption and photocatalysis kinetics of herbicide onto titanium oxide and powdered activated carbon. *Sep Purif Technol*, **58**: 335-342.

Jiang HW, Liu MJ, Chen C, Huang CH, Chao LY and Hsieh HL. 2010. A glutathione-*s*-transferase regulated by light and hormones participates in the modulation of *Arabidopsis* seedling development. *Plant Physiol*, **154**: 1646– 1658.

Kebeish R, Aboelmy M, El-Naggar A, El-Ayouty Y and Peterhansel C. 2015. Simultaneous overexpression of cyanidase and formate dehydrogenase in *Arabidopsis thaliana* chloroplasts enhanced cyanide metabolism and cyanide tolerance. *Environ Exp Bot*, **110**: 19-26.

Kebeish R and Al-Zoubi O. 2017. Expression of the cyanobacterial enzyme cyanase increases cyanate metabolism and cyanate tolerance in *Arabidopsis*. *Environ Sci Pollut Res Int*, **12**:11825-11835.

Komives T, Gullner G and Kiraly Z. 1998. Role of glutathione and glutathione- related enzymes in response of plants to environmental stress. *Ann NY Acad Sci*, **851**: 251-258.

Koncz C, and Schell J. 1986. The promoter of TL-DNA gene 5 controls the tissue-specific expression of chimeric genes carried by a novel type of *Agrobacterium* binary vector. *Mol Gen Genet*, **204**: 383-396.

Kumar S, Asif MH, Chakrabarty D, Tripathi RD, Dubey RS and Trivedi PK. 2013a. Differential expression of rice lambda class GST gene family members during plant growth, development, and in response to stress conditions. *Plant Mol Biol Rep*, **31**: 569–580.

Kumar S, Asif MH, Chakrabarty D, Tripathi RD, Dubey RS and Trivedi PK. 2013b. Expression of a rice lambda class of glutathione-*s*-transferase, OsGSTL2, in *Arabidopsis* provides tolerance to heavy metal and other abiotic stresses. *J Hazard Mater*, **248–249**: 228–237.

Kumar SV, Misquitta RW, Reddy VS, Rao BJ and Rajam MV. 2004. Genetic transformation of the green alga-*Chlamydomonas reinhardtii* by *Agrobacterium tumefaciens*. *Plant Sci*, **166**: 731-738.

Langmuir I. 1918. The adsorption of gases on plane surfaces of glass, mica and platinum. *J Am Chem Soc*, **40**: 1361-1403.

Liu XF and Li JY. 2002. Characterization of an ultra-violet inducible gene that encodes glutathione S-transferase in *Arabidopsis thaliana*. *Acta Genet Sin*, **29**: 458–460.

Loyall L, Uchida K, Braun S, Furuya M and Frohnmeyer H. 2000. Glutathione and a UV light–induced glutathione-*s*-transferase are involved in signaling to chalcone synthase in cell cultures. *Plant Cell*, **12**: 1939–1950.

Ma J. 2002. Differential sensitivity to 30 herbicides among populations of two green algae *Scenedesmus obliquus* and *Chlorella pyrenoidosa*. *Bull Environ Contam Toxicol*, **68**:275-281

Merchant SS, Prochnik SE, Vallon O, Harris EH, Karpowicz SJ, Witman GB, Terry A, Salamov A, Fritz-Laylin LK, Marechal-Drouard L and Marshall WF. 2007. The *Chlamydomonas* genome reveals the evolution of key animal and plant functions. *Sci*., **318**: 245 - 251.

Mishra DJ, Singh R, Mishra UK and Shahi SK. 2013. Role of bio-fertilizer in organic agriculture: A review. *Res J Recent Sci*, **2**: 39-41.

Mueller LA, Goodman CD, Silady RA and Walbot V. 2000. AN9, a petunia glutathione-s-transferase required for anthocyanin sequestration, is a flavonoid-binding protein. *Plant Physiol*, **123**: 1561–1570.

Nianiou-Obeidat I, Madesis P, Kissoudis C, Voulgari G, Chronopoulou E and Tsaftaris A. 2017. Plant glutathione transferase-mediated stress tolerance: functions and biotechnological applications. *Plant Cell Rep*, **36**: 791-805.

Niessen M, Thiruveedhi K, Rosenkranz R, Kebeish R, Hirsch HJ, Kreuzaler F and Peterhansel C. 2007. Mitochondrial glycolate oxidation contributes to photorespiration in higher plants. *J Exp Bot*; **58**: 2709-2715.

Noctor G, Arisi ACM, Jouanin L, Kunert KJ, Rennenberg H and Foyer CH. 1998. Glutathione biosynthesis, metabolism and relationship to stress tolerance explored in transformed plants. *J Exp Bot*, **49**: 623-647.

Nour El-Dien FA, Frag EYZ, Mohamed GG and Elmorsy K. 2010. Extractive spectrophotometric determination of sulphonamide drugs in pure and pharmaceutical preparations through ion-pair formation with molybdenum (V) thiocyanate in acidic medium. *J Adv Res*, **1**: 215-220.

Oakley AJ. 2011. Glutathione transferases: a structural perspective. *Drug Metab Rev*, **43**: 138-151.

Popescu CE and Lee RW. 2007. Mitochondrial genome sequence evolution in *Chlamydomonas*. *Genetics*, **175**: 819 - 826.

Prado R, Rioboo C, Herrero C and Cid A. 2009. The herbicide paraquat induces alterations in the elimental and biochemical composition of non-target microalgal species. *Chemosphere*, **76**:1440-1444.

Qi YC, Zhang SM, Wang LP, Wang MD and Zhang H. 2004. Overexpression of GST gene accelerates the growth of transgenic *Arabidopsis* under salt stress. *J Plant Physiol Mol Biol*, **30**: 517-522.

Ramadoss R and Subramaniam D. 2018. Adsorption of chromium using blue green algae-modeling and application of various isotherms. *Int J Chem Technol*, **10**: 1-22.

Reichel C, Mathur J, Eckes P, Langenkemper K, Koncz C, Schell J, Reiss B and Maas C. 1996. Enhanced green fluorescence by the expression of an Aequorea victoria green fluorescent protein mutant in mono-and dicotyledonous plant cells. *Proc Natl Acad Sci USA*, **93**: 5888-5893.

Robert RLG. 1979. Growth measurements. Division rate. In: Stein, R.J. (Ed.), **Physiological Methods. Culture and Growth Measurements**. Cambridge University Press, Cambridge, pp. 275.

Shamaan, N.A. 2005. Biochemistry of xenobiotics towards a healthy lifestyle and safe environment. Penerbit Universiti Putra Malaysia, http://www.penerbit.upm.edu.my.

Suwannahong K, Supa W, Chaysuk J and Kreetachat T. 2014. Adsorption of Herbicide onto Fly Ash Sample from Aqueous Solution. *Adv Mater Res*, **955-959**: 2118-2122.

Toribio F, Martinez-Lara E, Pascual P and Lopez-Barea J. 1996. Methods for purification of glutathione peroxidase and related enzymes. *J Chromatogr B Biom Appl*, **684**(1-2):77-97.

Whitcomb CE. 1999. An introduction to ALS-inhibiting herbicides. *Toxicol Ind Health*, **15**: 232-240

Zhang Y, Liu J, Zhou Y, Gong T, Wang J and Ge Y. 2013. Enhanced phytoremediation of mixed heavy metal (mercury)–organic pollutants (trichloroethylene) with transgenic alfalfa co-expressing glutathione-s-transferase and human P450 2E1. *J Hazard Mater*; **260**:1100-1107.

JJBS

Volume 12, Number 5,December 2019
ISSN 1995-6673
Pages 625 - 635

Jordan Journal of Biological Sciences

The Effectiveness of the Functional Components of Grape (*Vitis vinifera*) Pomace as Antioxidant, Antimicrobial, and Antiviral Agents

Alaa A. Gaafar[1*], Mohsen S. Asker[2], Ali M.A.[3] and Zeinab A. Salama[1]

[1] *Plant Biochemistry Department, ID: 60014618;* [2]*Microbial Biotechnology Department, ID: 60014618;* [3]*Center of Scientific Excellence for Influenza Viruses, National Research Centre, ID: 60014618, Dokki, Giza, P.O. 12622 Egypt*

Received March 13, 2019; Revised April 1, 2019; Accepted April 7, 2019

Abstract

This research describes the effectiveness of the bioactive compounds of two varieties of grape pomace (Romy and Banaty) extracts as antioxidant, antimicrobial, and antiviral agents. The antioxidant activity was assessed using $DPPH^{\bullet}$, $ABTS^{\bullet+}$ assays reducing power and iron-chelating methods. The results show that the total flavonoid (TF), total phenolic (TP), and total tannin (TT) of the red grape pomace (Romy) were high (17.38 mg/g DW, 16.39 mg/g DW and 5.79 mg/g DW) respectively, while for the white grape pomace (Banaty), these were (11.09 mg/g DW, 6.61 mg/g DW and 2.45 mg/g DW respectively. When using HPLC for the phenolic profile detection, the red grape 80 % acetone extract exhibited a high content of phenolic compounds, above all benzoic and pyrogallol compounds (122.54 and 44.11 mg/100g, respectively). While the chlorogenic compounds were mostly found in the red pomace aqueous extract (34.20 mg/100g). The highest antioxidant and antimicrobial activities were spotted in the red pomace extract. The red grape pomace has an antiviral activity slightly higher than that of the white grape pomace and the aqueous extract at 400µg was much better than the ethanol and acetone extracts. This study highlights the possibility of using grape pomace to develop new potential sources in the pharmaceutical industry as an antioxidant, antimicrobial, and antiviral materials.

Keywords: Antimicrobial, Antioxidant, Antiviral activities, Grape pomace, Phenolics.

1. Introduction

Grapes are among the most considerable and widely consumed fruits around the world. The prominence of grapes and their products is on the rise because of the many health benefits of this fruit to humans. Different grape extracts have been considered to be industrial derivatives of whole grapes, which contain high concentrations of phenols, flavonoids, and linoleic acid (Rathi and Rajput, 2014). As a byproduct, the grape pomace results during juice and wine industries. It consists of several parts: 1) the skin and pulp (10-12 %), 2) the seeds (2-6 %), and 3) part of the stalks (2.5-7.5 %) (Yu and Ahmenda, 2013). Grape pomaces are distinguished by their high contents of polyphenols and health phytochemical compounds due to the insufficient extraction through the process of grape processing. These phenols are known to be effective secondary plant-metabolite compounds that have beneficial properties for human health due to their antioxidant, antimicrobial, antiviral, anticancer and anti-inflammatory activities. Also, the agro-industrial residue of the grape pomace is rich in effective compounds that can be used in the pharmaceutical, cosmetic and food additives (Fontana *et al*., 2013). Strong correlations were confirmed between the presence of bioactive phenolic compounds and previous biological activities (Peixoto *et al*., 2018). In this context, the aim of the present study is to determine the active phenolic ingredients of the grape pomace and their effectiveness as antioxidant, antimicrobial and antiviral agents.

2. Material and Methods

2.1. Chemicals

$ABTS^{\bullet+}$ (2, 2'-azinobis (3-ethylbenzothiazoline- 6-sulfonic acid)), Folin–Ciocalteau reagents, Gallic acid, Quercetin, $DPPH^{\bullet}$ (2, 2-diphenyl-1-picrylhydrazyl), Ferrozine: (3-(2- pyridyl)- 5, 6-bis- (4-phenylsulfonic acid) -1,2,4-triazine, BHT: Butyl Hydroxytoluene and, potassium ferricyanide, were purchased from Sigma Chemical Co. (St. Louis, MO, USA).

2.2. Preparation of Samples

Two varieties of grapes (*Vitis vinifera*) (Romy and Banaty) were obtained from the local market in Giza-Cairo. The grapes were pressed, and the pressed residues were considered the grape pomace. Furthermore, each variety of pomace was dried at 40 °C in an air-circulating

* Corresponding author. e-mail: dr.gaafar2308@hotmail.com.

oven for constant weight. The dried pomace was ground in a knife mill, and vacuum-packed and stored at – 4 °C until analysis.

2.3. Preparation of Red and White Grapes Pomace Extracts

The dried powder (100 g) of the grape pomace was dispensed separately in 1 L of three different solvents as distilled water, 80 % ethanol and 80 % acetone, overnight at room temperature using a shaker. Each mixture was filtered through Whatman No. 1 filter paper, and the extraction step was repeated three times. The ethanol and acetone filtrates were concentrated at 40 °C in a rotary evaporator under vacuum, and the water was completely dried by lyophilization. The dried crude extracts were stored in a refrigerator until analysis.

2.4. Chemical Studies

2.4.1. Total Phenolic

The total phenolic (TP) was determined by Folin Ciocalteu reagent assay using Gallic acid as standard according to Singleton and Rossi (1965). A suitable aliquot (1 mL) of both local grape varieties was added into a 25 mL volumetric flask, containing 9 mL of distilled water. One milliliter of Folin Ciocalteu`s phenol reagent was added to the mixture and shaken. After five minutes. 10 mL of the 7 % Na_2CO_3 solution was added to the mixture. The solution was diluted to 25 mL with distilled water and mixed. After incubation for ninety minutes at room temperature, the absorbance was determined at 750 nm with a spectrophotometer (Unicum UV 300) against the prepared reagent as blank. The total phenolic content in the samples was expressed as mg Gallic acid equivalents (GAE)/g dry weight. All samples were analyzed in triplicates.

2.4.2. Total Flavonoid

The total flavonoid (TF) was determined by the aluminum chloride method using quercetin as a standard (Zhishen *et al*., 1999). One mL of both of the local grape pomace extracts was added into a 10 mL volumetric flask, containing 4 mL of distilled water. To the flask, 0.3 mL of $NaNO_2$ (5 %) was added and after five minutes, 0.3 mL of $AlCl_3$ (10 %) was added. After the sixth minute, 2 mL of 1M NaOH was added, and the total volume was made up to 10 mL with distilled water. The solutions were mixed well and the absorbance was measured against a prepared reagent blank at 510 nm using a spectrophotometer (Unicum UV 300). The total flavonoids in the samples were expressed as mg quercetin equivalents (QE)/ g dry weight. The samples were analyzed in triplicates.

2.4.3. Total Tannins

The total tannin (TT) was measured using the Folin-Ciocalteu reagent according to Polshettiwar *et al*. (2007). One mL of both of the local grape pomace extracts was added to 7.5 mL of distilled water (dH_2O) and then 0.5 mL of Folin reagent and 1 ml of sodium carbonate solution (35 %) were added. The volume was made up for 10 mL with distilled water, and absorbance was measured against prepared reagent blank at 775 nm using a spectrophotometer (Unicom UV 300). The total tannins in the samples were expressed as mg tannic acid equivalent (TE)/g dry weight. All of the samples were analyzed in triplicates.

2.4.4. Identification and Quantitation of Phenolic Compounds by HPLC

The phenolic compounds in the grape pomace (aqueous, 80 % ethanol and 80 % acetone) extracts were identified using HPLC according to Ben-Hammouda *et al.* (1995). All chemicals and solvents used were of an HPLC spectral grade, and were obtained from Sigma (St. Louis, USA (and Merck –Shcuchrdt Munich, Germany).

The HPLC system is Agilent 1100 series coupled with DAD detector (G1315B) and (G1322A) DEGASSER. Sample injections of 5 µL were made from an Agilent 1100 series auto-sampler. The chromatographic separations were performed on ZORBAX-EclipseXDB-C18 column (4.6×250 mm, particle size 5 µm). A constant flow rate of 1 mL/min was used with mobile phases: (A) 0.5 % acetic acid in distilled water at pH 2.65; and solvent (B) 0.5 % acetic acid in 99.5 % acetonitrile. The elution gradient was linear starting with A and ending with B over fifty minutes, using a DAD detector set at a wavelength of 280 nm. The phenolic compounds of the grape pomace extracts were identified by comparing their retention times with those of the standard mixture chromatogram. The concentration of an individual compound was calculated on the basis of peak area measurements, and the results were expressed as mg phenolic/100 g dry weight.

2.5. Antioxidant Activity

2.5.1. DPPH· Free Radical Scavenging Activity

The determination of $DPPH^{\cdot}$ (2, 2-diphenyl-1-picrylhydrazyl) free radical scavenging activity was measured spectrophotometrically according to Chu *et al.* (2000). 0.1 mM of $DPPH^{\bullet}$ in methyl alcohol was prepared and 0.5 mL of this solution was added to 1 ml of three grape pomace extracts at different concentrations (25, 50, 75, 100 µg/mL). Methanol was used as a blank. The mixture was shaken vigorously, and allowed to stand at room temperature (for thirty minutes.). Butyl Hydroxytoluene (BHT, Sigma) was used as positive control; and negative control contained the entire reaction reagent except for the extracts. Then the absorbance was measured at 515 nm against a blank.

The capacity to scavenge the $DPPH^{\cdot}$ radical was calculated using the following equation:

$$DPPH^{\cdot} \text{ scavenging activity } \% = [(A_c - A_s) / A_c] \times 100$$

Where (A_c) is the absorbance of the negative control reaction, and (A_s) is the absorbance in the presence of the plant extracts. The results were expressed as IC_{50} (the concentration (µg/mL) of the grape pomace extracts that scavenge 50 % of $DPPH^{\cdot}$ radical).

2.5.2. ABTS·+ Scavenging Activity

The $ABTS^{\bullet+}$ assay was generated by the oxidation of $ABTS^{\bullet+}$ with potassium persulphate. Arnao *et al*., (2001). $ABTS^{\bullet+}$ was dissolved in deionized water to a 7.4 mM concentration, and potassium persulphate was added to a concentration of 2.6 mM. The working solution was then prepared by mixing the two stock solutions in equal quantities and allowing them to react for twelve to sixteen hours at room temperature in the dark. The solution was then diluted by mixing the 1mL $ABTS^{\bullet+}$ solution with 60 mL of methanol to obtain an absorbance of 1.1 ± 0.02 at 734 nm using a spectrophotometer. A fresh $ABTS^{\bullet+}$ solution was prepared for each assay. The grape pomace

extracts (150 µL) at different concentrations (25, 50, 75, 100 µg/mL) were allowed to react with 2850 µL of the $ABTS^{\bullet+}$ solution for two hours in the dark. Then the absorbance was taken at 734 nm using the spectrophotometer. Results were expressed in comparison with the standard Trolox. The activity to scavenge the $ABTS^{\bullet+}$ radicals was calculated using the following equation:

$ABTS^{\bullet+}$ scavenging activity % = $[(A_0 - A_1) / A_0] \times 100$

Where A_0 is the $ABTS^{\bullet+}$ absorbance of the control reaction, and A_1 is the $ABTS^{\bullet+}$ absorbance in the presence of the sample. The results were expressed as IC_{50} (the concentration µg/ml of the grape pomace extracts that scavenge 50 % of $ABTS^{\bullet+}$ radical)

2.5.3. Reducing Power

The reducing power was assayed spectrophotometrically (Kuda *et al*., 2005). One ml of the grape pomace extracts at different concentrations (25, 50, 75, 100 µg/mL) were mixed with 2.5 ml of phosphate buffer (50 mM, pH 7.0) and 2.5 mL of potassium ferricyanide (1 %). The mixture was then incubated at 50 °C for twenty minutes. After the addition of 2.5 mL of trichloroacetic acid (10 %) to the mixture, centrifugation at 3000 rpm for ten minutes was performed. Finally, 1.25 mL from the supernatant was mixed with 1.25 mL of distilled water and 0.25 mL of a $FeCl_3$ solution (0.1%, w/v). The absorbance was measured at 700 nm. BHT was used as a standard. The results were expressed as EC_{50} (the concentration µg/mL of the grape pomace extracts that provided the reading of 0.5 absorbance's at 700 nm).

2.5.4. Ferrous Chelating Activity

The ferrous ion chelating activities were assessed colorimetrically (Hsu *et al*., 2003). One ml of the grape pomace extracts or EDTA solution (as a positive control at different concentrations (25, 50, 75, 100 µg/mL) was spiked with 0.1 mL of 2 mM $FeCl_2$- $4H_2O$. 0.2 mL of a 5 mM ferrozine solution and 3.7 mL of methanol were mixed in a test tube and reacted for ten minutes at room temperature. The absorbance was then measured at 562 nm. The mixture without the extract was used as the control. A lower absorbance indicates a higher ferrous ion chelating capacity.

The percentage of the ferrous ion chelating ability was calculated using the following equation:

Chelating activity (Inhibition %) = $[(A_c - A_s) / A_c] \times 100$

Where (A_c) is the absorbance of the control reaction, and (A_s) is the absorbance in the presence of the plant extracts. The results were expressed as IC_{50} (the concentration (µg/mL) of the grape pomace extracts that chelate 50 % of Fe^{2+} ions).

2.6. Antimicrobial Activity

2.6.1. Microbial Strains

Bacillus subtilis NRRL B-94, Escherichia coli NRRL B-3703, Pseudomonas aeruginosa NRRL, Staphylococcus aureus NRRL, Aspergillus niger NRRL313, Aspergillus flavus NRC, Saccharomyces cerevisiae NRC and Candida albicans NRRL477. The bacterial strains were cultured on a nutrient medium, while the fungi and yeast strains were cultured on a malt medium and a yeast medium, respectively.

2.6.2. Antimicrobial Activity of Grape Pomace Extracts

The disk diffusion method was used to evaluate the antimicrobial activity of each of the grape pomace extracts. The grape pomace extract residues (200, 400 and 600 µg/mL) were re-dissolved in 1 ml of a corresponding solvent (water, ethanol, and acetone) sterilized through Millipore filter (0.22 mm). Ten mL of an agar medium (nutrient, malt, and yeast) was poured into sterile Petri dishes followed with 15 mL of a seeded medium previously inoculated with the bacterial suspension to attain a 10^5 CFU/mL of medium. These microorganisms were cultured and incubated at 37°C for twenty-four hours. The inoculums' suspension was spread uniformly over the agar plates using a spreader, for a uniform distribution of bacteria. Subsequently using a sterile borer, a well of 0.6 cm diameter was made in the inoculated media then 100 µL of each extract was added, and the control Ciprofloxacin (10 µg) was filled into the well. The solvent was used as negative control. The plates were kept in the fridge at 4°C for two hours to permit the grape pomace extract diffusion. They were incubated at 35°C for twenty-four hours. The presence of inhibition zones was measured and considered an indication of antibacterial activity (Scott, 1989).

2.6.3. Determination of Minimum Inhibitory Concentrations (MIC) of the Effective Extract

MIC is defined as the lowest concentration of the antimicrobial agent that inhibits the microbial growth after twenty-four hours of incubation on the agar plates (NCCLS, 1990). The most effective grape pomace extracts which exhibited a strong antibacterial activity at 10 mg/mL were manipulated to determine their MIC using the disk diffusion method. Different concentrations of the effective grape pomace extracts (100-600 µg/mL) were prepared separately, sterilized through Millipore filter and their requisite amount was loaded over sterilized filter paper discs (8 mm in diameter). Agar was poured unto the sterile Petri dishes seeded with the microbial suspensions of the pathogenic strains. The loaded filter paper discs with different concentrations of the effective grape pomace extracts were placed on the top of the agar plates. The plates were kept in the fridge at 4°C for two hours, and were then incubated at 35°C for twenty-four to forty-eight hours

2.6.4. Mode of Action

The effects of different concentrations of the ethanolic extract on some biochemical activities were studied. Immediately after incubating the flasks with *B. subtilis* (for twenty-four hours), the cells were harvested during the middle logarithmic growth phase, and an aqueous extract was applied in concentrations of 1/4 and 1/2 MIC. Each test was repeated three times. Subsequently, the flasks were shaken using a rotary shaker of 150 rpm at 30°C. The samples were withdrawn at the onset of the experiment and after incubation periods of 24, 48, 72, 96, 120 and 144 minutes. The bacterial cells were subjected to the following determinations: total acid-soluble phosphorus compounds (Hogeboom and Schneider, 1950; Chen *et al*., 1956), total lipids (Bligh and Dyer, 1959; Knight *et al*., 1972), total soluble protein (Daughaday *et al*., 1952; Bradford, 1976), and total nucleic acids (Burton, 1957).

2.7. Antiviral Bioassay:

2.7.1. MTT Cytotoxicity Assay (TC50)

The extracts were diluted with Dulbecco's Modified Eagle's Medium (DMEM). The stock solutions of the test extracts were prepared in 10 % DMSO in ddH_2O. The cytotoxic activity of the extracts was tested in Madin-Darby Canine kidney (MDCK) cells by using the 3-(4, 5-dimethylthiazol-2-yl)-2, 5-diphenyltetrazolium bromide (MTT) method with minor modification (Mossman, 1983). Briefly, the cells were seeded in 96 well plates (100 µL/well at a density of 3×10^5 cells/mL) and were incubated for twenty-four hours at 37 °C in 5 % CO_2. After twenty-four hours, the cells were treated with various concentrations of the tested extracts in triplicates. After further twenty-four hours, the supernatant was discarded, and the cell monolayers were washed with a sterile phosphate buffer saline (PBS) three times. The MTT solution (20 µL of 5 mg/ml stock solution) was added to each well and incubated at 37 °C for four hours followed by medium aspiration. In each well, the formed formazan crystals were dissolved with 200 µL of acidified isopropanol (0.04 M HCl in absolute isopropanol = 0.073 ml HCl in 50 mL isopropanol). The absorbance of formazan solutions was measured at λmax 540 nm with 620 nm as a reference wavelength using a multi-well plate reader. The percentage of cytotoxicity compared to the untreated cells was determined with the following equation: $\%\ \text{Cytotoxicity} = [(A_0 - A_t) / A_0] \times 100$
Where A_0 is the absorbance of the cell without treatment, and A_t is the absorbance of the cell with treatment

The plot of % cytotoxicity versus the sample concentration was used to calculate the concentration which exhibited 50 % cytotoxicity (TC_{50})

2.7.2. Plaque Reduction Assay

The assay was carried out according to the method of Hayden *et al*., (1980) in a six-well plate where MDCK cells (10^5 cells/mL) were cultivated for twenty-four hours at 37°C. A/Chicken/ Egypt/M7217B/1/ (H5N1) virus was diluted to give a 104 PFU/ well, and was mixed with the safe concentration of the tested extracts and incubated for one hour at 37 °C before being added to the cells. The growth medium was removed from the cell culture plates and the cells were inoculated with (100 µL/well) virus. After one hour contact time for the virus adsorption, 3 mL of DMEM supplemented with 2 % agarose, and the tested compounds were added onto the cell monolayer. The plates were left to solidify and were incubated at 37 °C till the formation of viral plaques (3 to 4 days). Formalin (10 %) was added for two hours, then the plates were stained with 0.1 % crystal violet in distilled water. Control wells were included where the untreated virus was incubated with MDCK cells, and finally, the plaques were counted, and the percentage of reduction in the plaques' formation in comparison to the control wells was recorded as following
Inhibition (%) = viral count (untreated) -viral count (treated) / viral count (untreated) x100.

2.8. Statistical Analysis

Data were statistically analyzed using Costat statistical package (Anonymous, 1989).

3. Results and Discussion

3.1. Phenolics, Flavonoids, and Tannins Compounds

Table 1 shows that the red grape acetone (80 %) pomace extract had the highest level of TP, TF, and TT respectively. The lowest values of the same parameters were spotted with the ethanol (80 %) extract. The total phenolic content exhibited much higher TP (17.38 ± 0.19 mg/g) in the red grape acetone (80 %) pomace extract (0.81, 1.79, and 2.91 mg/g) than in the sesame cake, sugar beet pulp, and potato peels correspondingly (Mohdaly *et al*., 2010), and (5.60 and 4.90 mg/g) in blueberries and blackberries (Yu *et al*., 2005). It was extremely lower than that (62.00 mg /g) in tea leaves (Lee *et al*., 2005), (32.10-52.70 mg/g) and (15.00-20.30 mg/g) in grape seeds and grape skins (Yilmaz, 2002). There was a considerable distinction between the flavonoids content of grape pomace extracts for each variety. The very best level has been revealed in the acetone extract (16.39± 0.15 mg/g) followed by the aqueous and ethanolic extracts respectively. The white grape pomace aqueous extract manifested the very best amount (9.69± 0.12 mg/g) of flavonoids followed by the acetone and ethanol extracts. The Tannins content exhibited a similar tendency as TP and was the very best for the red and white grape pomace acetone extracts followed by the aqueous extracts, while the ethanolic extracts showed the lowest values for each variety (Table 1).

Table. 1. Bioactive compounds of grape pomace extracts

Extracts	TP (mg GAE/ g)		TF (mg QE/g)		TT (mg TE/g)	
	Red grape (Romy)	White grape (Banaty)	Red grape (Romy)	White grape (Banaty)	Red grape (Romy)	White grape (Banaty)
Aqueous	11.69 ^{b}± 0.12	7.02 ^{b}± 0.09	10.63 ^{b} ± 0.14	9.69 ^{c}± 0.12	4.38 ^{b} ± 0.04	3.22 ^{c} ± 0.04
Ethanol 80%	10.79 ^{a}± 0.23	5.81 ^{a}± 0.09	10.15 ^{a}± 0.14	5.89 ^{a} ± 0.20	3.32^{a}± 0.04	1.60 ^{a}± 0.03
Acetone 80%	17.38 ^{c}± 0.19	11.09 ^{c}± 0.19	16.39 ^{c}± 0.15	6.61 ^{b} ± 0.11	5.79 ^{c}± 0.03	2.45 ^{b} ± 0.02
LSD at 0.05	0.51	0.29	0.16	0.36	0.06	0.08

All values are the mean of three replicates ± S.D. Values with different letters are significantly different at $p \leq 0.05$.

A substantial diversity between the solvents at ($p \leq 0.05$) was discovered for the TP, TF, and TT contents. The separation and extraction of phenolic compounds from plant samples are influenced by the composition and sort of phenolic compounds as well as the polarity of the solvents used (Zhao *et al*., 2006). Condensed tannins (CT), which are also called proanthocyanidins, give too harsh tastes for grapes and wines (Alipour and Rouzbehan 2010; Fontoin *et al*., 2008). Prior *et al*. (2001) reported that about 32 to 54 % of the antioxidant capacity in blueberries, grapes, and cranberries can be accounted for by condensed tannins.

3.2. High- Performance Liquid Chromatograph (HPLC)

The HPLC could be the favored technique of separation and quantification of phenolic compounds (Lee *et al*., 2003). Considerable factors have an effect on the HPLC assessment of phenolics, which includes sample purification, column kinds, mobile phase, varieties and detectors (Katsube *et al*., 2004). Purified phenolics are utilized to an HPLC device making use of a reversed-phase C18 column (RP-C18), photograph diode array detector (PDA) (Lapornik *et al*., 2005). The phenolic compounds analyzed by HPLC are given in Table 2.

The results manifest that all extracts contained different components and contents of phenolic compounds.

Table 2. Identification of individual phenolics in different extracts of grape pomace

Phenolic compounds (mg/100g DW)	Red grape (Romy)			White grape (Banaty)		
	Aqueous	Ethanol 80%	Acetone 80%	Aqueous	Ethanol 80%	Acetone 80%
Ellagic	13.73	11.89	23.02	14.94	9.94	14.99
Tannic acid	2.04	7.16	17.52	2.59	3.42	6.34
Chlorogenic	34.32	19.82	-	5.90	16.54	-
Pyrogallol	44.04	38.68	44.11	36.77	7.62	9.23
Vanillic	-	-	4.87	-	-	4.22
quercetin	0.96	1.02	1.49	-	-	-
Benzoic	129.26	119.55	122.54	128.72	107.24	135.62
Rutin	-	-	-	0.08	0.07	0.08
Acacetin	0.20	0.18	0.27	0.20	0.19	0.10

It is clear from Table 2 that the red and white grape pomace contains a nearly similar phenolic profile. There is a component that is found in both varieties, but they differ in concentrations. The red pomace aqueous extract shows the highest content of phenolic compounds above all benzoic, pyrogallol, chlorogenic, and ellagic compounds followed by the acetone and ethanol extracts respectively. While the ethanol extract exhibited the lowest values of phenolic compounds. Benzoic, ellagic and pyrogallol compounds were found in the aqueous and acetone extract with high values in white grape pomace, respectively. Yilmaz and Toledo (2004) found that methanol was more effective than the aqueous extract in terms of the extraction of phenolics from Muscadine seeds. Rodtjer *et al*. (2006) maintain that the yields of phenolics depend on the solvent polarity and the variety and conditions of extraction.

3.3. Activity of Antioxidant

3.3.1. DPPH• Radical Scavenging Activity

The antiradical capability is resolved as the number of extracts requisite to depress the radical concentration by 50% (Ruberto *et al*., 2007; Wang *et al*., 2010). With respect to the DPPH• assay, the antioxidant capacity (IC_{50}) of the red grape pomace had the highest DPPH• radical scavenging activity compared to the white grape pomace. The red grape aqueous extract was found to be statistically superior to the white aqueous pomace extract when all results are compared (Table 3). These outcomes were higher than that formerly reported and conveyed by Anastasiadi *et al*. (2010) in the skin of the grape varieties of *Mandilaria*, *Voidomatis*, *Assyrtiko*, and *Aidani* with IC_{50} values 55.7, 177.5, 117.0 and 274.2 µg/mL, respectively. It was found that the results of the current study are higher than those obtained by Katalinic *et al*. (2010) in the grape skin extracts of seven *Vitis vinifera* red and white varieties with the DPPH• radical-scavenging ability (IC_{50}) of 156, 209, 239, 153, 58.0, 64.2 and 158 mg/L in *Vranac*, *Trnjak*, *Rudezusa*, *Merlot*, *Babic*, *Latin*, and *Plavina*, respectively.

Table 3. *In-vitro* antioxidant activity as (IC_{50}) for red and white grape pomaces

Sample	Extracts	DPPH• IC_{50} (µg / mL)	$ABTS^{•+}$ IC_{50} (µg / mL)	Reducing Power EC_{50} (µg /mL)	Fe^{2+}-chelating IC_{50} (µg / mL)
Red grape pomace	Aqueous	$2.67^{a} \pm 0.85$	$29.22^{c} \pm 0.57$	$59.45^{b} \pm 0.47$	$143.73^{b} \pm 5.17$
	Ethanol 80%	$33.29^{d} \pm 1.10$	$56.22^{d} \pm 0.45$	$160.97^{d} \pm 1.95$	$262.67^{d} \pm 0.35$
	Acetone 80%	$21.93^{c} \pm 0.61$	$16.32^{b} \pm 0.49$	$71.89^{c} \pm 1.06$	$199.77^{c} \pm 4.06$
	BHT	$7.61^{b} \pm 0.33$	-	$11.01^{a} \pm 0.32$	-
	Trolox	-	$4.28^{a} \pm 0.20$	-	-
	EDTA	-	-	-	$1.88^{a} \pm 0.46$
L.S.D at 0.05		1.74	0.88	1.15	0.76
White grape pomace	Aqueous	$24.31^{b} \pm 1.05$	$53.38^{c} \pm 0.79$	$126.69^{c} \pm 0.32$	$250.34^{d} \pm 5.03$
	Ethanol 80%	$54.02^{d} \pm 0.35$	$78.47^{d} \pm 0.79$	$141.50^{d} \pm 3.03$	$248.35^{c} \pm 1.92$
	Acetone 80%	$39.43^{c} \pm 0.40$	$37.31^{b} \pm 0.15$	$94.58^{b} \pm 0.58$	$203.14^{b} \pm 2.53$
	BHT	$7.61^{a} \pm 0.33$	-	$11.01^{a} \pm 0.32$	-
	Trolox	-	$4.28^{a} \pm 0.20$	-	-
	EDTA	-	-	-	$1.88^{a} \pm 0.46$
L.S.D at 0.05		1.13	1.31	1.25	0.47

All values demonstrated as mean ± S.D. Mean with different letters are significantly different at $p \leq 0.05$.

Hogan *et al*. (2009) inspected the efficiency of antioxidants for three fresh wine grapes from Virginia - Cabernet Franc clone1, Norton, and Cabernet Franc clone 313, and specified their DPPH$^{\bullet}$ scavenging activities as (8.8, 7.9, and 5.4μmol TE/g, respectively). The antioxidant activity of plants can be attributed to the flavonoid and polyphenolic compounds located in them (Yilmaz and Toledo 2004). Even so, the antioxidant capability also depends on numerous variables which include genetics, environmental circumstances, industrial methods employed, date of harvest and post-harvest and storage problems (Wang and Helliwell 2001). These outcomes are in accordance with Anastasiadi *et al*. (2010) and Ruberto *et al*. (2007) for red grape peels. Also, the outcomes of white grape pomace have been comparable to those reported by Katalinic *et al*. (2010).

3.3.2. ABTS$^{\bullet+}$ Radical Scavenging Activity

The outcomes show that the grape pomace has potent scavenging capacity for the ABTS$^{\bullet+}$ radical, and really should be explored as a potent antioxidant. Advanced reports have confirmed the radical scavenging activity of the red grape pomace from the seeds and outer skin extracts (Rockenbach *et al*., 2011). The IC_{50} values of ABTS$^{\bullet+}$ radical activity are varied significantly. The high activity was observed with the acetone (80 %) extract of both grape varieties parallel to Trolox as standard (Table 3). While the ethanol (80 %) extracts of the red and white pomaces showed lower antioxidant activity.

In the current research, the red and white grape pomace extracts showed a high anti-oxidant activity to scavenging ABTS$^{\bullet+}$ radical, compared to earlier studies conducted by (González-Centeno *et al*. 2013), who studied red and white grape pomaces (193–485 and 71–134 μmol TE/g).

3.3.3. Reducing Power

The reducing power of phytochemical compounds depends on their effectiveness in transmitting electrons. In the reducing power assay, the presence of antioxidant activity in the plant extracts improves the process of reduction of ferricyanide complex to the ferrous form by electron-donating. Therefore, the reducing ability of phytochemicals is fundamental evidence of its probable antioxidant activity. The occurrence of reductants in the samples would cause the reduction of (Fe^{3+}) to (Fe^{2+}) through the donation of an electron and the creation of the Perl Prussian blue complex. This kind of complex was estimated by measuring absorbance at 700 nm (Oyaizu, 1986). It was observed that the aqueous extract of the red grape and acetone extract of the white grape pomace had a higher reducing power (EC_{50} = 59.45 ± 0.47 and 94.58 ± 0.58 μg / mL), respectively (Table 3). This is probably due to the low viscosity of the solvent which possesses a low intensity and high diffusivity that allows them to be facilely diffused into the pores of the plant materials to create their way out of the bioactive matters (Sultana *et al*., 2007). Based on the results of this study, the extracts with the maximum antioxidant activity had the highest concentration of phenols (Katalinic *et al*. 2010).

3.3.4. Fe+2-chelating Activity

The chelation is a significant parameter because ferrous is desired to transport respiration oxygen and many enzyme activities. However, ferrous is an extremely invigorate metal and can stimulate oxidative changes in protein, lipid, and other ingredients in cells. Iron is essential to every single known living being, but increased iron can be unsafe, in light of the fact that free ferrous particles respond with peroxides to create free radicals, which can harm some neurological atoms, for example, genetics, proteins, lipids, and other cell segments (Wang *et al*., 2010).

The metals chelating capability is expressed as the percentage of suppression of the Fe^{2+} complex formation with various extracts Halliwell, and Gutteridge (1984). In the existent research, all of the extracts demonstrated a significant ability to chelate metal ions (Fe^{2+}). The capacity of grape pomace to chelate Fe^{2+} is given in Table 3. This study found that both varieties could chelate Fe^{2+} efficiently and reduce free ferrous realization. The IC_{50} values of both grape pomace extracts ranged from 143.73±5.17 to 262.67±0.35. The red grape pomace aqueous extract had the highest Fe^{+2} chelating capacity (IC_{50} =143.73±5.17 μg/mL), while the red grape pomace ethanol extract had the lowest capacity (262.67±0.35 μg/mL) (Table 3).

EDTA was used as a reference to this assay and its IC_{50} value for Fe^{2+}-chelation was 1.88 μg/mL. The results are in the range of those reported by Pal *et al*. (2015) and Maniyan *et al*. (2015) for kiwi byproducts. The results can be explained by the grape pomace's high content of phytochemical compounds acting as antioxidants such as anthocyanin, phenolics, flavonoids, and chlorophyll as previously reported by Cassano *et al*. (2006). Ethanol exhibited lower chelation activities than the aqueous and acetone extracts. The highest antioxidant activity of the aqueous and acetone extracts can be also attributed to the major components present in grape pomace, above all benzoic acid, and ellagic acid in the red Romy and white Banaty grape pomace extracts. This can be clarified by distinct factors, including the existence of diverse effective components in the plant which have the ability to mutate the antioxidant capacity, the synergistic effects of unlike components, the experimental circumstances, and the mechanisms of the methods utilized for antioxidant reactions (Cho *et al*., 2003).

3.4. Antimicrobial Activity of Grape pomace Extracts

Using natural products as antimicrobials for conserving food is on the rise. It has received an increasing awareness on the part of consumers regarding the appreciation of natural foods as well as increasing attention regarding microbial impedance by ordinary preservatives (Omidbeygi *et al*., 2007). Spices' antimicrobial properties have been recognized for thousands of years in the preservation of food. Biologically active molecules in food are important to stop dangerous outcomes to free radicals; they also prevent the degradation of foods resulting from the oxidation of lipid and microbial corruption. Spices are the most notable parts in the diets of humans to transfer the taste, color, and flavors of foods. Foodborne diseases due to food exhaustion contaminated by pathogenic toxins and/or bacteria are among the most serious public health concerns. Monitoring of pathogenic microorganisms can reduce outbreaks of foodborne diseases and ensure supplying consumers with nutritious, healthy, and safe foods. Plant extracts possess antimicrobial efficacy against distinct, pathogenic microorganisms (Luther *et al*., 2007; Allahghdri *et al*., 2010). Different microbial species were

utilized to recognize the antimicrobial capacity of extracts for both varieties of grape pomace. The study of antimicrobial activity of the red and white grape pomace extracts using the agar diffusion method revealed that the ethanolic extracts from the red and white grape can restrain the growth of all microorganisms tested as displayed in Table 4. The ethanol extract of the red and white grape pomace was the most effective extract inhibiting the microbial growth of all pathogenic microorganisms tested at 600 µg/mL, while the acetone and aqueous extracts of the red and white grape pomace were mediated by effective extract inhibition of the growth of microbials when testing all pathogenic microorganisms in all concentrations. The zone result of inhibition obtained in ethanolic extracts shows a higher inhibition at a concentration of 600 µg/mL. This is consistent with the previous reports of (Bradbury and Holloway, 1988; Furneri *et al*., 2002) which maintain that those action modes of phenolic compounds are concentration-dependent. The results of the present study are in part consistent with earlier studies of grape pomace extract which found that the extracts were efficient as anti-Gram+ve bacteria (Darra *et al*., 2012; Oliveira *et al*., 2013). The potent durability of Gram-ve bacteria to the grape pomace extracts in these results might be attributed to the double cell membrane and vigorous hydrophobicity of the exterior membranes of Gram-ve bacteria; this is in agreement with Smith-Palmer *et al*. (1998).

Table 4. Antimicrobial activity of Red and White grape pomace

Samples	Extracts	Conc. (µg/ml)	Inhibition Zone Diameter (mm)							
			Bacteria				Fungus		Yeast	
			B. subtilis	*S. aureus*	*E. coli*	*P. aeruginosa*	*A. niger*	*A. flavus*	*S. cerevisiae*	*C. albicans*
Red grape pomace	Aqueous	200	00.00	00.00	00.00	00.00	00.00	00.00	00.00	00.00
		400	11.55	10.86	09.87	10.95	09.76	10.20	11.47	10.30
		600	17.70	16.54	16.16	15.73	13.83	15.50	15.60	15.26
	Ethanol 80%	200	09.11	09.00	10.00	09.00	00.00	00.00	10.00	09.00
		400	17.20	15.30	15.00	14.00	12.67	11.42	14.00	15.43
		600	28.16	27.65	25.46	25.46	20.33	17.56	25.00	21.80
	Acetone 80%	200	00.00	00.00	00.00	00.00	00.00	00.00	00.00	00.00
		400	10.66	10.53	09.67	10.61	09.80	10.33	09.27	10.60
		600	15.32	14.17	15.23	15.86	13.65	12.76	14.22	14.44
White grape pomace	Aqueous	200	00.00	00.00	00.00	00.00	00.00	00.00	00.00	00.00
		400	12.63	13.70	11.00	12.00	10.62	11.30	10.56	11.43
		600	16.66	17.57	15.46	16.57	16.75	17.81	16.87	15.71
	Ethanol 80%	200	09.00	11.00	09.00	00.00	00.00	00.00	09.00	00.00
		400	15.50	17.55	15.00	13.80	11.70	11.00	12.87	11.76
		600	24.54	26.60	20.46	19.46	19.00	16.75	23.77	20.85
	Acetone 80%	200	00.00	00.00	00.00	00.00	00.00	00.00	00.00	00.00
		400	11.66	11.73	11.00	09.00	09.64	10.30	11.62	10.87
		600	14.82	15.50	14.46	13.46	14.85	13.85	16.81	15.50

Inhibition zone diameter was measured as the clear area was centered on agar containing the sample; well with non-inhibition zone was record 0.00. The measurements are taken after 24 h incubation by yeast, 24 to 48 h with bacteria and 48 to 72 h with fungus.

3.4.1. Minimum Inhibitory Concentrations (MIC)

The effects of MIC of the white and red grape pomace extracts on behaving Gram-ve bacteria, Gram +ve bacteria, yeasts, and fungi were tested and the results are shown in Table 5.

The ethanolic and aqueous extracts of each red and white grape pomace display a vigorous antimicrobial vigor against *B. subtilis* NRRL B-94, *E. coli* NRRL B-3703, *P. aeruginosa* NRRL, *S. aureus* NRRL, *A. niger* NRRL313, *A. flavus* NRC, *S. cerevisiae* NRC, and *C. albicans* NRRL477. They possess spacious vision competence against Gram-ve bacteria, Gram +ve bacteria, and molds with MIC extending between 210 to 325 ppm. The distinction in the efficiency of the red and white grape extracts against different strains depends on permeability variances between the cells of these microbes and chemical contents of each extract; this is in harmony with Dorman and Deans, (2000).

Table 5. The MIC of red and white grape pomace

Samples	Extract	MIC (ppm)							
		Bacteria				Fungus		Yeast	
		B.subtilis	*S. aureus*	*E. coli*	*P. aueginosa*	*A. niger*	*A. fluves*	*S. cervisiae*	*C. albicans*
Red grape pomace	Aqueous	260	285	290	260	280	270	236	250
	Ethanol 80%	255	230	300	285	290	290	270	260
White grape pomace	Aqueous	265	312	260	285	310	325	320	300
	Ethanol 80%	210	215	220	227	256	260	227	224

3.4.2. Mode of Action

The effects of specific concentrations of the ethanolic extract of the white grape pomace were evaluated through the bio-synthesis of total lipids, DNA & RNA, acids soluble phosphorus, and protein in *B. subtilis* cells and the data are shown in Figures 1 and 2. The ethanolic white grape extract from the grape pomace had a significant impact on protein synthesis and total lipid in the cells of *B. subtilis* NRRL B-94 (Figure. 1 A and B). The effect is increased by increasing the concentration (1/4 and 1/2 MIC) and incubation duration. The ethanolic white grape pomace extract had a slight effect on the synthesis of DNA, RNA, and acid-soluble phosphorus (Figure 2 A- C). These results point out that the ethanolic white grape pomace extracts significantly affect protein biosynthesis by the control of a few steps in the compound interpretation processes. The ultimately remarkable antibiotics with the same procedure are tetracycline. Some chemotherapy agents are affected by the assembly of DNA or/and RNA or can join DNA or/and RNA so that their messages cannot be read. However, most drugs are non-selective, affecting animal and bacterial cells; therefore, they have no therapeutic enforcement (Sahu, 1997; Shuichi et al., 2000).

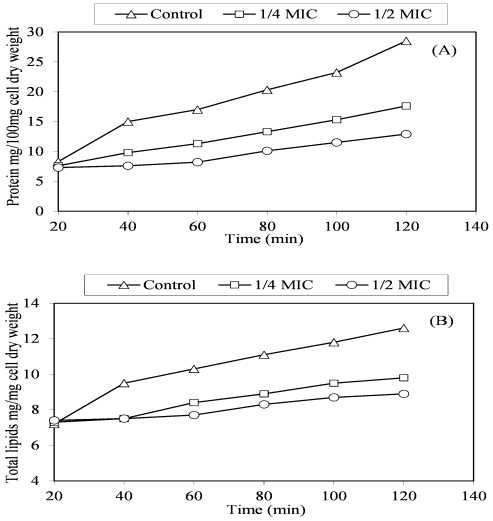

Figure 1. Effect of different concentrations of the ethanolic white grape extract on: (A) Biosynthesis of proteins. (B) Biosynthesis of total lipids in the cells of (*B. subtilis)* NRRL B 94.

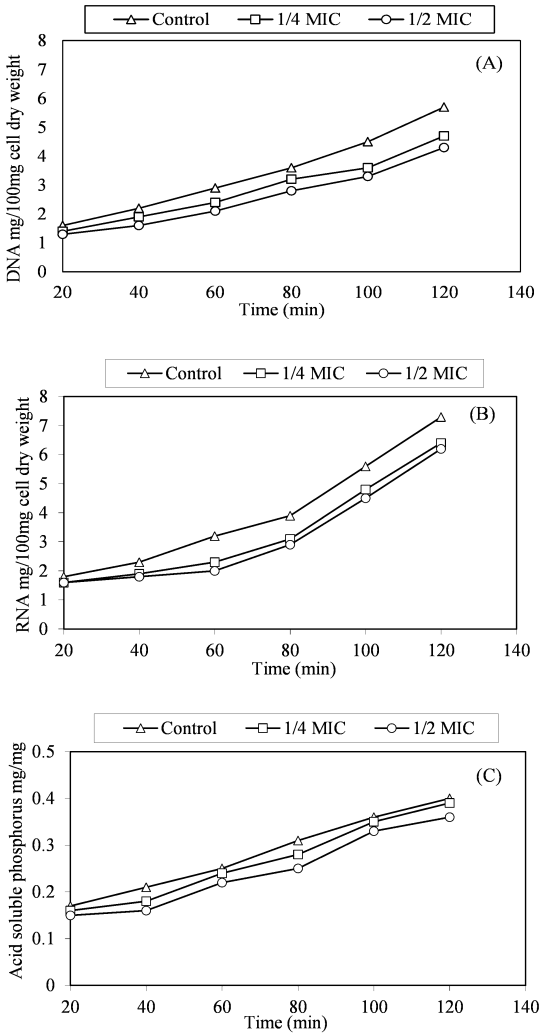

Figure 2. Effect of unlike concentrations of the white grape ethanolic extract on: (A) DNA synthesis in the cells of (*B. subtilis)* NRRL B-94. (B) RNA synthesis (C) Acid-soluble phosphorus synthesis

3.5. MTT Cytotoxicity

The cytotoxicity assay was carried on the studied extracts to choose the safe doses of the plant extract on cell culture Madin-Darby Canine kidney (MDCK) cells to be used for the antiviral activity assay. The results are presented in Table 6.

Table 6. MTT cytotoxicity

Samples	Extracts	Conc.µg/µL	Cytotoxicity TC_{50} µg/µL	Initial viral counts	Viral counts (PFU/mL)	Inhibition (%)
Red grape Pomace	Aqueous	200	443	7×10^6	4×10^6	43
		400			2.5×10^6	75
	Ethanol	200	1596	10×10^6	5×10^6	40
		400			4×10^6	60
	Acetone	200	796	10×10^6	6×10^6	50
		400			3×10^6	64
White grape pomace	Aqueous	200	502	10×10^6	6×10^6	21
		400			4.5×10^6	71
	Ethanol	200	5539	7×10^6	5.5×10^6	40
		400			2×10^6	55
	Acetone	200	3901	10×10^6	4×10^6	60
		400			3.5×10^6	65
Standard	Oseltamivir	5	-	10×10^6	0	100

To explore the antiviral activity of the target extracts, the plaque infectivity reduction assay was used in two concentrations. The results reveal that the red grape extract has a slightly higher antiviral activity compared to the white one and the aqueous extract at 400 µg and is much better than the ethanol and acetone extracts, consistent with (Gaafar et al., 2015). The extracts are examined against AIV H5N1 (A / chicken / Egypt /M7217B / (H5N1) as shown in Figure 3.

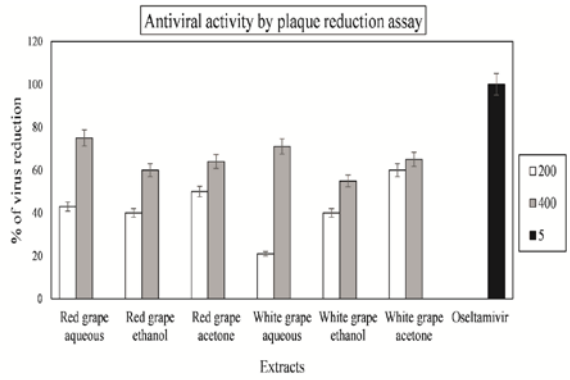

Figure 3. Antiviral activity (%) of pomace extracts expressed by the percentage of plaque reduction assay.

4. Conclusion

The considerable diversity of two grape pomace varieties (Romy and Banaty) with respect to the contents of TP, TF, TT, and antioxidant assays by $DPPH^{\bullet}$, $ABTS^{\bullet+}$, reducing power, and iron-chelating tests have been investigated in this study. The red grape pomace acetone extract displayed the highest quantity of phenolics and antioxidant activities. It was confirmed that all pomace extracts offered antimicrobial and antiviral activities. This study also shows that the grape pomace polyphenols exhibited activities against Gram+ve and Gram-ve bacteria which means that these underutilized grape pomaces could be a perfect provenance of antimicrobials for further utilization in the food manufacturing industries which oversight or deny food-borne pathogens. Red grape pomaces have been proven to have ~~a~~ great potential as sources of antioxidant, antimicrobial and antiviral agents. This investigation confirms the prospects of using grape pomaces to promote new potential sources of antioxidant, antimicrobial and antiviral materials in the pharmaceutical industry.

Conflict of Interests

The authors declare that there is no conflict of interest.

Acknowledgments

This work was supported and funded by the project entitled “Optimization of the agricultural wastes of food industries as a source of bioactive compounds” PI: Prof.Dr. ‘Zeinab Hanem Salama’ and funded by the National Research Centre (NRC), Egypt.

References

Alipour D and Rouzbehan Y. 2010. Effects of several levels of extracted tannin from grape pomace on intestinal digestibility of soybean meal. *Livest Sci*, 2010; **128**: 87-91.

Allahghdri T, Rasooli I, Owlia P, Nadooshan MJ, Ghazanfari T, Taghizadeh M and Astaneh SDA. 2010. Antimicrobial property, antioxidant capacity, and cytotoxicity of essential oil from cumin produced in Iran. *J Food Sci*, **75**: H54-H61.

Anonymous A. 1989. Cohort Soft Ware Crop. Costat user manual version 3.03, Berkeley CA, USA.

Anstasiadi M, Pratsinis H, Kletsas D, Skaltsounis A and Haroutounian S. 2010. Bioactive non-colored polyphenols content of grapes, wines and vilification by-products: Evaluation of the antioxidant activities of their extracts. *Food Res Int*, **43**: 805-813.

Arnao MB, Cano A and Acosta M. 2001. The hydrophilic and lipophilic contribution to total antioxidant activity. *Food Chem*, **73**: 239-244.

Ben-Hammouda M, Kremer RJ, minor HC and Sarwar MA. 1995. Chemical basis for differential allelopathic potential of sorghum hybrids on wheat. *J Chem Ecol*, **21**: 775-786.

Bligh EG, and Dyer WJ. 1959. A rapid method for total lipid extraction and purification. *Can J Biochem Physiol*, **37**: 911-917.

Bradbury JH and Holloway WD. 1988. Chemistry of tropical root crops: significance for nutrition and agriculture in the Pacific. Australian Centre for International Agricultural Research. Astralia.

Bradford MM. 1976. A rapid and sensitive method for the quotation of microgram quantities of protein utilizing the principle of protein-day binding. *Anal Biochem*, **72**: 248-254.

Burton K. 1957. A study of the conditions and mechanism of diphenylamine reaction for colorimetric estimation of deoxyribonucleic acid. *J Biochem*, **62**: 315-323.

Cassano A, Figoli A, Tagarelli A, Sindono G and Drioli, E. 2006. Integrated membrane process for the production of highly nutritional kiwi fruit juice. *Desalination*, **189**: 21-30.

Chen PS, Toribara TT And Warner H. 1956. Microdetermination of Phosphorus. *Anal Chem*, **28**: 1756-1758.

Chu YH, Chang CL and Hsu HF. 2000. Flavonoids content of several vegetables and their antioxidant activity. *J Sci Food Agric*, **80**: 561-566.

Cho EJ, Yokozava T, Rhyu DY, Kim SC, Shibahara N and Park JC. 2003. Study on the inhibitory effects of Korean medicinal plants and their main compounds on the DPPH radical. *Phytomed.*, **10**: 544-551.

Darra NE, Tannous J, Mouncef PB, Palge J, Yaghi J and Vorobiev E. 2012. A Comparative study on antiradical and antimicrobial properties of red grapes extracts obtained from different Vitis *vinifera varieties. Food Nutr Sci*, **3**:1420-1432.

Daughaday WH, Lowry OH, Rosebrough NJ and Fields WS. 1952. Determination of cerebrospinal fluid protein with the folin phenol reagent. *J Lab Clin Med*, **39**: 663-666.

Dorman HJD and Deans SG. 2000. Antimicrobial agents from plants: antibacterial activity of plant volatile oils. *J Appl Microbiol*, **88**: 308-316.

Fontana AR, Antoniolli A and Bottini R. 2013. Grape pomace as a sustainable source of bioactive compounds: extraction, characterization, and biotechnological applications of phenolics. *J Agric Food Chem*, **61**: 8987-9003.

Fontoin H, Saucier C, Teissedre PL and Glories Y. 2008. Effect of pH, ethanol, and acidity on astringency and bitterness of grape seed tannin oligomers in model wine solution. *Food Qual Prefer*, **19**: 286-291.

Furneri PM, Marino A, Saija A, Uccella N and Bisignano G. 2002. *In-vitro* antimycoplasmal activity of oleuropein. *Int J Antimicrob Agents*, **20**: 293-296.

Gaafar A, Asker M, Salama Z, Bagato O, Ali M. 2015. *In*-vitro, antiviral, antimicrobial and antioxidant potential activity of tomato pomace. *Int J Pharm Sci Rev Res*. **32**: 262-272.

González-Centeno MR, Jourdes M, Femenia A, Simal S, Rossello C and Teissedre PL. 2013. Characterization of polyphenols and antioxidant potential of white grape pomace byproducts (*Vitis vinifera* L.). *J Agric Food Chem*, **61**: 11579-11587.

Halliwell B and Gutteridge JMC. 1984. Oxygen toxicology, oxygen radicals, transition metals and disease. *J Biochem*, **219**: 1-4.

Hayden FG, Cote KM and Douglas RG. 1980. Plaque inhibition assay for drug susceptibility testing of influenza viruses. *Antimicrob Agents Chemother*, **17**: 865-870.

Hogan S, Zhang L, Li J, Zoecklein B and Zhou K. 2009. Antioxidant properties and bioactive components of Norton (*Vitis aestivalis*) and Cabernet Franc (*Vitis vinifera*) wine grapes. *LWT-Food Sci Technol*, **42**: 1269-1274.

Hogeboom GH and Schneider WC. 1950. Cytochemical studies of mammalian tissues III. Isocitric dehydrogenase and triphosphopyridine nucleotide-cytochrome c reductase of mouse liver. *J Biol Chem*, **186**: 417-427.

Hsu C, Chen W, Weng Y and Tseng C. 2003. Chemical composition, physical properties, and antioxidant activities of yam flours as affected by different drying methods. *Food Chem*, **83**: 85-92.

Katalinic V, Mozina SS, Skroza D, Generalic I, Abramovic H, Milos M, Ljubenkov I, Piskernik S, Pezo I, Terpinc P and Boban M. 2010. Polyphenolic profile, antioxidant properties and antimicrobial activity of grape skin extracts of 14 *Vitis vinifera* varieties grown in Dalmatia (Croatia). *Food Chem*, **119**: 715-723.

Katsube T, Tabata H, Ohta Y, Yamasaki Y, Anuurad E, Shiwaku K and Yamane Y. 2004. Screening for antioxidant activity in edible plant products: Comparison of low-density lipoprotein oxidation assay, DPPH radical scavenging assay, and Folin-Ciocalteu assay. *J Agric Food Chem*, **52**: 2391-2396.

Knight JA, Anderson S and James MR. 1972. Chemical basis of the sulfo-phospho-vanillin reaction for estimating total serum lipids. *Clin Chem*, **18**: 199-202.

Kuda T, Tsunekawa M, Goto H and Araki Y. 2005. Antioxidant properties of four edible algae harvested in the Noto Peninsula, Japan. *J Food Compos Anal*, **18**: 625-633.

Lapornik B, Prosek M and Wondra AG. 2005. Comparison of extracts prepared from plant by-products using different solvents and extraction time. *J Food Eng*, **71**: 214-222.

Lee KW, Lim YJ, Lee HJ and Lee CY. 2003. Cocoa has more phenolic phytochemicals and a higher antioxidant capacity than teas and red wine. *J Agric Food Chem*, **51**: 7292-7295.

Lee MG, Hassani OK, Alonso A and Jones BE. 2005. Cholinergic basal forebrain neurons burst with theta during waking and paradoxical sleep. *J Neurosci*, **25**: 4365-4369.

Luther M, Parry J, Moore J, Meng J, Zhang Y, Cheng Z and Yu L. 2007. Inhibitory effect of Chardonnay and black raspberry seed extracts on lipid oxidation in fish oil and their radical scavenging and antimicrobial properties. *Food Chem*, **104**: 1065-1073.

Maniyan A, John R and Mathew A. 2015. Evaluation of fruit peels for some selected nutritional and anti-nutritional factors. *Emergent Life Sci Res.*, **1**: 13-19.

Mohdaly AAA, Sarhan MA, Smetanska I and Mahmoud A. 2010. Antioxidant properties of various solvent extracts of potato peels, sugar beet pulp, and sesame cake. *J Sci Food Agric*, **90**: 218-226.

Mosman T. 1983. Rapid colorimetric assay for cellular growth and survival: application to proliferation and cytotoxic assays. *J Immunol Methods*, **65**:55-63

NCCLS. 1990 Methods for Dilution Antimicrobial Susceptibility Tests for Bacteria that Grow Aerobically, 2nd Ed., Approved Standard NCCLS Document M7-A2, Villanova, PA.

Oliveira DA, Salvadora AA, Smânia Jr A, Smâniab EFA, Maraschinc M and Ferreiraa SRS. 2013. Antimicrobial activity and composition profile of grape (*Vitis vinifera*) pomace extracts obtained by supercritical fluids. *J Biotechnol*, **164**: 423-432.

Omidbeygi M, Barzegar M, Hamidi Z and Naghdibadi H. 2007. Antifungal activity of thyme, summer savory and clove essential oils against Aspergillus *xavus* in liquid medium and tomato paste. *Food Control*, **18** : 1518-1523

Oyaizu M. 1986. Studies on products of browning reaction. *Jap J Nutrition and Dietetics*, **44**:307-315.

Pal RS, Kumar VA, Arora S, Sharma AK, Kumar V and Agrawa S. 2015. Physicochemical and antioxidant properties of kiwi fruit as a function of cultivar and fruit harvested month. *Braz Arch Biol Technol*, **58**:262-271.

Peixoto CM, Dias MI, Alves MJ, Calhelha RC, Barros L, Pinho SP and Ferreira IC. 2018. Grape pomace as a source of phenolic compounds and diverse bioactive properties. *Food Chem*, **253**: 132-138.

Polshettiwar SA, Ganjiwale RO, Wadher SJ and Yeole PG. 2007. Spectrophotometric estimation of total tannins in some ayurvedic eye drops. *Indian J Pharm Sci*, **69**: 574-576.

Prior R, Lazarus S, Cao G, Muccitelli H and Hammerstone J. 2001. Identification of procyanidins and anthocyanins in blueberries and cranberries (*Vaccinium* spp.) using high-performance liquid chromatography/mass spectrometry. *J Agric Food Chem*, **49**: 1270-1276.

Rathi P and Rajput CS. 2014. Antioxidant potential of grapes (*Vitis vinifera*): A review. *J Drug Deliv Technol*, **4**: 102-104.

Rockenbach II, Gonzaga LV, Rizelio VM, Gonçalves AEDSS, Genovese MI and Fett R. 2011. Phenolic compounds and antioxidant activity of seed and skin extracts of red grape (*Vitis vinifera* and *Vitis labrusca*) pomace from Brazilian wine making. *Food Res Int*, **44**: 897-901.

Rodtjer A, Skibsted LH and Andersen ML. 2006. Antioxidative and prooxidative effect of extracts made from cherry liqueur pomace. *Food Chem*, **99**: 6-14.

Ruberto G, Renda A, Daquino C, Amico V, Spatafora C, Tringali C and De Tommasi N. 2007. Polyphenol constituents and antioxidant activity of grape pomace extract from five Sicilian red grape cultivars. *Food Chem*, **100**: 203-210.

Sahu SC and Green S. 1997. Food antioxidants: Their dual role in carcinogenesis, *In*: Oxidants, Antioxidants and Free Radicals**,** S. Baskin and H. Salem, eds., Taylor and Francis, Washington, pp. 329-330.

Scott AC. 1989. Laboratory control of antimicrobial therapy. *In*: Mackie & McCartney Practical Medical Microbiology**,** Collee JG, Duguid JP, Fraser AG, and Marmion B P (Eds) 13th Edn. Vol 2, United Kingdom-Edinburgh: Churchill Livingstone. 161-181.

Shuichi A, Hidenori N, Sumito I, Hiroaki T, Hiroshi S, Shuichi K, Naofumi M, Kouji M and Hitonodu T. 2000. Interleukin-8 gene repression by clarithromycin is mediated by the activator protein-1 binding site in human bronchial epithelial cells. *Am J Respir Cell Mol Biol*, **22**: 51-60.

Singleton VL and Rossi JA. 1965. Colorimetric of total phenolics with phosphomolybdic– phosphor tungstic acid reagents. *Am J Enol Vitic*, **16**: 144-158.

Smith-Palmer A, Stewart J and Fyfe L. 1998. Antimicrobial properties of plant essential oils and essences against five

important food-borne pathogens. *Lett Appl Microbiol*, **26**: 118-122.

Sultana B, Anwar F and Przybylski R. 2007. Antioxidant activity of phenolic components present in barks of barks of *Azadirachta indica*, *Terminalia arjuna*, *Acacia nilotica*, and *Eugenia jambolana* Lam. trees. *Food Chem*, **104**: 1106-1114.

Wang H and Helliwell K. 2001. Determination of flavonols in green and black tea leaves and green tea infusions by high-performance liquid chromatography. *Food Res Int*, **34**: 223-227.

Wang X, Tong H, Chen F and Gangemi JD. 2010. Chemical characterization and antioxidant evaluation of muscadine grape pomace extract. *Food Chem*, **123**: 1156-1162.

Yilmaz Y. 2002. Antioxidant activities of grape skin and grape seed polyphenolics and potential use of antioxidants in foods as a functional food ingredient. Ph.D. Thesis. The University of Georgia.

Yilmaz Y and Toledo RT. 2004. Major flavonoids in grape seeds and skins antioxidant capacity of catechin, epicatechin and gallic acid. *J Agric Food Chem*, **52**: 255-260.

Yu J, Ahmedna M and Goktepe I. 2005. Effects of processing methods and extraction solvents on concentration and antioxidant activity of peanut skin phenolics. *Food Chem*, **90**:199-206

Yu J and Ahmenda M. 2013. Functional properties of grape pomace, their composition, biological properties and potential applications. *Int J Food Sci Technol*, **48**: 221-237.

Zhao M, Yang B, Wang J, Li B and Jiang Y. 2006. Identification of the major flavonoids from pericarp tissues of lychee fruit in relation to their antioxidant activities. *Food Chem*, **98**: 539-544.

Zhishen J, Mengcheng T and Jianping W. 1999. The determination of flavonoid contents in mulberry and their scavenging effects on superoxide radicals. *Food Chem*, **64**: 555-559.

JJBS

Volume 12, Number 5,December 2019
ISSN 1995-6673
Pages 637 - 647

Jordan Journal of Biological Sciences

Re-evaluation of Molecular Phylogeny of the Subfamily Cephalophinae (Bovidae: Artiodactyla); with Notes on Diversification of Body Size

Taghi Ghassemi-Khademi[1*] and Kordiyeh Hamidi[2]

[1] Department of Biology, Faculty of Sciences, University of Shiraz, Shiraz, [2]Department of Biology, Faculty of Science, Ferdowsi University of Mashhad, Mashhad, Iran

Received February 20, 2019; Revised April 2, 2019; Accepted April 9, 2019

Abstract

Duikers from the subfamily Cephalophinae are small to medium-sized antelope native to sub-Saharan Africa. Since most of the species belonging to this group are considered at-risk due to the process of population decline and probable extinction, recognizing their evolutionary biology will be useful toward preventing their extinction. Herein, molecular phylogeny of fourteen species of duikers were re-evaluated using complete mitochondrial genome sequences (n=17), cytochrome *b* (n=64), cytochrome *c* oxidase I (n=81), as well as the tRNA-proline gene and D-loop sequences. The analysis of a total of 225 gene sequences showed the average base composition of mtDNA sequences, based on mitogenome sequences, as follows: 26.8 % T, 26.5 % C, 33.3 % A, and 13.4 % G, with a great AT bias (60.1 %). According to the phylogenetic trees which resulted from maximum likelihood analysis, five distinct groups were indicated as West African red (*Cephalophus callipygus*, *C. ogilbyi*), East African red (*C. leucogaster*, *C. natalensis*, *C. rufilatus*, *C. nigrifrons*), savanna (*Sylvicapra grimmia*), giant (*C. dorsalis*, *C. jentinki*, *C. silvicultor*, *C. spadix*), and dwarf (*Philantomba maxwellii*, *P. monticola*) duikers. Furthermore, the current study showed that results will be similar using limited mitochondrial genes or either mitogenomes. Giving a careful attention to the phylogeny of duikers, two distinct evolutionary lineages were observed which could be defined as two distinct tribes (i.e. dwarf duikers and other species) within this subfamily. It means that their phylogeny is in accordance with their body-size classes. Therefore, similar approaches would be useful for those animals in which phylogeny is in accordance with their geographic position and body size, as can be seen in duikers.

Keywords: Duikers, Molecular phylogeny, Body size, Geographical location, Bovidae.

1. Introduction

The subfamily, Cephalophinae (Bovidae), consists of several artiodactyl species, commonly named as duikers, which are widely distributed in sub-Saharan Africa, but mainly inhabit tropical forests of Africa (Wilson and Reeder, 2005). Although they can be easily recognized due to their typical body form, they differ significantly in size. Unlike most bovids, females are slightly larger than males in this subfamily. Moreover, in contrast to most other bovids, duikers are primarily frugivorous (Castelló, 2016). However, they also feed on foliage, leaves of bushes, vines, and lower branches of trees. Sometimes they eat meat and may take nestlings, bird eggs, insects, and carrion. In captivity, they are sometimes fed dog food as a diet supplement (Burton and Burton, 2002). Duikers are very shy, elusive, and highly active creatures which need to eat large amounts of food (fruits) to maintain their energy levels (Burton and Burton, 2002). In most species, both sexes bear short pointed horns facing back over the neck with a tuff of hair between them, with the exception of the females of common duikers (*Sylvicapra grimmia*) which have only stunted horns or none at all. Just beneath the eyes, there are crescent-shaped glandular openings that secrete a kind of scent. Duikers rub this scent on each other for future recognition, and also use it to mark out their territories (Burton and Burton, 2002; Castelló, 2016).

Duikers in the subfamily Cephalophinae contain three genera (Vuuren and Robinson, 2001; Grubb and Groves, 2005; Johnston and Anthony, 2012). The monotypic savanna specialist *Sylvicapra* genus contains a single savannah dwelling species, *S. grimmia*, and several subspecies widely distributed across the area from the Sahel to Austral Africa. The recently derived, species-rich, forest dwelling, genus *Cephalophus*, has several species and numerous subspecies inhabiting humid African tropical lowlands and mountain forests (Johnston and Anthony, 2012). Finally, the dwarf *Philantomba* contains the two smallest and most widely-distributed duiker species, namely *P. maxwelli* and *P. monticola* (Colyn *et al*., 2010; Johnston and Anthony, 2012). They both occupy a range of natural habitats, including mosaic shrubby and wooded savannah habitats near human settlements. These two species are considered as the most frequently hunted antelopes in western and central Africa, and thus, represent a significant proportion of the local bushmeat market (Colyn *et al*., 2010).

* Corresponding author e-mail: t.ghassemi@shirazu.ac.ir.

Today, the most significant issues about duikers are the declining of their populations and the risk of extinction in Africa. Most species of duikers are common and widespread across sub-Saharan Africa (Burton and Burton, 2002). However, the destruction of fruit trees and the development of land in their place for settlement and agriculture (Burton and Burton, 2002), in addition to several other factors, have severely reduced the population of duikers to the point that, presently, all the members of the subfamily are mentioned on the red list of IUCN (Table 1).

Table 1. Scientific names and the IUCN red list categories for the duiker species of the subfamily Cephalophinae.

Scientific Name	Red List Category	Reference
C. adersi	Critically Endangered	(Finnie, 2008)
C. callipygus	Least Concern	IUCN
C. dorsalis	Near Threatened	IUCN
C. harveyi	Least Concern	IUCN
C. jentinki	Endangered	IUCN
C. leucogaster	Near Threatened	IUCN
C. natalensis	Least Concern	IUCN
C. niger	Least Concern	IUCN
C. nigrifrons	Least Concern	IUCN
C. ogilbyi	Least Concern	IUCN
C. rufilatus	Least Concern	IUCN
C. silvicultor	Near Threatened	IUCN
C. spadix	Endangered	(Moyer *et al*., 2016)
C. weynsi	Least Concern	IUCN
C. zebra	Vulnerable	IUCN
P. maxwellii	Least Concern	IUCN
P. monticola	Least Concern	IUCN
Sylvicapra grimmia	Least Concern	IUCN

Although several researchers (Hassanin and Douzery, 1999; Rebholz and Harley, 1999, Wronski *et al*., 2010; Manuel *et al*., 2005; Gatesy *et al*., 1997; Groves, 2000; Kuznetsova and Kholodova, 2003; Marcot, 2007; Bärmann *et al*., 2013; Ghassemi-Khademi, 2017a,b; Ghassemi-Khademi and Madjdzadeh, 2019; Hassanin *et al*., 2012) have studied the phylogenetic relationship among the species belonging to Bovidae, there are few studies which are specifically focused on phylogenetic relationships within the subfamily, Cephalophinae (Johnston and Anthony, 2012; Jansen-van Vuuren and Robinson, 2001). Furthermore, based on previous studies, four major lineages for duikers have been introduced (Johnston and Anthony, 2012; Johnston, 2011; Jansen-van Vuuren and Robinson, 2001).

On the whole, since these animals and also all bovids are ecologically, economically, and biologically important animals in the world, the determination of phylogenetic relationships among them is an effective step toward planning for the conservation and enhancement of multiplication of these animals in the world. In this regard, phylogenetic analyses based on the complete mitochondrial genomes can provide most accurate inferences (Ghassemi-Khademi, 2017a).

In the present study, the taxonomical validation of the existent evolutionary lineages in Cephalophinae has been evaluated based on different genes and complete genomes of mitochondria.

2. Materials and Methods

Totally, 225 gene sequences belonging to the Cephalophinae were obtained from NCBI, including all complete mitochondrial genome sequences (n=17), as well as sequences of cytochrome *b* (cyt *b*) (n=64), cytochrome *c* oxidase I (COI) (n=81), and tRNA-proline-D-loop (n=63). Sequences were aligned with Mega6 (Tamura *et al*., 2013) using the clustral W alignment method. In all analyses, the corresponding gene sequences of *Tragelaphus spekii* and *T. eurycerus* were used as outgroups.

The evolutionary history was inferred using the Maximum Likelihood (ML) method for each of the studied genes separately. Evolutionary divergence over sequence pairs between groups (different species) was also evaluated based on mitogenomes. The variance estimation method was bootstrap with 1000 replications. Herein, each species belonging to the subfamily Cephalophinae was considered as a separate group. Considering the outgroups, there were a total of fifteen groups (Table 2). Those positions containing gaps and missing data were eliminated. All of the evolutionary analyses were computed using the Kimura 2-parameter method (Kimura, 1980) in Mega6 (Tamura *et al*., 2013). Moreover, the robustness of clades was calculated by the bootstrap method. In this study, a bootstrap value of 50-60 % was considered as weak, 64-75 % as moderate, 76-88 % as good, and ≥ 89 % as a strong support (Win *et al.*, 2017).

3. Results

The phylogenetic analysis of fourteen species belonging to Cephalophinae was carried out using mitogenomes, cyt *b*, COI, and tRNA-proline-D-loop genes. The average length of complete mitochondrial genomes was calculated to be 16,427.9 base pairs. In 16427.9, the average base composition of mtDNA sequences was 26.8 % T, 26.5 % C, 33.3 % A, and 13.4 % G, showing a strong AT bias (60.1 %).

The molecular phylogenetic trees for the complete mtDNA genomes and also for the cyt *b*, COI, and the tRNA-proline-D-loop genes were constructed using the ML method, which all provided nearly the same topologies (Figures 1-4). In all of the trees, five different groups of duikers, namley dwarf, giant, savanna, east African and west African duikers, were clearly separated from each other. Four phylogenetic trees based on four different genes, revealed a great main clade; all of the species belonging to the subfamily Cephalophinae, with the exception of the two species of *P. maxwellii* and *P. Monticola*, constructed a great monophyletic clade.

Moreover, as the results indicate, *T. spekii* and *T. eurycerus* (used as outgroups) were completely separated from other species. The outgroups were at a far distance (Table 3) and separated from the members of Cephalophinae in all of the constructed phylogenetic trees (Figures 1-4), which implies the presence of relative close genetic distances among duikers. Based on mitogenomes, the shortest phylogenetic distances were obtained between the two species of *C. silvicultor* and *C. spadix* (= 0.25), and also *C. callipygous* and *C. ogilbyi* (= 0.24). Furthermore, in all phylogenetic trees, the two species of *C. silvicultor* and *C. spadix*, as well as the two species of *C. callipygous* and *C. ogilbyi* were located close to each other. Thus, it can be inferred that these species are phylogenetically the closest species within the Cephalophinae.

As mentioned earlier, based on mitogenomes, the longest distance was obtained between the outgroups (*T.*

spekii and *T. eurycerus*) and other species. Besides, after the outgroups, dwarf duikers (*P. maxwellii* and *P. monticola*) had the most phylogenetic distances with other members of the subfamily, and in all phylogenetic trees, the two species of *P. maxwellii* and *P. monticola* were located separately from other species and did not construct a single cluster with them. Moreover, based on the mitogenomes, among the five groups of duikers (Giant, Dwarf, East African, West African, and Savanna duikers) and *C. adersi*, the shortest phylogenetic distances were obtained between west African red and giant duikers (= 0.89), savanna and giant duikers (= 0.85), east and west African red duikers (= 0.82), and *C. adersi* and west African red duikers (= 0.89) (Table 3).

Using complete mitochondrial genome sequences, two distinct groups were distinguished within the great monophyletic clade of the constructed phylogenetic tree; in these distinct groups, six species including *C. callipygous*, *C. ogilbyi*, *C. leucogaster*, *C. natalensis*, *C. rufilatus*, and *C. nigrifrons* showed the highest supported monophyly values (≥ 99). Based on the topology of ML phylogenetic tree of mitogenomes, the relationship of species in this group was as follows: [(*C. callipygous*+ *C. callipygous*)+ (*C. callipygous*+ *C. ogilbyi*)]+ [*C. leucogaster*+ {*C. natalensis*+ (*C. rufilatus* and *C. nigrifrons*)}]. In group two, five species including *S. grimmia*, *C. dorsalis*, *C. jentinki*, *C. silvicultor*, and *C. spadix* showed the highest supported monophyly values (= 100) in the ML phylogenetic tree. Based on the topology of the ML tree of mitogenomes, the relationship of species in this group was as follows: [*S. grimmia*+ {(*C. dorsalis*)+ (*C. jentinki*)+ (*C. silvicultor*+ *C. spadix*}].

In the four phylogenetic trees, *C. adersi* was located separately from other species, and is considered as a sister taxon for other species belonging to *Cephalophus* and *Sylvicapra* genera. As mentioned before, this species along with the species mentioned above, constructed a monophyletic cluster. In addition, in all of the resulting trees, *C. adersi* was located close to dwarf duikers (Tables 4-7).

Table 2. Phylogenetic distances between species belonging to the subfamily Cephalophinae based on complete mitochondrial sequences. Gp refers to Group.

Name	Gp_1	Gp_2	Gp_3	Gp_4	Gp_5	Gp_6	Gp_7	Gp_8	Gp_9	Gp_10	Gp_11	Gp_12	Gp_13	Gp_14
Gp_1														
Gp_2	0.025													
Gp_3	0.053	0.053												
Gp_4	0.056	0.057	0.059											
Gp_5	0.086	0.088	0.087	0.091										
Gp_6	0.085	0.085	0.083	0.089	0.090									
Gp_7	0.090	0.090	0.091	0.095	0.088	0.098								
Gp_8	0.089	0.091	0.089	0.094	0.024	0.094	0.091							
Gp_9	0.090	0.090	0.092	0.094	0.082	0.099	0.096	0.087						
Gp_10	0.093	0.093	0.092	0.098	0.082	0.100	0.096	0.086	0.061					
Gp_11	0.091	0.090	0.090	0.094	0.080	0.097	0.092	0.083	0.030	0.061				
Gp_12	0.090	0.091	0.091	0.095	0.081	0.099	0.096	0.084	0.007	0.060	0.029			
Gp_13	0.110	0.115	0.111	0.115	0.110	0.115	0.113	0.112	0.114	0.112	0.111	0.114		
Gp_14	0.111	0.113	0.110	0.113	0.105	0.114	0.110	0.108	0.114	0.111	0.112	0.114	0.067	
Gp_15	0.167	0.168	0.167	0.166	0.168	0.168	0.164	0.170	0.171	0.166	0.170	0.170	0.168	0.163

Note: Group 1: *Cephalophus silvicultor*, Group 2: *C. spadix*, Group 3: *C. dorsalis*, Group 4: *C. jentinki*, Group 5: *C. callipygus* (three sequences), Group 6: *C. grimmia*, Group 7: *C. adersi*, Group 8: *C. ogilbyi*, Group 9: *C. rufilatus*, Group 10: *C. leucogaster*, Group 11: *C. natalensis*, Group 12: *C. nigrifrons*, Group 13: *Philantomba maxwellii*, Group 14: *P. monticola* (two sequences), Group 15: *Tragelaphus spekii*, *T. eurycerus*.

Table 3. Phylogenetic distances between different groups belonging to the subfamily Cephalophinae based on complete mitochondrial sequences.

	Giant duiker	West African red duiker	Savanna duiker	Aders's duiker	East African red duiker	Dwarf duiker
Giant duiker						
West African red duiker	0.089					
Savanna duiker	0.085	0.091				
Aders's duiker	0.092	0.089	0.098			
East African red duiker	0.092	0.082	0.099	0.095		
Dwarf duiker	0.112	0.107	0.114	0.111	0.113	
Outgroups	0.167	0.168	0.168	0.164	0.169	0.165

Table 4. Nucleotide composition of mtDNA of the studied species of the Cephalophinae (n=17) and their accession numbers obtained from GenBank (www.ncbi.nlm.nih.gov) (n=19).

Scientific Name	T(U)	C	A	G	Total	Accession Number	Reference
Cephalophus silvicultor	27.0	26.3	33.4	13.4	16425.0	JN632622	(Hassanin *et al*., 2012)
Cephalophus spadix	27.0	26.2	33.3	13.5	16430.0	JN632623	(Hassanin *et al*., 2012)
Cephalophus dorsalis	26.7	26.6	33.4	13.4	16425.0	JN632615	(Hassanin *et al*., 2012)
Cephalophus jentinki	27.0	26.1	33.5	13.3	16391.0	NC_020688	(Hassanin *et al*., 2012)
Cephalophus callipygus	26.5	26.7	33.3	13.5	16427.0	JN632613	(Hassanin *et al*., 2012)
Cephalophus callipygus	26.5	26.6	33.3	13.5	16427.0	JN632614	(Hassanin *et al*., 2012)
Sylvicapra grimmia	26.7	26.6	33.4	13.3	16437.0	JN632701	(Hassanin *et al*., 2012)
Cephalophus callipygus	26.4	26.8	33.3	13.5	16422.0	JN632612	(Hassanin *et al*. 2012)
Cephalophus adersi	26.7	26.5	33.6	13.2	16435.0	JN632611	(Hassanin *et al*., 2012)
Cephalophus ogilbyi	26.4	26.7	33.3	13.6	16374.0	JN632620	(Hassanin *et al*., 2012)
Cephalophus rufilatus	26.3	27.0	33.0	13.7	16429.0	JN632621	(Hassanin *et al*., 2012)
Cephalophus leucogaster	26.8	26.5	33.2	13.5	16426.0	JN632617	(Hassanin *et al*., 2012)
Cephalophus natalensis	26.5	26.8	33.1	13.6	16429.0	JN632618	(Hassanin *et al*., 2012)
Cephalophus nigrifrons	26.4	26.9	33.0	13.7	16406.0	JN632619	(Hassanin *et al*., 2012)
Philantomba maxwellii	27.7	25.7	33.4	13.2	16440.0	JN632685	(Hassanin *et al*., 2012)
Philantomba monticola	27.4	26.0	33.7	13.0	16501.0	JN632686	(Hassanin *et al*., 2012)
Philantomba monticola	27.5	25.9	33.6	13.0	16451.0	JN632687	(Hassanin *et al*., 2012)
Avg.	26.8	26.5	33.3	13.4	16427.9		
Tragelaphus spekii						NC_020620	(Hassanin *et al*., 2012)
Tragelaphus eurycerus						JN632703	(Hassanin *et al*., 2012)

Table 5: Accession numbers of cytochrome *b* genes for the studied species belong to the subfamily Cephalophinae (n=64) obtained from GenBank (www.ncbi.nlm.nih.gov) (n=66).

Scientific Name	Accession Number	Scientific Name	Accession Number
Cephalophus callipygus	AF153886	*Cephalophus dorsalis*	AF153884
	AF153885		AF153884
	FJ807612		AF091634
	FJ807575		FJ807596
	FJ807574		FJ807595
	FJ807573		FJ807590
	JN632614		FJ807589
Cephalophus leucogaster	AF153889		FJ807588
	FJ807606		FJ807577
	JN632617		FJ807576
Cephalophus natalensis	AF153890		JN632615
	FJ807611	*Cephalophus jentinki*	AF153888
	FJ807610		JN645578
	JN632618		NC_020688
Cephalophus rufilatus	AF153890	*Cephalophus silvicultor*	AF153898
	FJ807626		FJ807622
	FJ807625		FJ807587
	JN632621		FJ807579
Cephalophus nigrifrons	AF153896		FJ807571
	FJ807627		JN632622
	FJ807609	*Cephalophus adersi*	AF153883
	FJ807572		FJ807617
	JN632619		FJ807616
Cephalophus ogilbyi	AF153897		JN632611
	FJ888512	*Philantomba maxwellii*	JF728780
	FJ807628		JN632685
	FJ807618	*Philantomba monticola*	JF728781
	JN632620		JN632687
Sylvicapra grimmia	FJ807613		JN632686
	FJ807591	*Tragelaphus spekii*	JF728788
	FJ807592	*Tragelaphus euryceros*	AF036276
	FJ807593		

Table 6. Accession numbers of Cytochrome *c* oxidase I (COX1) genes for the studied species from the subfamily Cephalophinae (n=81) obtained from GenBank (www.ncbi.nlm.nih.gov) (n=85).

Scientific Name	Accession Number	Scientific Name	Accession Number
Cephalophus ogilbyi	KJ192792	*Cephalophus dorsalis*	HQ644091
	KJ192791		GQ144514
	KJ192789		GQ144513
	KJ192790		KJ192767
Cephalophus leucogaster	HQ644098		KJ192768
	HQ644097		KJ192965
	GQ144515		KJ192975
	GQ144516		KJ192982
	GQ144517		GQ144511
	HQ644096		GQ144507
	HQ644095		KJ192980
	GQ144521		GQ144509
	GQ144519	*Cephalophus jentinki*	HQ644094
Cephalophus natalensis	HQ644104	*Cephalophus silvicultor*	HQ644113
	HQ644103		HQ644112
Cephalophus rufilatus	HQ644111		KJ192969
	HQ644110	*Cephalophus spadix*	HQ644115
Cephalophus nigrifrons	HQ644108		HQ644114
	HQ644107	*Cephalophus adersi*	HQ644087
	GQ144550		HQ644086
	GQ144549	*Philantomba maxwellii*	KJ192888
	GQ144548		KJ192889
	GQ144547		KJ192890
	GQ144546		KJ192891
Philantomba monticola	HQ644102		KJ192892
	KJ192774		KJ192893
	HM144016		KJ192974
	HM144015		HM144021
	HM144026		HQ644099
	HM144022		KJ192976
	HM144020	*Cephalophus callipygus*	HQ644090
	KJ192775		HQ644089
	HM144024		HQ644088
Tragelaphus spekii	HQ644120		GQ144491
	KJ192918		GQ144492
Tragelaphus eurycerus	EU623454		GQ144494
	LC143641		GQ144498
Sylvicapra grimmia	HQ644119		GQ144504
	HQ644118		HM144025
	KX012658		GQ144499
			GQ144500
			HM144023
			GQ144502
			GQ144493
			GQ144505

Table 7. Accession numbers of tRNA-proline gene and D-loop sequences for the studied species from the subfamily Cephalophinae (n=63) obtained from GenBank (www.ncbi.nlm.nih.gov)(n=67).

Scientific Name	Accession Number	Scientific Name	Accession Number
Cephalophus callipygus	FJ823345	*Cephalophus dorsalis*	FJ823384
	FJ823338		FJ823383
	FJ823339		FJ823379
	FJ823340		FJ823375
	FJ823342		FJ823371
	FJ823341		FJ823367
Cephalophus ogilbyi	FJ823363		FJ823372
	FJ823362		FJ823381
	FJ823360		FJ823376
Cephalophus leucogaster	FJ823333		FJ823373
	FJ823337		FJ823382
	FJ823335	*Cephalophus jentinki*	NC_020688
	FJ823334	*Cephalophus silvicultor*	FJ823359
	FJ823336		FJ823358
Cephalophus natalensis	FJ823314		FJ823357

	FJ823315		FJ823353
Cephalophus rufilatus	FJ823325		FJ823356
	FJ823326		FJ823354
	FJ823323	*Cephalophus spadix*	AM903086
	FJ823324		HG323850
Cephalophus nigrifrons	FJ823331		AM903085
	FJ823328		AM903084
Cephalophus adersi	FJ823312		HG323849
	FJ823313		FJ823351
Philantomba maxwellii	FJ823311		FJ823352
	FJ823310		HG323852
	FJ823309		FJ823349
Tragelaphus spekii	FJ823283	*Sylvicapra grimmia*	FJ823297
	FJ823286		FJ823296
	FJ823282		FJ823295
Tragelaphus eurycerus	JN632703		FJ823294
		Philantomba monticola	FJ823304
			FJ823305
			FJ823306
			FJ823308
			FJ823303

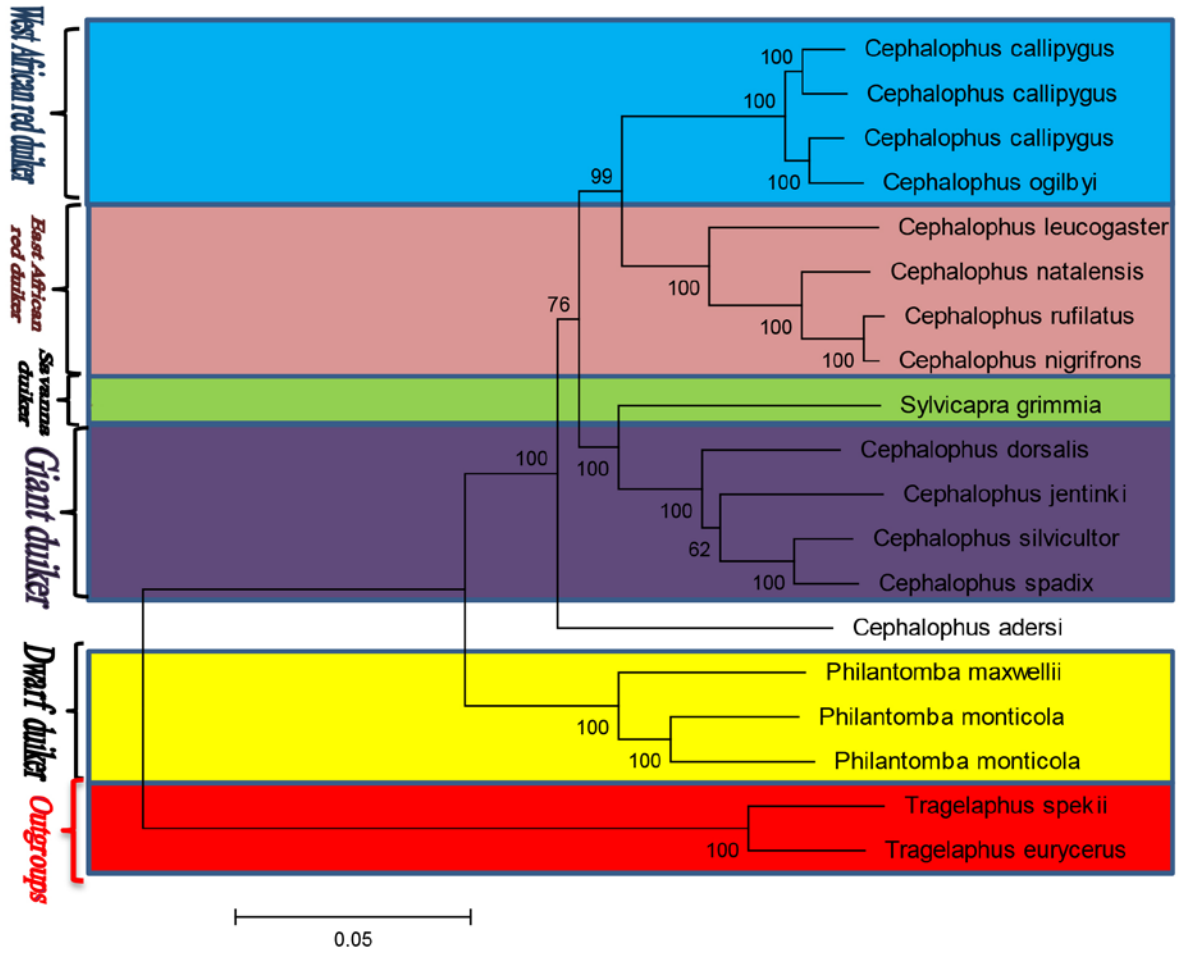

Figure 1. Maximum Likelihood tree based on Kimura 2- parameter distance using complete mitochondrial genome sequences. The numbers on each branch correspond to bootstrap support values. The tree was rooted with two *Tragelaphus* species sequences.

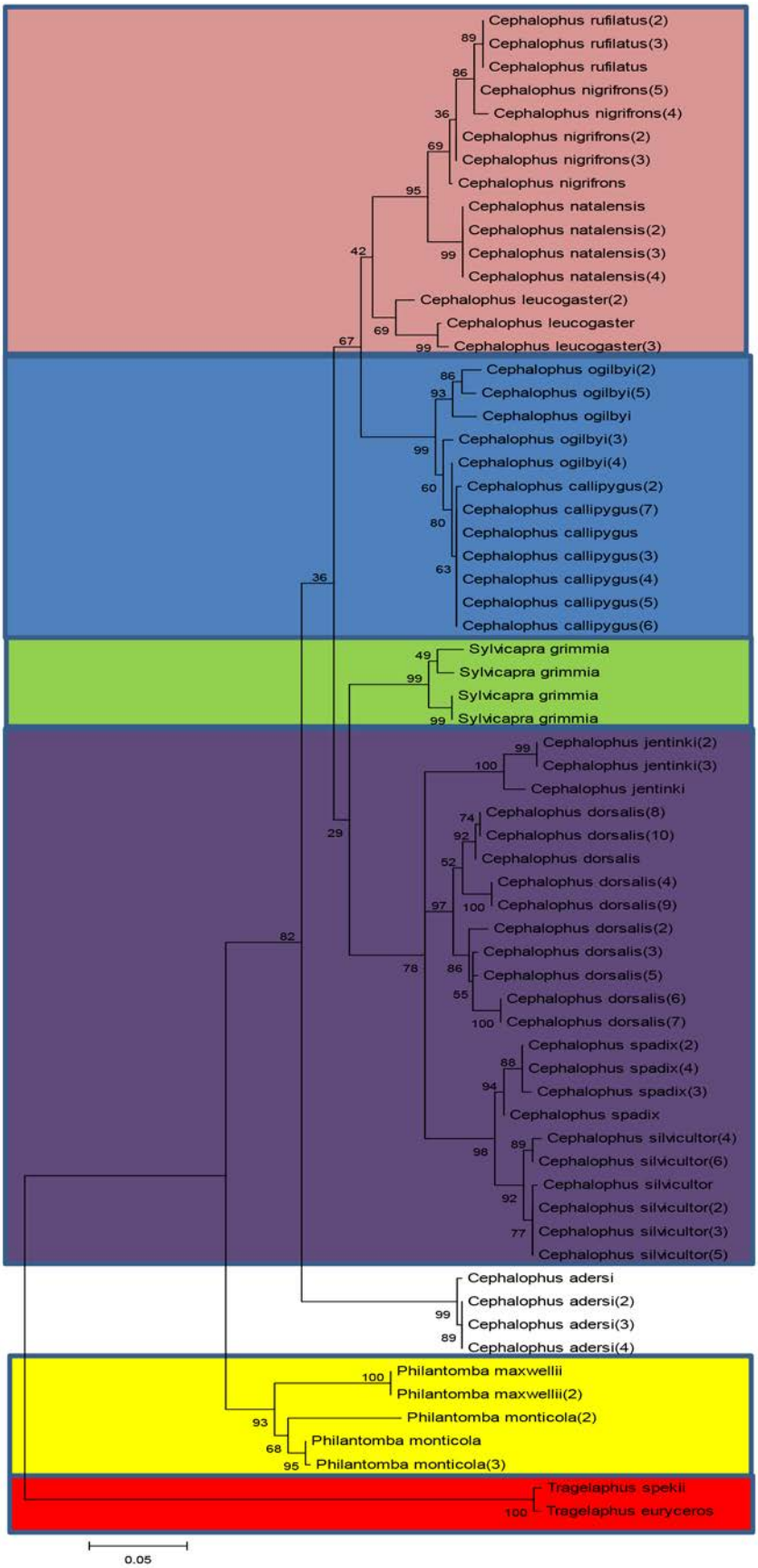

Figure 2. Maximum Likelihood tree based on Kimura 2- parameter distance using Cytochrome *b* sequences. The numbers on each branch correspond to bootstrap support values. The tree was rooted with two *Tragelaphus* species sequences.

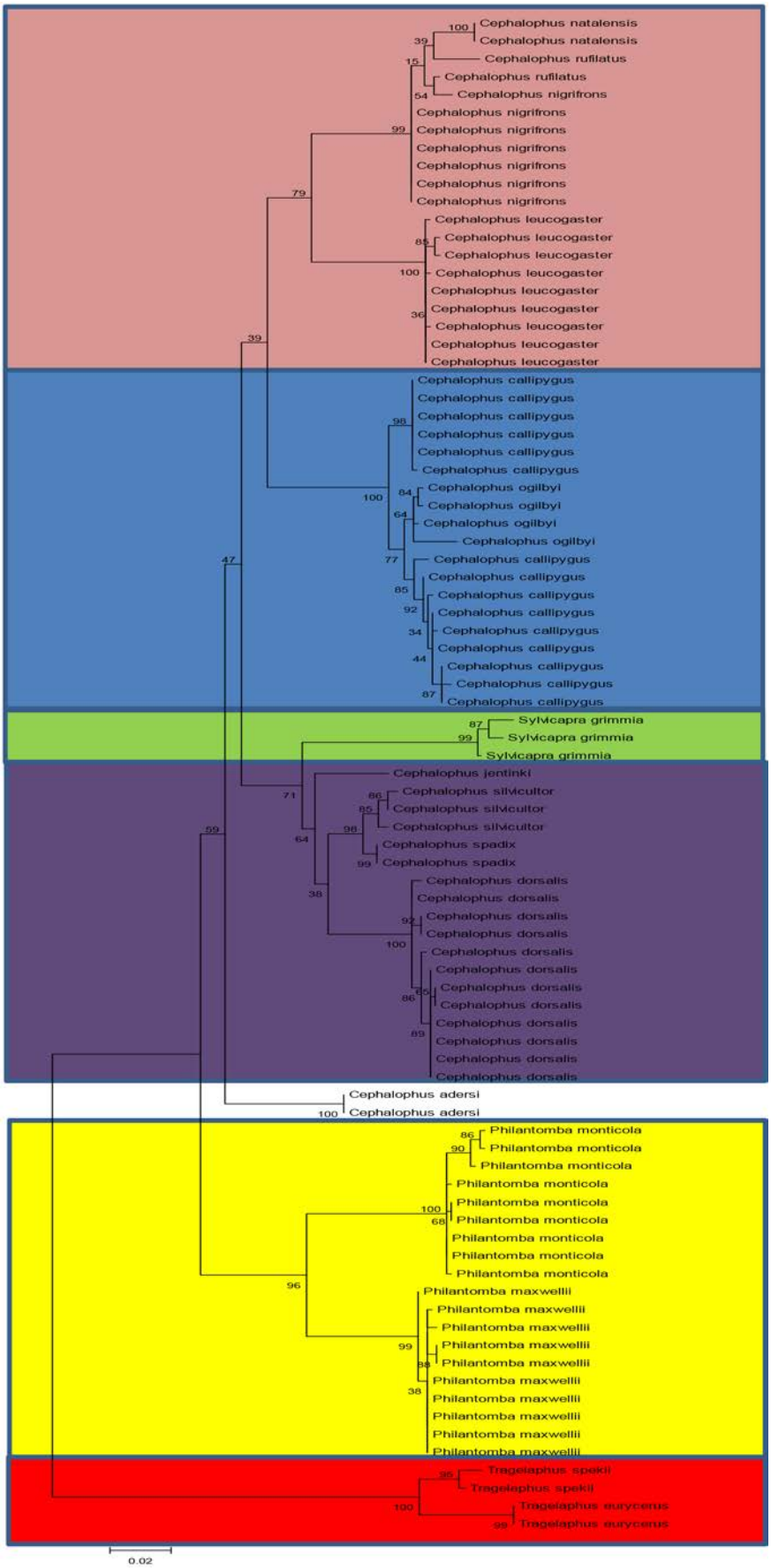

Figure 3. Maximum Likelihood tree based on Kimura 2- parameter distance using Cytochrome *c* oxidase I (COX1) sequences. The numbers on each branch correspond to bootstrap support values. The tree was rooted with two *Tragelaphus* species sequences.

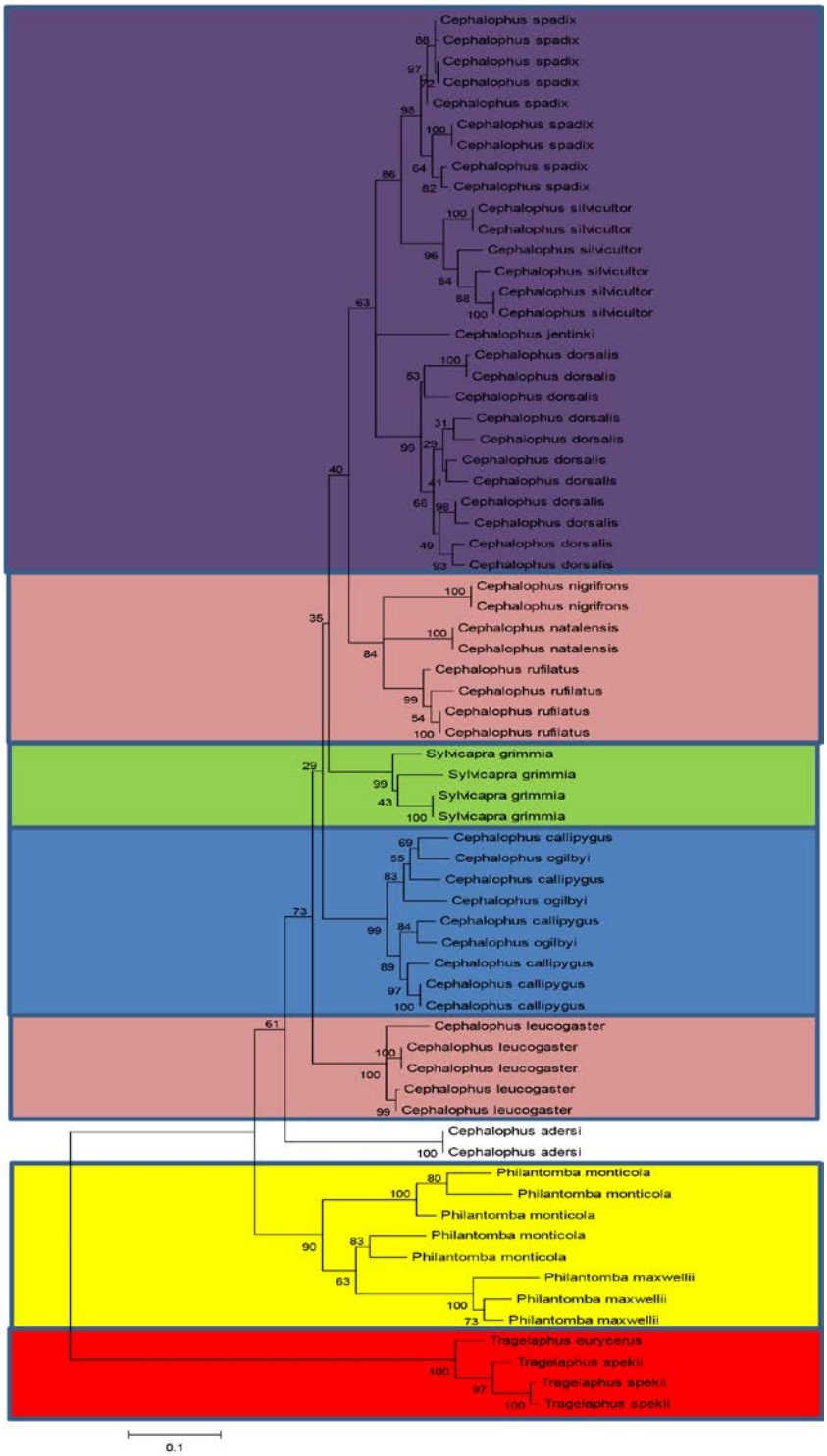

Figure 4. Maximum Likelihood tree based on Kimura 2- parameter distance using tRNA-proline gene and D-loop sequences. The numbers on each branch correspond to bootstrap support values. The tree was rooted with two *Tragelaphus* species sequences.

4. Discussion

Today, the subfamily Cephalophinae is introduced with three duiker genera: 1) the recently derived, species-rich, and forest-dwelling *Cephalophus*, 2) the dwarf *Philantomba*, and 3) the monotypic savanna specialist *Sylvicapra* (Johnston and Anthony, 2012). Using two mitochondrial genes (cyt *b* and 12S rRNA) and fluorescence *in situ* hybridization, Jansen-van Vuuren and Robinson (2001) retrieved four adaptive lineages in dwarf duikers (as the basal lineage), giant duikers (*C. silvicultor*, *C. spadix*, *C. dorsalis*, and *C. jentinki*), the red duikers with a subdivision comprising an East African red duikers group (including *C. leucogaster*, *C. rufilatus*, *C. nigrifrons*, *C. natalensis*, *C. rubidus*, and *C. harveyi*), a West African red duiker group (including *C. callipygous*, *C. weynsi*, *C. ogilbyi*, and *C. niger*), and a savanna specialist (*S. grimmia*) (Jansen-van Vuuren and Robinson, 2001).

Moreover, Johnston and Anthony (2012) used portions of two coding mDNA genes including 514 base pairs of the cyt *b* gene, 658 base pairs of COXI, and four nuclear

DNA markers including mechano growth factor (MGF), protein kinase CI (PRKCl), spectrin beta chain, non-erythrocytic (SPTBN1), and thyrotropin (THY) for evaluating the phylogenetic relationships within the subfamily Cephalophinae. The results of this study confirmed Jansen-van Vuuren and Robinson's statements and also confirmed four adaptive lineages of duikers completely separated from each other (Johnston and Anthony, 2012) (Figures 1- 4).

Therefore, using the complete mitochondrial genomes and three different genes of mtDNA, in addition to the confirmation of the presence of four phylogenetic lineages of duikers, resulted in inferences that are nearly compatible with those achieved when using limited mitochondrial genes. Accordingly, in the case of the phylogenetic studies of duikers, the fastest and economic method is to use limited mitochondrial genes, as it does not require using complete mitochondrial genomes. However, using mitogenomes in phylogenetic studies resulted in more accurate and reliable inferences in the world of animal diversification (Ghassemi-Khademi, 2017a, b).

Herein, similar to previous studies (Jansen-van Vuuren and Robinson, 2001; Johnston, 2011; Johnston and Anthony, 2012) the position of the genus *Philantomba* as a sister clade to the remaining Cephalophinae was confirmed considering it as a separate genus. Relations between West African red and giant duikers, savanna and giant duikers, east and West African red duikers, and finally, *C. adersi* and West African red duikers showed the shortest phylogenetic distances based on mitogenomes (Table 2). However, in all phylogenetic trees except those of the tRNA-proline-D-loop genes, savanna and giant duikers, and also East and West African red duikers were located close to each other. These observations are similar to results obtained by previous studies (Johnston, 2011; Johnston and Anthony, 2012). The East and West African red duiker lineages which are monophyletic and are considered as sister taxa (Johnston, 2011), sistered with each other in all of the resulted phylogenetic trees except in the tRNA-proline-D-loop genes tree. This result implies that they belong to a single lineage. Based on mitogenomes, the savanna duiker (*Sylvicapra grimmia*) and giant duikers had one of the shortest phylogenetic distances together, and were located as the sister group of giant duikers which leave the genus *Cephalophus* as a paraphyletic group (Johnston and Anthony 2012). Hence, this genus (*Cephalophus*) cannot be considered as a monophyletic group.

In all of the phylogenetic trees, *C. adersi* was located separately from other species belonging to a paraphyletic group of the genus *Cephalophus*, and constructed a sister taxon. Similar to the previous results (Johnston, 2011), in all of the phylogenetic trees, this species was basal to East and West African red, savanna, and giant duikers. Although it seems necessary to re-evaluate the phylogenetic position of this species carefully (Johnston and Anthony, 2012), this taxon is, undoubtedly, a member of the paraphyletic group of the genus *Cephalophus*. Furthermore, two species of dwarf duikers, *P. maxwellii* and *P. monticola* were located separately from other species, and did not construct a single cluster with them. Besides, after the outgroups, these species showed the greatest phylogenetic distances with other members of subfamily Cephalophinae. Given this evidence, one can probably identify two distinct tribes within the subfamily; one for dwarf duikers and the other for the rest of the species.

On the other hand, the correlation of phylogeny with animal body size and ecological traits (e.g. geographical locality) has been evaluated in several studies (Barnagaud *et al*., 2014; Leonhardt *et al*., 2013; Abellán and Ribera, 2011; Diniz-filho and d-sant Ana, 2000; Diniz-filho and Torres, 2002; Wollenberg *et al*., 2011; Carrascal *et al*., 2008). Meanwhile, the results of the current study and some earlier studies (Johnston, 2011; Johnston and Anthony, 2012) show that phylogenetic relationships of species belonging to the subfamily Cephalophinae correspond to their body size and geographic location. An example of such situation in the animal world belongs to the Apini tribe of honey bees. Based on body size, this kind of bees is divided into three giant, medium, and dwarf groups and their phylogenetic status correspond exactly to this morphological classification (Hepburn and Radloff, 2011). Geographic and phylogenetic relationships also shape the chemical profiles of stingless bees on a global scale (Leonhardt *et al*., 2013). Furthermore, Barnagaud and his colleagues (2014) stated that ecological traits influence the phylogenetic structure of bird species (Barnagaud *et al*., 2014). Given the above studies, and the results of the present study, it can be inferred that there is a strong correlation in some animal species between phylogeny with body size and ecological traits. It seems that the phylogeny of duikers is a specific example in this case, because these animals are divided into two different groups, phylogenetically.

In conclusion, the correlation between the phylogenetic situation and the morphological status (body size) as well as the geographical location in the world of invertebrates and vertebrates is, undoubtedly, an important and interesting subject for future studies.

4. Conclusion

The analysis of a total of 225 gene sequences showed five distinct groups within the subfamily Cephalophinae. Based on the complete mitochondrial genome sequences, cytochrome *b*, cytochrome *c* oxidase I, as well as the tRNA-proline gene and the D-loop sequence phylogenetic trees, these five groups of duikers were divided into two different clusters, dwarf duikers and non-dwarf duikers. This means that their phylogeny corresponds to their body-size classes. Probably, differences in the body size may create distinctive phylogenetic paths for taxa within a group or those with a close relationship. Finding relationships between the body size and phylogeny in a group of animals, requires comprehensive studies including, above all, ecological, biological, and phylogenetic approaches which will, undoubtedly, reveal many hidden facts in the worlds of animals.

Acknowledgment

The authors would like to thank the Department of Biology of Shiraz University for supporting this scientific research.

References

Abellán P and Ribera I. 2011. Geographic location and phylogeny are the main determinants of the size of the geographical range in aquatic beetles. *BMC Evol Biol*., **11:** 344.

Bärmann EV, Rössner GF and Wörheide G. 2013. A revised phylogeny of Antilopini (Bovidae, Artiodactyla) using combined mitochondrial and nuclear genes. *Mol Phylogenet Evol*, **67(2):** 484-493.

Barnagaud JY, Kissling WD, Sandel B, Eiserhardt WL, Şekercioğlu ÇH, Enquist BJ, Tsirogiannis C and Svenning JC. 2014. Ecological traits influence the phylogenetic structure of bird species co-occurrences worldwide. *Ecol Lett*, **17(7):** 811-820.

Burton M and Burton R. 2002. **The International Wildlife Encyclopedia: Volume 6.** Cavendish Square Publishing, Third Edition, New York, United States of America (USA), 864 pp.

Colyn M, Hulselmans J, Sonet G, Oude P, Winter JD, Natta A, Tamas-Nagyz and Verheyen E. 2010. Discovery of a new duiker species (Bovidae: Cephalophinae) from the Dahomey Gap, West Africa. *Zootaxa*, **2637:** 1–30.

Castelló JR. 2016. **Bovids of the world: Antelopes, Gazelles, Cattle, Goats, Sheep, and Relatives**. Princeton University Press, Princeton, New Jersey, 664 pp.

Carrascal LM, Seoane J, Palomino D and Polo V. 2008. Explanations for bird species range size: ecological correlates and phylogenetic effects in the Canary Islands. *J Biogeogr*, **35:** 2061–2073.

Diniz-Filho JAF and de Sant'Ana CER. 2000. Phylogenetic correlograms and the evolution of body size in South American owls (Strigiformes). *Genet. Mol. Biol*, **23(2):** 285-292.

Diniz-Filho JAF and Torres N. 2002. Phylogenetic comparative methods and the geographic range size - Body size relationship in new world terrestrial carnivora. *Evol Ecol*, **16(4):** 351-367.

Ghassemi-Khademi T. 2017a. Evaluation of phylogenetic relationships of Antilopini and Oreotragini tribes (Bovidae: Artiodactyla) based on complete mitochondrial genomes. *JWB*, **1:** 1-11.

Ghassemi-Khademi T. 2017b. A re-evaluation of phylogenetic relationships within the tribe Tragelaphini (Bovinae: Bovidae), based on complete mitochondrial genomes. *J Entomol Zool Stud*, **5(5):** 1025-1032.

Ghassemi-Khademi T., Madjdzadeh S.M. 2019. A re-evaluation of phylogenetic relationships within the subfamily Hippotraginae. *Jordan J Biol Sci*, **12(3):** 297-305.

Gatesy J., Amato G., Vrba E.S., Schaller G.B., DeSalle R. 1997. A cladistic analysis of mitochondrial ribosomal DNA from the Bovidae. *Mol. Phylogenetics Evol*, **7:** 303–319.

Groves CP. 2000. Phylogenetic relationships within recent Antilopini (Bovidae)**.** *In*: Vrba, ES., Schaller, George B. (Eds.), **Antelopes, Deer, and Relatives: Fossil Record, Behavioral Ecology, Systematics, and Conservation**, New Haven and London, Yale University Press,pp 223–233.

Grubb P. 2005. Artiodactyla. *In*: **Mammal species of the World. A Taxonomic and Geographic Reference** (3rd edition). Wilson D.E., Reeder D.M., (Eds), Johns Hopkins University Press, Baltimore, pp. 637–722.

Grubb P and Groves C.P. 2005. Revision and classification of the Cephalophinae. *In*: Wilson V.J., (Ed), **Duikers and Rainforests of Africa**,. Chipangali Wildlife Trust, Ascot, Bulawayo, Zimbabwe, pp. 703–728.

Hassanin A and Douzery EJP. 1999. The tribal radiation of the family Bovidae (Artiodactyla) and the evolution of the mitochondrial cytochrome b gene. *Mol Phylogenet Evol*, **13:** 227.

Hassanin A, Delsuc F, Ropiquet A, Hammer C, Jansen-van-vuuren B, Matthee C, Ruiz-Garcia M, Catzeflis F, Areskoug V, Nguyen TT and Couloux A. 2012. Pattern and timing of diversification of Cetartiodactyla (Mammalia, Laurasiatheria), as revealed by a comprehensive analysis of mitochondrial genomes. *C R Biol*, **335:** 32–50.

Hepburn HR and Radloff SE. 2011. **Honeybees of Asia**. Springer Heidelberg Dordrecht London New York 669 p p.

Jansen-van-Vuuren B and Robinson TJ. 2001. Retrieval of four adaptive lineages in duiker antelope: Evidence from mitochondrial DNA sequences and fluorescence in situ hybridization. *Mol Phylogenet Evol*, **20:** 409-425.

Johnston AR. 2011. Evolutionary relationships among duiker antelope (Bovidae: Cephalophinae). Ms.C thesis of biological sciences. University of New Orleans, Louisiana, United States of America.

Johnston AR and Anthony NM. 2012. A multi-locus species phylogeny of African forest duikers in the subfamily Cephalophinae: evidence for a recent radiation in the Pleistocene. *BMC Evol Biol*, **12:** 120.

Kimura M. 1980. A simple method for estimating evolutionary rate of base substitutions through comparative studies of nucleotide sequences. *J Mol Evol*, **16:** 111-120.

Kuznetsova MV and Kholodova MV. 2003. Revision of phylogenetic relationships in the Antilopinae subfamily on the basis of the mitochondrial rRNA and b-spectrin nuclear gene sequences. *Dokl Biol Sci*, **391:** 333–336.

Leonhardt SD, Rasmussen C and Schmitt T. 2013. Genes versus environment: geography and phylogenetic relationships shape the chemical profiles of stingless bees on a global scale. *Proc R Soc Lond B Biol Sci*, **280:** 280: 20130680.

Manuel H, Ferna N and Elisabeth S. 2005. A complete estimate of the phylogenetic relationships in Ruminantia: A dated species level supertree of the extant ruminants. *Biol Rev*, 269–302.

Marcot JD. 2007. Molecular phylogeny of terrestrial artiodactyls**.** *In***:** Prothero, DR. and Foss, SE. (Eds.),**The Evolution of Artiodactyls ,**. Baltimore, Johns Hopkins University Press.

Moyer D, Jones T and Rovero F. 2016. *Cephalophus spadix*. The IUCN Red List of Threatened Species 2016: e.T4151A50184413.

Rzhetsky A and Nei M. 1992. A simple method for estimating and testing minimum evolution trees. *Mol Biol Evol*, **9:** 945-967.

Rebholz W and Harley E. 1999. Phylogenetic relationships in the bovid subfamily Antilopinae based on mitochondrial DNA sequences. *Mol. Phylogen Evol*, **12:** 87–94.

Saitou N and Nei M. 1987. The neighbor-joining method: A new method for reconstructing phylogenetic trees. *Mol Biol Evol*, **4:** 406-425.

Tamura K, Stecher G, Peterson D, Filipski A and Kumar S. 2013. MEGA6: Molecular Evolutionary Genetics Analysis version 6.0. *Mol Biol Evol*, **30:** 2725-2729.

Wronski T, Wacher T, Hammond RL, Winney B, Hundertmark JK, Blacket MJ, Mohammed OB, Flores B, Omer SA, Macasero W, Plath M, Tiedemann R and Bleidorn C. 2010. Two reciprocally monophyletic mtDNA lineages elucidate the taxonomic status of mountain gazelles (*Gazella gazella*). *Syst Biodivers*, **8:** 119–129.

Wilson DE and Reeder DM. 2005. **Antilopinae, in Mammal Species of the World: A taxonomic and geographic reference**. Johns Hopkins University Press, 3ª ed.

Win NZ, Choi EY, Park J and Park JK. 2017. Molecular phylogenetic relationship of the subfamily Nymphalinae (Lepidoptera: Nymphalidae) in Myanmar, inferred from mitochondrial gene sequences. *J Asia Pac Biodivers*, **10:** 86-90.

Wollenberg KC, Vieites DR, Glaw F and Vences M. 2011. Speciation in little: the role of range and body size in the diversification of Malagasy mantellid frogs. *BMC Evol Biol*, **11:** 217.

Zhang WQ and Zhang MH. 2013. Complete mitochondrial genomes revealphylogeny relationship and evolutionaryhistory of the family Felidae. *Genet Mol Res*, **12(3):** 3256-3262

JJBS
Jordan Journal of Biological Sciences

Volume 12, Number 5,December 2019
ISSN 1995-6673
Pages 649 - 656

The Role of the Dietary Supplementation of Fenugreek Seeds in Growth and Immunity in Nile Tilapia with or without Cadmium Contamination

Wafaa T. Abbas*, Iman M.K. Abumourad, Laila A. Mohamed, Hossam H. Abbas, Mohammad M.N. Authman, Waleed S.E. Soliman and Mamdouh Y. Elgendy

Department of Hydrobiology, National Research Centre, 33 El Bohouth St. Dokki, P.O. Box 12622, Giza, Egypt

Received February 6, 2019; Revised March 29, 2019; Accepted April 13, 2019

Abstract

This study is aimed at evaluating fenugreek seeds (*Trigonella foenum-graecum*) as a feed additive for the enhancement of growth and immunity in Nile tilapia (*Oreochromis niloticus*). It is also aimed at assessing their role in fish experimentally exposed to cadmium toxicity. Fish was distributed into five groups as follows: two groups were given crude fenugreek seeds at the concentrations of 5 % and 2.5 %, two groups received 3 % and 1 % concentrations of an alcoholic fenugreek seed extract, in addition to the control group. Each group contained two subgroups; one subjected to cadmium and the other without cadmium exposure. After thirty days of feeding, the fish were bacterially challenged with *Aeromonas hydrophila*. Then the growth and hematological parameters were assessed. The interleukins IL6 & IL8 gene expressions were also estimated. The results indicate a decrease in growth parameters in the cadmium-exposed groups, whereas the growth parameters improved in the fenugreek-fed fish, especially those that received the crude fenugreek seeds at 5 % and the seed extract at 3 % concentrations. Hemoglobin, lymphocyte percentages and the total leukocyte count increased in the group treated with a 2.5 % concentration of crude fenugreek seeds. Also the crude fenugreek seeds at a 5 % concentration induced the lowest mortality (70 %) following the bacterial challenge test. Moreover, the IL6 and IL8 genes expressions were up-regulated in the groups treated with crude fenugreek seeds at 5 % and the seed extract at 3 % concentrations. It can be concluded that fenugreek seeds can be used as feed additives to improve fish growth and immunity, and to help reduce the hazardous effects of cadmium pollution.

Keywords: *Oreochromis niloticus*, Fenugreek, Growth performance, Cadmium, *Aeromonas hydrophila*, Interleukins.

1. Introduction

Aquaculture is the fastest growing sector in the world of food production accounting for almost 50 % of the world's food fish (Martins *et al.*, 2011; FAO, 2018). Aquaculture production should be increased to cover the continuous outpaced population growth (Aly, 2009). Such high rates of aquaculture production depend mainly on raising the growth rates and immunity of fish to afford the disease outbreaks which constitute the main impediment to aquaculture development. The strength of aquaculture lies in growing fish that are resistant to diseases and contamination with heavy metals, pesticides, and other stressful contaminants. Unfortunately the agricultural drainage and irrigation waters contain high concentrations of different pesticides, fertilizer runoff and heavy metals (Abumourad *et al.*, 2013).

Heavy-metal pollution is one of the greatest problems for fish consumers. Heavy metals are inorganic non-biodegradable chemicals that cannot be metabolized and broken down into harmless forms since they leave the biological cycles very slowly (Abumourad *et al.*, 2013 and Wani *et al.*, 2017). Elements such as cadmium, copper, lead, and zinc are considered the most dangerous in the ecotoxicological effects (Golovanova, 2008). Cadmium (Cd) is a xenobiotic which is widely used in electronics, metal plating, batteries, dye, and plastic industries. It has toxic effects on animal health even at very low concentrations (Sorensen, 1991). Filipoviæ and Raspor (2003) reported that Cd enters the aquatic ecosystems from different resources and causes many physiological alterations and DNA disorders.

Although chemical drugs are traditionally used for fish-disease treatment (Herman, 1970 and Chowdhury *et al.*, 2015), they can give rise to the emergence of drug-resistant bacteria, environmental pollution and residues (Lee and Gao, 2012). Recently, more interest has been directed at the development of immunostimulants especially those of natural origins that operate on the principle of stimulating innate immunity which is the first line of defense against pathogenic invaders (Abbas and Awad, 2016; Awad and Awaad, 2017). Medicinal plants are biodegradable, cheap, easy to prepare, and effective, with fewer side effects during the treatment. They also act as immunostimulants and have anti-bacterial activities in

* Corresponding author e-mail: wtabbas2005@yahoo.com.

fish and shellfish without causing any environmental problems (Harikrishnan *et al.*, 2011). Accordingly, they can be used in aquaculture as a natural source of food and immunostimulant in exchange for many chemical additives.

The effect of some plant extracts on several physiological functions in different fish species have been investigated by many studies; for example, Awad *et al.* (2013) studied the effect of black cumin seed oil (*Nigella sativa*) and nettle extract (Quercetin) on the enhancement of immunity in rainbow trout (*Oncorhynchus mykiss*). The effects of fenugreek (*Trigonella foenum graecum*) on gilthead seabream's (*Sparus aurata L.*) immune status and growth performance were also studied by Awad *et al.* (2015).

Studies of different growth parameters, hematological changes, and immune gene expressions create good biomarkers for aquaculture production and fish health. In this context, this work has been carried out for studying the effect of fenugreek seeds (*Trigonella foenum-graecum*) on different growth, hematological, and immune parameters of Tilapia being the most common freshwater-cultured fish all over the world. Also the study aims to evaluate the role of fenugreek seeds in reducing the toxic effects of cadmium on fish.

2. Materials and Methods

2.1. Medicinal Plant

Crude crushed fenugreek (*Trigonella foenum-graecum*) seeds and an alcoholic extract of seeds were prepared to be used as fish feed additives. The alcoholic extract was obtained by washing, drying, and crushing 1 Kg of fenugreek seeds to be soaked in a double volume of absolute ethyl alcohol in a stopper container for five days. The mixture was shaken more than once each day. It was filtered, evaporated by a rotary evaporator. Finally it was left for complete dryness and was weighed (Azwanida, 2015).

2.2. Fish Diets

A commercial pellet diet (35 % protein) was firstly crushed, mixed with the appropriate ratios of crude crushed fenugreek seeds or their alcoholic extract, and wet with water, then turned again into pellets. The diet was allowed to dry in the open air, and was then stored at 4^{o}C until use.

2.3. Fish and Experimental Design

Around 450 Nile Tilapia fish (*Oreochromis niloticus*), of about 30-40 g were obtained from the private fish farm at Kafr El-Shaik, Egypt. The fish were allowed to acclimatize in an aerated free-flowing and de-chlorinated tap water for two weeks. Water quality parameters during the study period were as follows: temperature (23.3^{o}C); pH (7.6); dissolved oxygen (6.4 ppm); alkalinity (115 ppm $CaCO_3$) and hardness (130 ppm $CaCO_3$). After acclimatization, the fish were distributed into five groups as follows: two groups received crude fenugreek seeds of 5 % and 2.5 % concentrations, while the other two groups which fed on the alcoholic seed extract of 3 % and 1 % concentrations. The last group was the control group that fed on the basal diet. Each group was subdivided into two subgroups; a group subjected to 1/10 LC_{50} of cadmium toxicity [1.5 mg of $CdCl_2$, according to Garcia-Santos *et al.*, 2006], and another group non-treated with Cd. The applied ratios of the crude and extract fenugreek seeds were chosen based on some previous references (Zaki *et al.*, 2012; Awad *et al.*, 2015). Fish were fed twice daily at 3 % of fish body weight. After thirty days of feeding, the growth performance and hematological parameters were investigated. The other subgroups of fish that were not exposed to Cd were bacterially challenged, and noticed for mortality rates for ten days, and tissue samples were collected for interleukins (6 & 8) gene expressions to assess the immune function induction by the fenugreek plant.

2.4. Growth Performance

Fish sampling was done twice; at the beginning of the experiment and after thirty days of being fed on the fenugreek. Fish were firstly anaesthetized by keeping them in aquaria containing clove oil (Merck, Germany) at a concentration of 50µl L^{-1} for five minutes. (Hamackova *et al*., 2006). Total length and total weight were recorded in cm and gram respectively. After the dissection of each fish from each treated group, the liver and gonads weights were recorded to calculate growth indices. Weight gain (WG), specific growth rate (SGR), and some growth indices [hepato-somatic index (HSI), gonado-somatic index (GSI) and the condition factor (CF)] were calculated according to the following formulas (Tukmechi *et al*., 2011).

WG = final weight – initial weight

SGR = 100* (ln final weight – ln initial weight)/days of feeding

HSI = (liver weight/total weight)*100

GSI = (Gonads weight/total weight)*100

CF = (total weight/total length^3)*100

2.5. Hematological Assays

Blood samples were collected from the caudal veins in EDTA tubes. Red blood cells (RBCs) and white blood cells (WBCs) were counted using an improved Neubauer hemocytometer (Natt and Herrick, 1952). Leukocytic differential counts were also recorded using Giemsa stain. Hematocrit (Hct %) was determined using heparinized capillary tubes, centrifuged in a microhematocrit centrifuge. Hemoglobin concentration (Hb) was recorded using spectrophotometer according to the cyanmethemoglobin method (Drabkin, 1948). The red blood indices [mean corpuscular volume (MCV), mean corpuscular Hemoglobin (MCH), and mean corpuscular Hemoglobin concentrations (MCHC)] were calculated using Hct, Hb and RBC measurements.

2.6. Immunological Assays

2.6.1. Experimental Challenge with Bacteria

At the end of the feeding experiment, a Cd non-treated subgroup was injected intra-peritoneally with 0.2 ml of a suspension containing 4×10^7 CFU/ml live *Aeromonas hydrohila* that were prepared according to Zhang *et al.* (2016). The challenged fish were observed for ten days for the recording of the mortality rates, clinical signs, and post mortem lesions. Re-isolation of *A. hydrophila* from dead fish was processed to confirm the specificity of pathogenicity. Tissue samples were collected and maintained in -80^{o}C for interleukins (6&8) gene expression determination.

2.6.2. Evaluation of IL6 & IL8 Gene Expressions Using Real-time PCR

RNA extraction: After two days of the bacterial challenge test, total RNA was extracted from the liver using a Gene JET RNA Purification Kit (Fermantus, UK) according to the manufacturer's protocol.

cDNA synthesis: 2 µg RNA was reverse transcribed with Revert Aid First Strand cDNA Synthesis Kit™ (Fermentus life science) using hexa-nucleotides and was used as templates for Real-time PCR.

Primer designing: Primers for target genes and the internal control (18s ribosomal RNA) (Table 1) were designed through the NCBI web site and were purchased from Invitrogen Corporation (Van Allen Way, Carlsbad, Canada).

Table 1. Sequences of the 5' and 3' synthetic primers used in PCR

Accession number	Primers (sense and antisense 5'→3')	Annealing Temp.
IL-6 XM_019350387.1	Sense: 5'-TCCGATTGAAGACGGAAGTGT-3' Antisense: 5'-GGAGCAGTGCACTCGAAGG3'	58 ℃
IL-8 NM_001279704	Sense: 5'-AGAGAACAGAGGAGACCGGG A3' Antisense: 5'-CTCCACCTTCTCGATGTGGC 3'	58℃
18sRNA JF698683.1	Sense: 5'-GGACACGGAAAGGATTGACAG3´ Antisense:5´-GTTCGTTATCGGAATTAACCAGAC3´	58℃

Quantitative Real-Time PCR

cDNA was PCR amplified using corresponding primers for IL6, IL8, and 18S rRNA was used as a reference housekeeping gene. PCR-Applied Biosystems was used with the use of SYBR green PCR Master Mix (Applied Biosystems) and gene specific primers where specimens' analysis were done in a final volume of 12 µ L in MicroAmp® Optical 96-well reaction plates (Applied Biosystems, Foster City, CA) using ABI PRISM 7500 instrument, Applied Biosystems (The qPCR mixture consisted of 1 µl of cDNA (equivalent to 10 ng of RNA), 1 µl of 0.5 µM gene-specific forward primer, 1 µl of 0.5 µM gene-specific reverse primer, 6 µl of 2× SYBR Green SuperMix and 3 µl of DEPC-treated water. Q PCR was performed in triplicate for each cDNA sample. The qPCR thermal cycling parameters were 50 ºC for two minutes, 95 ºC for two minutes followed by forty cycles of 95 ºC for fifteen seconds and 60 ºC for one minute. Th e PCR products were also gel-excised, purified, and sequenced to confirm that they match the target genes sequences.

2.6.3. Molecular Data Analysis

The relative transcriptional levels of different genes were determined by subtracting the cycle threshold (Ct) of the sample by that of the 18S ribosomal RNA, the calibrator, using the formula: ΔCt =Ct (sample) - Ct (calibrator). T he relative expression level of a s pecific gene in the immunized fish was compared to that of non-immunized fish to obtain 2ΔΔCt, where ΔΔCt = ΔCt (control) - ΔCt (Pfaffl 2001). Statistical analyses for the mRNA transcription levels were performed with the aid of the SPSS.16 statistical package (SPSS Inc., Microsoft Co., Redmond, USA).

2.7. Statistical analysis

Results are presented as means ± standard error (SE). Significant differences were determined by one-way ANOVA test (Duncan, 1955). All statistical analyses were performed using a computer program of SPSS Inc. (version 17.0 for Windows) at P <0.05.

2.8. Ethical Approval

The study was ethically cleared by the ethical review board of the National Research Centre.

3. Results

3.1. Clinical Investigation

The clinical investigation of *O. niloticus* subjected to 1/10 LC_{50} of Cadmium (1.5 mg/l) for thirty days showed some pictures of illness-like ascites, dark liver, distended gall bladders and enlarged intestines (Figure 1).

Figure 1. *Oreochromis niloticus* subjected to 1/10 LC_{50} (1.5 mg/l)

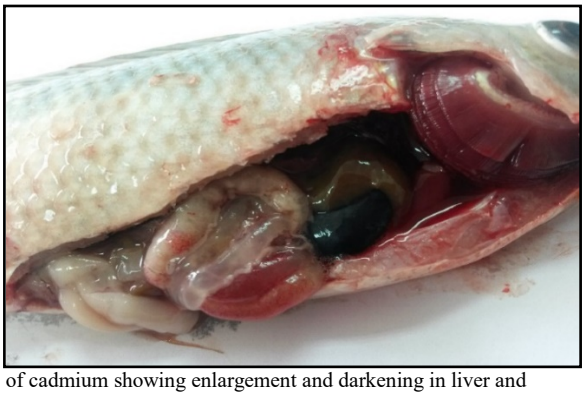

of cadmium showing enlargement and darkening in liver and gallbladder, enlargement of intestines with ascites

3.2. Weight Gain (WG) and Specific Growth Rate (SGR)

The results of the current study showed that the highest fenugreek concentrations; of crude fenugreek seeds at a 5 % concentration and the seed extract at a concentration of 3 % showed the highest significant increase (P>0.05) of WG (10.14 and 9.88 g, respectively) compared to the control (3.3 g) and SGR (0.76 and 0.81, respectively) compared to control (0.32) (Figures 2 and 3). Regarding the cadmium treated groups, there was a decrease in WG and SGR compared to their corresponding non-cadmium treated groups. Whereas the fish that fed on f enugreek seeds and subjected to Cd revealed insignificant increase in WG and SGR, especially at higher fenugreek concentrations; (crude fenugreek seeds at 5 % and the seed extract at 3 %) (Figures 2 and 3).

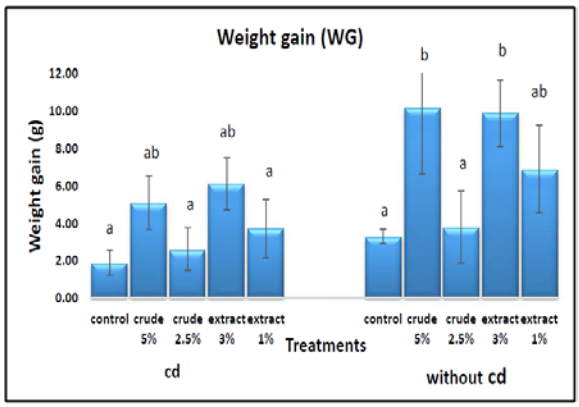

Figure 2. Weight gain (WG) of *Oreochromis niloticus* after experimental feeding on fenugreek seeds for 30 days with and without being subjected to 1/10 LC_{50} of cadmium (1.5 mg/l). The same letters at the columns are not significantly different at $P > 0.05$

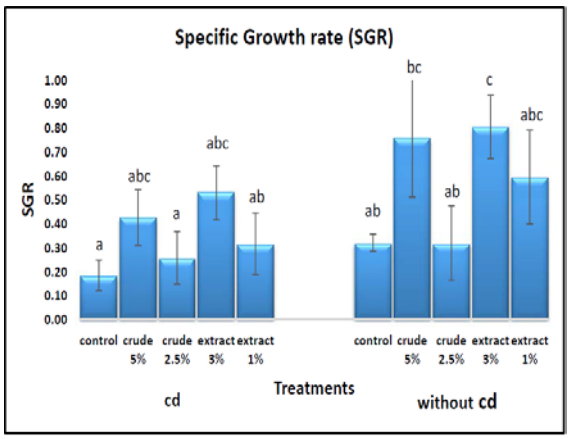

Figure 3. Specific growth rate (SGR) of *Oreochromis niloticus* after experimental feeding on fenugreek seeds for 30 days with and without being subjected to 1/10 LC_{50} of cadmium (1.5 mg/l). The same letters at the columns are not significantly different at $P > 0.05$.

3.3. Hepatosomatic Index, Gonadosomatic Index and Condition Factors

Generally, the fish group that was exposed to cadmium toxicity showed a d ecrease in the hepatosomatic index (HSI) and gonadosomatic index (GSI) (1.35 and 1.39, respectively) compared to the control group (1.46 and 2.60, respectively) (Table 2). There was a significant increase in HSI values (P>0.05) in the Cd-exposed groups at lower fenugreek concentrations; that is crude fenugreek seeds at 2.5 % and the seed extract at 1 % (2.03 and 2.2, respectively). Regarding GSI values, the group treated with crude fenugreek seeds exhibited a significant increase in the Cd-exposed groups (P>0.05); they were (4.09 and 3.41) in the groups that fed on the crude fenugreek seeds at 5 % and at 2.5 % concentrations, respectively compared to their comparable control groups. CF values in all groups showed insignificant changes (Table 2).

Table 2. Hepatosomatic index (HSI), Gonadosomatic index (GSI) and Condition factor (CF) values of *Oreochromis niloticus* that fed on fenugreek seeds for 30 days with and without being subjected to 1/10 LC_{50} of cadmium (1.5 mg/l).

Treatment		Hepatosomatic Index (HSI)	Gonadosomatic index (GSI)	Condition factor (CF)
		Mean ± SE	Mean ± SE	Mean ± SE
Cd	Control	1.35 ± 0.08^{a}	1.39 ± 0.12^{a}	1.70 ± 0.07^{a}
	Crude 5%	1.23 ± 0.33^{a}	4.09 ± 0.88^{c}	1.54 ± 0.03^{a}
	Crude 2.5%	2.03 ± 0.40^{bc}	3.41 ± 0.90^{bc}	1.47 ± 0.12^{a}
	Extract 3%	1.50 ± 0.19^{ab}	2.13 ± 0.64^{ab}	1.51 ± 0.05^{a}
	Extract 1%	2.20 ± 0.22^{c}	1.61 ± 0.58^{ab}	1.50 ± 0.09^{a}
Without Cd	Control	1.46 ± 0.08^{ab}	2.60 ± 0.76^{abc}	1.63 ± 0.02^{a}
	Crude 5%	2.07 ± 0.10^{bc}	1.64 ± 0.31^{ab}	1.57 ± 0.06^{a}
	Crude 2.5%	1.31 ± 0.09^{a}	1.19 ± 0.20^{a}	1.51 ± 0.08^{a}
	Extract 3%	2.02 ± 0.17^{bc}	1.86 ± 0.31^{ab}	1.60 ± 0.10^{a}
	Extract 1%	1.62 ± 0.03^{abc}	1.29 ± 0.35^{a}	1.79 ± 0.28^{a}
	F-Value	3.216	2.869	0.794
	Sig.	0.004**	0.008**	0.623†

Means with the same letter within the same column are not significantly different (P>0.05) SE= standard error F-value = ANOVA F-test. Sig. = significance level. **ANOVA (Highly significant difference, P<0.01). †ANOVA (Insignificant difference, P>0.05).

3.4. Hematological Results

While there was a g eneral decrease in the red blood cells count (RBCs), hemoglobin (Hb), packed cell volume (Hct%) values in all cadmium-treated groups compared to the control groups, only the group treated with a 2.5 % crude fenugreek seeds showed a s ignificant increase in RBCs, Hb, Hct % and hematological indices (Table 3). Cadmium toxicity decreased the total WBCs count, while the group treated with 2.5 % crude fenugreek seeds showed a significant increase in WBCs count compared to the control cadmium group (Figure 4). Also, the Cd-exposed group showed a significant decrease in lymphocyte %, and fenugreek treatments revealed an increase in their percentages (Figure 5).

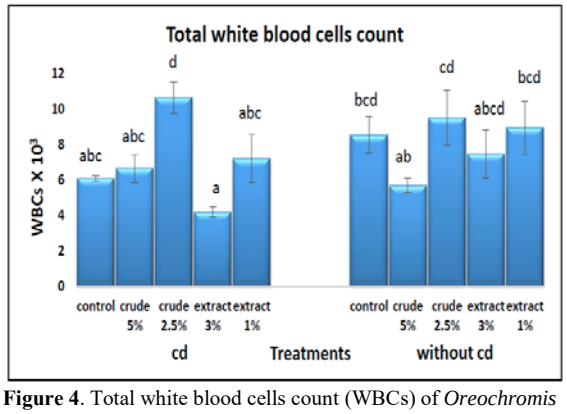

Figure 4. Total white blood cells count (WBCs) of *Oreochromis niloticus* after experimental feeding on fenugreek seeds for 30 days with and without subjection to 1/10 LC_{50} of cadmium(1.5 mg/l) (1.5 mg/l). The same letters at the columns are not significantly different at $P > 0.05$.

Table 3. RBC_S count, Hb, Hct and hematological indices of *Oreochromis niloticus* fish feeding on fenugreek seeds for 30 days with and without being subjected to 1/10 LC_{50} of cadmium (1.5 mg/l).

Treatments		RBC_S X 10^6/µl	Hb (g/dl)	Hct (%)	MCV	MCH	MHCH
		Mean ± SE	Mean±SE	Mean ± SE	(fl)	(pg)	(g/dl)
Cd	Control	1.41±0.02[a]	4.60±0.06[a]	21.50±0.29[a]	152.48	32.62	21.40
	Crude 5%	1.36±0.23[a]	4.83±0.55[a]	20.75±3.59[a]	153.14	35.61	23.25
	Crude 2.5%	1.91±0.26[b]	7.13±0.87[b]	30.75±4.15[b]	160.99	37.30	23.17
	Extract 3%	1.26±0.10[a]	4.18±0.29[a]	19.25±1.44[a]	152.78	33.13	21.69
	Extract 1%	1.45±0.01[a]	4.60±0.06[a]	21.50±0.29[a]	148.28	31.72	21.40
Without Cd	Control	1.40±0.03[a]	4.80±0.12[a]	21.75±0.48[a]	155.64	34.35	22.07
	Crude 5%	1.58±0.12[ab]	5.08±0.48[a]	24.00±1.91[a]	151.90	32.12	21.15
	Crude 2.5%	1.50±0.06[ab]	5.13±0.22[a]	23.25±1.03[a]	154.74	34.11	22.04
	Extract 3%	1.52±0.11[ab]	4.83±0.14[a]	22.25±0.75[a]	146.38	31.74	21.69
	Extract 1%	1.53±0.12[ab]	5.05±0.20[a]	23.50±0.87[a]	153.59	33.01	21.49
	F-Value	1.776	4.163	2.500			
	Sig.	0.115†	0.001**	0.029*			

Means with the same letter within the same column are not significantly different *at* $P>0.05$. SE= standard error. *F*-value = ANOVA *F*-test. Sig. = significance level.†ANOVA (Insignificant difference, $P>0.05$). *ANOVA (Significant difference, $P<0.05$). **ANOVA (Highly significant difference, $P<0.01$).

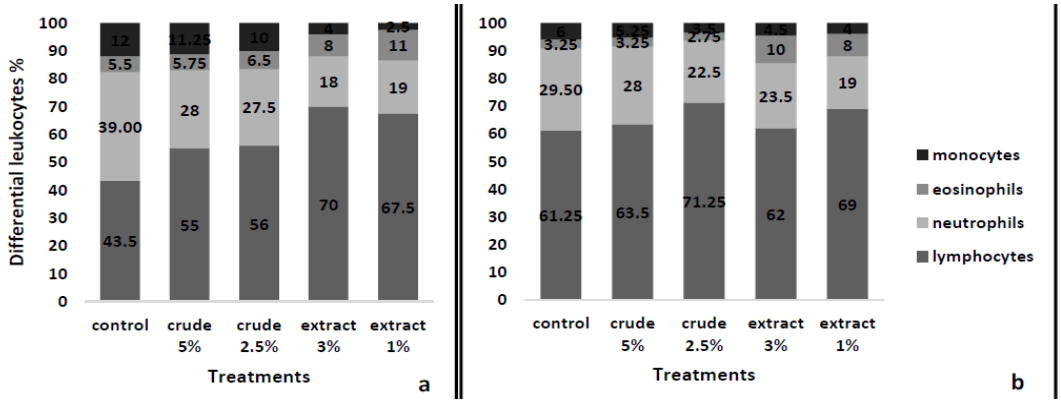

Figure 5. : Differential white blood cells of *Oreochromis niloticus* after experimental feeding on fenugreek seeds for 30 days with subjection to 1/10 LC_{50} of cadmium (**a**) and without cadmium subjection (**b**).

3.5. Immunological Results

3.5.1. Bacterial Challenge

After thirty days of fenugreek feeding, the *A. hydrophila* injection revealed the lowest mortality rate in the group that fed on the 5 % crude fenugreek seed concentration followed by the groups that fed on the seed extract at 3 % and 1 % concentrations, and finally followed by the group that fed on the crude fenugreek seeds at a 2.5 % concentration compared to the control group (Figure 6). Some clinical observations were noticed in the injected fish such as the external hemorrhage in the abdominal region (Figure 7).

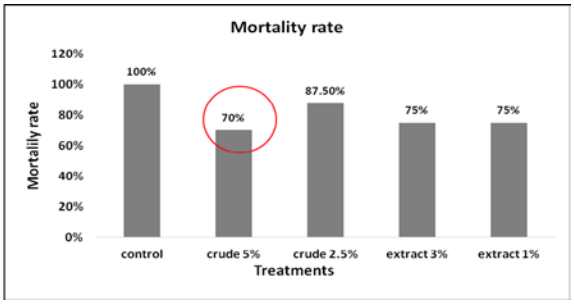

Figure 6. Mortality rate of *Oreochromis niloticus* injected with *Aeromonas hydrophila* after 30 days feeding on fenugreek seeds.

Figure 7. *Oreochromis niloticus* injected with *Aeromonas hydrophila* showed external hemorrhage in the abdomen and anal prolapse.

3.5.2. Molecular Studies (Interleukins 6 & 8 (IL 6 &IL 8) Immune Genes Expression)

The changes in the IL6 & IL8 gene expression fold with the different concentrations of the fenugreek crude seeds and seed extract show that the expressions of these genes were increased significantly with high fenugreek doses (P>0.05). They were up-regulated better in the groups treated with crude fenugreek seeds at 5 %, or with the seed extract at 3 % following the bacterial challenge. However, it was clear that the fold change of IL6 expression (8.24-8.46) was higher than the fold change of IL 8 expression (1.34-3.16) (Figure 8).

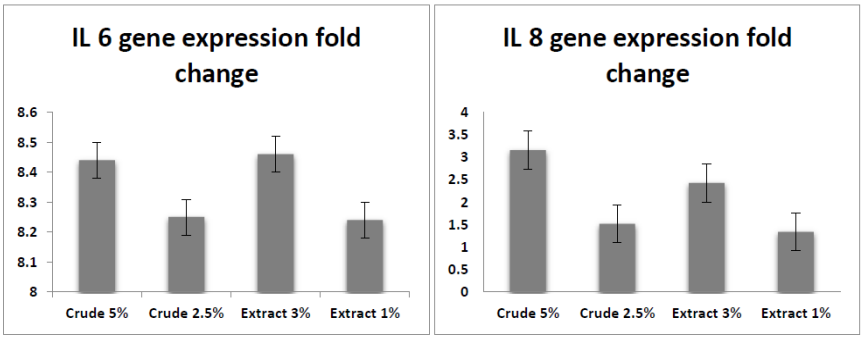

Figure 8. IL6 and IL8 gene expression fold changes after *Aeromonas hydrophila* bacterial challenge in fish that fed on Fenugreek crude and extracts with different concentrations.

4. Discussion

Aquaculture is an important industrial sector which needs combined efforts to boost its production as it constitutes the last frontier to solve the world's protein-deficiency problem. To grow fish that are bigger and healthy, alternatives from natural products must been found as feed additives and immunostimulants instead of drugs and chemicals. Many plants that possess several biological activities are currently used in traditional medicine, including fenugreek seeds. This study reveals that *O. niloticus* that were given crude fenugreek seeds at 5 % and fenugreek seeds' extract at 3 % concentrations showed a significant increase in growth performance. Also it has been found that fenugreek can modulate the growth retardation in the cadmium-exposed groups, especially at higher fenugreek concentrations; crude fenugreek seeds at 5 % and fenugreek seed extract at 3 %. T he growth-promotion effect of fenugreek may be attributed to its high nutritive value, as it is rich in protein, carbohydrates and many minerals. Fenugreek also improves the digestion of protein and absorption of fats (Mansour and El-Adawy, 1994). Some previous studies reported the effect of fenugreek as food additive in rabbits (Zeweil *et al.*, 2015) and ensured its growth-promotion effect in fish (Zaki *et al.* 2012; Awad *et al.*, 2015). Similarly, the obtained results suggest that using a concentration of 5 % of crude fenugreek seeds and 3 % of an alcoholic fenugreek seed extract as a feed additive enhances fish growth and equilibrates the cadmium inhibitory effect on the growth of the Nile tilapia fish.

Environmental pollution causes a lot of physiological and metabolic changes to fish that can have bad effects on growth and reproduction (Heath, 1995). Hepatosomatic index (HSI) represents one of the main indicators of metabolic activity and status of energy reserve in animals. Thus, HSI value provides information about the health status of fish and the quality of water surrounding it. In this study, the exposure of *O. niloticus* to 1/10 LC_{50} of Cd for thirty days decreased the HSI value. This may be attributed to the excessive usage of energy reserve in the liver of the cadmium-exposed group (Çiftçi *et al.*, 2015). Such result was corroborated by previous studies which reported that HSI values decreased in catfish and tilapia fish when exposed to water pollution, especially heavy-metal pollution (Bekmezci, 2010; Çiftçi *et al.*, 2015).

Also, gonadosomatic index (GSI) is another parameter that reflects the health status of fish. It was decreased in this study in the cadmium-exposed group; such result was similar to that of Çiftçi *et al.* (2015) who reported a decrease in GSI in tilapia fish after exposure to cadmium and zinc heavy metals. They attributed such decrease in the GSI value to the inhibition of some enzymes and reproductive hormones due to chemical pollution. Fortunately, feeding on f enugreek for thirty days can neutralize the cadmium toxic effects on liver and gonads. This was obvious in some fenugreek groups that showed a significant increase in HSI and GSI values in the

cadmium-exposed groups, which may be explained by the catalyst-promoting effects of fenugreek and its usage as a growth stimulus which can also increase reproductive hormones.

Moreover, condition factor (CF) indicates the state of general health of fish that is affected by many environmental factors. It has been used to compare growth conditions of fish, since high CF values can indicate good environmental quality and vice versa. In the current study, the insignificant changes in CF in mostly all of the the treated groups may be attributed to the short duration of feeding (thirty days). Similarly, the CF values were not affected in *Clarias gariepinus* under the effect of lead acetate toxicity (Balawi *et al*., 2011).

Regarding the hematological changes, only the group that fed on a concentration of 2.5 % of crude fenugreek seeds showed a significant increase in RBCs, Hb and Hct % in cadmium- treated groups, while other groups were insignificantly affected. This may be attributed to the inability of the short duration of time to affect the hematological parameters. Also cadmium decreased the fish immunity which is represented in the total leukocyte count and lymphocyte %; however, feeding on fenugreek modulated such toxic effect of cadmium and increased the WBCs count in the group which fed on t he crude fenugreek seeds at 2.5 % and the lymphocyte percentage in all of the cadmium-exposed groups, which explains the increase in the immunity response of fish, especially after the bacterial challenge (Awad and Awaad, 2017).

The immune system plays an essential role in protecting fish against stressful environmental conditions. Immunological effects of natural plants depend on the dose and time of administration as well as on the fish species (Chakrabarti, 2005; Awad and Awaad, 2017). An important and a large category of proteins that are crucial to many immunological processes are the pro-inflammatory cytokines. Cytokine genes are glycoprotein mediators produced by immune cells and contribute to cell growth and differentiation and defense mechanisms of the host against bacterial invasions (Biswas *et al*., 2012). Liver is the central organ regulating the acute-phase response by releasing specific cytokines including interleukin 1 be ta (IL-1beta), interleukin 6 (IL-6) and interleukin 8 (IL-8) (Panigrahi *et al*., 2007). Some investigations have identified cytokines and immune genes in the salmonid immune systems (Secombes *et al*., 2001) and their response to invading bacteria in rainbow trout (Komatsu *et al*., 2009). The present study evaluated IL6 & IL8 cytokines gene expressions after a bacterial challenge with *A. hydrophila*, the causative agent for hemorrhagic septicemia and some frequent diseases among fish and other aquatic animals (Longyant *et al*., 2010). IL-8 is an important cytokine, which can attract neutrophils, T-lymphocytes, and basophils to inflammatory sites (Mukaida *et al*., 1998). This protein was detected in the head kidney, and spleen of catfish, and its expression was up-regulated three to five fold in channel catfish and blue catfish after infection with the pathogenic bacterium *Edwardsiella ictaluri* (Chen *et al*., 2005). IL-6 is another cytokine that plays important roles in regulating immune gene response, hematopoiesis, and inflammation in many cell types such as lymphocytes and macrophages (Naka *et al*., 2002; Zante *et al*., 2015). The present results show that fenugreek up-regulated the expression of IL6 and IL8 after the *A. hydrophila* infection more than the control group. Also it can be seen that there is a d ose- immune genes expression positive relationship, which means that a high dose of fenugreek can enhance interleukins better. This may be attributed to the fact that fenugreek seeds are rich in active principles of flavonoid and alkaloids, and their high quantity led to improve the immune response. Similarly, the feeding of rainbow trout on l upin and stinging nettle stimulated the expression of IL-1b and IL-8 after being challenged with *A. hydrophila* (Awad *et al*., 2013). Also, the up-regulation of IL6 and IL8 expressions confirmed the inflammatory response in zebra fish after being challenged (Pressley & Gaskins, 2006). PCR analysis of Japanese puffer fish showed a constitutive expression of IL-6 in kidney following a bacterial infection (Bird *et al*., 2005).

5. Conclusion

In conclusion, this study highlights the promising role of fenugreek seeds in the *O. niloticus* production, since it can improve the growth and immunity parameters in tilapia fish. Also, fenugreek was shown to have an antibacterial effect and to decrease the mortality rate in fish challenged with *A. hydrophila*. Moreover, fenugreek plays a significant role in reducing the toxic effects of cadmium. However, further studies are still needed to assure its efficiency.

Acknowledgement

This work has been supported financially by project no. 11020301 from the National Research Centre (NRC), Egypt.

References

Abbas WT and Awad E. 2016. Effect of leek (*Allium ampeloprasum* L.) extract on biotransformation enzymes and innate immunity of catfish (*Clarias gariepinus)* exposed to Benzo [a] Pyrene. *Res J Pharma Biol Chem Sci*, **7**: 2211-2224.

Abumourad IM, Authman MM and Abbas WT. 2013. Heavy metal pollution and metallothionein expression: a survey on Egyptian tilapia farms. *J App Sci Res*, **9**: 612-619.

Aly SM. 2009. Probiotics and aquaculture .CAB Reviews: *Perspec in*, **403**: 1-16.

Awad E, Austin D and Lyndon AR. 2013. Effect of black cumin seed oil (*Nigella sativa*) and nettle extract (Quercetin) on enhancement of immunity in rainbow trout, *Oncorhynchus mykiss* (Walbaum). *Aquaculture*, **15**: 193-197.

Awad E and Awaad A. 2017. Role of medicinal plants on growth performance and immune status in fish. *Fish Shellfish Immunol*, **67**: 40-54.

Awad E, Cerezuela R and Esteban MÁ. 2015. Effects of fenugreek (*Trigonella foenum graecum*) on gilthead seabream (*Sparus aurata* L.) immune status and growth performance. *Fish Shellfish Immunol*, **45**: 454-464.

Azwanida N. 2015. A review on the extraction methods use in medicinal plants, principle, strength and limitation. *Med Aromat Plants*, **4**: 3-8.

Balawi H, Ahmad Z, Al-Akel A, Al-Misned F, Suliman E and Al-Ghanim K. 2011. Toxicity bioassay of lead acetate and effects of its sublethal exposure on growth, haematological parameters and reproduction in Clarias gariepinus. *Afr J Biotechnol*, **10**: 11039-11047.

Bekmezci H. 2010. Aşağı Seyhan Ovası drenaj sistemlerindeki kirlilik etmenlerinin *Clarias gariepinus*' da toksik etkileri. Çukurova Üniversitesi. Fen Bilimleri Enstitüsü, Biyoloji ABD, Doktora Tezi, 145.

Bird S, Zou J, Kono T, Sakai M, Dijkstra JM and Secombes C. 2005. Characterisation and expression analysis of interleukin 2 (IL-2) and IL-21 homologues in the Japanese pufferfish, *Fugu rubripes*, following their discovery by synteny. *Immunogenetics*, **56**: 909-923.

Biswas G, Korenaga H, Takayama H, Kono T, Shimokawa H and Sakai M. 2012. Cytokine responses in the common carp, *Cyprinus carpio* L. treated with baker's yeast extract. Aquaculture, 356: 169-175. Chakrabarti R. 2005. Stimulation of immunity in Indian major carp *Catla catla* with herbal feed ingredients. *Fish Shellfish Immunol*, **18**: 327-334.

Chen L, He C, Baoprasertkul P, Xu P, Li P, Serapion J, Waldbieser G, Wolters W and Liu Z. 2005. Analysis of a catfish gene resembling interleukin-8: cDNA cloning, gene structure, and expression after infection with *Edwardsiella ictaluri*. *Dev Comp Immunol*, **29**: 135-142.

Chowdhury AA, Uddin MS, Vaumik S and Al Asif A. 2015. Aqua drugs and chemicals used in aquaculture of Zakigonj upazilla, Sylhet. *Asian J Med Biol Res*, **1**: 336-349.

Çiftçi N, Ay Ö, Karayakar F, Cicik B and Erdem C. 2015. Effects of zinc and cadmium on condition factor, hepatosomatic and gonadosomatic index of *Oreochromis niloticus*. *Fresenius Environ Bull*, **24**: 1-4.

Drabkin DL. 1948. The standardization of hemoglobin measurement. *Am J Med Sci*, **215**: 110-110.

Duncan DB. 1955. Multiple range and multiple F tests. *Biometrics*, **11**: 1-42.

FAO. 2018. The State of World Fisheries and Aquaculture 2018 - Meeting the sustainable development goals. Food & Agriculture Organization of the United Nation, Rome.

Filipović V and Raspor B. 2003. Metallothionein and metal levels in cytosol of liver, kidney and brain in relation to growth parameters of *Mullus surmuletus* and *Liza aurata* from the Eastern Adriatic Sea. *Water res*, **37**: 3253-3262.

Garcia-Santos S, Fontaínhas-Fernandes A and Wilson JM. 2006. Cadmium tolerance in the Nile tilapia (*Oreochromis niloticus*) following acute exposure: assessment of some ionoregulatory parameters. *Environ Toxicol: An International Journal*, **21**: 33-46.

Golovanova I. 2008. Effects of heavy metals on the physiological and biochemical status of fishes and aquatic invertebrates. *Inland Water Biol*, **1**: 93.

Hamackova J, Kouril J, Kozak P and Stupka Z. 2006. Clove oil as an anaesthetic for different freshwater fish species. *Bulg J Agric Sci*, **12**: 185.

Harikrishnan R, Balasundaram C and Heo MS. 2011. Impact of plant products on innate and adaptive immune system of cultured finfish and shellfish. *Aquaculture*, **317**: 1-15.

Heath AG. 1995. Water pollution and fish physiology. CRC press., 337pp.

Herman RL. 1970. Chemotherapy of fish diseases: a review. *J Wild Dis*, ***6*(1)**: 31-34.

Komatsu K, Tsutsui S, Hino K, Araki K, Yoshiura Y, Yamamoto A, Nakamura O and Watanabe T. 2009. Expression profiles of cytokines released in intestinal epithelial cells of the rainbow trout, *Oncorhynchus mykiss,* in response to bacterial infection. *Dev Comp Immunol*, **33**: 499-506.

Lee JY and Gao Y. 2012. Review of the application of garlic, Allium sativum, in aquaculture. *J World Aquacult Soc*, **43**: 447-458.

Longyant S, Chaiyasittrakul K, Rukpratanporn S, Chaivisuthangkura P and Sithigorngul P. 2010. Simple and direct detection of *Aeromonas hydrophila* infection in the goldfish, *Carassius auratus* (L), by dot blotting using specific monoclonal antibodies. *J Fish Dis*, **33**: 973-984.

Mansour E and El-Adawy T. 1994. Nutritional potential and functional properties of heat-treated and germinated fenugreek seeds. *LWT-Food Sci Tech*, **27**: 568-572.

Martins CI, Eding EH and Verreth JA. 2011. The effect of recirculating aquaculture systems on the concentrations of heavy metals in culture water and tissues of Nile tilapia *Oreochromis niloticus*. *Food Chem*, **126**: 1001-1005.

Mukaida N, Harada A and Matsushima K. 1998. Interleukin-8 (IL-8) and monocyte chemotactic and activating factor (MCAF/MCP-1), chemokines essentially involved in inflammatory and immune reactions. *Cytokine Growth Factor Rev*, **9**: 9-23.

Naka T, Nishimoto N and Kishimoto T. 2002. The paradigm of IL-6: from basic science to medicine. *Arthritis Res Ther*, **4**: S233.

Natt MP and Herrick CA. 1952. A new blood diluent for counting the erythrocytes and leucocytes of the chicken. *Poultr Sci*, **31**: 735-738.

Panigrahi A, Kiron V, Satoh S, Hirono I, Kobayashi T, Sugita H, Puangkaew J and Aoki T. 2007. Immune modulation and expression of cytokine genes in rainbow trout *Oncorhynchus mykiss* upon probiotic feeding. *Dev Comp Immunol*, **31**: 372-382.

Pfaffl M. 2001. Development and validation of an externally standardised quantitative insulin-like growth factor-1 RT-PCR using Light Cycler SYBR Green I technology. In: **Rapid Cycle Real-Time PCR.** (pp. 281-291), Springer, Berlin, Heidelberg.

Pressley M and Gaskins IW. 2006. Metacognitively competent reading comprehension is constructively responsive reading: how can such reading be developed in students? *Metacognition and Learning*, **1**: 99-113.

Secombes C, Wang T, Hong S, Peddie S, Crampe M, Laing KJ, Cunningham C and Zou J. 2001. Cytokines and innate immunity of fish. *Dev Comp Immunol*, **25**: 713-723.

Sorensen EM. 1991. Cadmium. In: **Metal Poisoning in Fish**. CRC press, Boca Raton, Florida.

Tukmechi A, Andani HRR, Manaffar R and Sheikhzadeh N. 2011. Dietary administration of beta-mercapto-ethanol treated *Saccharomyces cerevisiae* enhanced the growth, innate immune response and disease resistance of the rainbow trout, *Oncorhynchus mykiss*. *Fish Shellfish Immunol*, **30**: 923-928.

Wani RA, Ganai BA, Shah MA and Uqab B. 2017. Heavy metal uptake potential of aquatic plants through phytoremediation technique, a review. *J Bioremediat Biodegrad*, ***8:*** 404.

Zaki M, Labib E, Nour A, Tonsy H and Mahmoud S. 2012. Effect some medicinal plants diets on mono sex Nile tilapia (*Oreochromis niloticus*), growth performance, feed utilization and physiological parameters. *APCBEE Procedia*, **4**: 220-227.

Zante MD, Borchel A, Brunner RM, Goldammer T and Rebl A. 2015. Cloning and characterization of the proximal promoter region of rainbow trout (*Oncorhynchus mykiss*) interleukin-6 gene. *Fish Shellfish Immunol*, **43**: 249-256.

Zeweil H, Zahran S, El-Rahman M, El-Gindy Y and Embark J. 2015. Effect of fenugreek and anise seeds as natural growth promoter on the performance, carcass, blood constituents and antioxidant status of growing rabbits. *Egypt Poultr Sci J,* **35**: 909-921.

Zhang D, Xu DH and Shoemaker C. 2016. Experimental induction of motile Aeromonas septicemia in channel catfish (*Ictalurus punctatus*) by waterborne challenge with virulent *Aeromonas hydrophila*. *Aquacult Rep*, **3**: 18-23.

JJBS

Volume 12, Number 5,December 2019
ISSN 1995-6673
Pages 657 - 658

Jordan Journal of Biological Sciences

Short Communication

First Record of the Western Conifer Seed Bug, *Leptoglossus occidentalis* Heidemann, 1910 (Hemiptera, Coreidae), from Palestine

Elias N. Handal* and Mazin B. Qumsiyeh

Palestine Museum of Natural History, Bethlehem University, Bethlehem, Palestine

Received February 14, 2019; Revised March 5, 2019; Accepted March 12, 2019

Abstract

This is the first report of the invasive Western conifer seed bug *Leptoglossus occidentalis* Heidemann, 1910 (Hemiptera, Coreidae) from the Palestine geography representing its southern-most record in Asia. The record is from Wadi Al Makhrour, a valley considered as a key biodiversity area (KBA) and a UNESCO World Heritage site. *L. occidentalis* is a significant pest of pine trees and an invasive species to the Mediterranean region originally from western North America. More studies are needed on its ecology, status, genetics, distribution, and potential damage in Palestine.

Keywords: Hemiptera, Heteroptera, invasive species, pest, historic Palestine, *Leptoglossus occidentalis*.

1. Introduction

The family Coreidae of the insect Order Heteroptera has 270 genera and around 1900 described species world-wide (Henry 2009; Packauskas 2010); though a more recent reference is recommended. The genus *Leptoglossus* has sixty-one species restricted to the Nearctic ecozone except for one species that is the Western conifer seed bug, *L. occidentalis* (Heidemann, 1910) which has been spreading elsewhere (Brailovsky 2014). This is a damaging invasive species originally native to western North America which has been spreading to eastern North America and other parts of the world (Kulijer and Ibrahimi, 2017; Lesieur *et al*., 2019). The first record of this species in Europe was in Italy in 1999 (Taylor *et al*. 2001) to be soon followed by observations in further parts of Europe and then in Turkey in 2009 (Arslangündoğdu and Hizal 2010; Fent and Kment, 2011). From Turkey, the species has started to spread southwards to Lebanon (Nemer 2015) and the nearby Syrian Golan Heights (van der Heyden 2018).

This paper records the southern-most distribution of the Western conifer seed bug, *L. occidentalis* so far in a significant area and discusses the implication of finding the species in Wadi Al-Makhrour, near Bethlehem, Palestine. The area in question is a key biodiversity area and was also designated as a UNESCO World Heritage Site (see MoTA 2013) which really prompted the researchers to study such invasive and other threats to the local area. This area is the last remaining biodiversity hotspot in Western Bethlehem and the Southern Jerusalem areas. The valley is mentioned earlier in travel books (e.g. Robinson, 1856) and is undergoing a biodiversity reduction (Qumsiyeh *et al*. 2014; Amr *et al*. 2016).

2. Materials and Methods

Field trips were made to Al Makhrour Valley as part of the ongoing projects by the Palestine Museum of Natural History (PMNH) and the Palestine Institute for Biodiversity and Sustainability (PIBS) to study biodiversity in an area of significant conservation value coming under threats (Qumsiyeh *et al*. 2017). Wadi Al-Makhrour is a valley located about 7 km south of the old city of Jerusalem and about 6 km northeast of the old city of Bethlehem. Al-Makhrour is an important part of the system that refills the water aquifer of Bethlehem District area. The Genus *Leptoglossus* is easy to distinguish Coreid genera by having a denticulate hind femora and leaf-like dilations on the hind tibiae (Moulet 1995, Figure 1). The identification of the specimen at the PMNH lab shows the existence of the species *Leptoglossus occidentalis* which was confirmed by using keys to the genus *Leptoglossus* (Brailovsky 2014).

3. Results and Discussion

A living specimen of *L. occidentalis* was collected from Wadi Al-Makhrour under a pine tree of the species *Pinus halepensis* Miller (specimen number PMNH E11620, collected on 4 September 2018, Figure 1). The closest records from the Eastern Mediterranean region are from Turkey (Fent and Kment, 2011), Lebanon (Nemer 2015), and the Syrian Golan (van der Heyden 2018). The range spread from western North America to other parts of the world including Morocco, Turkey, Lebanon, and Syria

* Corresponding author e-mail: eliashandal93@gmail.com.

in the MENA region (van der Heyden 2018). This invasive pest species is found on conifer trees mostly of the genus *Pinus*, and is highly damaging (Fent and Kment 2011; Farinha *et al*. 2018).

This is the first record of the species from Palestine which raises a significant alarm concerning its potential damage to conifers such as *P. halepensis* and accordingly the potential damage to a highly sensitive ecosystem. Unfortunately, the sampling in the area was not intensive enough to understand the extent of the presence of a population of this species.

Locally, Handal (2017) have found another invasive species of Heteroptera, *Deroplax silphoides* Thunberg 1783, in the Bethlehem district. The finding of a second invasive pest species may signal significant changes in the environment already evident by decline of biodiversity in this region (e.g. Qumsiyeh *et al*. 2014; Amr *et al*. 2016). A more detailed survey of Heteroptera in Palestine is warranted in addition to using mitochondrial DNA analysis which has already shown its utility in understanding the spread of this species from western to eastern North America and then to Europe (Lesieur *et al*. 2019). This study concludes that such data, though limited, are important to create an understanding of the distributional changes of species and are especially relevant in the case of invasive species.

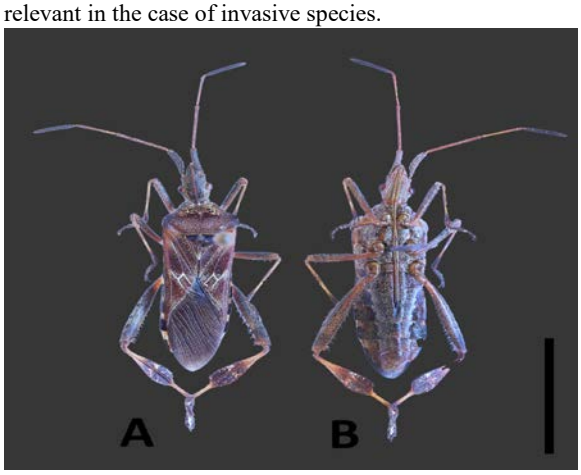

Figure 1. Adult of *Leptoglossus occidentalis*, A: Dorsal view, B: Ventral view, Scale Bar = 10mm.

Acknowledgment

The biodiversity work in Al-Makhrour valley is supported by grants from the National Geographic and the Darwin initiative and for the entomology collection from the Ministry of Education and Higher Education.

References

Amr ZS, Handal, EN, Bibi F, Najajrah MH and Qumsiyeh MB. 2016. Change in diet of the Eurasian eagle owl (*Bubo bubo*) suggests decline in biodiversity in Wadi Al Makhrour, Bethlehem Governorate, Palestinian Territories. *Slovak Raptor J*, **10**(1): 75-79.

Arslangündoğdu Z and Hizal E. 2010. The western conifer seed bug, *Leptoglossus occidentalis* (Heidemann, 1910), recorded in Turkey (Heteroptera: Coreidae). *Zool Middle East,* **50**(1): 138-139.

Brailovsky H. 2014. Illustrated key for identification of the species included in the genus *Leptoglossus* (Hemiptera: Heteroptera: Coreidae: Coreinae: Anisoscelini), and descriptions of five new species and new synonyms. *Zootaxa,* **3794**(1):143-178.

Farinha ACO, Silva JEP, Correia AC, Sousa EMR, Roques A and Branco M. 2018. Is *Leptoglossus occidentalis* entirely responsible for the high damage observed on cones and seeds of *Pinus pinea*? Results from a fertirrigation trial in Portugal. *Forest Ecol Management,* **429**: 198-206.

Fent M and Kment P. 2011. First record of the invasive western conifer seed bug *Leptoglossus occidentalis* (Heteroptera: Coreidae) in Turkey. *North-Western J Zool*, **7**(1):72-80.

Handal EN. 2017. First record of *Deroplax silphoides* (Thunberg, 1783) from the West Bank – Palestine. *Entomol Hellenica*, **26**: 13-16.

Henry TJ. 2009. **Biodiversity of Heteroptera**. 223-263 In: Foottit RG and Adler PH, (Eds.) **Insect Biodiversity,** Science and society. Oxford: Wiley-Blackwell.

Kulijer D and Ibrahimi H. 2017. First Report of Invasive Species *Leptoglossus occidentalis* in Kosovo (Heteroptera: Coreidae). *Acta Entomol Slovenica*, **25**:1.

Lesieur V, Lombaert E, Guillemaud T, Courtial B, Strong W, Roques A and Auger-Rozenberg MA. 2019. The rapid spread of *Leptoglossus occidentalis* in Europe: A bridgehead invasion. *J Pest Sci*., **92(1)**: 189-200.

MoTA (Ministry of Tourism and Antiquities), 2013. **Palestine, Land of Olives and Vines: Cultural Landscape of Southern Jerusalem, Battir**. World Heritage Site Nomination Document. Palestinian Ministry of Tourism and Antiquities. Department of Antiquities and Cultural Heritage Palestine

Moulet P. 1995. **Hémiptères Coreoidea (Coreidae, Rhopalidae, Alydidae), Pyrrhocoridae, Stenocephalidae EuroMéditerranéens**. Faune de France 81. Fédération Française des Sociétés de Sciences Naturelles, Paris.

Nemer N. 2015. **Report on insect pests associated with conelet losses and their management in Pinus pinea forests in Lebanon**. FAO, Rome.

Packauskas RJ. 2010. Catalog of the Coreidae, or leaf-footed bugs, of the New World. *Fort Hays Studies, Fourth Series,* **5**: 1–270

Qumsiyeh MB, Zavala SS and Amr ZS. 2014. Decline In vertebrate biodiversity In Bethlehem, Palestine. *Jordan J Biol Sci.,* **7**:101-107.

Qumsiyeh M, Handal E, Chang J, Abualia K, Najajreh M and Abusarhan M. 2017. Role of museums and botanical gardens in ecosystem services in developing countries: Case study and outlook. *Inter J Environ Studies*, **74**(2): 340-350.

Robinson E. 1856. **Biblical Researches in Palestine and the Adjacent Regions: A Journal of Travels in the Years 1838 & 1852**: in Three Volumes (Vol. 2). Murray, London.

Taylor SJ, Tescari G, Villa M. 2001. A Nearctic pest of Pinaceae accidentally

introduced into Europe: *Leptoglossus occidentalis* (Heteroptera: Coreidae) innorthern Italy. *Entomol News,* **112**: 101–103.

van der Heyden T. 2018. First record of *Leptoglossus occidentalis* Heidemann, 1910 (Hemiptera: Heteroptera: Coreidae: Coreinae: Anisoscelini) in the Golan Heights. *Revista Gaditana de Entomol*., **9**(1): 1-3.

JJBS

Volume 12, Number 5,December 2019
ISSN 1995-6673
Pages 659 - 662

Jordan Journal of Biological Sciences **Short Communication-2**

Salicylic Acid Modifies the Active Ingredients of Sour Orange

Khalid A. Khalid[1*] and Aisha M. A. Ahmed[2]

[1]Medicinal and Aromatic Plants Department, [2]Botany Department, National Research Centre, Cairo, Egypt

Received March 13, 2019; Revised April 10, 2019; Accepted April 13, 2019

Abstract

The essential oils of sour orange have been used for different purposes especially for the food and pharmaceutical industries. Salicylic acid plays significant roles in essential oil metabolism. In the present work, the effects of salicylic acid on the essential oil composition are examined. Sour orange trees were exposed to foliar spray of salicylic acid (0, 20 and 40 mg/L), and the essential oil of each treatment was isolated from young leaves and peels using the hydro distillation method (HD); then it was analyzed by the GC and GC/MS equipment's. The obtained results indicate that the essential oil percentage and its characterized constituents are affected by the salicylic acid significantly. The major components of the peel and leaf oils were limonene and linalool. The highest percentage of the essential oil and its major constituents were recorded with salicylic acid at 40 mg/L. Oxygenated monoterpenes (OM) was the major chemical class of the leaf oil, while monoterpene hydrocarbons (MH) was formed as a major fraction of the peel oil. Sesquiterpene hydrocarbons (SH) and oxygenated sesquiterpenes (OS) were the minor classes. Salicylic acid resulted in different variations of all chemical classes, i.e., MH, OM, SH and OS.

Keyword: Salicylic acid, Sour orange, Essential oil, Limonene, Linalool

1. Introduction

Sour orange (*Citrus aurantium* L.) belongs to the Family Rutaceae which is grown in South and Central America as well as in the Mediterranean region (Ait *et al*., 2005). Sour orange trees resist the worst environmental conditions, and the most popular rootstock of various citrus trees in Egypt is that of the sour orange tree (Reams and Furr, 1972). The essential oils of the leaves and peels of sour orange have been used for various purposes including cosmetics, perfumes, and for food and pharmaceutical industries (Lawless, 1992; Lehrner *et al*., 200l; Lota e*t al*,. 2001).

The exogenous application of bio-stimulants such as salicylic acid has been a successful method in scientific research with the potential of improving essential oils' composition to be used as natural sources in food and drug industries (Bukar *et al.*, 2016). Salicylic acid caused significant increases in essential oils isolated from young shoots and the peels of grapefruit (Khalid *et al.*, 2018). The effects of salicylic acid on essential oils isolated from yarrow (*Achillea millefolium* Boiss) were investigated (Rowshan and Bahmanzadegan, 2013); results indicated that salicylic acid resulted in significant increments in essential oil yield, 1, 8-cineol and β-caryphyllene compared with the control. Summer savory (*Satureja hortensis* L.) plants exposed to 5 mg/L of salicylic acid (as foliar spray) produced higher values in carvacrol, γ-terpinene, and monoterpene hydrocarbons than in the control, 10 and 20 mg/L of salicylic acid (Pirbalouti *et al.*, 2016). Salicylic acid caused significant increases in carvacrol, α-thujene, α-pinene and p-cymene detected in the thyme (*Thymus daenensis* Celak.) essential oil (Pirbalouti *et al*., 2014). Peppermint (*Mentha piperita* L.) plants were treated with salicylic acid, and significant variations were detected due to different applications of salicylic acid (Saharkhiz and Goudarzi, 2014; Khanam and Mohammad, 2017). Responses of *Ammi visnaga*'s essential oil to salicylic acid (0, 5, 10 and 20 mg/L) were investigated by Talaat *et al.* (2014), and the data indicated that the treatment with 20 mg/L produced the greatest amounts of essential oil and its major constituents. The essential oil of tansy (*Tanacetum vulgare* L.) plants was significantly changed due to salicylic acid applications (Goudarzi *et al.*, 2016). Significant increases were recorded in essential oil yield, limonene, β-selinene, sedanolide, and sedanenolide of Celery (*Apium graveolens* L.) with salicylic acid treatments (Ahmed *et al.*, 2018).

Improving the productivity of essential oil-bearing plants was required to increase the natural recourses. Therefore, the aim of the present study is to evaluate essential oils isolated from young leaves and peels of sour orange trees treated with various doses of salicylic acid.

2. Materials and Methods

2.1. Location

The experiments were carried out at the citrus experimental farm of the Faculty of Agriculture, Cairo University during 2017-18. The sour orange trees were divided into three groups. The first and second groups were exposed to salicylic acid of 20 and 40 mg/L. The

* Corresponding author e-mail: ahmed490@gmail.com .

third group was subjected to distilled water (as control). The salicylic acid was applied as foliar spray to run-off to foliage at the end of January and the first week of February in both seasons. The analyses of soil used in this study are presented in Table 1.

Table 1. Soil analysis used in this study.

Physical properties		Ions (mg/100g soil)	
Sand	26.1%	P	18.7
Silt	33.5%	K	25.3
Clay	40.4%	Ca	75.7
Chemical properties		Na	37.9
pH	7.9 (1 : 2.5)	HCO_3	22.9
EC	1.7 (dS/m)	Cl	10.3
OM	0.9%	CO_3	12.8
$CaCO_3$	0.8%	SO_4	23.9
Total N	78.9%	NO_3	9.8

2.2. Harvesting

During the first week of April and last week of October (2017 and 2018), young leaves and fruits were collected respectively. The fresh young leaves and peels of fruit were divided into small pieces with a knife. Then, they were weighed to isolate the essential oil.

2.3. Essential oil Isolation

The fresh young leaves and peels were collected from each treatment, and then 250g from each replicate (3 replicates) of all treatments were subjected to hydro-distillation for three hours using a Clevenger-type apparatus (Clevenger, 1928). The essential yield was calculated as a relative percentage (v/w).

2.4. Essential Oil Analysis

2.4.1. GC and GC–MS Conditions

GC analyses were performed using a Shimadzu GC-9 gas chromatograph equipped with a DB-5 (dimethyl-siloxane, 5 % phenyl) fused silica column (J & W Scientific Corporation) (30 m X 0.25 mm i. d., film thickness 0.25µm). Oven temperature was held at 50 ºC for five minutes and then programmed to rise to 240 ºC at a rate of 3 ºC/ min. The flame ionization detector (FID) temperature was 265 ºC and the injector temperature was 250 ºC. Helium was used as carrier gas with a linear velocity of 32 cm/s. The percentages of compounds were calculated by the area normalization method, without considering response factors. GC–MS analyses were carried out in a Varian 3400 GC-MS system equipped with a DB-5 fused silica column (30 m X 0.25 mm i. d., film thickness 0.25 lm); oven temperature was 50–240 ºC at a rate of 4 ºC/min, transfer line temperature was 260 ºC, carrier gas was helium, with a linear velocity of 31.5 cm/s, split ratio was 1:60, ionization energy was 70 eV, scan time was 1s, and mass range was 40–300 amu.

2.4.2. Identification of Volatile Components

The components of the oils were identified through the comparison of their mass spectra with those of a computer library or with authentic compounds, and these were confirmed through comparing their retention indices (RI^L), either with those of authentic compounds or with data published in the literature (Adams, 1995). Mass spectra from the literature were also compared (Adams 1995). Further identification was made by comparison of their mass spectra on both columns with those stored in NIST-98 and Wiley-5 Libraries. The retention indices (RI^C) were calculated for all volatile constituents using a homologous series of n-alkanes.

2.5. Statistical Analysis

In this vary experiment, one factor was considered: salicylic acid (0, 20 and 40 mg/L). For each treatment there were three replicates, the experimental design followed a complete random block design (RCBD). The average data of essential oil contents of both seasons were statistically analyzed using 1-way analysis of variance (Snedecor and Cochran, 1990). The applications of that technique were according to the STAT-ITCF program version 7 (Foucart, 1982).

3. Results

3.1. Effect of Salicylic Acid on Essential Oil Contents

The effects of salicylic acid doses (0, 20 and 40 mg/L) on essential oils isolated from the leaves and peels of sour orange trees are presented in Table 2. In both seasons, it was clear that the values of the leaf and peel oils were significantly increased with various doses of salicylic acid compared with the control. The highest amounts of the leaf and peel oils were reported with the application of 40 mg/L of salicylic acid recording the values of 0.5, 0.6 % and 0.8, 0.9 % of the leaf and peel oils during the first and second seasons, respectively.

Table 2. Effect of Salicylic acid on essential oil contents.

Salicylic acid (mg/L)	Essential oil content (%)			
	Young leaves		Peels	
	Seasons			
	2017	2018	2017	2018
0	0.2	0.3	0.2	0.3
20	0.3	0.4	0.5	0.5
40	0.5	0.6	0.8	0.9
LSD: 0.05	0.1	0.1	0.2	0.2

3.2. Effect of Salicylic Acid on Essential Oil Constituents

The various components that are detected using the GC/MS analysis are presented in Table 3. Different variations were observed in all of the components with different doses of salicylic acid. The major components recorded under all treatments with the salicylic acid were limonene and linalool for the essential oils extracted from the peels and leaves respectively. Higher values of limonene were recorded in the peel oil than in the leaf oil, while the linalool component was produced in higher amounts in the leaf oil than in the peel oil. The greatest amounts of limonene and linalool were produced under the treatment of 40 mg/L of salicylic acid with the values of 75.3 % and 62.9 % of the peel and leaf oils respectively. All characterized constituents in this investigation were classified into four chemical groups as follows: 1) Monoterpene hydrocarbons (MH), 2) Oxygenated monoterpenes (OM), 3) Sesquiterpene hydrocarbons (SH) and 4) Oxygenated sesquiterpenes (OS). The MH was the major group in the peel oil while OM was the major one in

the leaf oil. The highest amounts of MH (81.5 %) and OM (67.5 %) were obtained from the treatments of control and salicylic acid at 40 mg/L of the peel and leaf oil, respectively. The greatest amounts of SH (2.3 %) and OS (1.6 %) resulted from the treatment of the leaf oil with the dose of 20 mg/L.

Table 3. Effect of Salicylic acid on essential oil components in young leaves and peels.

No	Components	Class	RI^C	RI^L	Salicylic acid treatments (mg/L)					
					Young leaves			Peels		
					0	20	40	0	20	40
1	α-Pinene	MH	949	939	0.5	0.6	0.6	1.1	0.4	0.5
2	Camphene	MH	955	953	0.9	1.3	1.1	-	-	-
3	Sabinene	MH	977	976	0.9	0.1	0.7	0.3	0.5	0.1
4	β- Pinene	MH	081	980	0.7	0.9	0.3	0.4	0.2	0.1
5	β-Myrcene	MH	991	991	1.8	1.5	1.6	0.1	0.3	0.3
6	Octanal	MH	1003	1001	-	-	-	0.9	0.7	0.4
7	α-Phellandrene	MH	1006	1005	1.9	1.7	1.3	0.4	0.5	0.5
8	ʒ-Carene	MH	1011	1011	0.7	0.5	0.7	0.4	0.5	0.6
9	Limonene	MH	1032	1031	18.8	19.9	20.5	74.7	74.9	75.3
10	*cis*-β-Ocimene	MH	1041	1040	0.6	0.9	0.8	0.4	0.8	0.9
11	*trans*-β-Ocimene	MH	1050	1050	0.4	0.5	0.9	1.2	0.9	0.7
12	α-Terpinene	MH	1063	1062	0.3	0.2	0.6	0.9	0.5	1.1
13	α-Terpinolene	MH	1089	1088	1.8	0.6	0.2	0.7	0.5	0.1
14	*trans*-Linalool oxide	OM	1077	1074	0.2	0.5	0.7	0.4	0.6	0.5
15	Linalool	OM	1099	1098	59.8	61.9	62.9	11.7	12.8	12.9
16	Terpinen-4-ol	OM	1190	1189	1.8	1.0	0.1	0.7	0.3	0.3
17	Decanal	OM	1206	1204	-	-	-	0.2	0.3	0.5
18	Nerol	OM	1230	1228	1.6	1.2	0.4	0.4	0.5	0.4
19	Citral	OM	1242	1240	0.8	0.5	0.9	0.2	0.3	0.4
20	Carvone	OM	1243	1242	-	-	-	0.3	0.1	0.1
21	Geraniol	OM	1256	1255	0.1	0.5	0.9	1.5	0.2	0.4
22	Neryl acetate	OM	1366	1365	0.6	0.2	0.7	0.2	0.3	0.2
23	Geranyl acetate	OM	1385	1383	1.7	0.7	0.9	0.4	0.5	0.5
24	β-Caryophyllene	SH	14120	1418	0.7	0.6	0.5	-	-	-
25	α-Caryophyllene	SH	1455	1454	-	-	-	0.1	0.7	0.4
26	E-β-Farnesene	SH	1459	1458	0.8	0.9	0.3	0.7	0.5	0.3
27	Germacrene D	SH	1482	1480	0.7	0.8	0.1	0.1	0.8	0.2
28	Nerolidol	OS	1566	1564	0.5	0.8	0.4	0.1	0.4	0.6
29	Caryophyllene oxide	OS	1582	1581	0.4	0.7	0.6	0.7	0.2	0.4
30	α-Bisabolol	OS	1685	1683	0.5	0.4	0.6	0.1	0.4	0.4
MH (Monoterpene Hydrocarbons).					29.3	28.7	29.3	81.5	80.7	80.6
OM (Oxygenated Monoterpenes).					66.6	66.5	67.5	16.0	15.9	16.2
SH (Sesquiterpene Hydrocarbons).					2.2	2.3	0.9	0.9	2.0	0.9
OS (Oxygenated Sesquiterpenes).					1.4	1.9	1.6	0.9	1.0	1.4
Total identified					99.5	99.4	99.3	99.3	99.6	99.1

4. Discussion

The results obtained in this study indicate that salicylic acid can cause various changes in peel and leaf oils extracted from sour orange. These results may be attributed to the fact that salicylic acid (phenol compounds) has been recognized as a regulator of plant physiological processes when applied exogenously to plants. The most investigated roles of salicylic acid are associated with its interference in plant resistance response to pathogen attacks and less than optimal biotic conditions (Jalal *et al.,* 2012). The stimulating effects of salicylic acid on essential oil composition may be attributed to the salicylic acid influences on nutrient uptake, cell elongation, cell division, cell differentiation, sink / source regulation, changes in the hormonal status, improvement of photosynthesis, transpiration and stomatal conductance that reflect various increases in essential oil composition (Blokhina *et al.,* 2003; Shakirova, 2007; El-Tayeb, 2005; Abreu and Munne-Bosch, 2009). The salicylic acid has improved the level of cell metabolism, a prerequisite for the synthesis of auxin and/or cytokinin that may cause an increase in essential oil composition (Metwally *et al.*, 2003; Gharib, 2006). Rowshan and Bahmanzadegan (2013) indicated that salicylic acid may increase the essential oil composition through increasing the numbers of oil glands and enzyme activities of mono and sesquiterpenes biosynthesis.

5. Conclusion

The effects of salicylic acid on sour-orange essential oils were observed in this trial. 40 mg/L of Salicylic acid resulted in highest values of essential oil content and major constituents of the leaves and peels. Different changes were found in the chemical classes (monoterpene hydrocarbons, oxygenated monoterpenes, sesquiterpene hydrocarbons and oxygenated sesquiterpenes) of both of the leaf and peel oils.

Acknowledgment

The authors extend their thanks to the National Research Centre for the encouragement and support in this research work through the internal project no. 11080301.

References

Abreu ME and Munne-Bosch S. 2009. Salicylic acid deficiency in NahG transgenic lines and sid2 mutants increases seed yield in the annual plant *Arabidopsis thaliana*. *J Exp Bot*, **60:** 1261-1271.

Adams RP. 1995. **Identification of Essential Oil Components by Gas Chromatography/ Mass Spectrometry**. Allured Publ. Corp., Carol Stream, IL.

Ahmed AMA, El-Kady FA and Khalid AK. 2018. Comparison between salicylic acid and selenium effect on growth and biochemical composition of celery. *Asian J Plant Sci*, **17:** 150-159.

Ait ML, Kouhila M, Jamali A, Lahsasni S and Mahrouz M. 2005. Moisture sorption isotherms and heat of sorption of bitter orange leaves (*Citrus aurantium*). *Eng Food J*, **67:** 491-498.

Blokhina O, Virolainen E and Fagerstedt KV. 2003. Antioxidants, oxidative damage and oxygen deprivations stress. A Review. *Ann Bot*, **91:**179-194.

Bukar BB, Dayom DW and Uguru MO. 2016. The growing economic importance of medicinal plants and the need for developing countries to harness from it: A Mini Review. *IOSR J Pharm*, **6:** 42-52.

Clevenger JF. 1928. Apparatus for determination of essential oil. *J Amer Pharm Ass*, **17:** 346 - 349.

El-Tayeb MA. 2005. Response of barley grains to the interactive effect of salinity and salicylic acid. *Plant Growth Reg*, **45:** 215-224.

Foucart T. 1982. **Analyse Factorielle, Programmatiol Sur Micro- Ordinateur**. Masson, ITCF, Paris, France.

Gharib FA. 2006. Effect of salicylic acid on the growth, metabolic activities and oil content of basil and marjoram. *Int J Agric Bio*, **8:** 485-492.

Goudarzi T, Saharkhiz MJ, Rowshan V and Taban A. 2016. Changes in essential oil content and composition of Tansy (*Tanacetum vulgare* L.) under foliar application of salicylic and ortho-phosphoric acids. *J Ess Oil Res*, **28:** 64-70.

Jalal RS, Bafeel SO and Moftah AE. 2012. Effect of salicylic acid on growth, photosynthetic pigments and essential oil components of Shara (*Plectranthus tenuiflorus)* plants grown under drought stress conditions. *Int Res J Agric Soil Sci*, **2:** 252-260.

Khalid AK, El-Gohary AE and Ahmed AMA. 2018. Effect of the interaction between salicylic acid and geographical locations on grapefruit essential oil. *J Ess Oil Bear Plant*, **21:** 1594 -1603.

Khanam D and Mohammad F. 2017. Effect of structurally different plant growth regulators (PGRs) on the concentration, yield, and constituents of peppermint essential oil. *J Herb Spic Med Plant*, **23:** 26-35.

Lawless J 1992. The Encyclopaedia of Essential oils. The complete guide to the use of aromatis in aromatherapy, herbalism, health and well being. Element. Shaftesbury, *Dorset Rockport Massach*, 12-155.

Lehrner J, Eckersberger C, Walla P, Potsch G and Deecke L. 2000. Ambient odor of orange in a dental office reduces anxiety and improves mood in female patients. *Phys Behav*, **67:** 739-748.

Lota ML, Rocca Serra D, Jacquemond C, Tomi F and Casanova J. 2001. Chemical variability of peel and leaf essential oils of sour orange. *Flav Frag J*, **16:** 89-96.

Metwally A, Finkemeier I, Georgi M and Dietz KJ. 2003. Salicylic acid alleviates the cadmium toxicity in barley seedlings. *Plant Phys*, **132:** 272-281.

Pirbalouti AG, Immalek MR, Nejhad LE and Hamedi B. 2016. Essential oil compositions of summer savory under foliar application of jasmonic acid and salicylic acid. *J Ess Oil Res*, **26:** 342-347.

Pirbalouti AG, Samani MR, Hashemi M and Zeinali H. 2014. Salicylic acid affects growth, essential oil and chemical compositions of thyme (*Thymus daenensis* Celak.) under reduced irrigation. *Plant Growth Reg*, **72:** 289–301.

Reams LC and Furr JR. 1976. Salt tolerance of some Citrus species, relatives and hybrids tested as rootstocks. *J Amer Soc Hort Sci*, **101:** 265-267.

Rowshan V and Bahmanzadegan A. 2013. Effects of salicylic acid on essential oil components in Yarrow (*Achillea millefolium* Boiss). *Int J Bas Sci App Res*, **2:** 453-457.

Saharkhiz MJ and Goudarzi T. 2014. Foliar application of salicylic acid changes essential oil content and chemical compositions of peppermint (*Mentha piperita* L.). *J Ess Oil Bear Plant*, **17:** 435-440.

Shakirova FM. 2007. Role of hormonal system in the manifestation of growth promoting and anti stress action of salicylic acid. *In*: Hayat, S. and Ahmad, A. (Eds.). **Salicylic acid. A Plant Hormone**. Springer Publishers, Dordrecht, The Netherlands.

Snedecor GW and Cochran WG. 1990. **Statistical Methods**. 11th Ed. Iowa State Univ. Press. Ames, Iowa, USA.

Talaat IM, Khattab HI and Ahmed AM. 2014. Changes in growth, hormones levels and essential oil content of *Ammi visnaga* L. plants treated with some bio-regulators. *Saudi J Bio Sci*, **21:** 355–365.

Subscription

Jordan Journal of Biological Sciences

An International Peer – Reviewed Research Journal

Published by the Deanship of Scientific Research, The Hashemite University, Zarqa, Jordan

Name: ..... الاسم:

Specialty: ..... التخصص:

Address: ..... العنوان:

P.O. Box: ..... صندوق البريد:

City &Postal Code:..... المدينة: الرمز البريدي:

Country: ..... الدولة:

Phone: ..... رقم الهاتف

Fax No.: ..... رقم الفاكس:

E-mail: ..... البريد الإلكتروني:

Method of payment: ..... طريقة الدفع:

Amount Enclosed: ..... المبلغ المرفق:

Signature: ..... التوقيع:

Cheque should be paid to Deanship of Research and Graduate Studies – The Hashemite University.

I would like to subscribe to the Journal

For

- ☐ One year
- ☐ Two years
- ☐ Three years

One Year Subscription Rates

	Inside Jordan	Outside Jordan
Individuals	JD10	$70
Students	JD5	$35
Institutions	JD 20	$90

Correspondence

Subscriptions and sales:

Prof. Khaled H. Abu-Elteen
The Hashemite University
P.O. Box 330127-Zarqa 13115 – Jordan
Telephone: 00 962 5 3903333 ext. 4399
Fax no. : 0096253903349
E. mail: jjbs@hu.edu.jo

المجلة الأردنية للعلوم الحياتية
Jordan Journal of Biological Sciences (JJBS)

http://jjbs.hu.edu.jo

المجلة الأردنية للعلوم الحياتية: مجلة علمية عالمية محكمة ومفهرسة ومصنفة، تصدرعن الجامعة الهاشمية وبدعم من صندوق البحث العلمي والابتكار – وزراة التعليم العالي والبحث العلمي.

ترسل البحوث الى العنوان التالي:

رئيس تحرير المجلة الأردنية للعلوم الحياتية

الجامعة الهاشمية

ص.ب , 330127 , الزرقاء, 13115 , الأردن

هاتف: 0096253903333 فرعي 4357

E-mail: jjbs@hu.edu.jo, Website: www.jjbs.hu.edu.jo

المملكة الأردنية الهاشمية

المجلة الأردنية

للعلوم الحياتية

مجلة علمية عالمية محكمة

تصدر بدعم من صندوق دعم البحث العلمي و الابتكار

http://jjbs.hu.edu.jo/